



• **Solid State NMR**  
AVANCE Solids  
User Manual

Version 001

think forward

NMR Spectroscopy

The information in this manual may be altered without notice.

BRUKER BIOSPIN accepts no responsibility for actions taken as a result of use of this manual. BRUKER BIOSPIN accepts no liability for any mistakes contained in the manual, leading to coincidental damage, whether during installation or operation of the instrument. Unauthorized reproduction of manual contents, without written permission from the publishers, or translation into another language, either in full or in part, is forbidden.

This manual was written by:

Hans Foerster, Jochem Struppe, Stefan Steuernagel, Fabien Aussenacc,  
Francesca Benivelli, and Peter Gierth

Desktop Published by:

Stanley J. Niles

© November 25, 2008: Bruker Biospin GmbH

Rheinstetten, Germany

P/N: Z31848  
DWG-Nr.: Z4D10641 001

For further technical assistance on Solid State NMR, please do not hesitate to contact your nearest BRUKER dealer or contact us directly at:

BRUKER BioSpin GMBH  
am Silberstreifen  
D-76287 Rheinstetten  
Germany

Phone: + 49 721 5161 0  
FAX: + 49 721 5171 01  
E-mail: [service@bruker.de](mailto:service@bruker.de)  
Internet: [www.bruker.com](http://www.bruker.com)

# Contents

<b>Contents .....</b>	<b>3</b>	
<b>1</b>	<b>Introduction .....</b>	<b>9</b>
1.1	Disclaimer .....	9
1.2	Safety Issues .....	10
1.3	Contact for Additional Technical Assistance .....	10
<b>2</b>	<b>Test Samples .....</b>	<b>11</b>
<b>3</b>	<b>Basic Setup Procedures .....</b>	<b>13</b>
3.1	General Remarks .....	14
3.2	Setting the Magic Angle on KBr .....	15
	RF-Routing .....	15
	Setting Acquisition Parameters .....	17
3.3	Calibrating $^1\text{H}$ Pulses on Adamantane .....	23
3.4	Calibrating $^{13}\text{C}$ Pulses on Adamantane and Shimming the Probe .....	31
3.5	Calibrating Chemical Shifts on Adamantane .....	32
3.6	Setting Up for Cross Polarization on Adamantane .....	33
3.7	Cross Polarization Setup and Optimization for a Real Solid: Glycine ..	35
3.8	Some Practical Hints for CPMAS Spectroscopy .....	41
3.9	Literature .....	43
<b>4</b>	<b>Decoupling Techniques .....</b>	<b>45</b>
4.1	Hetero-nuclear Decoupling .....	45
	CW Decoupling .....	45
	TPPM Decoupling .....	46
	SPINAL Decoupling .....	47
	XiX Decoupling .....	47
	Pi-Pulse Decoupling .....	47
4.2	Homo-nuclear Decoupling .....	47
	Multiple Pulse NMR: Observing Chemical Shifts of Homo-nuclear Coupled Nuclei .....	47
	Multiple Pulse Decoupling .....	48
	BR-24, MREV-8, BLEW-12 .....	48
	FSLG Decoupling .....	48
	DUMBO .....	53
	Transverse Dephasing Optimized Spectroscopy .....	54
<b>5</b>	<b>Practical CP/MAS Spectroscopy on Spin 1/2 Nuclei .....</b>	<b>55</b>
5.1	Introduction .....	55
5.2	Possible Difficulties .....	55
5.3	Possible Approaches for $^{13}\text{C}$ Samples .....	55

5.4	Possible Approaches for non- <sup>13</sup> C Samples .....	57
5.5	Hints, Tricks, Caveats for Multi-nuclear (CP-)MAS Spectroscopy .....	58
5.6	Setup for Standard hetero-nuclear Samples <sup>15</sup> N, <sup>29</sup> Si, <sup>31</sup> P .....	58
<b>6</b>	<b>Basic CP-MAS Experiments .....</b>	<b>61</b>
6.1	Introduction .....	61
	Pulse Calibration with CP .....	61
6.2	Total Sideband Suppression TOSS .....	62
6.3	SELTICS .....	66
6.4	Non-Quaternary Suppression (NQS) .....	69
6.5	Spectral Editing Sequences: CPPI, CPPISPI and CPPIRCP .....	72
<b>7</b>	<b>FSLG-HETCOR .....</b>	<b>75</b>
7.1	Introduction .....	75
7.2	Pulse Sequence Diagram for FSLG HETCOR .....	76
7.3	Setting FSLG HETCOR Experiments .....	77
7.4	Results .....	81
<b>8</b>	<b>Modifications of FSLG HETCOR .....</b>	<b>83</b>
8.1	Carbon Decoupling During Evolution .....	84
8.2	HETCOR with DUMBO, PMLG or w-PMLG, Using Shapes .....	85
	The Sequence pmlghet .....	85
	w-pmlghet .....	88
	edumbohet .....	89
	dumbohet .....	90
8.3	HETCOR with Cross Polarization under LG Offset .....	91
<b>9</b>	<b>RFDR .....</b>	<b>93</b>
9.1	Experiment .....	94
9.2	Set-up .....	94
9.3	Data Acquisition .....	95
	Set-up 2D Experiment .....	95
9.4	Spectral Processing .....	96
<b>10</b>	<b>Proton Driven Spin Diffusion (PDSD) .....</b>	<b>99</b>
10.1	Pulse Sequence Diagram .....	101
10.2	Basic Setup .....	101
	2D Experiment Setup .....	101
10.3	Acquisition Parameters .....	103
	Processing Parameters .....	104
10.4	Adjust the Rotational Resonance Condition for DARR/RAD .....	104
10.5	Example Spectra .....	106
<b>11</b>	<b>SUPER .....</b>	<b>109</b>
11.1	Overview .....	109
11.2	Pulse Program .....	110
11.3	Experiment Setup .....	110
	Experiment setup .....	110
	Setup 2D Experiment .....	111

11.4	Data Acquisition .....	113
11.5	Spectral Processing .....	114
<b>12</b>	<b>Symmetry Based Recoupling .....</b>	<b>119</b>
12.1	Pulse Sequence Diagram, Example C7 .....	121
12.2	Setup .....	121
	Spectrometer Setup for $^{13}\text{C}$ .....	123
	Setup for the Recoupling Experiment .....	123
	Setup of the 2D SQ-DQ Correlation Experiment .....	125
12.3	Data Acquisition .....	126
12.4	Spectral Processing .....	127
12.5	$^{13}\text{C}$ - $^{13}\text{C}$ Single Quantum Correlation with DQ Mixing .....	128
12.6	Data Acquisition .....	129
12.7	Spectral Processing .....	130
<b>13</b>	<b>PISEMA .....</b>	<b>131</b>
13.1	Introduction .....	131
13.2	Pulse Sequence Diagram .....	132
13.3	Setup .....	133
	Setup 2D Experiment .....	134
13.4	Data Acquisition .....	135
13.5	Processing .....	137
<b>14</b>	<b>Relaxation Measurements .....</b>	<b>141</b>
14.1	Describing Relaxation .....	141
14.2	T1 Relaxation Measurements .....	142
	Experimental Methods .....	142
	The CP Inversion Recovery Experiment .....	143
	Data Processing .....	145
	The Saturation Recovery Experiment .....	147
	T1p Relaxation Measurements .....	148
14.3	Indirect Relaxation Measurements .....	149
	Indirect Proton T1 Measurements .....	150
<b>15</b>	<b>Basic MQ-MAS .....</b>	<b>151</b>
15.1	Introduction .....	151
15.2	Pulse sequences .....	151
15.3	Data Acquisition .....	153
	Setting Up the Experiment .....	153
	Two Dimensional Data Acquisition .....	158
15.4	Data processing .....	160
15.5	Obtaining Information from Spectra .....	163
<b>16</b>	<b>MQ-MAS: Sensitivity Enhancement .....</b>	<b>169</b>
16.1	Split-t1 Experiments and Shifted Echo Acquisition .....	169
16.2	Implementation of DFS into MQMAS experiments .....	171
	Optimization of the Double Frequency Sweep (DFS) .....	171
	2D Data Acquisition .....	176
	Data Processing .....	178

## Contents

16.3	Fast Amplitude Modulation - FAM .....	180
16.4	Soft Pulse Added Mixing - SPAM .....	180
<b>17</b>	<b>STMAS .....</b>	<b>183</b>
17.1	Introduction .....	183
17.2	Experimental Particularities and Prerequisites .....	183
17.3	Pulse Sequences .....	185
17.4	Data Acquisition .....	187
	Set-up of the Experiment .....	187
	Two Dimensional Data Acquisition .....	189
17.5	Data Processing .....	191
<b>18</b>	<b>Double-CP .....</b>	<b>193</b>
18.1	Pulse Sequence Diagram, Double CP (DCP) .....	194
18.2	Spectrometer Setup for DCP .....	194
	Setup for DCP, <sup>13</sup> C channel .....	194
	<sup>15</sup> N Channel Setup .....	196
	Setup of the Double CP Experiment .....	197
	Setup of the 2D Double CP Experiment .....	201
18.3	2D Data Acquisition .....	202
18.4	Spectral Processing .....	203
18.5	Example Spectra .....	204
<b>19</b>	<b>CRAMPS: General .....</b>	<b>207</b>
19.1	Homo-nuclear Dipolar Interactions .....	207
19.2	Multiple Pulse Sequences .....	207
19.3	W-PMLG and DUMBO .....	208
19.4	Quadrature Detection and Chemical Shift Scaling .....	208
<b>20</b>	<b>CRAMPS 1D .....</b>	<b>211</b>
20.1	Pulse Sequence Diagram of W-PMLG or DUMBO .....	211
20.2	Pulse Shapes for W-PMLG and DUMBO .....	212
20.3	Analog and Digital Sampling Modi .....	213
	Analog Mode Sampling .....	214
	Digital Mode Sampling .....	214
20.4	Setup .....	215
20.5	Parameter Settings for PMLG and DUMBO .....	215
20.6	Fine Tuning for Best Resolution .....	217
20.7	Fine Tuning for Minimum Carrier Spike .....	217
20.8	Correcting for Actual Spectral Width .....	217
20.9	Digital Mode Acquisition .....	218
20.10	Examples .....	218
<b>21</b>	<b>Modified W-PMLG .....</b>	<b>221</b>
21.1	Pulse Sequence Diagram for Modified W-PMLG .....	221
21.2	Pulse Shapes for W-PMLG .....	222
21.3	Set-up .....	222
21.4	Parameter Settings for PMLG and DUMBO .....	223
21.5	Fine Tuning for Best Resolution .....	224

21.6	Correcting for Actual Spectral Width .....	224
21.7	Digital Mode Acquisition .....	224
<b>22</b>	<b>CRAMPS 2D .....</b>	<b>225</b>
22.1	Proton-Proton Shift Correlation (spin diffusion) .....	225
22.2	Pulse Sequence Diagram .....	226
22.3	Data Processing .....	227
22.4	Examples .....	228
22.5	Proton-Proton DQ-SQ Correlation .....	230
22.6	Pulse Sequence Diagram .....	231
22.7	Data Processing .....	233
22.8	Examples .....	233
<b>A</b>	<b>Appendix .....</b>	<b>237</b>
A.1	Form for Laboratory Logbooks .....	237
	<b>Figures .....</b>	<b>243</b>
	<b>Tables .....</b>	<b>249</b>
	<b>Index .....</b>	<b>253</b>

## Contents

# Introduction

1

This manual is intended to help users set up a variety of different experiments that are to date more or less standard in solid state NMR.

Previously, the manuals described the hardware in some detail, and also basic setup procedures. Armed with this knowledge, it was assumed the users would be in a position to manage the setup of even complicated experiments themselves.

In this manual however, the hardware is not discussed in detail, since there is no longer much hardware which is specific to solid-state NMR. There are still transmitters with higher power, and preamps and probes that take this power, but for the purposes of experimental setup, detailed knowledge is not required, since the setup does not generally depend on the details of the hardware. So, this manual is now much more specific to the type of experiment which is to be executed, and includes tricks and hints required to set the experiment up properly for best performance. If any special hardware (or software) knowledge is required, it is indicated within the experimental section.

This manual begins with the most frequently used solid-state NMR experiments, and will be extended as time permits and as it is required by new development in NMR. The manual is written primarily for Bruker AVANCE III instruments, but the experimental part will be identical, or similar, for AVANCE I and AVANCE II instruments. For example, pulse programs will have slightly different names, differing usually in the pulse program name extension. Contact your nearest applications scientist if you do not find the experiment/pulse program that you are looking for. Users of older instruments (DSX, DMX, DRX) should refer to the Solids Users Manual delivered within the Help system at Help -> Other topics -> Solids Users Manual. Even though the pulse programs may look similar, they will not run on these instruments.

The first five chapters deal with basic setup procedures, subsequent chapters are dedicated to specific types of experiments. There may be many different „sub“ experiments within a given type, since the same information can often be obtained with pulse sequences differing by sub-units only, or in using a totally different principle. The experiments outlined here are usually the most important ones and/or the ones that were common at the time when the manual was written.

New chapters will be added, as the manual consists of largely self-contained units rather than being a comprehensive single volume. This structure was adopted in order to be more flexible in updating/replacing individual chapters. So do not be surprised if some chapters are still missing, they will be completed in the near future and implemented as they are finished and proofread. The individual chapters are written by different people, so there will be some differences in style and composition.

## Disclaimer

1.1

Any hardware units mentioned in this manual should only be used for their intended purpose as described in their respective manual. Use of units for any purpose other than that for which they are intended is taken only at the users own risk and invalidates any and all manufacturer warranties.

Service or maintenance work on the units must be carried out by qualified personnel.

## **Introduction**

Only those persons schooled in the operation of the units should operate the units.

Read the appropriate user manuals before operating any of the units mentioned. Pay particular attention to any safety related information.

## **Safety Issues**

**1.2**

Please refer to the corresponding user manuals for any hardware mentioned in this manual for relevant safety information.

## **Contact for Additional Technical Assistance**

**1.3**

For further technical assistance on the BPSU36-2 unit, please do not hesitate to contact your nearest BRUKER dealer or contact us directly at:

BRUKER BioSpin GMBH  
am Silberstreifen  
D-76287 Rheinstetten  
Germany

Phone: + 49 721 5161 0  
FAX: + 49 721 5171 01  
E-mail: [service@bruker.de](mailto:service@bruker.de)  
Internet: [www.bruker.de](http://www.bruker.de)

# Test Samples

2

Table 2.1. Setup Samples for Different NMR Sensitive Nuclei

Nucleus	Sample	Method	O1P	Remarks
<sup>3</sup> H				
<sup>1</sup> H	Silicone paste Silicone rubber Adamantane  Glycine Malonic Acid	<sup>1</sup> HMAS <sup>1</sup> HMAS <sup>1</sup> HMAS  CRAMPS CRAMPS	0 0 0  -3 -3	setup proton channel, shim, set field setup proton channel, set field setup proton channel, set field, shim under CRAMPS conditions setup CRAMPS resolution CRAMPS, d1=60s
<sup>19</sup> F	PVDF  PTFE	<sup>19</sup> F MAS CP <sup>19</sup> FMAS		direct observe <sup>19</sup> F CP <sup>1</sup> H/ <sup>19</sup> F, <sup>1</sup> H/ <sup>13</sup> C, <sup>19</sup> F/ <sup>13</sup> C (low sensitivity) direct observe
<sup>3</sup> He				
<sup>203,209</sup> Tl				
<sup>31</sup> P	(NH <sub>4</sub> )H <sub>2</sub> PO <sub>4</sub>	<sup>1</sup> H/ <sup>31</sup> PCP	0	powdered sample, piezoelectric, 4s
<sup>7</sup> Li	LiCl	MAS		
<sup>117,119</sup> Sn	Sn (cyclohexyl) <sub>4</sub> Sm <sub>2</sub> Sn <sub>2</sub> O <sub>7</sub> /SnO <sub>2</sub>	CP MAS		5ms contact, d1>10s VT shift thermometer, d1<1s Sm <sub>2</sub> Sn <sub>2</sub> O <sub>7</sub> ,>60s SnO <sub>2</sub> (temp. independent)
<sup>87</sup> Rb	RbNO <sub>3</sub> , RbClO <sub>4</sub>	MQMAS	0	0.5s repetition
<sup>11</sup> B	BN Boric Acid	MAS MQMAS		>5s repetition
<sup>71</sup> Ga	Ga <sub>2</sub> O <sub>3</sub>	hahn echo		CT 300 kHz wide
<sup>65</sup> Cu	Cu-metal powder	wideline		knight shift +2500ppm
<sup>71</sup> Ga				
<sup>129</sup> Xe	as hydroquinon Clathrate gas in air	CPMAS	0 0	d1>5s single pulses overnight, 1s
<sup>23</sup> Na	Na <sub>2</sub> HPO <sub>4</sub> Na <sub>3</sub> P <sub>3</sub> O <sub>9</sub>	MQMAS MQMAS	0	dep. on crystal water 2-5 lines
<sup>51</sup> V	NH <sub>4</sub> VO <sub>4</sub>			
<sup>123</sup> Te				

## Test Samples

Table 2.1. Setup Samples for Different NMR Sensitive Nuclei

<sup>27</sup> Al	AlPO-14	MQMAS	0	d1 05-1s, 4 lines
<sup>13</sup> C	Adamantane α-glycine	CP,DEC CP	50 110	HH setup, shim sensitivity,decoupling.Prep.: precipitate with acetone from aq. solution, C,N fully labelled for fast setup, recoupling, REDOR (10% in natrl. abundance)
<sup>79</sup> Br	KBr	MAS		d1< 50msec, angle setting finely powdered, reduced volume
<sup>59</sup> Co	Co(CN) <sub>6</sub>	MAS		shift thermometer
<sup>55</sup> Mn	KMnO <sub>4</sub>	MAS		>500 MHz pattern
<sup>93</sup> Nb				
<sup>207</sup> Pb	PbNO <sub>3</sub> Pb(p-tolyl) <sub>4</sub>	MAS CP		shift thermometer, 0,753 ppm/degr. d1>10s 5ms, 15s
<sup>29</sup> Si	Q <sub>8</sub> M <sub>8</sub> DSS,TMSS	CPMAS CPMAS	-50 0	d1>5s, reference sample 12.6/-108 ppm reference sample 0 ppm
<sup>77</sup> Se	H <sub>3</sub> SeO <sub>3</sub> (NH <sub>4</sub> ) <sub>2</sub> SeO <sub>4</sub>	CPMAS CPMAS	1800 -200	HH setup, 8ms contact, d1>10s 3ms, d1>4s
<sup>113</sup> Cd	Cd(NO <sub>3</sub> ) <sub>2</sub> *4H <sub>2</sub> O	CPMAS	350	15ms contact, d1>8s
<sup>195</sup> Pt	K <sub>2</sub> Pt(OH) <sub>6</sub>	CPMAS	- 12000	1ms contact, d1>4s
<sup>199</sup> Hg	Hg(acetate) <sub>2</sub>	CPMAS	2500	5ms contact, d1>10s
<sup>2</sup> H	d-PMMA d-PE d-DMSO <sub>2</sub>	WL WL WL	0 0 0	wideline setup d1 5s wideline setup d1 0.5s/10s amorphous/ crystalline exchange expt. at 315K
<sup>6</sup> Li	LiCl, Li (org.)			make sure it is not <sup>6</sup> Li depleted, d1>60s
<sup>17</sup> O	D <sub>2</sub> O		0	pulse determination, 100scans,0.5s
<sup>15</sup> N	α-glycine	CP	50	sensitivity, 4ms contact,4s labelled for fast setup
<sup>35</sup> Cl	KCl	WL,MAS	0	pulse determ., 100 scans
<sup>33</sup> S	K <sub>2</sub> S	MAS	0	100 scans in a >=500 MHz instr.
<sup>14</sup> N	NH <sub>4</sub> Cl	MAS,WL	0	100 scans, narrow line
<sup>25</sup> Mg				
47/49-Ti	Anatas	MAS		
<sup>39</sup> K	KCl	MAS,WL	0	100 scans
<sup>109</sup> Ag	AgNO <sub>3</sub>	MAS		1scan, 500s, finely powdered
<sup>89</sup> Y	Y(NO <sub>3</sub> ) <sub>3</sub> *6H <sub>2</sub> O	CPMAS	-50	10ms contact, d1>10s

# **Basic Setup Procedures**

**3**

This chapter contains information and examples on how to set up basic solid-state NMR (SSNMR) experiments. We'll begin with the settings for the RF-routing of the spectrometer, some basic setup procedures for MAS probes and how to measure their (radio frequency) RF-efficiency and RF-performance. Accurate measurement of the pulse lengths and the associated RF-power levels is essential for solid-state NMR experiments. In SSNMR, RF-field amplitudes are often expressed as spin nutation frequencies instead of 90° pulse widths. Spin nutation frequency  $n_{rf}$  and 90° pulse width are related through the reciprocal of the 360° pulse duration  $4t_{p90}$  such that:

$$n_{rf} = 1/(4t_{p90}) = \text{RF-field in Hz (with } t_{p90} \text{ in } \mu\text{sec})$$

Setting up the magic angle, shimming a CPMAS probe, setting up cross polarization and measuring probe sensitivity for  $^{13}\text{C}$  will also be explained. This is part of probe setup and performance assessment during installation. However, regularly scheduled performance measurements should be part of the hardware, probes and spectrometer maintenance. Therefore, these checks should be performed periodically.

The checks also need to be performed if an essential piece of hardware has been exchanged. In the following, we describe all steps which are necessary to assess performance of a CPMAS probe, along with all necessary settings. Detailed information about TopSpin software commands is available in the help section within the appropriate chapter.

**Setting up a CPMAS probe from scratch** requires the following steps:

- Mount the probe in the magnet and connect the RF connectors of the probe to the appropriate preamps.
- Connect the spinning gas connectors and the spin rate monitor cable.
- Insert a spinner with finely ground KBr and spin at 5 kHz.

It is assumed that these operations are known. If not, please refer to the following sources:

- Probe manual.
- MAS-II pneumatic unit manual in TopSpin/help.
- SBMAS manual in TopSpin/help.
- Solids manual in TopSpin/help.

This chapter will include:

**"Setting the Magic Angle on KBr"**

**"Calibrating 1H Pulses on Adamantane"**

**"Calibrating 13C Pulses on Adamantane and Shimming the Probe"**

**"Calibrating Chemical Shifts on Adamantane"**

**"Setting Up for Cross Polarization on Adamantane"**

**"Cross Polarization Setup and Optimization for a Real Solid: Glycine"**

**"Some Practical Hints for CPMAS Spectroscopy"**

**"Literature"**

### General Remarks

3.1

Despite the fact that most spectra taken on a CP/MAS probe look like liquids spectra, the conditions under which they are taken must account for the presence of strong interactions. This basically means that:

- fast spinning, and
- high power pulses are applied.

Fast spinning requires a high precision mechanical system to allow spinning near the speed of sound. This requires careful operation of the spinning devices. Please read the probe manual carefully!

High power decoupling in solids requires 20-fold RF fields compared to liquids spectroscopy, since we are dealing with >20 kHz dipolar couplings rather than maximum 200 Hz J-couplings! This means that RF voltages near the breakthrough limit must be applied, and that currents of far more than 20 A occur.

It is therefore essential that:

- Power levels for pulses must be carefully considered before they are applied. Always start at very moderate power levels with an unknown probe, find the associated RF field or pulse length and then work your way towards specified values. The same applies for pulse lengths, especially decoupling periods, since the power dissipation inside the probe is proportional to pulse power and duration. Always observe the limits for duty cycle and maximum pulse power. Please refer to the probe specifications for more information. Never set acquisition times longer than required!
- Spinners and turbine must be kept extremely clean. Any dirt, especially oil, sweat from fingers, water will decrease the breakthrough voltage dramatically. Make sure the spinner is always clean (wipe before inserting, touch the drive cap only) and the spinning gas supply is carefully checked to provide oil-free and dry (dew point below 0 °C) spinning gas. Compressors and dryers must be checked and maintained on a regular basis. Any dirt inside the turbine will eventually cause expensive repairs.

The following setup steps need only be executed upon installation or after a probe repair. The test spectrum on glycine should be repeated in regular intervals to assure probe performance.

**Setting the Magic Angle on KBr**

3.2

For all following steps, generate new data sets with appropriate names using the **edc** command to record all individual setup steps.

**RF-Routing**

3.2.1

The spectrometer usually has 2 or more RF generation units (SGU's), transmitters and preamplifiers. In order to connect the appropriate SGU to the appropriate transmitter and the transmitter to the associated preamp where the probe channels are connected, there are several routing possibilities. In order to minimise errors in hardware connections, the routing is under software control where possible. Where cable connections need to be done manually, the software does not allow a change. These connections are made during instrument installation.

Enter the “**edasp**” command (or click the **Edit** button in the nucleus section in the acquisition parameter window **eda**) in order to get the spectrometer router display.

Alternatively, click on the routing icon in **eda**.

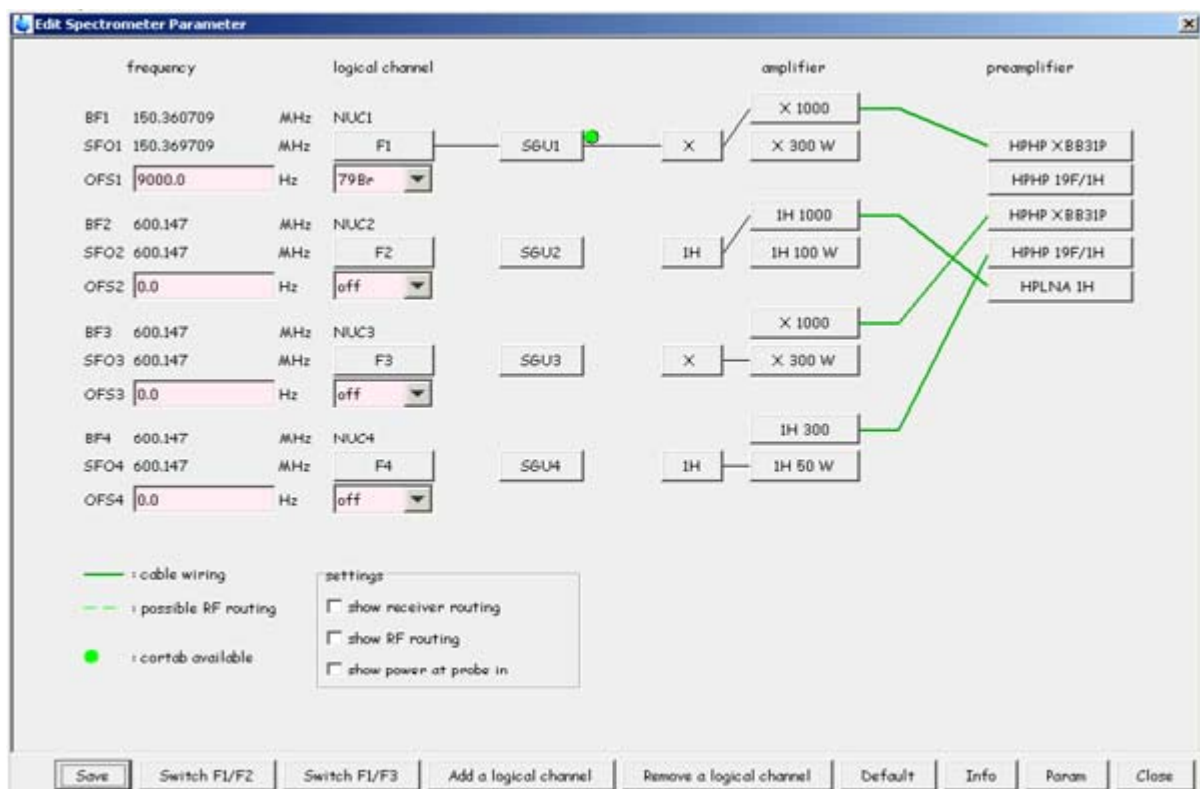


Figure 3.1. Routing for a Simple One Channel Experiment

The figure above shows the routing for a simple one channel NMR experiment using the 1000 W output from the high power amplifier.

In this menu, 4 RF channels are available. These 4 RF channels can be set up for 4 different frequencies. The two left most columns labelled frequency and logical channel define the precise irradiation frequency by setting the nucleus and the offset **O1** from the basic frequency. In

this example, we want to set up for pulsing/observe on the nucleus  $^{79}\text{Br}$ . Selecting  $^{79}\text{Br}$  for channel F1 defines the basic frequency **BF1** of  $^{79}\text{Br}$  (in this case on a 600 MHz spectrometer, 150.360709) and the adjustable offset (9000 Hz in this case). Both values are added to show the actual frequency setting, **SFO1**. The frequency setting is taken from a nucleus table which is calculated for the respective magnetic field  $B_0$ . The index 1 in **O1**, **BF1**, and **SFO1** refers to the RF channel 1 (which is also found in the pulse program where the pulse is defined as p1:f1). Note that this index does not exist for the following columns which represent the hardware components (SGU1-4 refers to the slot position in the AQS-rack). The lines connecting the (software) channel F1 to the actual frequency generation and amplification hardware can be drawn ad libitum as long as the required hardware connections are present. The connections between transmitter and preamp cannot be routed arbitrarily, because every transmitter output is hardwired to a preamplifier, so the lines are drawn in green. Please note that the nucleus in channel F1 is always the observe nucleus.

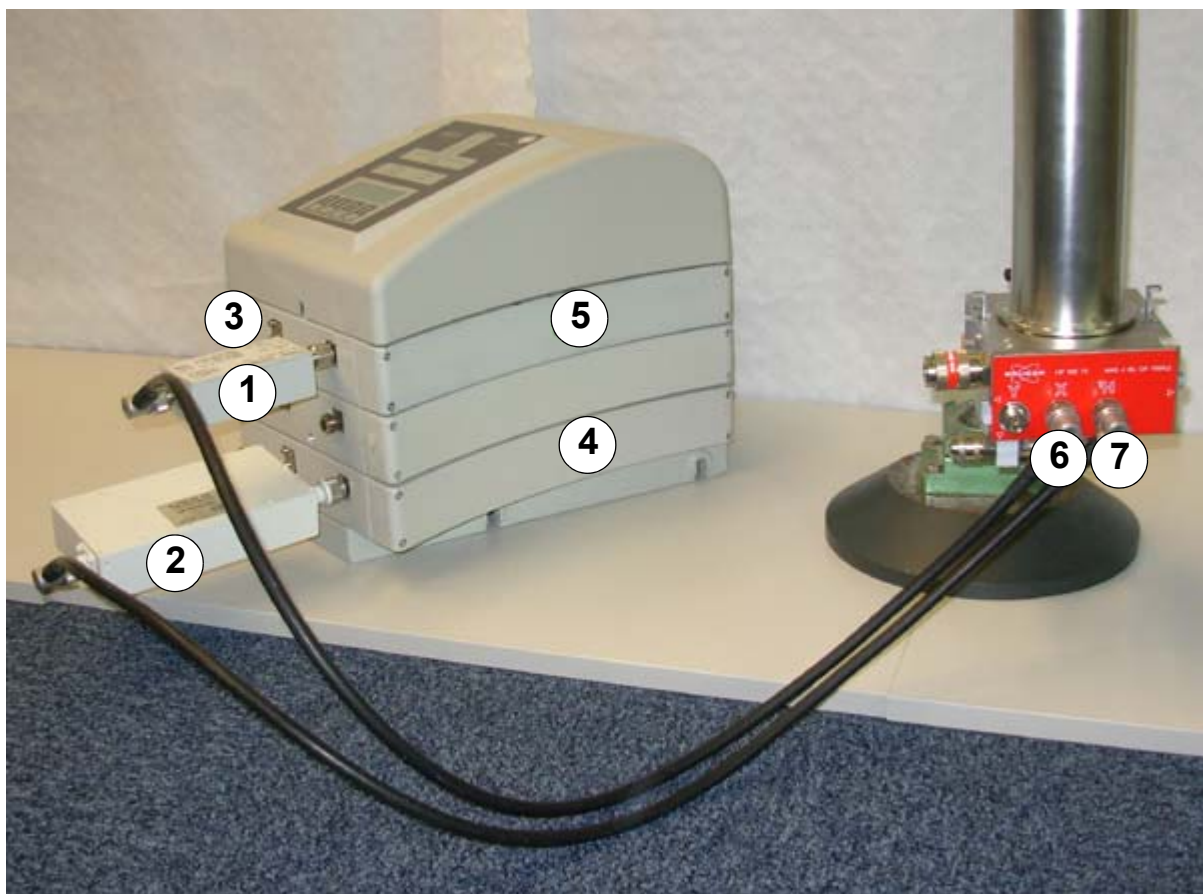
To set up for  $^{79}\text{Br}$  observation, click on **Default** and the correct routing will be shown.

The green dot between SGU1 and amplifier 1 indicates that for this nucleus in this connection, the transmitter has been calibrated for amplitude and phase linearity (CORTAB).

For example, if you select a nucleus where this has not been calibrated and the green dot is not visible, the same power level setting in dB will produce >6 dB more power (> 4-fold power) which may destroy your probe. Calibrate power levels in such a case starting with 10 dB less power (higher  $p/(n)$ -value) to prevent destruction of your probe!

The connections between SGU(n) and transmitter (n) can be altered by clicking on either side of the connecting line (removes the connection), and clicking again on both units you want to connect (route). In case of high power transmitters, you have two power stages which you select by clicking on the desired stage. High power stages require the parameter **powmod** to be set to "high". Selecting a path which is not fully routed will generate an error message.

To leave the display, click on **Save**. Make sure your probe X-channel is connected to the selected preamplifier (the sequence of preamplifiers in **edasp** represents the physical position of the preamplifier in the stack). If the preamp is a high power type, make sure the correct matching box is inserted into the preamp (for 500-800 MHz systems, it would be labelled for the frequency range 120-205 MHz). Connections are shown in the figure below:



- 1: X Low Pass Filter  
2: Proton Bandpass Filter  
3: X-BB Preamplifier  
4: 1H HP Preamplifier

- 5: 13C Matching Box  
6: X Probe Connector  
7: 1H Probe Connector

Figure 3.2. Probe Connections to the Preamplifier

The figure above shows the probe connections to the preamplifier with appropriate filters, placed on a table for better illustration.

### Setting Acquisition Parameters

#### 3.2.2

Create a new data set for the experiment by typing **edc** in the command line.

## Basic Setup Procedures

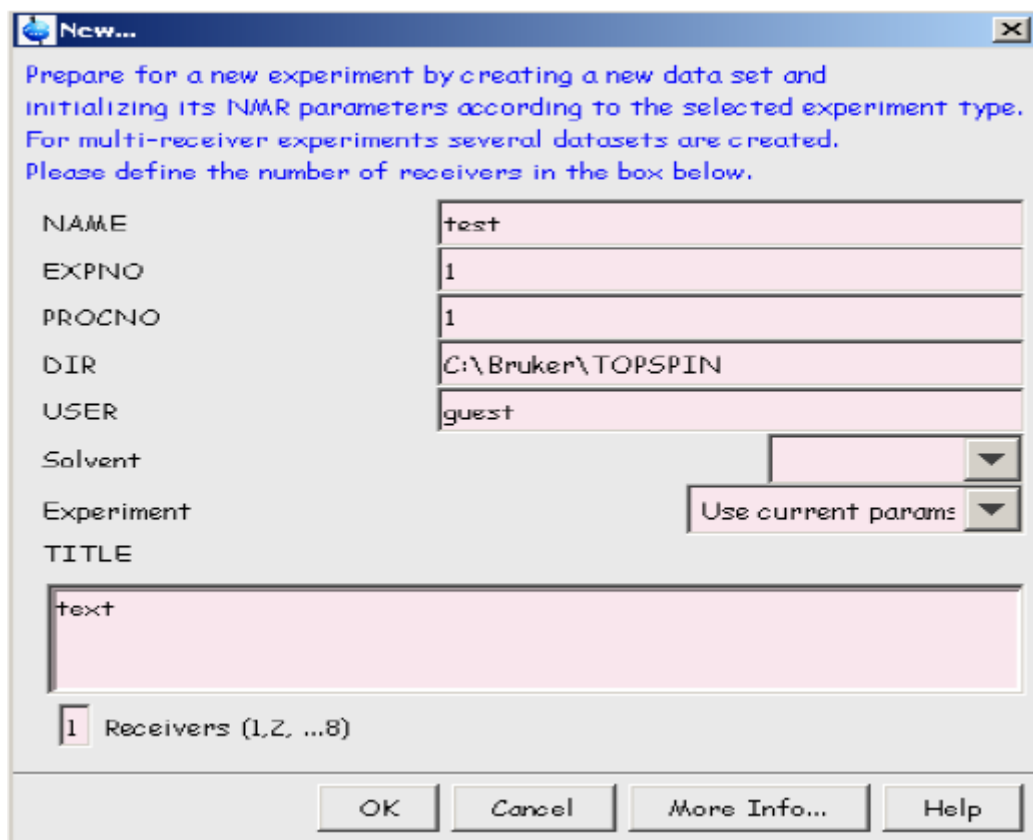


Figure 3.3. Pop-up Window for a New Experiment

Spin the KBr sample moderately (~5, 2.5mm: 10 kHz). In order to set up the experiment, type **ased** in the command line to open the table with parameters used for this experiment.

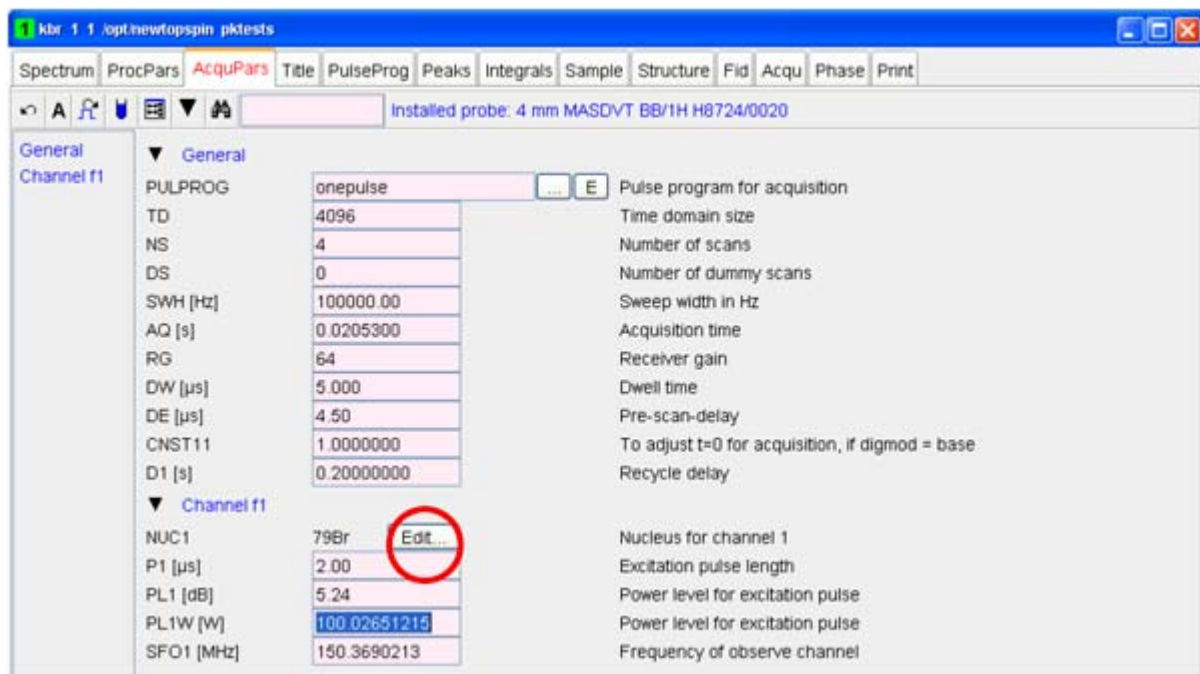


Figure 3.4. *ased Table with Acquisition Parameters for the KBr Experiment*

Then check rf routing by clicking on the **Edit** button in figure 4 or by typing **edasp** in the command line and check **powmod** by clicking the *default* button (as described above). The rf routing for this experiment is shown in figure 1. Next set **p1** = 2 ms, **ns** = 8 or 16. The power level at which **p1** is executed is **pl1**. Having high power transmitters it is important to be aware of the pulse power that is applied. With TopSpin 2.0 and later, **ased** shows **pl1** and **pl1w**, if the transmitter has been linearized (green dot in **edasp**) and the transmitter power has been measured. Set the power to about 100W.

For a non linearized transmitter, **pl1** should be set to 10 in case of a 1000W transmitter and to 4 (5) for a 300W or 500W transmitter. You can also check durations and power levels in a graphical display by clicking the *experiment* button in the **Pulprog** window as it is shown in the figure below.

## Basic Setup Procedures

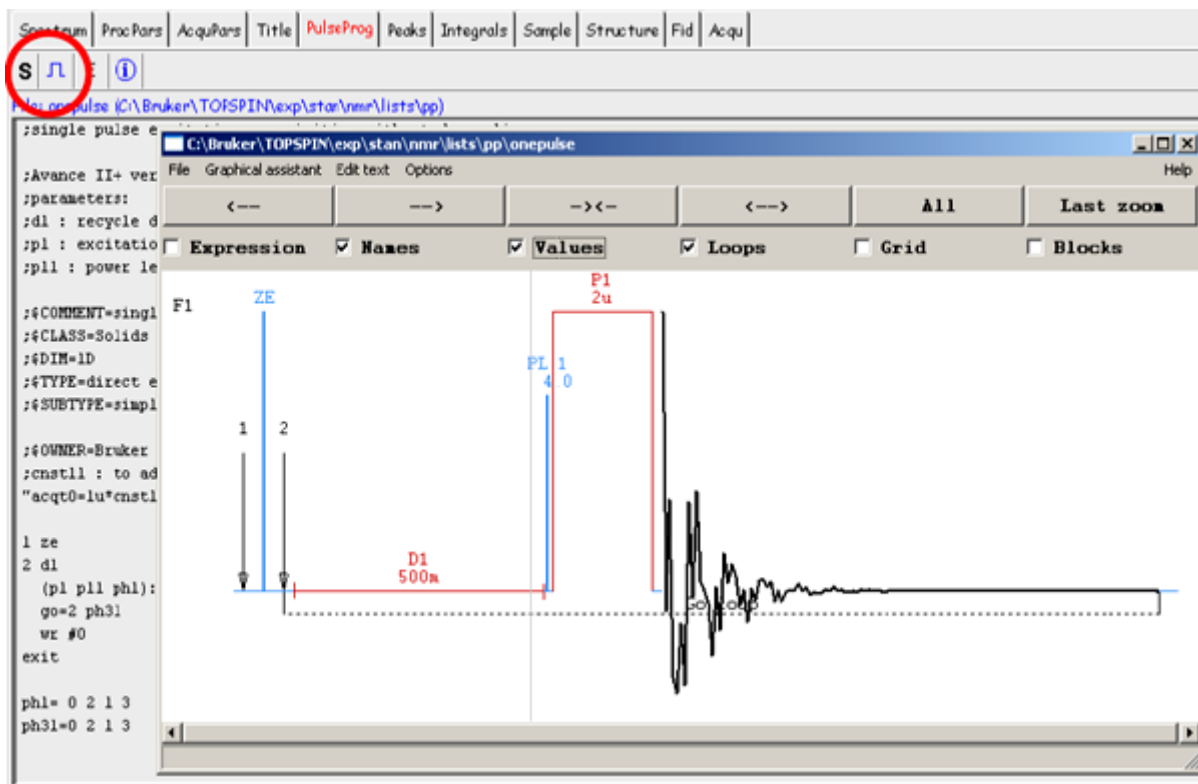


Figure 3.5. Graphical Pulse Program Display

In the figure above, the experiment button for opening the graphical display is marked with a red circle.

Then match and tune the probe for this sample using the command **wobb**. This will start a frequency sweep over the range of **SFO1+-WBSW/2**. The swept frequency will only be absorbed by the probe at the frequency to which it is tuned.

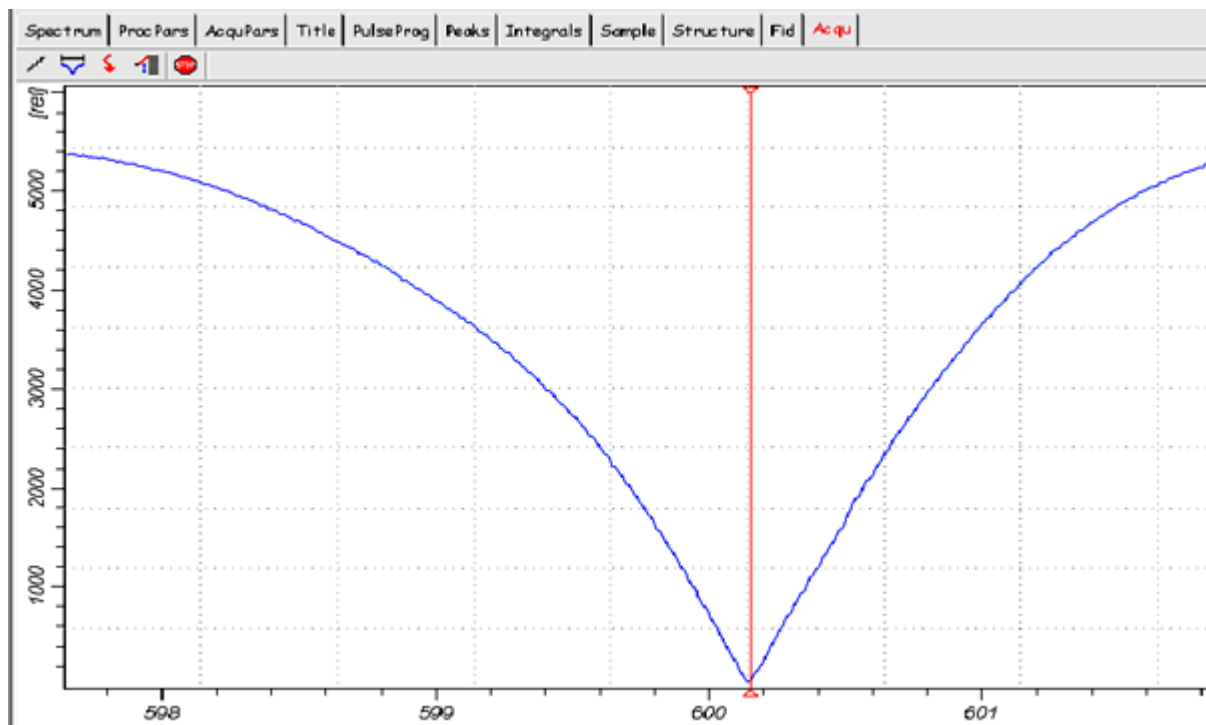


Figure 3.6. Display Example of a Well-tuned Probe

At frequencies, where the probe is not matched to 50 Ohms, the curve will lift off the zero line. If tuned to a frequency within **SFO1+/-WBSW/2**, but  $\neq$  **SFO1**, the probe response will be off center. N.B.: Fake resonances may appear which do not shift with probe tuning. It is always a good idea to keep track which nucleus was tuned last so it is clear what direction to tune to. Usually, turning the tuning knob counter clockwise (looking from below) will shift to higher tuning frequency.

## Basic Setup Procedures

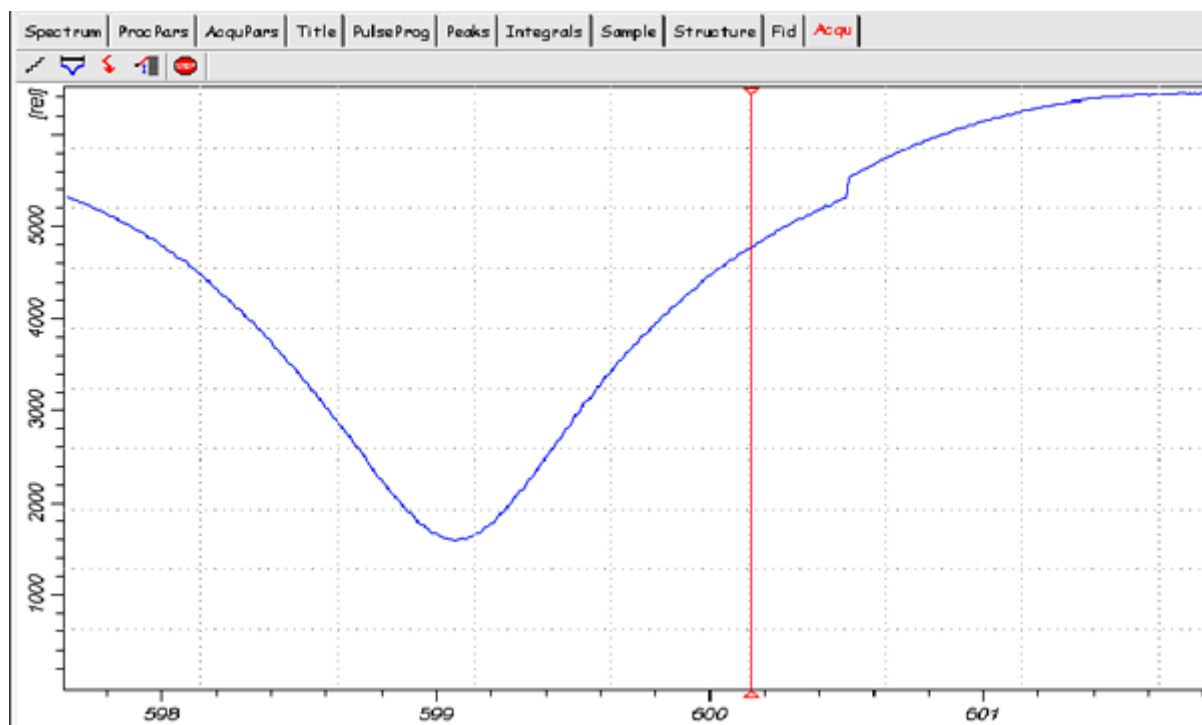


Figure 3.7. Display Example of an Off-Matched and Off-Tuned Probe

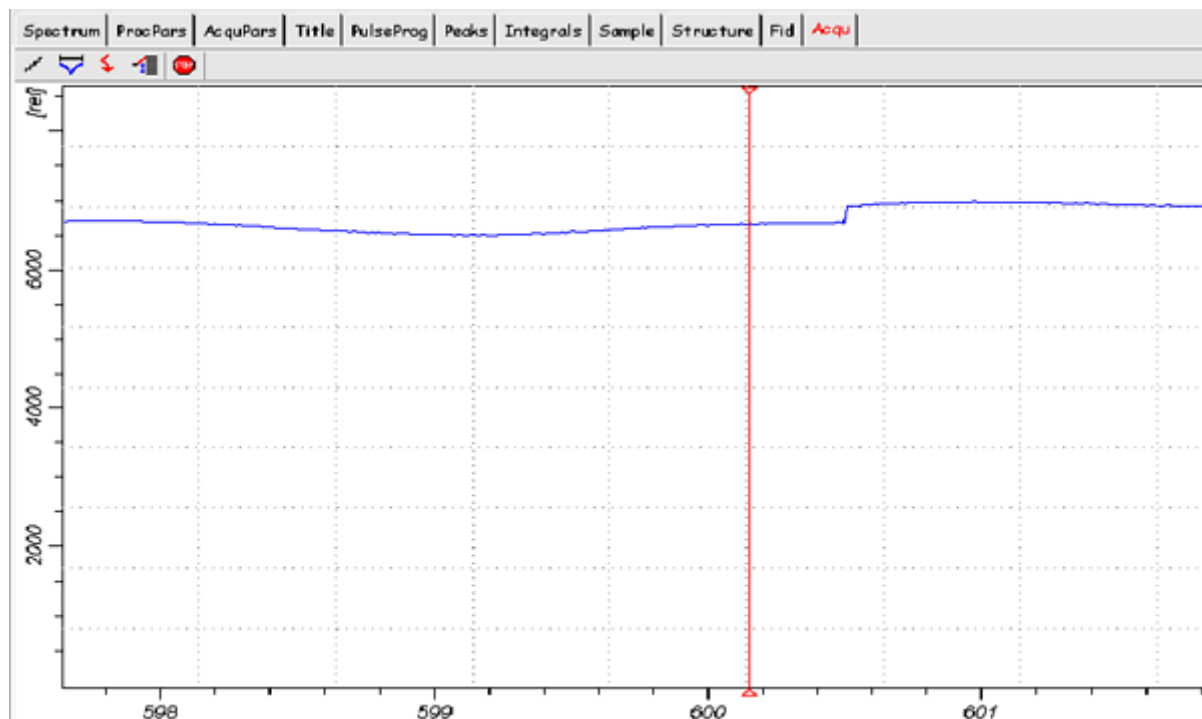


Figure 3.8. Display Example Where Probe is Tuned to a Different Frequency

The figure above is an example of where the probe is either tuned to a completely different frequency outside this window or the probe is not connected to the selected preamp. Check **edasp** for correct routing, Check for correct matching box frequency range. Increase WBSW to 50 or 100 and try to find the probe resonance position.

Next start an acquisition by typing **zg** in the command line or clicking on the black triangle (upper left side) in the acquisition display. Do a *Fourier Transformation* and a *phase correction* by typing **ft** and **phase correct**.

Set offset **O1** to the value obtained for the center peak (see **fig. 13**) and start “**xau angle**”. This will allow you to view the fourier transformed spectrum or the FID after **ns** scans. The magic angle is adjusted best when the spikes on the FID or the spinning sidebands in the *Spectrum* display have maximum size, like shown in **figure 9**. This is most easily seen with the carrier exactly on resonance and the un shuffled FID display mode. The spinning sidebands should have maximum intensity, the rotational echoes on the FID should extend out to at least 8msec in the FID-display.

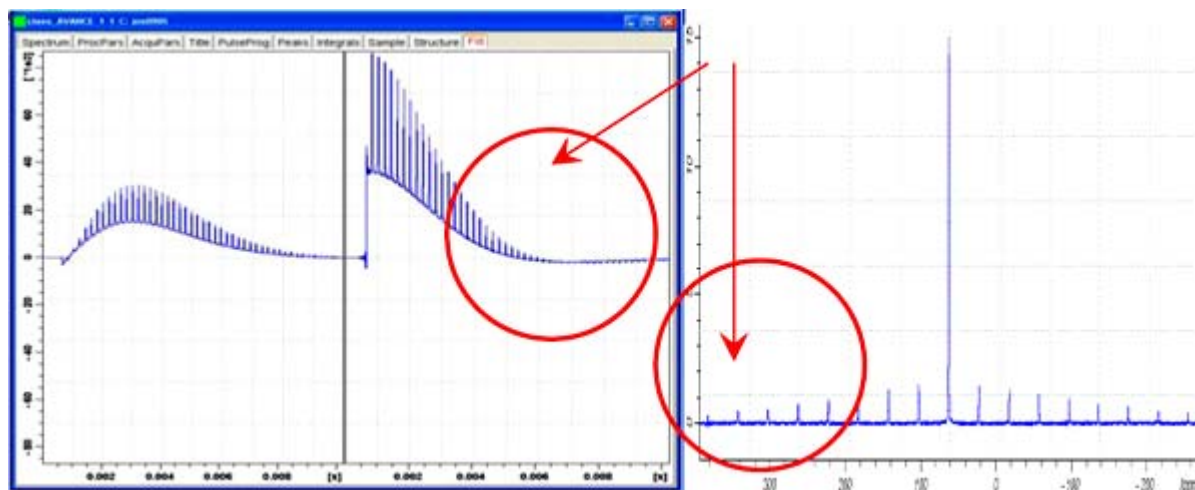


Figure 3.9. FID and Spectrum of the  $^{79}\text{Br}$  Signal of KBr used to Adjust the Magic Angle

### Calibrating 1H Pulses on Adamantane

### 3.3

Spin the KBr sample down and change to a spinner filled with adamantane. Spin at 5-10 kHz. Generate a new data set from the KBr data set by typing **new**. Set the instrument routing for  $^{13}\text{C}$  observe and  $^1\text{H}$  decoupling, as shown in the following figure:

## Basic Setup Procedures

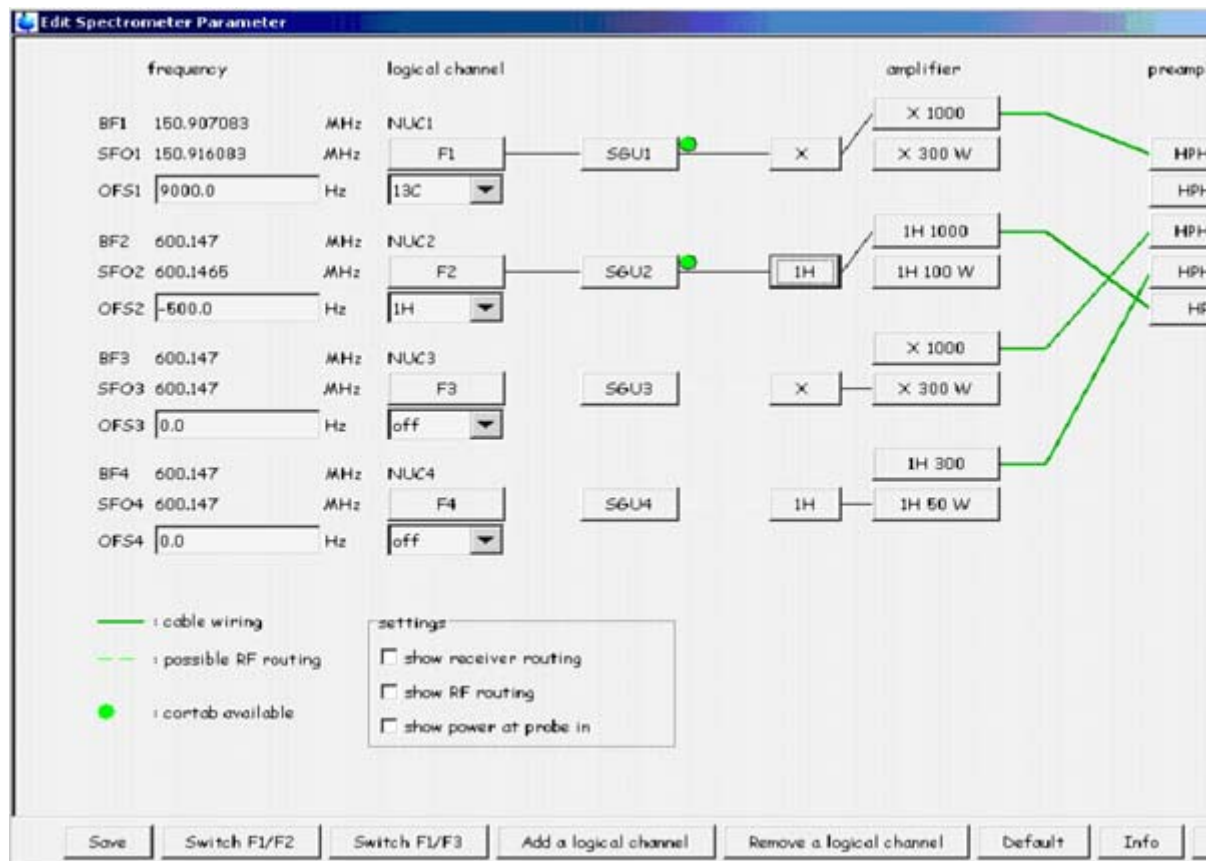


Figure 3.10. Routing for a Double Resonance Experiment using High Power Stage for H and X-nucleus

The figure above shows the routing for a double resonance experiment, e.g. a  $^{13}\text{C}$  experiment with  $^1\text{H}$  decoupling. For high power transmitters, the parameter **powmod** must be set to **high**. To check which power mode is selected, one may click the **default** button, change to **powmod high** in the command line if necessary. Note: the routing is only effective if the parameter **powmod = high**.

To change to proton observe, click **SwitchF1/F2**.

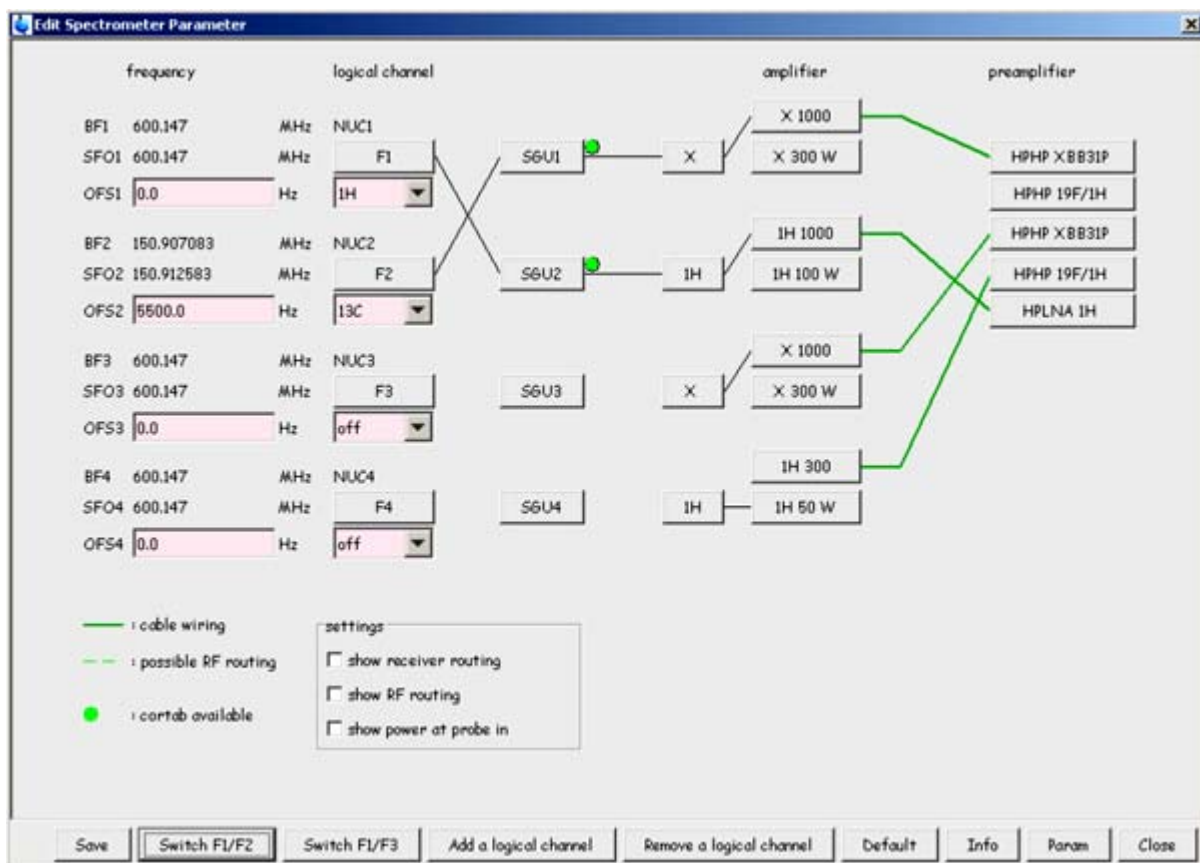


Figure 3.11. Routing for a Double Resonance Experiment, Changed for Proton Observation

In the figure above channel F2 need not be used.

The settings for F1 and F2 are interchanged. Change **rg** to 8-16 and **d1** to 4 sec. Set **pl1w** to 50W, or to 10 dB (high power proton transmitter), 7 dB (500W proton transmitter), 5dB (300W proton transmitter) or -4 (100W transmitter), if the green dot does not appear in the <sup>1</sup>H channel in **edasp**. Connect the probe proton channel to the proton preamp. A proton band pass filter must be inserted between preamp and probe. Tune the proton channel of the probe using the command **wobb high**. This means that the highest frequency is tuned first. Stop and type **wobb** again. Then adjust the tuning of the X channel to <sup>13</sup>C. Alternatively, you can switch to the lower frequency channel within **wobb high** by clicking on the frequency table symbol in the **wobb** display or by pressing the second touch button on the preamp cover module twice. Then acquire **ns =2** scans on the protons of adamantane.

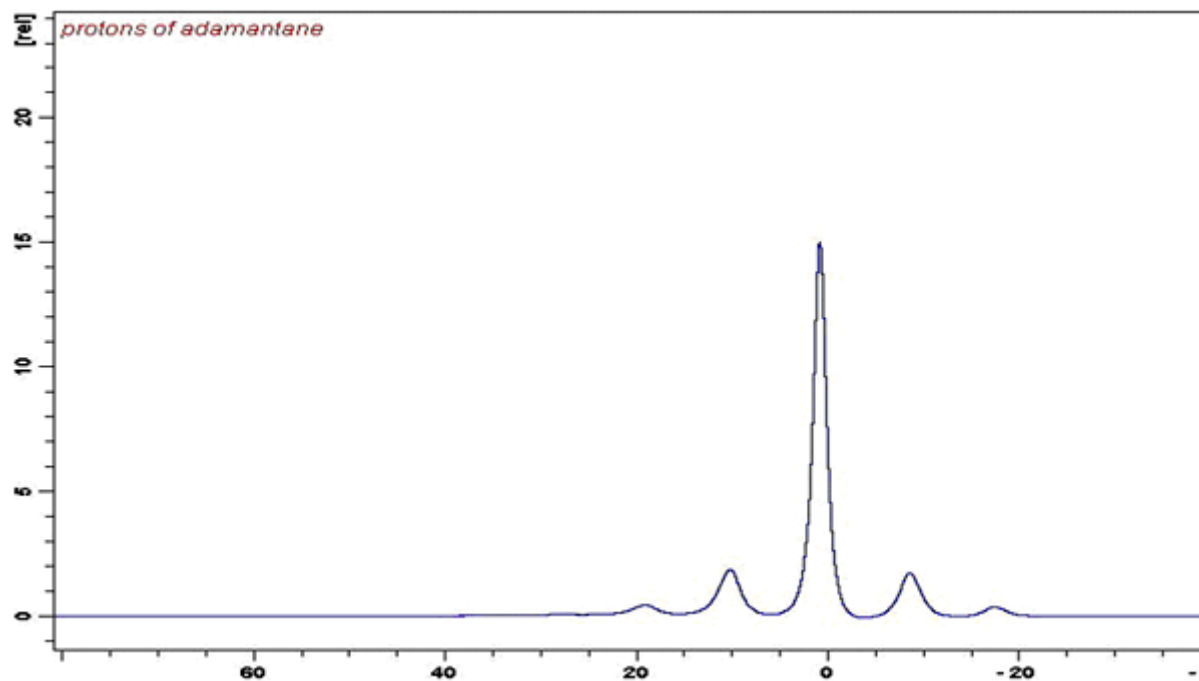


Figure 3.12. Proton Spectrum of Adamantane at Moderate Spin Speed

Set the carrier frequency O1 on top of the biggest peak using the encircled button in TopSpin.

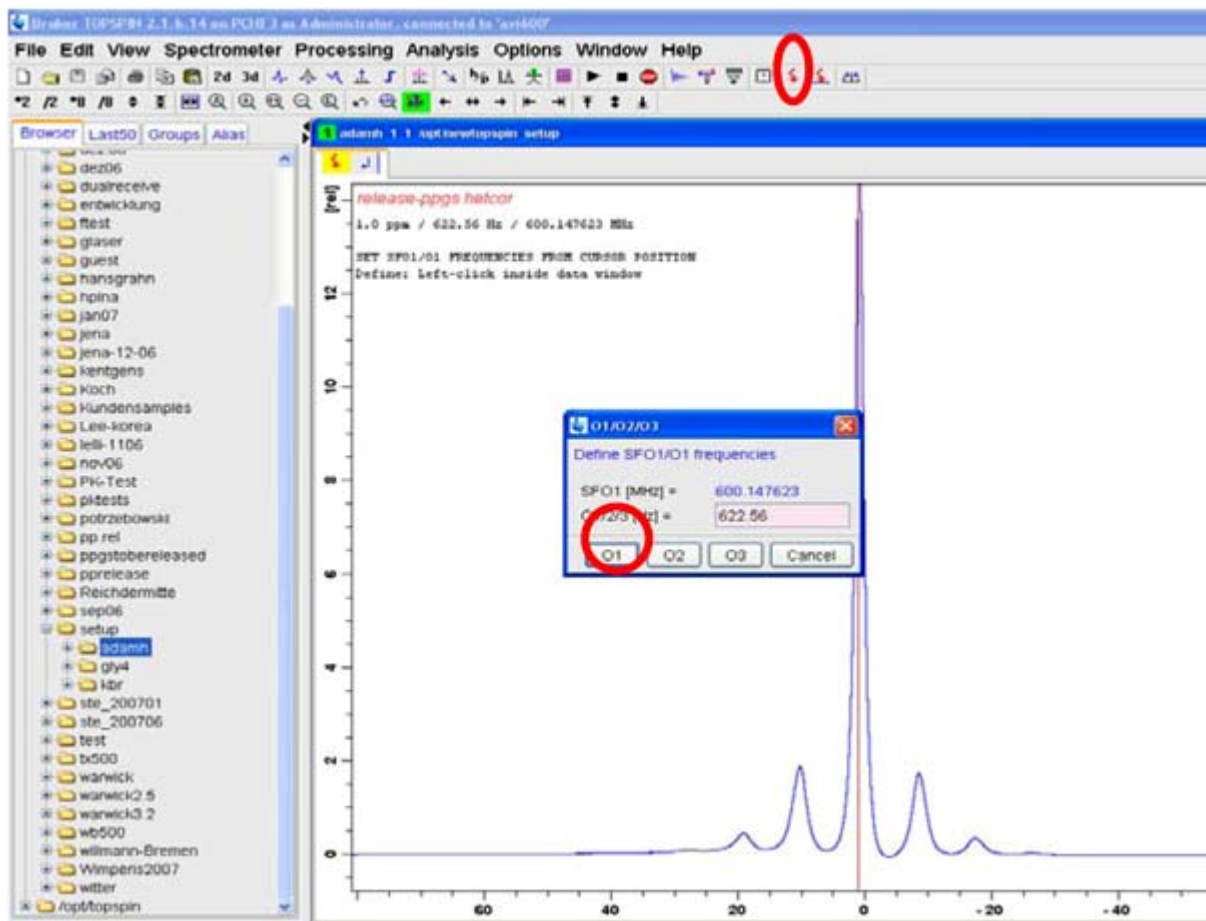


Figure 3.13. Setting the Carrier on Resonance

Click on the marked red arrow to set the observe frequency, set the position of the cursor line, and left click on the **O1** button. Acquire another spectrum, ft and phase.

Then expand the spectrum around the adamantane proton signal including the spinning sidebands by clicking on the left margin of the region of interest and pulling the mouse to the right margin of the region of interest as shown in the following figure:

## Basic Setup Procedures

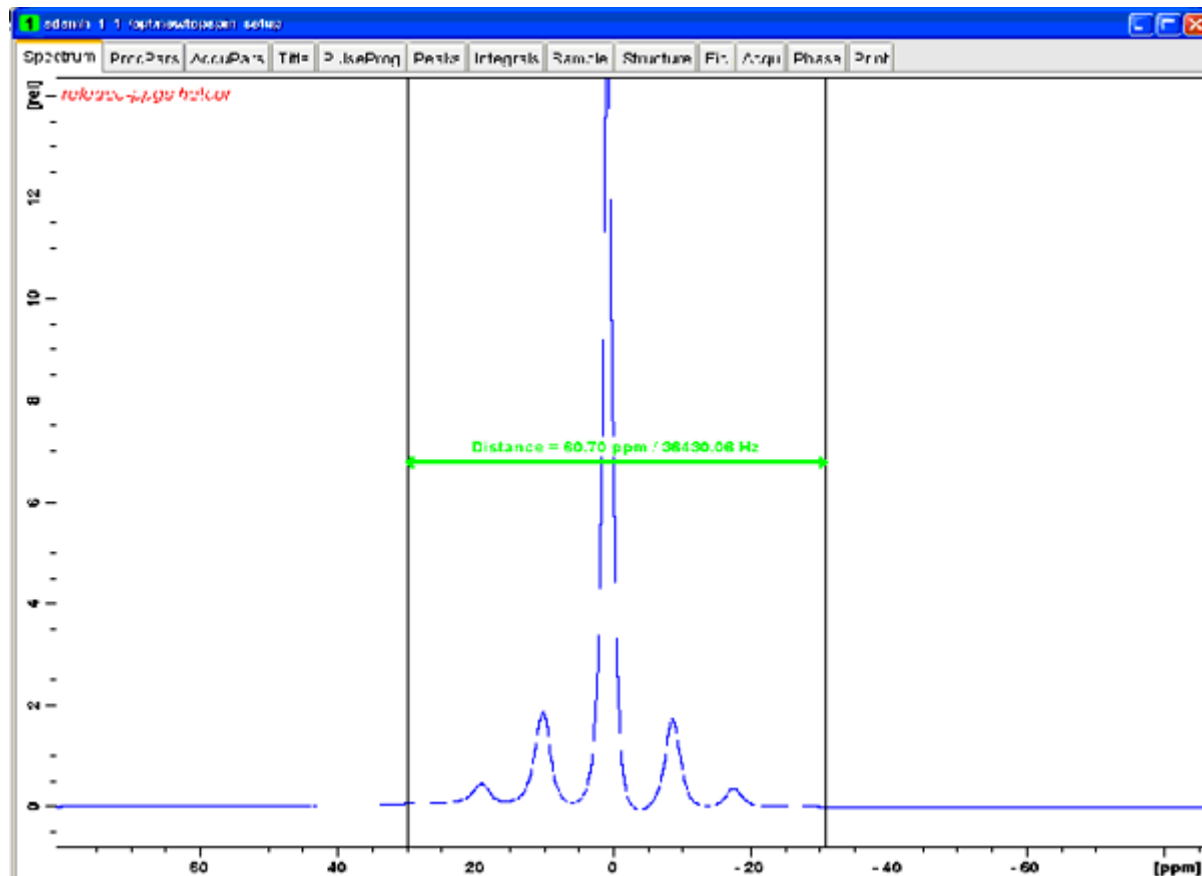


Figure 3.14. Expanding the Region of Interest

Click right mouse button in the **Spectrum** window. When the **Save Display Region to** menu pops up, select *Parameters F1/2* and OK or type **dpl** in the command line.

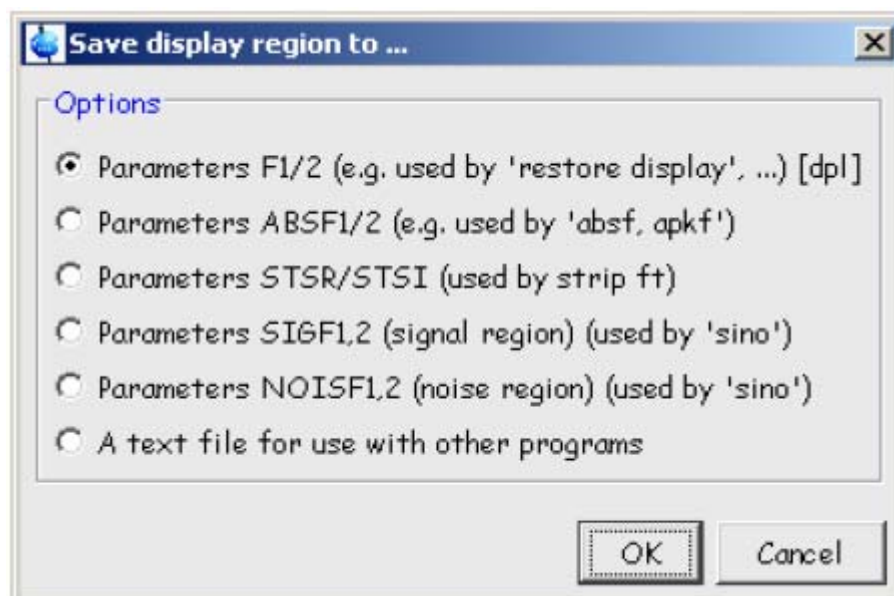


Figure 3.15. Save Display Region to Menu

Start parameter optimization by typing **popt** in the command line. The **popt** window will appear.

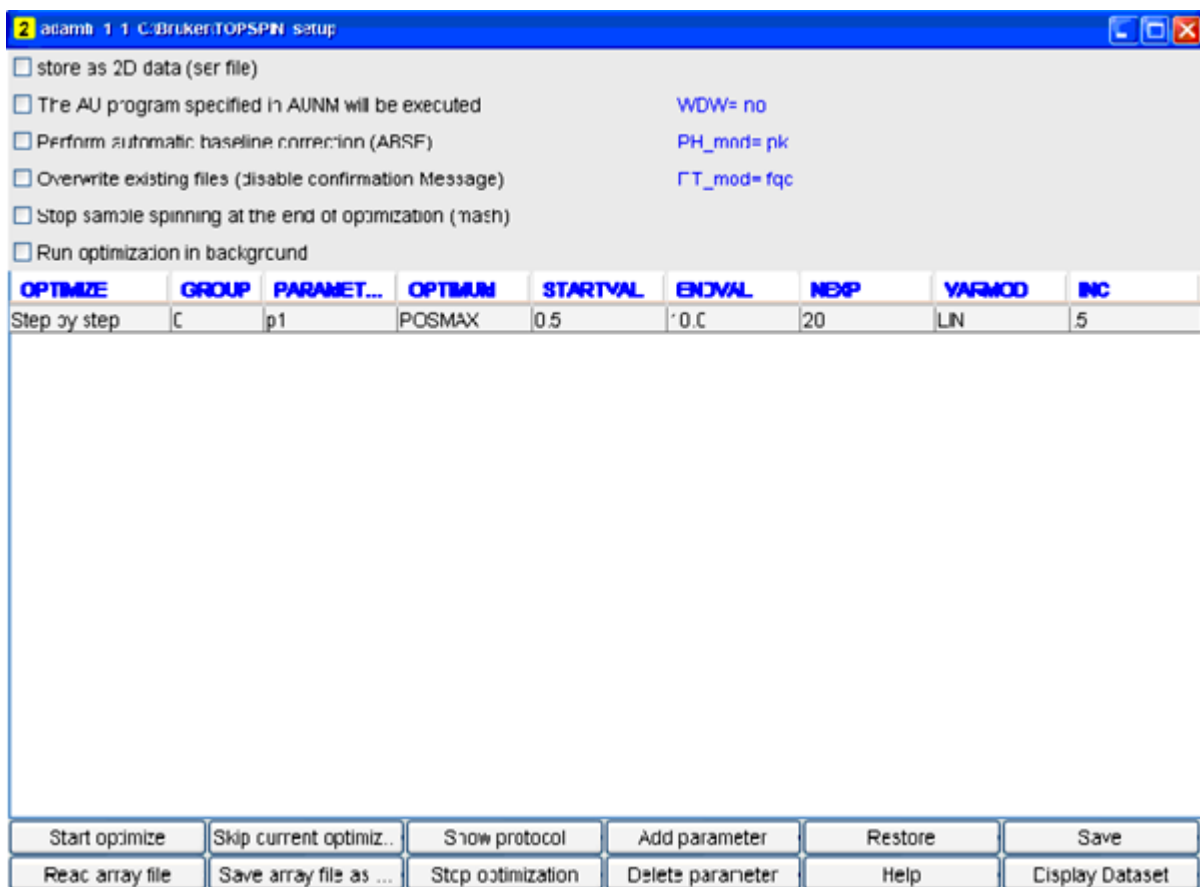


Figure 3.16. The **popt** Window

Use **optimize step by step**, **parameter p1** to optimize parameter **p1**, **optimum posmax** to find the highest signal intensity (90 degree pulse) for the given value of **p1w** or **p1l**, and **varmod lin** to use linear increments for optimization. The value for **group** is not used for optimizing only one parameter and the number of experiments **nexp** is set automatically when clicking on the save button. Then save table by clicking on the **save** button and click on **start optimize** to start optimization procedure.

The parameter value obtained by the program is written into the parameter set of the actual experiment at the end of the optimization.

In order to stop the execution of **popt** use the **skip** or **stop optimization** buttons. **Skip optimization** will evaluate the obtained data as if **popt** had finished regularly and writes the parameter into the parameter set. **Stop optimization** will stop without evaluation of the data. You can also type **kill** in the command line and click on the bar with "**poptau.exe**" to stop optimization. This will work like **stop optimization**.

**Popt** will generate a data set, where the selected expansion part of the spectrum is concatenated for all different parameter values (in this case, for **p1**). It will have a **procno** around 999. To achieve this, processing parameters are changed appropriately. Fourier transforming a normal FID in such a window will generate an incorrect spectrum window.

## Basic Setup Procedures

Therefore:

Never start an acquisition in such a window, first read in the **procno** where popt was started using the **rep n** command where n is the source **procno**.

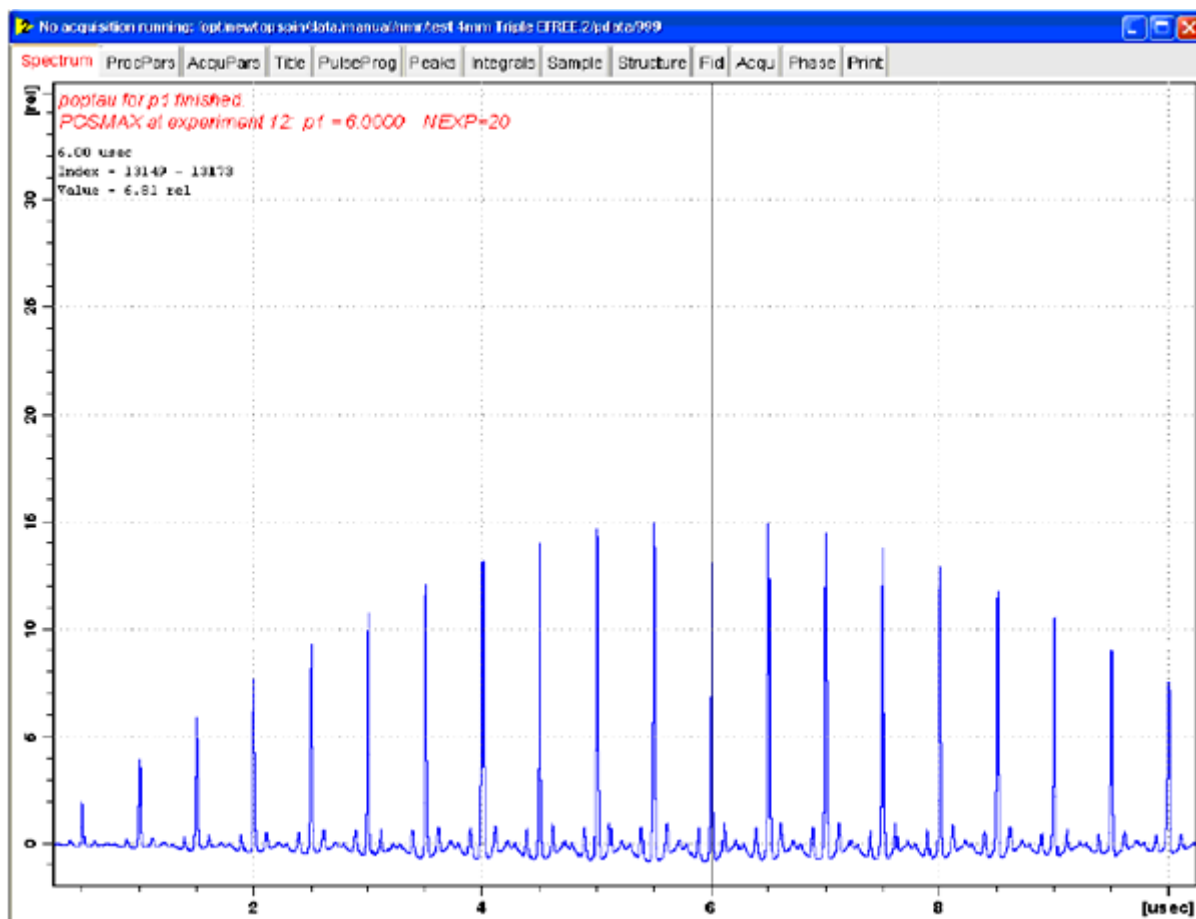


Figure 3.17. The **popt** Display after Proton p1 Optimization

The figure above shows the **popt** display after proton p1 optimization, the biggest signal is obtained at 6  $\mu$ sec in this case.

Once you have obtained a 90-degree pulse for a given power setting, you can calculate power levels for different rf fields using the AU program **calcpowlev**. Type **xau calcpowlev** into the command line and follow the instructions in the popup window.

Calculate the power level (in Watts or dB) required to achieve a 4.5  $\mu$ sec proton 90 degree pulse. In this case, 6  $\mu$ sec were obtained. The command **calcpowlev** calculates a power level 2.5 dB higher than used above to achieve 4.5  $\mu$ sec pulse length. Check whether  $2 \times 4.5 \mu\text{sec}$  for **p1** will give a close to zero signal. This is a safe power level for all probes for pulses up to 100 msec. length.

Calibrating  $^{13}\text{C}$  Pulses on Adamantane and Shimming the Probe

3.4

A high power decoupling experiment on  $^{13}\text{C}$  of adamantane is used to measure  $^{13}\text{C}$  pulse parameters.

**NOTE:** For experiments where long decoupling pulses on protons are executed, the proton preamplifier must be bypassed, i.e. the transmitter should be wired to the probe directly (via the proton bandpass filter) without going through the preamp if a high power proton preamplifier is not available. For HP-HPPR modules  $^1\text{H}/^{19}\text{F}$  this is not absolutely necessary, but recommended. For HPLNA  $^1\text{H}$  modules it is not required to bypass. Note that when bypassing the preamp which attenuates by about 1 dB, the proton power levels should be corrected by adding 1 dB to the pl-values.

Type **edasp** in the command line. You should get a display like in [Figure 3.11](#). Click on **SwitchF1/F2** to set for  $^{13}\text{C}$  observation with proton decoupling. Load the pulse program **hpdec**. Set **cpdprg2=cw**. Set **pl12** to the power level that yields a 4.5  $\mu\text{sec}$  proton pulse. Set **pl1** such that in **ased** the power displayed is 200W for  $^{13}\text{C}$  (7mm probe), 150W (4mm probe) or 80W (2.5 mm probe). If the green dot is not visible in **edasp** for the  $^{13}\text{C}$  channel, set **pl1** to 12 dB (1 kW transmitter), 9 dB (500W transmitter) or 7 dB (300W transmitter) for any probe. Make sure the proton channel is tuned (**wobb high**) and the carbon channel is also tuned (**wobb**). With **d1 = 4s**, **rg = 256** **swh = 100000**, **td = 4k**, **o2** set to be on resonance on the adamantane protons as found above, accumulate 4 scans. Set the carrier frequency between both adamantane  $^{13}\text{C}$  peaks. Reduce the spectral width **swh** to 50 kHz, set **aq = 50 msec**.

Acquire 2-4 scans and define the plot limits (as shown in [Figure 3.14](#)) for the larger of the two peaks. Define the plot limits and determine the 90 degree carbon pulse **p1**, using **popt**. Recalculate **pl1** for a 4.5  $\mu\text{sec}$  carbon pulse using **calcpowlev**.

Pulse continuously using **gs** and shim the z gradient for highest FID integral.

The gradient settings can be conveniently changed in the **setsh** display. [Figure 3.18](#) and [Figure 3.19](#) show the adamantane  $^{13}\text{C}$  FID without shims, with z-shim adjusted and the corresponding **setsh** displays.

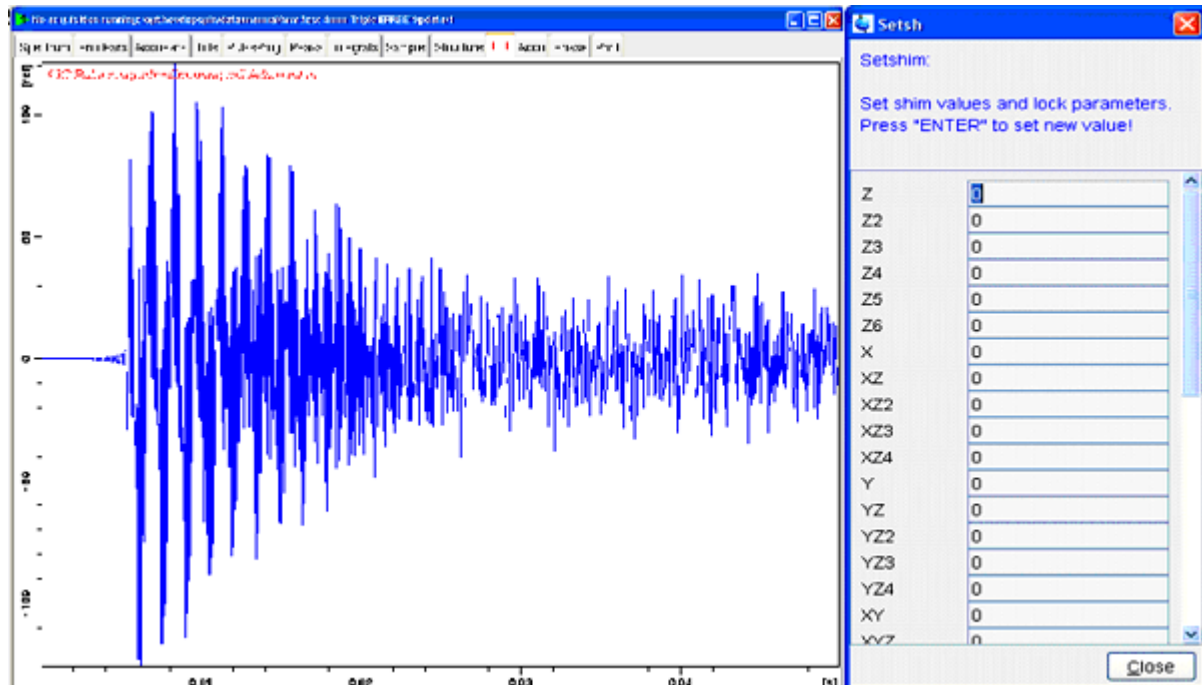


Figure 3.18. Adamantane  $^{13}\text{C}$  FID with 50 msec **aq**. **setsh** Display

## Basic Setup Procedures

The figure above is an Adamantane  $^{13}\text{C}$  FID with 50 msec **aq**, with **setsh** display showing no shim values. N.b.: spinning removes part of the  $B_0$  in homogeneities. Probes which do not use susceptibility compensated coil wire can show much shorter  $T_2^*$  and require much more shimming effort (only with older probes up to 400 MHz proton frequency).

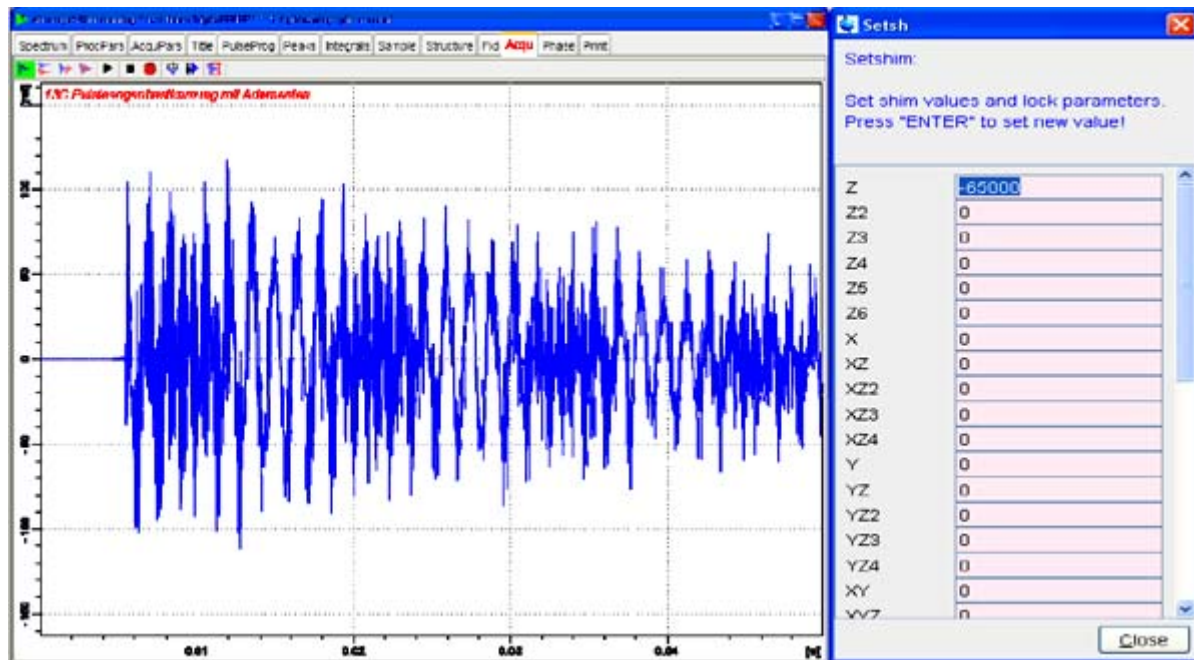


Figure 3.19. Adamantane  $^{13}\text{C}$  FID with 50 msec **aq**. **setsh** with Optimized Z-Shim Value

For optimum shims (rarely required) set the shims x, y,  $z^2$ ,  $xy$  and  $x^2-y^2$ , as well as  $xz$  and  $yz$ . You may need to increase the acquisition time **aq** to see the effect of increasing resolution. Save the shims using the command **wsh** followed by a suitable name.

Note: For long acquisition times (**aq** > 0.05 s) the decoupling power level **p12** must be set to +3 dB and d1 must be increased to 6s. To allow longer acquisition times than 50 msec, the **ZGoption -Dlacq** must be set in **ased**, if the pulse program contains the include file **aq\_prot.incl**. Make sure the **-Dlacq** option is not left set for the following steps.

## Calibrating Chemical Shifts on Adamantane

## 3.5

In TOPSPIN (as well as in the XWIN-NMR 3.5 release) the frequency list for NMR nuclei follows the IUPAC recommendations (see: R.K. Harris, E.D. Becker, S.M. Cabral de Menezes, R. Goodfellow and P. Granger, *NMR Nomenclature. Nuclear Spin Properties and conventions for Chemical Shifts*, Pure Appl. Chem. Vol. 73, 1795-1818 (2001) for reference).

Set the  $^{13}\text{C}$  low field signal of adamantane to 38.48 ppm. This will set the parameter **SR** which is used to calculate the chemical shift axis and the peak positions in the spectrum.

**Note:** All data sets generated from this data set will have the peak positions correctly calibrated, if the magnetic field  $B_0$  is not changed. However, you must make sure that the magnetic field is always the same. It may change, if the magnet has a slight drift, or if different shim settings are loaded. Therefore the same shim file should be loaded and the field be set to the same value using the **BSMSD/SP** command. If the magnet drift is noticeable, the calibration should be redone in suitable intervals and the **field** value recorded in the lab notebook.

One can also use a spinner filled with H<sub>2</sub>O to set the field position more precisely. Do not spin the sample and make sure the cap is well fitted. Set **o1p** to 4.85 ppm, set for proton observe (as described above for adamantane), and use **gs** for continuous pulsing and FID display. Change the field value in **bsmsdisp** until the FID is exactly on resonance. Then all spectra taken should be correctly referenced with **sr = 0**.

For all these experiments the field sweep must be off! When the BSMS unit is turned off and on again, the sweep will always be on. Running spectra with the sweep on will superimpose spectra at different fields! One can set the sweep amplitude to 0 in order to avoid such an accidental error condition.

## Setting Up for Cross Polarization on Adamantane

## 3.6

Cross polarization is used to enhance the signals of X-nuclei like <sup>13</sup>C. The strong proton polarization is transferred (cross polarized) to the X-nuclei coupled to the protons via strong dipolar couplings. To achieve this, the protons and the X-nuclei must nutate at the same frequency. This frequency is the RF field applied to both nuclei at the same time (contact time). If this condition (Hartmann-Hahn-condition) is met, the transfer of proton magnetization to carbon is optimum. Since the proton signal of adamantane is resolved into spinning sidebands even at slow spin rates, this Hartmann-Hahn condition can be set to match for every proton spinning sideband. Using a ramp for the proton contact pulse, the Hartmann-Hahn match is swept over these possible match conditions and becomes insensitive to miss-sets and different spin rates.

Start from the data set used for observing <sup>13</sup>C under proton decoupling (1.4). Load the pulse program cp (in **eda** or typing **pulprog cp**). The pulse sequence is depicted in the following figure:

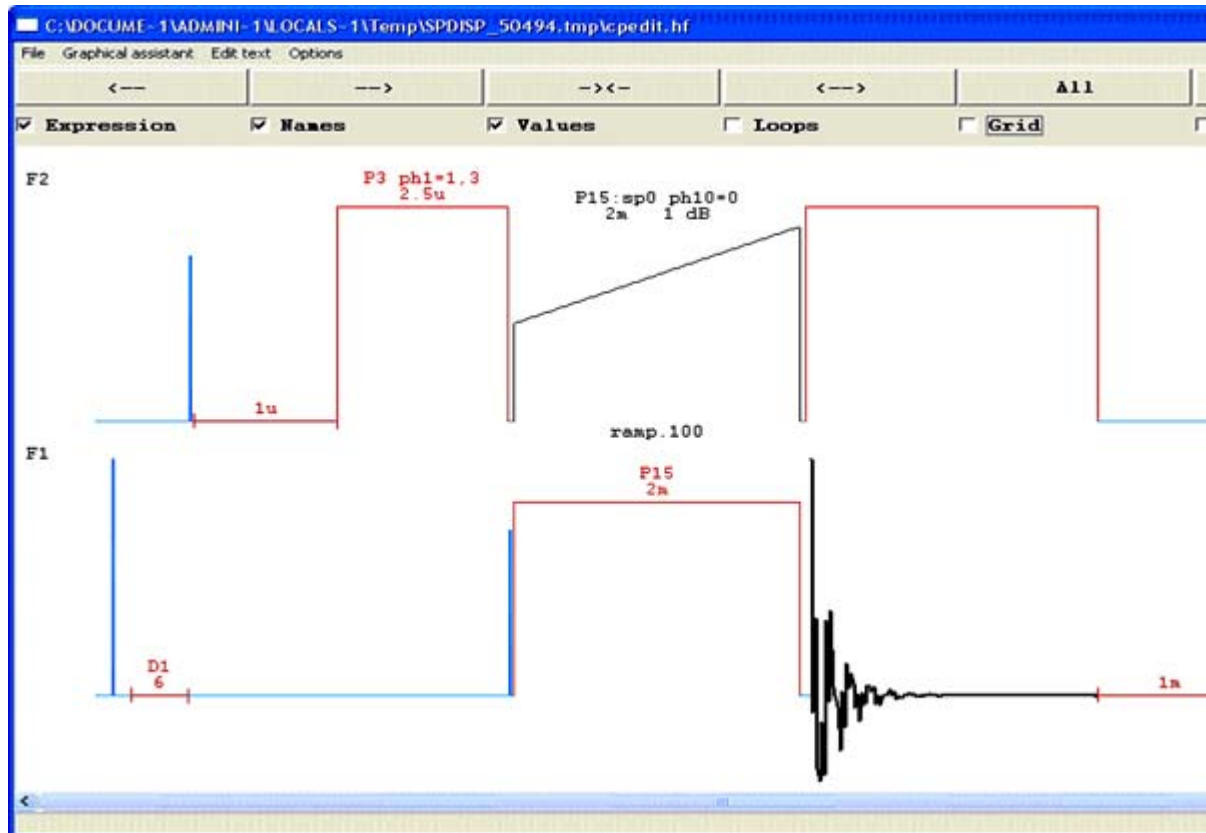


Figure 3.20. A cp Pulse Sequence

## Basic Setup Procedures

The following parameters are set:

- **p12**, for the initial 90 degree pulse and the decoupling during acquisition: set for a 4.5  $\mu$ sec proton 90 degree pulse (as previously determined)
- **p1**, for the carbon contact pulse, set for a 4.5  $\mu$ sec carbon pulse (as previously determined)
- **p3**, 4.5  $\mu$ sec
- **spnam0**, set to ramp.100 to sweep the proton contact RF field from 50 to 100%
- **sp0**, set to **p12** -3 dB, to account for the lower average RF over the ramp.
- **p15**, 2-5 msec (after the value, specify m to make it milliseconds, else it is taken as microseconds)
- **cpdprg2**, select cw
- **o1**, set between both adamantane peaks
- **o2**, set to be on resonance on adamantane protons

Acquire 2 or 4 scans, then set plot limits for both peaks, and optimise p3 ( $\pm$  2  $\mu$ sec) and p1 ( $\pm$  2 dB) for best signal. **Fig. 21** shows a Hartmann-Hahn match optimization over 4 dB using a ramp contact pulse going from 50 to 100% amplitude.

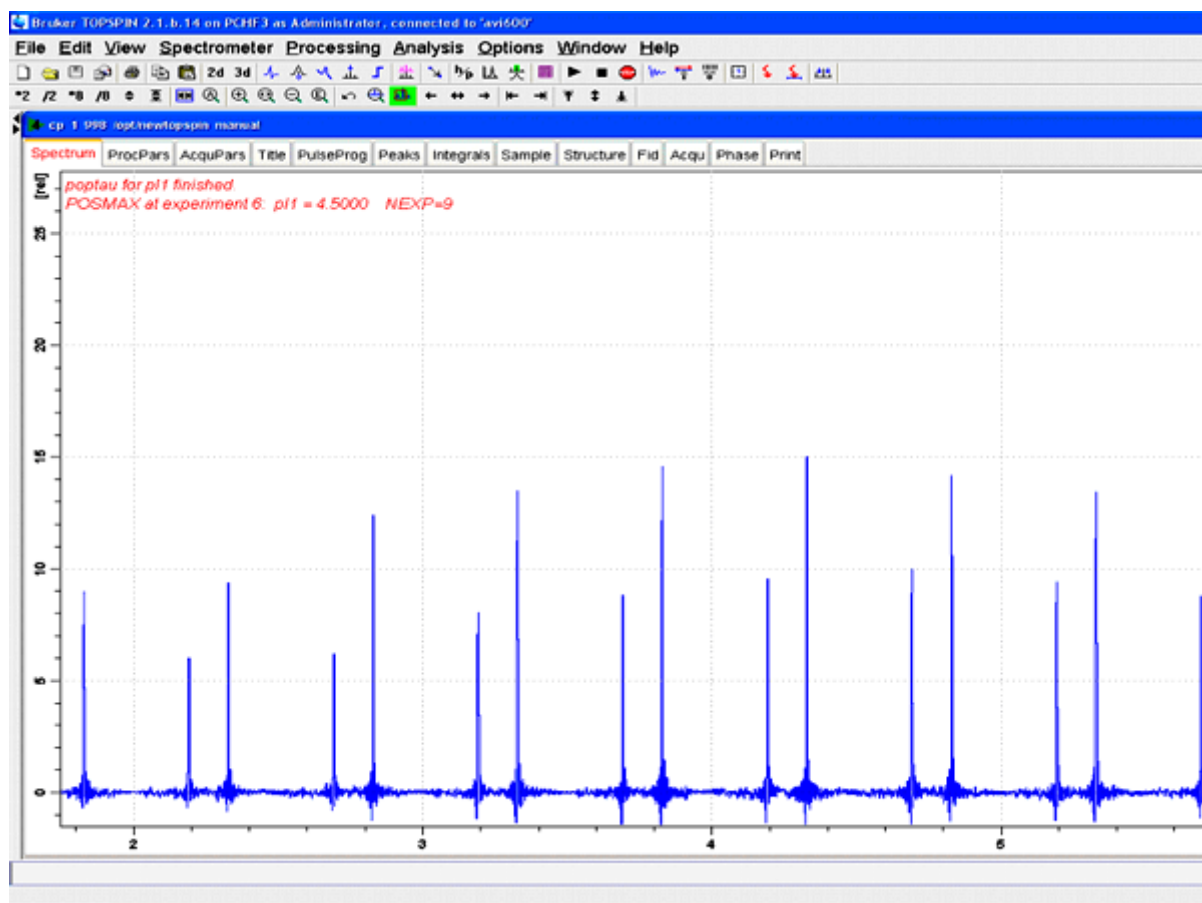
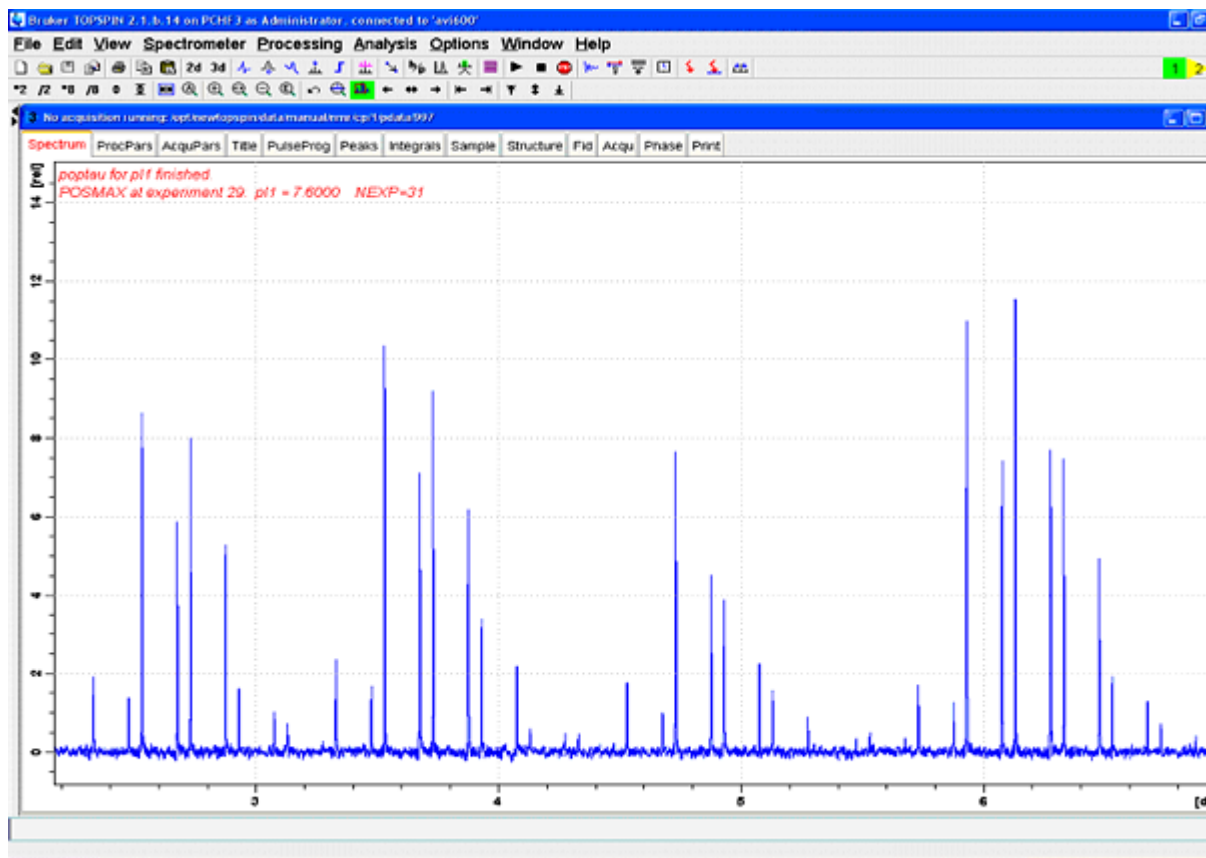


Figure 3.21. Hartmann-Hahn Optimization Profile

The wiggles besides the signals stem from truncation of the FID after 50 msec acquisition time.

To exemplify the existence of several HH-conditions on a spinning adamantane samples, another HH profile (**Figure 3.22.**) is shown where a square proton contact pulse is used. There are several maxima corresponding to matches on the sideband orders  $n+2$ ,  $n+2$ ,  $n+1$ ,  $n+0$ , and  $n-1$ . The largest intensity is seen for  $n+/-1$ , the intensities are very sensitive to the RF-level which is varied in 0.2 dB steps. Using a ramp makes the experiment much more stable and more quantitative. Problems may arise if the proton  $T_{1p}$  is short, since usually longer contact times must be employed. It makes therefore sense to use a flatter ramp (70-100%) and optimize for the spin rate which is used.



*Figure 3.22. Hartmann-Hahn Optimization Profile Using a Square Proton Contact Pulse*

The sideband order 0 at 4.8 dB gives a rather small intensity. A ramp sweeping over 3.5-6.5 dB would cover both most efficient HH conditions. Note that increasing the spin rate would shift all maxima except the one at 4.8 dB further out.

### Cross Polarization Setup and Optimization for a Real Solid: Glycine

3.7

Adamantane is highly mobile even in the solid state. Therefore it behaves differently from a "hard" solid like glycine. For instance, it is not sensitive to decoupling mis-adjustments, and also not sensitive to miss-sets of the magic angle. It is however extremely sensitive to HH mis-adjustment. Glycine is therefore used for fine tuning of the decoupling parameters and signal-to-noise assessment. Start with the parameters found for adamantane, using a 50-100% ramp (ramp.100) and  $p15=2$  msec for contact,  $aq = 20$  msec. Change the sample from adamantane to glycine.

## Basic Setup Procedures

Since glycine may exist in two different crystal modifications with very different CP-parameters, and since packing of the spinner determines crucially the achievable S/N value, it is useful to prepare a reference spinner with pure  $\alpha$ -glycine, finely powdered and densely packed.  $\alpha$ -glycine is prepared by dissolution of glycine in distilled water and precipitation with acetone, quick filtering and careful drying in a desiccator. Drying is important because wet glycine may readily transform, especially when kept warm, into  $\gamma$ -glycine.  $\alpha$ -glycine has two carbons with shifts of 176.03 and 43.5 ppm.  $\gamma$ -glycine shows resonances somewhat shifted to higher field, sharper lines, longer proton  $T_1$  and shorter proton  $T_{1p}$  which results in longer experiment time and less signal to noise.

Spin the glycine sample at 5 kHz (7mm spinner), or 10 kHz (smaller spinners 4, 3.2 or 2.5), tune and match the probe.

The glycine cp/mas 13C-spectrum taken under the same conditions as adamantane previously will look like in [Figure 3.23](#), far from optimum:

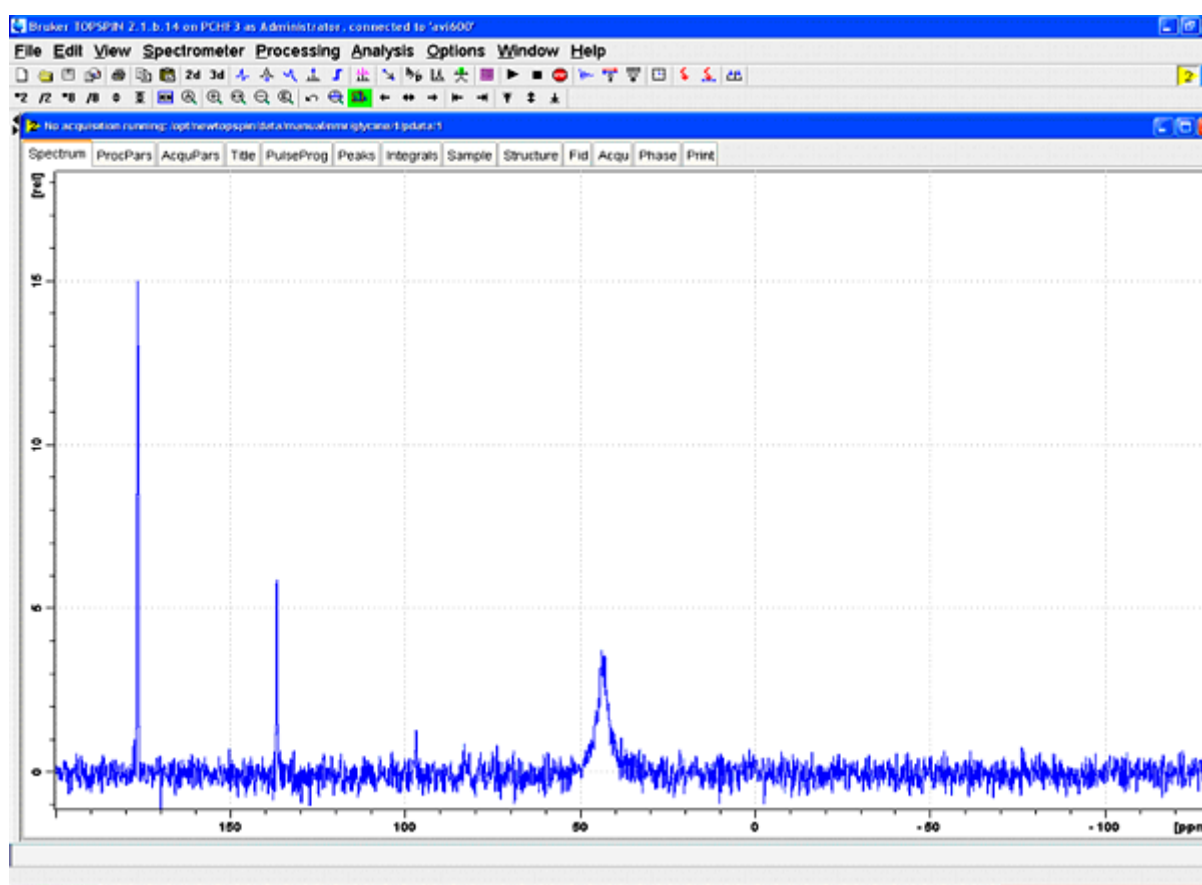
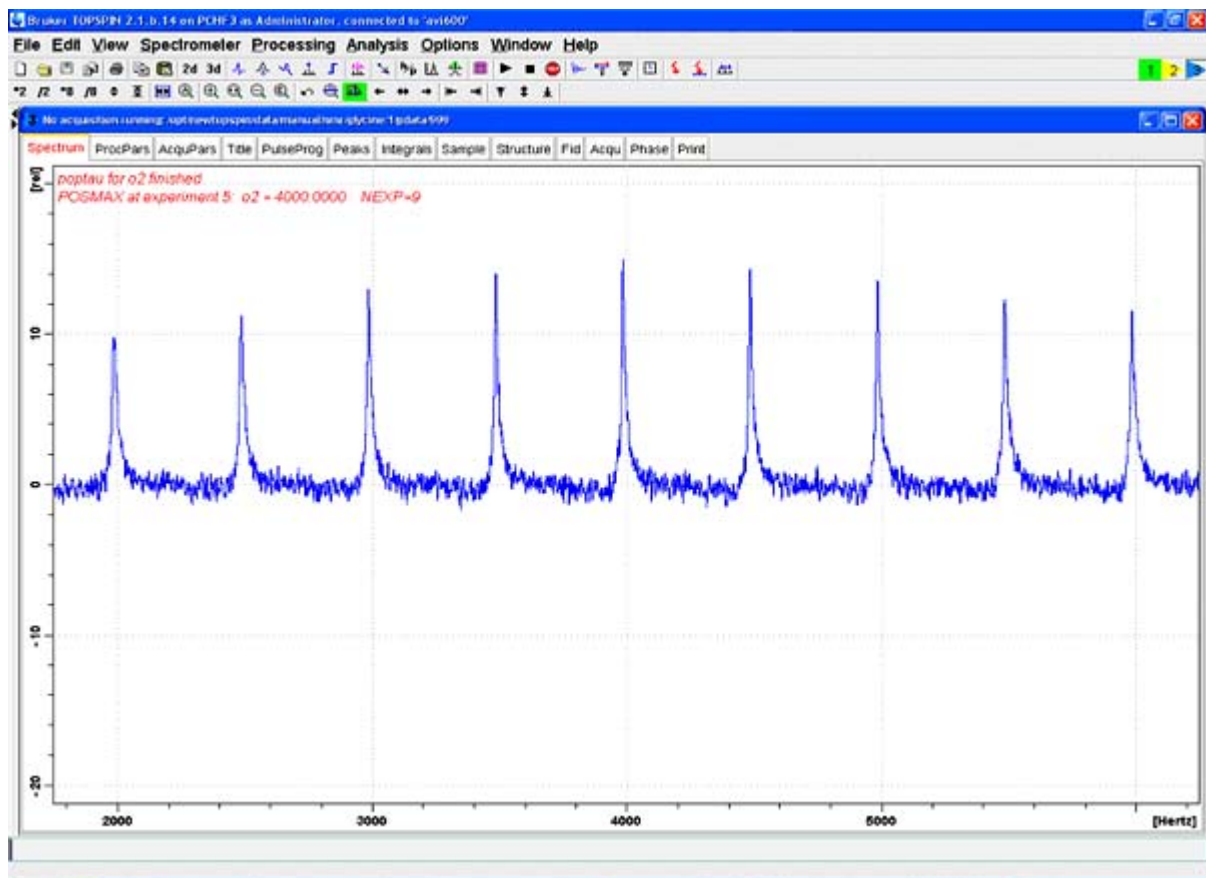


Figure 3.23. Display Showing  $\alpha$ -Glycine Taken Under Adamantane Conditions, 4 scans

The figure above shows  $\alpha$ -glycine taken under adamantane conditions, 4 scans: Incorrect carrier setting,  $\alpha$ -carbon at 43 ppm insufficiently decoupled. Angle is set correctly, because carboxyl peak at 176.03 ppm shows a narrow lorentzian line shape. HH condition looks okay.

Now reset the carrier as shown in [Figure 3.13](#).  $\text{o1p}$  should be around 100 ppm, in the middle of most carbon spectra. Acquire a spectrum, set the plot limits ([Figure 3.14](#), [Figure 3.15](#)) for the peak at 43 ppm, and start  $popt$ , optimizing  $\text{o2}$  for maximum signal (+/- 2000 Hz around the current position) in steps of 500 Hz. The following result will be obtained:



*Figure 3.24. Optimization of the Decoupler Offset **o2** at Moderate Power, Using cw Decoupling*

Since the proton spectrum of glycine extends around 5 ppm, the optimum decoupler offset will be obtained at higher frequency than the adamantane proton peak (around 1.2 ppm). Decoupling is still inefficient, since cw decoupling is used which does not cover the whole proton shift range. Also decoupling power is too low with a proton pulse of 4.5  $\mu$ sec. Glycine requires about 90 kHz of decoupling RF, corresponding to a 2.7  $\mu$ sec proton 90 degree pulse. This can be obtained with probes of 4mm spinner diameter and smaller (2.5, 3.2 mm). For a 7 mm probe, 3.5 (4 $\mu$ sec) can be expected at proton frequencies below 500 (at 500) MHz. Use **calcpowlev** to calculate the required power level **p12** and set **p3** to twice the expected proton pulse width. Check with 4 scans whether a close to zero signal is obtained. Compared to 4.5  $\mu$ sec, a 2.7  $\mu$ sec pulse requires about 4.5 dB more power (corresponding to almost 4 times more power!!!).

With **p3** properly set, a spectrum like in **Figure 3.25.** should be obtained, with about 93 kHz decoupling RF field.

## Basic Setup Procedures

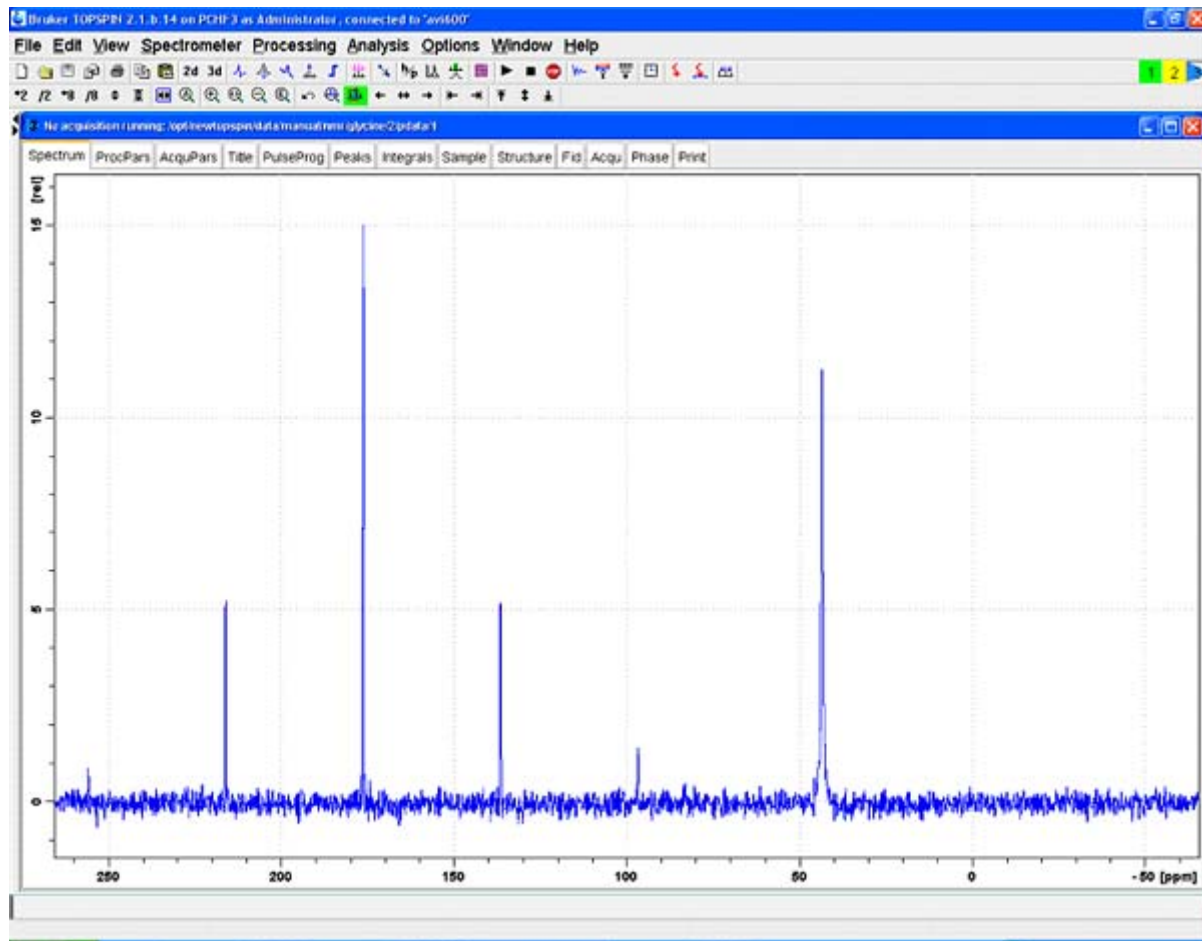


Figure 3.25. Glycine with cw Decoupling at 90 kHz RF Field

In the spectrum above, a lorentzian deconvolution (**Analysis** menu) shows a line width of 71 Hz for the peak at 43 ppm. The line width achievable under optimum decoupling conditions varies with the magnetic field. At fields below 9.4 Tesla (400 MHz) this line is substantially broadened by second order quadrupolar interaction to  $^{14}\text{N}$ . At fields above 9.4 Tesla (500 MHz and higher), the residual line width is mostly determined by chemical shift dispersion and insufficient decoupling. Here less than 60 Hz (at 600 MHz) are expected. More efficient decoupling schemes must be applied especially at higher magnetic fields. A more efficient decoupling scheme is spinal64. Select **cpdprg2** = spinal64, set **pcpd2** to proton 180 degree pulse – 0.2  $\mu\text{sec}$  for a start. A glycine spectrum as shown in [Figure 3.26](#), is obtained.

Table 3.1. Summary of Acquisition Parameters for Glycine S/N Test

Parameter	Value	Comments
PULPROG	cp	cp.av for AV1 and 2
NUC1	13C	Nucleus on f1 channel
O1P	100 ppm	$^{13}\text{C}$ offset
NUC2	1H	Nucleus on f2 channel.
D1	4 s	Recycle delay.
NS	4	Number of scans.
SWP	300 ppm	Spectral width for Glycine.
TD	2048	Number of acquired complex points.
CPDPRG2	SPINAL64	Decoupling scheme f2 channel ( $^1\text{H}$ ).
SPNAM0	ramp.100 or ramp 70100.100	For ramped CP.
P15	2 ms	Contact pulse (f1 and f2 channel).
PL1		Set for 4-4.5 $\mu\text{sec}$ P90.
SP0 (or pl2 AV1+2)		Set for 4-4.5 $\mu\text{sec}$ P90 – 2 dB (optimize).
PL12		High power level f2 channel ( $^1\text{H}$ ) excitation and decoupling.
P3		90° $^1\text{H}$ pulse at PL12 (f2 channel).
PCPD2 or P31 (AV1+2)		SPINAL64 decoupling pulse.
O2P	2.5 - 3 ppm	$^1\text{H}$ offset - optimize in 400 - 500 Hz steps for maximum signal of aliphatic peak.

Note that the spectral window (**swp**) is set in ppm which makes the acquisition time dependant on the  $B_0$ -field at a given **td** of 2k. This is intended and accounts for the linewidths dependence on the  $B_0$ -field. The glycine lines show a broadening proportional to  $B_0$  due to chemical shift dispersion. To make S/N values more comparable, this accounts for shorter  $T_2$  at higher field.

## Basic Setup Procedures

Table 3.2. Processing Parameters for the Glycine S/N-Test

Parameter	Value	Comment
SI	2-4 k	Twofold or fourfold zero filling.
WDW	No	No apodization used for S/N measurement in this case.
PH_mod	Pk	Phase correction if needed.
BC_mod	Quad	DC offset correction on FID.
FT_mod	Fqc	

Note: No line broadening is applied since the acquisition time is set appropriately.

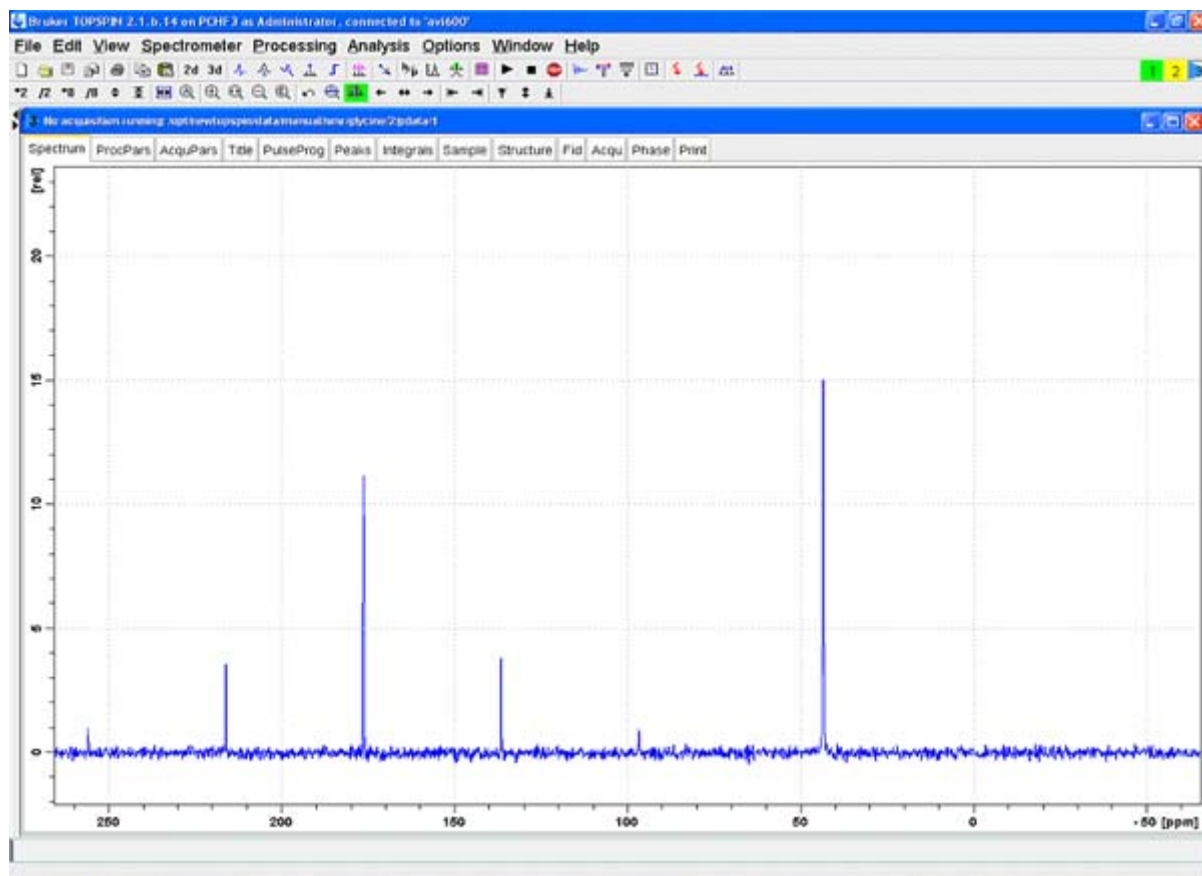


Figure 3.26. Glycine Spectrum with Spinal64 Decoupling at 93 kHz RF field

Here, the line width of the line at 43 ppm is fitted to be about 50 Hz: Correspondingly, the intensity is much higher. The **sinocal** routine calculates 80:1 S/N, using 250 to -50 ppm spectrum range, 50 to 40 signal range and 10 ppm noise range. On this triple probe, more than 100:1 is expected. What else needs to be optimized? Two more parameters are essential:

1. The power level at HH contact
2. The decoupling pulse **pcpd2**.

The spectrum of **Figure 3.26**, was taken at contact power levels as set for adamantane. Furthermore, a 50% ramp was used, which has a rather low average RF level corresponding to about 5.7  $\mu$ sec in this case (25% less than 4.5  $\mu$ sec). This does not spin lock the protons well enough. So the power level of the contact needs to be increased. Set ***spnam0*** = **ramp70100.100**. Set ***sp0*** and ***pl1*** to about 2 dB less attenuation and check S/N again. Re-optimize the HH condition observing the peak at 176 ppm (which is less strongly coupled to protons and therefore exhibits a sharper HH matching condition) in steps of 0.3 dB. In this case, S/N improves to 100:1. Then optimize the decoupling pulse **pcpd2** in steps of 0.2  $\mu$ sec, observing the peak at 43 ppm (which is more sensitive to decoupling mis-sets). Here, this led to another 10% improvement in S/N.

**Good Laboratory Practice** requires that evaluation measurements be taken in suitable periods. Store the optimized glycine spectrum together with the following important information:

1. Value of field setting.
2. Name of the shim file.
3. Name of the operator.
4. Probe setup (triple mode or double mode, high range or low range setting, WB probes only, name or part number of the probe).
5. Description of the sample (which reference rotor, weight of glycine and spinner).
6. Any additional comments, for instance the reading of the micrometer setting for the X tuning adjustment (not available on all probes).

Write this information into the title file so it is stored with the data set as well as all other acquisition and processing parameters. Recalling this data set and acquiring a new data set should give the same spectrum within +/- 10% of S/N.

### Some Practical Hints for CPMAS Spectroscopy

### 3.8

Some general recommendations for reasonable RF-fields used in WB probes:

Table 3.3. Reasonable RF-fields for Max. 2% Duty Cycle

Probe	Nucleus	Decoupling power over 50 ms, 200ms, 500ms. Contact pulse up to 10 ms
2.5mm CPMAS double resonance 35 kHz max sample rotation	<sup>1</sup> H	115 kHz (2.2 $\mu$ s 90° pulse), 75 kHz, 40 kHz 71 kHz (3.5 $\mu$ s) contact
2.5mm CPMAS double resonance 35 kHz max sample rotation	<sup>13</sup> C	83 kHz (3 $\mu$ s 90° pulse) 71 kHz (3.5 $\mu$ s)
3.2mm CPMAS double resonance 24 kHz max sample rotation	<sup>1</sup> H	110 kHz (2.3 $\mu$ s), 60 kHz, 35 kHz 68 kHz (3.7 $\mu$ s)
3.2mm CPMAS double resonance 24 kHz max sample rotation	<sup>13</sup> C	78 kHz (3.2 $\mu$ s) 68 kHz (3.7 $\mu$ s)
4 mm CPMAS double resonance probe (15 kHz max. sample rotation)	<sup>1</sup> H	92.5 kHz (2.7 $\mu$ s 90°), 50 kHz, 30 kHz 62 kHz (4 $\mu$ s)
4 mm CPMAS double resonance probe (15 kHz max. sample rotation)	<sup>13</sup> C	71 kHz (3.5 $\mu$ s) 62 kHz (4 $\mu$ s)

## Basic Setup Procedures

Table 3.3. Reasonable RF-fields for Max. 2% Duty Cycle

4 mm CPMAS triple resonance probe (15 kHz max. sample rotation)	<sup>13</sup> C	66 kHz (3.8 µs) 50 kHz (5 µs)
7mm CPMAS double resonance probe (7 kHz sample rotation)	<sup>1</sup> H	70 kHz (3.6 µs 90° pulse), 35 kHz, 20 kHz 50 kHz (5 µs)
7mm CPMAS double resonance probe (7 kHz sample rotation)	<sup>13</sup> C	55 kHz (4.5 µs) 50 kHz (5 µs)

**Note:** Higher RF power levels should only be applied if necessary and within specifications. For special probes, max. allowed RF fields may be lower. Check with your Bruker BioSpin applications support if in doubt.

In order to have quantitative information about the precision of your magic angle, one may measure the line width of the KBr central peak and compare it with the line width of the 5<sup>th</sup> spinning sideband. If the linewidths compare within ±8% then the MA-setting is acceptable. The line-width comparison is conveniently achieved with the command **peakw**, expanding the display first around the center line, typing **peakw** and then repeating this with the 5<sup>th</sup> sideband to either side.

Most cp/mas probes are tunable over a large range of X-frequencies. It can sometimes be fairly difficult to retune a probe to an arbitrary frequency within the tuning range. NEVER just load a nucleus and blindly tune and match the probe, using a small wobble width (**wbsw**) of 10 MHz or less. Instead, either note the current tuning position of the probe into the lab notebook and start retuning to the new nucleus frequency from this frequency on, following the probe response over the whole frequency range using a large **wbsw** of 50 MHz. Alternately, check the micrometer setting of the X-tuning adjustment and conclude from that to which nucleus the probe is tuned. Make a list of micrometer settings for the most frequently measured nuclei.

Remember which way to turn the tuning knob to tune to higher and lower frequencies. On most probes, turning the adjustment counter clockwise tunes to higher frequency. Do not change the matching adjustment until you have found the current tuning position of the probe, else you may lose the probe response totally. Do not tune without having the appropriate matching box fitted to the preamp. Fake resonances may appear due to filters between probe and preamp, because filters are also tuned circuits. Remove all filters before tuning over a wide range, and fine tune again (**wbsw** ≤ 10 MHz) when the probe is tuned close to the desired frequency.

Changing the proton tuning will affect the X tuning, so always tune the proton channel first, then the X-channel.

Setting a probe from high range to low range mode (lambda/4 switch) will shift the X tuning to lower frequency by many MHz, the proton frequency will only change by a few MHz.

An empty probe may tune as much as 10 MHz higher on the proton channel compared to a probe with a spinner in.

When a probe has not been used over an extended period, humidity may collect inside the turbine, causing a few harmless arcs (RF-breakthrough) on the proton channel. If the arcing does persist and/or gets worse, have the probe checked. Usually this means that dirt has accumulated inside the turbine or on the RF-coil. Cleaning should be done by a trained person only.

- Regular probe performance checks comprise
- Checking the magic angle setting (KBr)
- Checking the shims (Adamantane)
- Checking S/N performance on glycine

These checks must also be performed after a probe repair. Since a repair may result in a more efficient power conversion, start with slightly reduced power settings.

**SB probes** flip the stator vertical for sample eject. These probes require some more effort to assure a correct angle setting.

Remember to always approach the magic angle setting from the same side!

To check the reproducibility of the magic angle setting, take a KBr spectrum, stop spinning, eject and reinsert the sample, take another spectrum into a new data set, compare in dual display mode.

If the second spectrum is worse, dial less than 1/8<sup>th</sup> of a turn **countrerclockwise**.

Take another spectrum, compare again.

**A laboratory notebook** should be kept with the following entries:

(a suitable form for printout is supplied in the "**Appendix**")

- Name of the shim file and field value for every probe.
- Value of power level in dB and power in watt (if available) for proton decoupling (**p12**, **p12W**) and associated pulse lengths **p3**, **pcpd2**.
- Value of proton contact power level in dB and watt (**sp0**, **sp0W**).
- Value of carbon contact power level (**p1**, **p1W**) and associated pulse length **p1**.
- S/N value obtained on glycine, **SR** value for shift calibration, line width on  $\alpha$ -carbon in Hz.

## Literature

3.9

### Shift referencing:

R.K Harris, E.D. Becker, S.M. Cabral de Menezes, R. Goodfellow, and P. Granger, *NMR Nomenclature. Nuclear Spin Properties and conventions for Chemical shifts*, Pure Appl. Chem. Vol. 73, 1795-1818 (2001).

W.L. Earl, and D.L. VanderHart, *Measurement of <sup>13</sup>C Chemical Shifts in Solids*, J. Magn. Res. 48, 35-54 (1982).

C.R. Morcombe, and K.W. Zilm, J. Magn. Reson. 162 p479-486 (2003)

IUPAC recommendation (Harris et al.):

[http://sunsite.informatik.rwth-aachen.de/iupac/reports/provisional/abstract01/harris\\_310801.html](http://sunsite.informatik.rwth-aachen.de/iupac/reports/provisional/abstract01/harris_310801.html)

### Cross polarization:

D. Michel, and F. Engelke, *Cross-Polarization, Relaxation Times and Spin-Diffusion in Rotating Solids*, NMR Basic Principles and Progress 32, 71-125 (1994).

G. Metz, X. Wu, and S.O. Smith, *Ramped amplitude Cross Polarization in Magic-Angle-Spinning NMR*, J. Magn. Reson. A 110, 219-227 (1994).

B.H. Meier, *Cross Polarization under fast magic angle spinning: thermodynamical considerations*, Chem. Phys. Lett. 188, 201-207 (1992).

K. Schmidt-Rohr, and H.W. Spiess, Multidimensional Solid-State NMR and Polymers, Academic Press (1994).

S. Hediger, B.H. Meier, R.R. Ernst, *Adiabatic passage Hartmann-Hahn cross polarization in NMR under magic angle sample spinning*, Chem. Phys. Lett. 240, 449-456 (1995).

## **Basic Setup Procedures**

# Decoupling Techniques

# 4

Line shapes in solids are often broadened by dipolar couplings between the spins. If the coupled spins are of the same kind, it is called homo nuclear dipolar coupling. Hetero nuclear dipolar couplings exist between nuclei of different kind. While most dipolar couplings between X-range nuclei can be removed by magic angle spinning, couplings between  $^1\text{H}$ ,  $^{19}\text{F}$  and X nuclei cannot easily and efficiently be removed by spinning. Decoupling of homo nuclear and hetero nuclear interactions can be obtained by different forms of rf-irradiation with or without sample spinning. It is possible to suppress homo nuclear couplings without suppressing hetero nuclear couplings. Most frequently, the nucleus  $^1\text{H}$  must be decoupled when X-nuclei like  $^{13}\text{C}$  or  $^{15}\text{N}$  are observed, since it is abundant and broadens the line shapes of coupled X-nuclei strongly.

## Hetero-nuclear Decoupling

4.1

### CW Decoupling

4.1.1

CW decoupling simply means irradiating the decoupled spins (usually protons) with RF of constant amplitude and phase. The decoupling program is called cw or cw13 and it uses **pl12** or **pl13**, respectively. The decoupling programs select the power level and **pl12** does not need to be specified in the pulse program, if it is not used elsewhere. In the decoupling program there is also a statement setting the RF carrier frequency, according to the parameter **cnst21**, which is zero (on resonance) by default. In order to optimize decoupling, one uses the highest permitted rf-field (e.g. 100 kHz for 4mm probes) and optimizes the carrier frequency **o2** or **o2p** using **popt**.

The cw –decoupling program is written as follows:

```
0.5μ pl=pl12      ; reset power level to default decoupling power level  
1 100up:0 fq=cnst21 ; reset decoupling carrier frequency to o2+cnst21  
jump to 1          ; repeat until decoupler is switched off by do in the  
                      ; main ppg
```

CW decoupling suffers from the fact that protons have different chemical shifts, so irradiating at a single frequency does not decouple all protons evenly. At higher magnetic fields this becomes more evident, since the separation due to the magnetic field increases. CW decoupling requires fairly high decoupling power to be efficient.

## TPPM Decoupling

## 4.1.2

TPPM decoupling surpasses the traditional cw decoupling. The decoupling programs tppm15 and tppm20 use a 15 and 20 degree phase shift between the two pulses, respectively. Both operate at power level **p112**. The cpd program tppm13 uses 15 degree phase shift, as tppm15, but operates at power level **p113**.

In order to optimize the decoupling one optimizes **pcpd2** (AV3, or p31, AV1+2) with **popt** and the carrier frequency, by varying **o2** or **o2p**. Strongly proton coupled  $^{13}\text{C}$ -resonances narrow substantially, especially at high magnetic fields (>300 MHz).

The figure below shows an arrayed optimization using **popt** for the TPPM phase tilt and **pcpd2** (available in TS2.0 and higher).

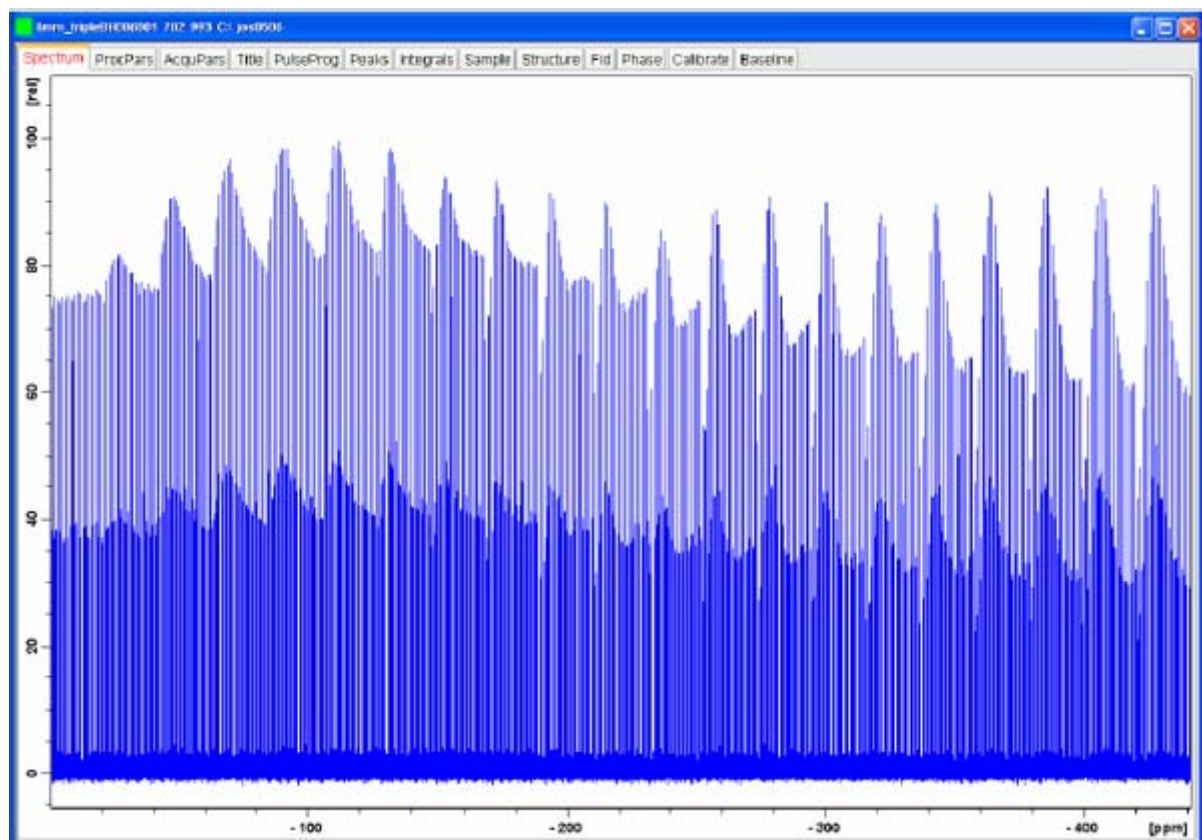


Figure 4.1. Optimization of TPPM Decoupling, on Glycine at Natural Abundance

The figure above shows optimization of TPPM decoupling, on glycine at natural abundance,  $^{13}\text{C}$  CPMAS at 5 kHz spin rate. Each block represents a 2° degree increment of the phase toggle and the variation in each block stems from incrementation of the pulse width in 0.2  $\mu\text{s}$  increments. Optimum decoupling was found with a 4.5  $\mu\text{s}$  pulse at a 16° phase toggle. It is obvious that more than one near optimum combinations of phase toggle and pulse length exist.

**Reference:**

A.E. Bennett, C.M. Rienstra, M. Auger, K.V. Lakshmi, and R.G. Griffin; *Hetero nuclear decoupling in rotating solids*, J. Chem. Phys. 103 (16); 6951 – 6958 (1995).

***SPINAL Decoupling*****4.1.3**

SPINAL decoupling is a super-cycled TPPM decoupling sequence. SPINAL16 provides adequate low power (B1 field around 50 kHz) decoupling for static samples exceeding decoupling performance of higher power cw decoupling and provides an adequate decoupling bandwidth at  $n_{rf}$  of approximately 50 kHz.

For rotating samples SPINAL64 and SPINAL128 exceed TPPM15 decoupling at high decoupling fields >80 kHz. SPINAL64 can be optimized in the same way as TPPM, by incrementing **pcpd2** (**p31**) (the phase shifts are fixed). The decoupling pulse is an approximate 180° pulse.

**Reference:**

B.M. Fung, A.K. Khitrin, K. Ermolaev, J. Magn. Reson. 142, 97-101 (2000).

***XiX Decoupling*****4.1.4**

XiX decoupling requires high spinning speeds, but decouples at a moderate RF level. 180° proton pulses are used, synchronized to the rotor speed such that recoupling does not occur (**pcpd2** $\neq$ n/4\*rotor periods). Usually, **pcpd2** is selected to be about 1/3 rotor period. The decoupler power level must be adjusted to produce a 180° pulse of (rotor period)/3.

**Reference:**

A. Detken, E. H. Hardy, M. Ernst, and B. H. Meier, Chem. Phys. Lett. 356, 298-304 (2002).

***Pi-Pulse Decoupling*****4.1.5**

Pi-pulse decoupling is a decoupling program, for weaker nuclear interactions like J couplings or weak dipolar interactions, using rotor synchronized 180° pulses.  $\pi$ -pulse decoupling uses the xy-16 phase cycle for large bandwidth. Abundant protons cannot be sufficiently decoupled with this method, but it is very suitable to remove couplings to  $^{31}P$ , which is hard to do by cw or tppm, since the chemical shift range is wide. Likewise, it can be used to decouple dilute spins or spins which are homo nuclear decoupled by spinning ( $^{19}F$ ).

**Reference:**

S.-F. Liu and K. Schmidt-Rohr, Macromolecules 34, 8416-8418 (2001).

***Homo-nuclear Decoupling*****4.2**

Homo-nuclear decoupling refers to methods which decouple dipolar interactions between like spins. Those are only prominent between abundant spins like  $^1H$ ,  $^{19}F$  and  $^{31}P$  (and potentially some others). This interaction cannot easily be spun out in most cases and renders NMR-parameters like chemical shifts of the homo-nuclear coupled spins or hetero-nuclear couplings and J-couplings to other (X)-nuclei unobservable.

***Multiple Pulse NMR: Observing Chemical Shifts of Homo-nuclear Coupled Nuclei*** **4.2.1**

Multiple pulse NMR methods are covered in the chapters about CRAMPS of this manual collection. The principle of those methods (CRAMPS, if MAS is used to average CSA interactions simultaneously), is to set the magnetization of the spins into the magic angle, using a suitable

pulse sequence. In this case, the dipolar couplings between those spins are suppressed. Short observation windows between pulses allow observation of the signal from the decoupled nuclei.

### Reference:

S. Hafner and H.W. Spiess, *Multiple-Pulse Line Narrowing under Fast Magic-Angle Spinning*, J. Magn. Reson. A 121, 160-166 (1996) and references therein.

### Multiple Pulse Decoupling

4.2.2

#### **Multiple Pulse Decoupling: Observing Dipolar Couplings and J-couplings to Homo-nuclear Coupled Nuclei**

Homo-nuclear couplings between abundant spins (usually protons) superimpose their hetero-nuclear dipolar couplings to X-spins and J-couplings to X-spins so these (distinct) couplings are not observable. Homo-nuclear decoupling protons while observing X-spins makes these couplings observable. Any method used in multiple pulse NMR (section [4.2.1](#)) may be used to achieve this.

#### **BR-24, MREV-8, BLEW-12**

Used as hetero-nuclear decoupling methods, the window between pulses may be shortened or omitted (semi-windowless or windowless sequences). These sequences work well, but have rather long cycle times and are therefore not suitable for fast spinning samples. Else they work in a similar fashion as the sequences covered in the following. BLEW-12 decoupling is supplied as a standard cpd-program. It consists of a windowless sequence of 90° pulses with suitable phases. High RF levels for decoupling provide better resolution.

#### **FSLG Decoupling**

The **F**requency **S**witched **L**ee **G**oldburg (FSLG) sequence may be used at spin rates up to 15 kHz. It is a Homo-nuclear decoupling sequence which rotates the interaction Hamiltonian around an effective field, aligned at the magic angle ( $\arctan \sqrt{2}$ ) with respect to the Zeeman field in the rotating frame. The tilt is achieved by off resonance irradiation at the Lee Goldburg frequency  $f_{LG}$  according to the Lee Goldburg condition,  $f_{LG} = \sqrt{2} f_1$ , with  $f_1 = 1/(4\tau_p)$  being the nutation frequency of the magnetization in the rotating field under on resonance conditions.  $\tau_p$  is the 90° pulse width. In the rotating frame, the frequency switching induces 2p rotations in opposite directions in the tilted rotating frame. Such rotations can be achieved by irradiation periods at the Lee Goldburg frequency  $f_{LG}$  of duration  $t_{LG} = (\sin 54.7/f_1 = \sqrt{2}/3/f_1)$  with the rf carrier jumping between the two frequencies  $f_{LG}$  and  $-f_{LG}$  with a simultaneous  $\pi$  phase shift.

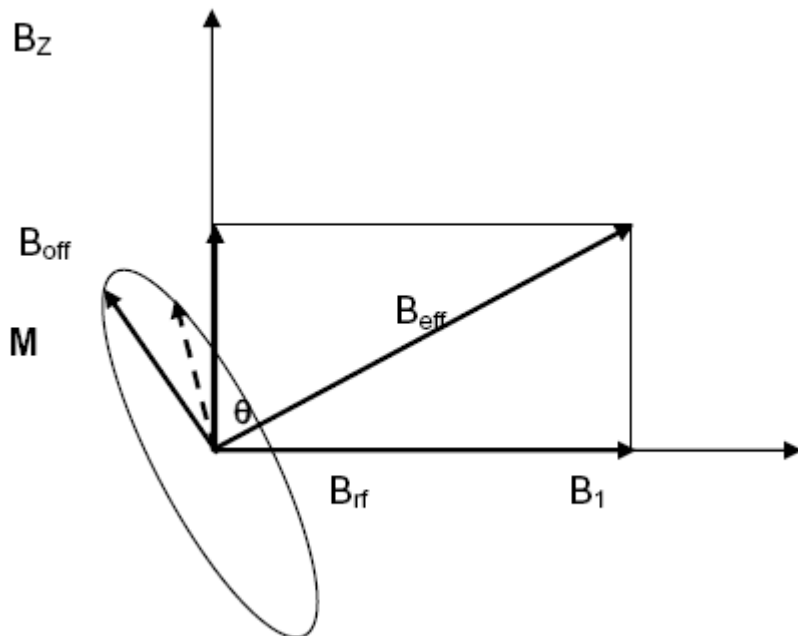


Figure 4.2. Geometry for the FSLG Condition

Note that  $B_{eff}$  points along the 1 1 1 direction in the 3 dimensional space (see Reference 2). Note the sign of  $B_{off}$  when calculating the actual direction of the effective field. A positive  $B_{off}$  and a  $B_1$  with phase 0 results in the effective field being in the positive quadrant along the magic angle in the X-Z plane of the rotating frame.

Two methods are available to achieve such a frequency switch experimentally. One method is simultaneous switching of frequencies and phases. The other method uses phase-modulation. Frequency, time and phase relate to each other as derivative of phase and time as  $\theta(t)$  to get  $2\pi f = \partial\theta/\partial\tau$ . The relationship describes the rate at which a phase of the rf-pulse must be changed in order to achieve a certain frequency offset. Vinogradov et al. describe this approach under the acronym PMLG (Phase Modulated Lee Goldburg).

Used in combination with cp signal generation, both methods allow observing proton-J-couplings to the observed X-nucleus. However, only samples with very narrow lines will produce well resolved J-couplings as shown below on adamantane. Harder solids require careful adjustment and fairly high power levels to show barely resolved couplings, since the linewidths achieved are broader than what can be achieved with standard decoupling sequences like tppm. Since the hetero-nuclear X-H-coupling remains, there may be spinning sidebands from this coupling, in addition to CSA sidebands.

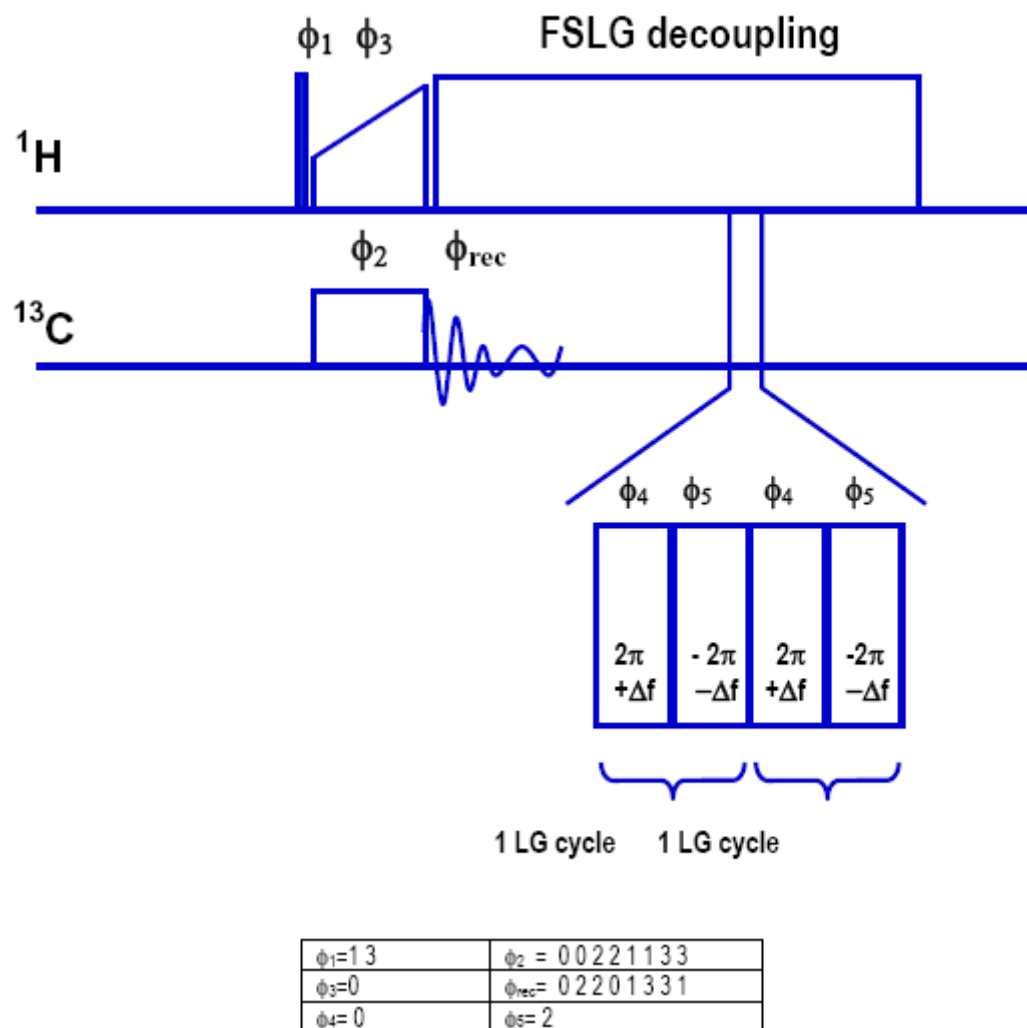


Figure 4.3. FSLG Decoupling Pulse Sequence Diagram

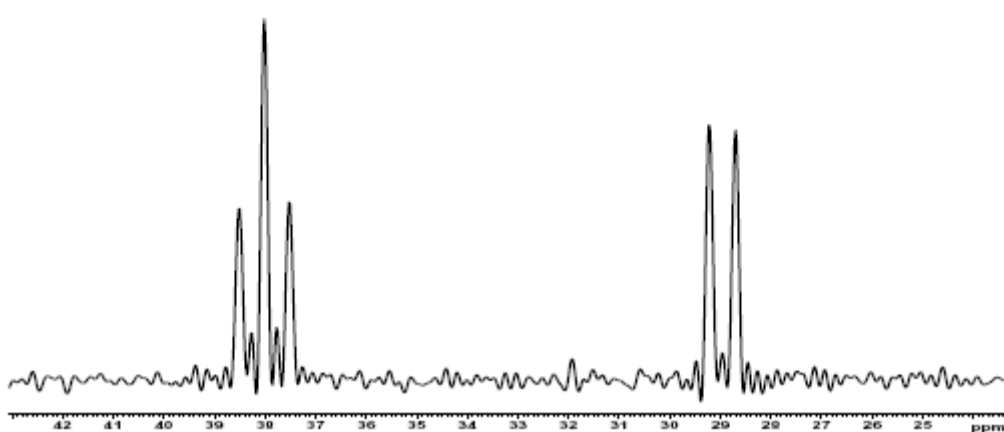


Figure 4.4. Adamantane, FSLG Decoupled. The C-H J-Couplings Shown.

The figure above shows Homo-nuclear proton decoupling on center packed adamantane sample rotating at 7 kHz, 100 kHz  $^1\text{H}$  decoupling field. Note that good  $\text{B}_1$ -homogeneity is required. Use a CRAMPS spinner (12  $\mu\text{l}$  sample volume in a 4mm spinner).

### Setting up the experiment:

1. Use center packed adamantane in a CRAMPS rotor, unlabeled and a spinning rate of 10 kHz for adamantane.
2. Start from a data set with well adjusted HH condition on adamantane.
3. Generate a new data set with ***edc***.
4. Readjust decoupling power ***pl12*** and ***p3, pcpd2*** for 70-100 kHz RF field, determine the precise RF field (preferably via a 360° proton pulse ***p3***).
5. Load the pulse program ***fqlg***. This uses frequency shifts with simultaneous phase shifts for FSLG-decoupling at ***pl13***.
6. Set ***pl13*** to achieve the same RF-field as measured in step 4, set ***cnst20*** to the value of RF field in Hz. The pulse program contains the include file <lcalc.incl> which calculates the required frequency shifts to either side (shown in ***ased*** as ***cnst22*** and ***cnst23***). ***Cnst24*** provides an additional overall offset to compensate for phase glitch. With proper probe tuning and 50Ω match, ***cnst24*** should be close to zero.
7. Set acquisition and processing parameters according to [\*\*Table 4.1\*\*](#), and [\*\*Table 4.2\*\*](#).

A spectrum like in **fig. 4** should be obtained. If the splitting is worse, optimize with ***pl13*** and ***cnst24***. Usually, somewhat less power than calculated is required.

The FSLG decoupling scheme is also implemented as cpd-program cwlgs. The include file lcalc.incl is also required. With ***cpdprg2*** = cwlgs, the standard cp pulse program can be used. The **ZGOPTN -Dlacr (ased)** should be set in order to allow decoupling times >50 ms.

*Table 4.1. Acquisition Parameters*

Parameter	Value	Comments
pulprog	fqlg	AV3, use fqlg.av for AV1+2.
d1	4 s	Recycle delay.
ns	4-16	Number of scans.
aq	80 ms	Acquisition time.
spnam0	ramp.100 or ramp70100.100	For ramped CP.
pl12, p3	set for p3=90°	
sp0, pl1	set for cp	
p15	5-10m	
pl13	set for 70-100 kHz	Optimize for best resolution.
cnst20	70000-100000	Equals the applied RF-field.
cnst24	0	To be optimized.
cnst21	0	Reset proton frequency to SFO2.

## Decoupling Techniques

Table 4.2. Processing Parameters

Parameter	Value	Comment
SI	2*td	Adequate 4fold zero filling.
WDW	no	No apodization.
PH_mod	pk	Phase correction if needed.
BC_mod	quad	DC offset correction.

As mentioned above, frequency shifts can also be generated by a phase gradient shape. A phase change of  $360^\circ$  per second corresponds to a frequency of 1 Hz, as can easily be visualized. The frequency shift which needs to be achieved is  $\pm \text{RF-field}/\sqrt{2}$ . Since the pulse duration must achieve a  $2\pi$  rotation off resonance, corresponding to a  $293^\circ$  flip angle on resonance, it can easily be calculated that a phase change over  $209^\circ$  during a  $293^\circ$  flip angle pulse is required to achieve this.

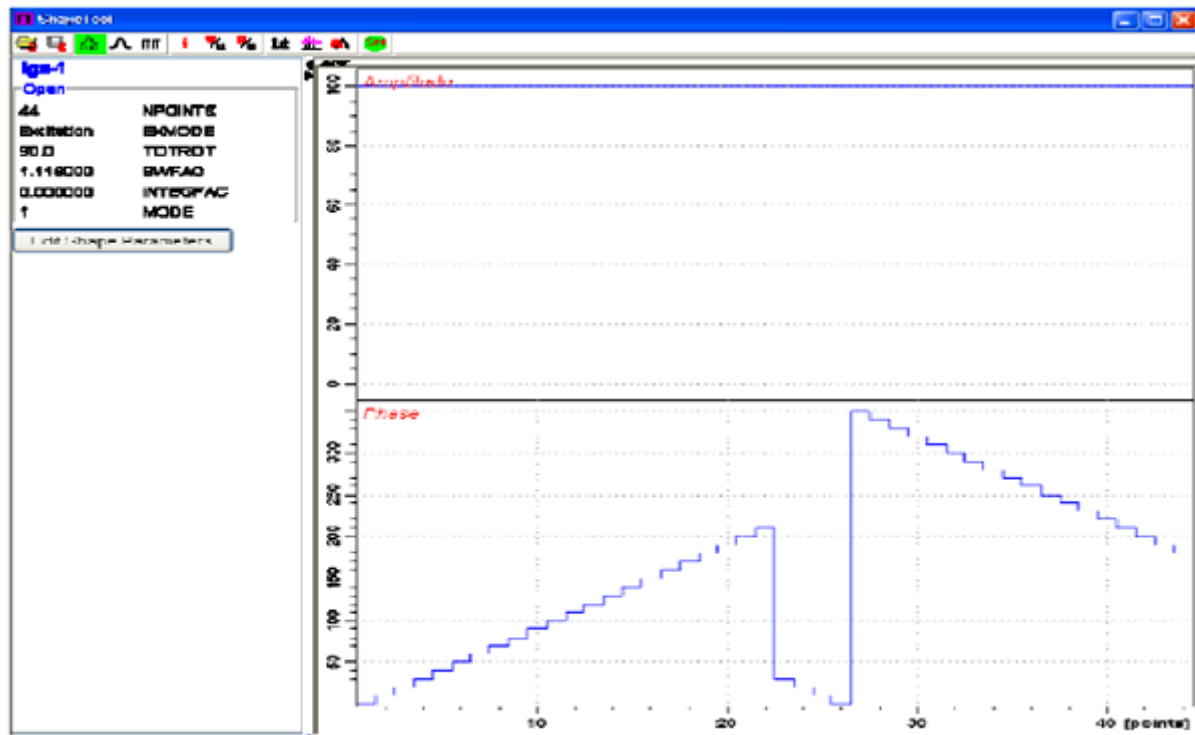


Figure 4.5. Shape with Phase Gradients

In the figure above: Shape with phase gradients for positive and negative offsets and corresponding phase change, **stdisp** –display of lgs-1 shape. Amplitude is 100% throughout.

Vinogradov et. al. have published shapes with much fewer steps and different phases. The pulse length for the shape does not depend on the number of steps, but only on the applied RF-field. Using the include file lgcalc.incl, a pulse  $p5$  is calculated from  $\text{cnst20}=\text{RF-field}$  in Hz. The total shape pulse length must be  $2*p5$ .

To use pmlg decoupling, save the pulse program fqlg under a different filename and change calculations and loop as follows:

```

define loop counter count;calculate number of LG periods according to aq
"count=aq/(2*p5)"

define pulse pmlg
"pmlg=2*p5"

"sp1=pl13" set shape power to pl13 for LG (TS2.1 only)

.

3 (pmlg:sp1 ph3):           f2 for one full PMLG unit, as for lgs-1 shape
lo to 3 times count

```

### References:

- A. Bielecki, A.C. Kolbert, and M.H. Levitt, *Frequency-Switched Pulse Sequences: Homo-nuclear Decoupling and Dilute Spin NMR in Solids*, Chem. Phys. Lett. 155, 341-346 (1989).
- A. Bielecki, A.C. Kolbert, H.J.M. deGroot, R.G. Griffin, and M.H. Levitt, *Frequency-Switched Lee-Goldburg Sequences in Solids*, Advances in Magnetic Resonance 14, 111-124 (1990).
- E. Vinogradov, P.K. Madhu, and S. Vega, High-resolution proton solid-state NMR spectroscopy by phase-modulated Lee-Goldburg experiments, Chem. Phys. Lett. 314, 443-450 (1999) and references cited therein.

### DUMBO

DUMBO (Decoupling Uses Mind Boggling Optimization) is a phase modulation scheme where the phase modulation +is described in terms of a Fourier series

$$\phi(t) = \sum_{n=0}^{+\infty} a_n \cos(n\omega_c t) + b_n \sin(n\omega_c t)$$

The shape can be created using the AU-program **DUMBO**. The DUMBO shape file in the release version of TOPSPIN is calculated for 32 $\mu$ s pulses. To create your own DUMBO shape you can also use the au-program **dumbo**. See instructions in the header of the au-program for proper use.

The above pulse program to observe J-couplings with DUMBO decoupling would be written as follows:

```

define loop counter count      ;calculate number of LG periods according to aq
"count=aq/(p10)"

.

3 (p10:sp1 ph3):f2          ;p10 set by AU-program DUMBO (n*32  $\mu$ sec)
lo to 3 times count

```

### References:

- D. Sakellariou, A. Lesage, P. Hodgkinson, and L. Emsley, *Homo-nuclear dipolar decoupling in solid-state NMR using continuous phase modulation*, Chem. Phys. Lett. 319, 253-260 (2000).
- Lyndon Emsley's home page: <http://www.ens-lyon.fr/STIM/NMR/NMR.html>

### Transverse Dephasing Optimized Spectroscopy

Decoupling optimized under refocused conditions:

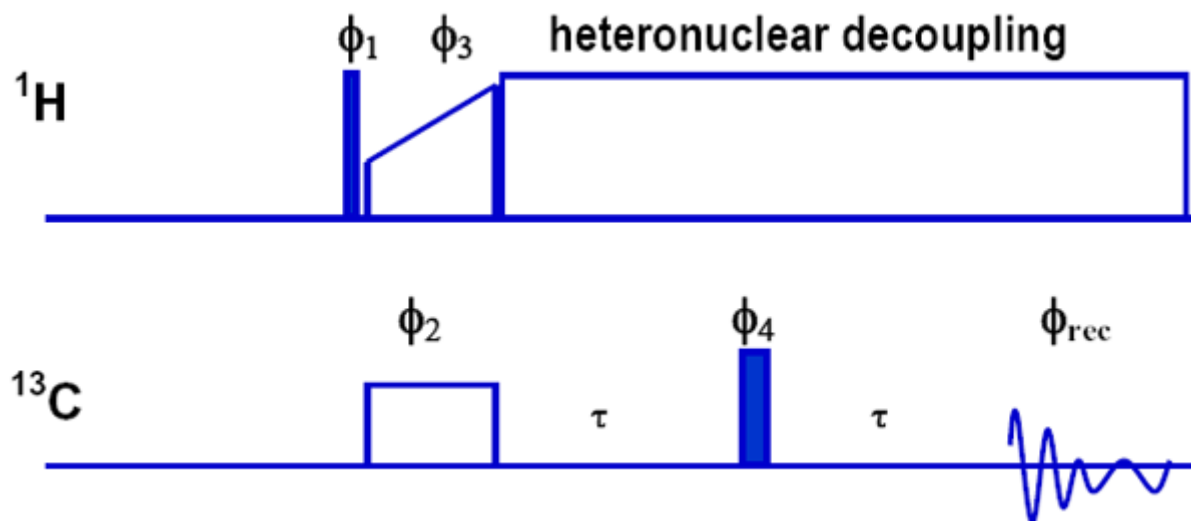


Figure 4.6. Pulse Program for Hahn Echo Sequence

Transverse Dephasing Optimized spectroscopy (G. De Paepe et al. 2003) uses a spin echo sequence for optimizing hetero-nuclear decoupling. The idea behind it is simply the removal of the normally dominant  $J_0$  term (describing coherent residual line broadening effects) in the transverse relaxation rate  $R_2$  (A. Abragam chapter 8). With the normal CP experiment the observed line broadening (coherence decay time  $T_2^*$ ) might be caused by other heterogeneous effects, such as distribution of chemical shifts or susceptibility effects and not reflect the true  $T_2'$  (coherence lifetime). The true  $T_2'$  achieved through good hetero-nuclear decoupling can then be observed with a hahn-echo experiment. Optimization is done by looking for the maximum signal amplitude of the decoupled resonances of interest. Be careful not to exceed the maximum decoupling time with high power decoupling.

#### Reference:

G. De Paepe, N. Giraud, A. Lesage, P. Hodgkinson, A. Böckmann, and L. Emsley, *Transverse Dephasing Optimized Solid-State NMR Spectroscopy*, JACS 125, 13938 – 13939 (2003).

# *Practical CP/MAS Spectroscopy on Spin 1/2 Nuclei*

**5**

## ***Introduction***

**5.1**

Once good setup parameters have been obtained to observe  $^{13}\text{C}$  and get good S/N on glycine, it should be easy to also observe  $^{13}\text{C}$ -CP/MAS spectra on other samples and on nuclei different from  $^{13}\text{C}$ . Nevertheless, sometimes one comes across samples where it is difficult to observe  $^{13}\text{C}$ . This chapter deals with strategies to optimize acquisition parameters for  $^{13}\text{C}$  and other spin  $\frac{1}{2}$  nuclei.

## ***Possible Difficulties***

**5.2**

Usually,  $^{13}\text{C}$  spectra are easily acquired. Several sample properties may however make observation difficult:

1. Low concentration of  $^{13}\text{C}$  in the sample.
2. No or too few protons in the sample
3. Long proton  $T_1$
4. Long  $T_{I-S}$
5. Short proton  $T_{1\rho}$

If a nucleus different from  $^{13}\text{C}$  should be observed, there are additional potential difficulties:

6. Unknown chemical shift
7. Unknown Hartmann-Hahn-condition
8. Unknown relaxation properties (proton  $T_1$ ,  $T_{1\rho}$ ,  $T_{I-S}$ )

## ***Possible Approaches for $^{13}\text{C}$ Samples***

**5.3**

1. Collect as much information about the sample as possible. Do not accept samples for measurement with unknown composition. Request information about:
  - possible hazards (upon a rotor explosion)
  - concentration of the nucleus to be measured
  - structural information about the molecular environment of the nucleus of interest:
    - mobility (rigid environment: expect long  $T_1$  and repetition delay),
    - proximity to protons (can one use cross polarization)
  - conductivity, dielectric loss (expect tuning and RF-heating problems if sample is dielectrically lossy or even conductive)

### 2. Collect information about the sample first by running an “easy” nucleus:

Feasibility of cross polarization parameters is the required key information, because it decides the steps to follow.

If the sample information which you have collected shows that a  $^{13}\text{C}$  CP/MAS experiment should be feasible (sample contains more than 20% protonated carbons), load a reference cross polarization data set (S/N test spectrum of glycine), spin the sample at the same spin rate, set contact time (**p15**) to 1ms, wait 1 min., do one scan. There should be a visible signal.

From there on, optimize the required repetition rate (**d1**), contact time (**p15**), number of scans (**ns**), spin rate (**masr**) and Hartmann-Hahn adjustment until the signal is optimum. In very few cases, the decoupler offset (**o2**) may require readjustment.

If no  $^{13}\text{C}$ -signal is found, the reasons may be:

- incorrect setup (recheck reference sample)
- concentration lower than expected
- unusual relaxation properties (long  $T_{1,S}$ , long proton  $T_1$ , short proton  $T_{1p}$ ).

### 3. Then the most important information about the sample (proton $T_1$ , proton $T_{1p}$ ) can be obtained by looking at the protons in the sample. Set up for proton observation, set **swh** to 100000-500000, **rg** to 4 and **pulprog cpoft** (if not found in the library, copy the pulse program in the appendix), **p3** and **p12** for **p3=p90**. Set **spnam0 = ramp.100**, **sp0** = power level for HH, **p15=100** us. Do 1 scan and fourier transform/phase correct. Using popt, optimize **d1** for maximum signal.

**Note:** CP/MAS probes usually have a substantial proton background signal. Do not be misled by this, it will not behave like a regular signal:

- it will grow steadily with longer pulses
- it will not show spinning sidebands
- it will cancel when a background suppression pulse program like **aring** is used with a full phase cycle.

### 4. Knowing the required relaxation delay, the following step is to determine the cross polarization (contact time). On protons, we measure the time constant $T_{1p}$ . Using popt in the previous setup, vary **p15** between 100 $\mu\text{sec}$ and 10 ms (even 20 ms at reduced power, if a long $T_{1,S}$ is expected, as the distance between nucleus of interest is long or the mobility is high, leading to a small hetero-nuclear dipolar coupling between nucleus of interest and protons). This measurement will tell you how long the contact time **p15** may be. A value of p15 giving 50% of the initial proton signal amplitude will still give a 2-fold enhancement on $^{13}\text{C}$ . If the proton signal is below 50% at 1ms spin lock time or even less, a full cp-enhancement cannot be expected.

### 5. Now we know the minimum relaxation delay and the maximum contact time. With these parameters used as d1 and p15, the measurement is just a matter of patience.

**Possible Approaches for non-<sup>13</sup>C Samples****5.4**

If an arbitrary X-nucleus of spin  $\frac{1}{2}$  is under investigation (quadrupolar spins must be treated separately), the strategy follows the one described above, if the sample contains the protons bound to <sup>13</sup>C. In this case, running a <sup>13</sup>C cp/mas spectrum allows setting and determining all proton parameters (recycle time, contact time) from the <sup>13</sup>C setup. To run the X-nucleus, cross polarized from protons, one just needs to set the HH-condition from the known proton RF-field, the spin rate, and the transmitter power at the NMR-Frequency of the X-nucleus such that the effective field at the X-frequency equals the effective field at proton frequency  $\pm$  spin rate.

Example: setting the HH-condition for <sup>15</sup>N from known parameters for <sup>13</sup>C-CP/MAS. The gyromagnetic ration of <sup>15</sup>N is lower by a factor of 2.5 compared to carbon (proton frequency: 400 MHz, <sup>13</sup>C-frequency: 100 MHz, <sup>15</sup>N frequency: 40 MHz). The probe efficiency is about the same for <sup>13</sup>C and <sup>15</sup>N (but not <sup>1</sup>H!), so one needs about 2.5 times higher RF-voltage for the <sup>15</sup>N-contact pulse than for the <sup>13</sup>C-contact pulse, if the spin rate and the proton RF-field are the same. This is equivalent to  $2.5^2=6.25$  times the power in watts! So if *p1W* =150W for a well optimized <sup>13</sup>C-CP setup, <sup>15</sup>N will require  $6.25 \times 150$  W= 938 W! This is far above specs, so the same proton contact power level cannot be used, it needs to be lowered. The maximum allowed power for a contact pulse on <sup>15</sup>N is 500W. This means that the proton contact power should be lowered by approximately a factor of  $\sqrt{938/500} \approx 1.37$ . Precalculating power levels like this will get the parameters close enough to see a cp-signal on a good test sample, so further optimization is possible. See "[Test Samples](#)" for suitable test samples.

The most efficient way of precalculating power levels for multi-nuclear spectroscopy is the following:

1. Determine the power conversion factor for some nuclei of interest on a suitable test sample, from the low end to the high end of the probe tuning range. This means measuring a precise 360° pulse (make sure it is 360°, not 180° or 540°!) and the associated power level. Make a table in your lab notebook as follows (see "[Appendix](#)"):

*Table 5.1. Power Conversion Table*

Probe: 4mm Triple				
Nucleus Frequency	P90 (μs)	Rf-field (Khz)	Power (W or dB)	Remarks
<sup>1</sup> H/400.13	2.5	100	100	Low range
<sup>19</sup> F/376.3				Not available
<sup>15</sup> N/40.5	6.5	38.6	300	Probe in double mode
<sup>15</sup> N/40.5	6.5	38.6	500	Probe in triple mode C/N
<sup>29</sup> Si/79.5	6	41.7	300	Double mode low range
<sup>13</sup> C/100.5	4	62.5	150	Double mode low range
<sup>13</sup> C/100.5	5	50	200	Triple mode C/N
<sup>119</sup> Sn/149.1	4	62.5	100	Double mode high range
<sup>31</sup> P/161.9	3.5	71.4	150	Range switch up, double mode

2. Once these values are measured, any HH condition can be calculated. Assumed you want to cross polarize  $^{119}\text{Sn}$ , the sample spins at 12 kHz. The contact time is anticipated to be rather long, because  $^{119}\text{Sn}$  atoms are large and far away from protons. So the power level for the contact should not be too high. Let us set the RF-field to 50 kHz for the contact. We decide to apply a ramp shape on the proton contact pulse, covering the  $\pm 1$  spinning sidebands. This means that we need to apply a ramp from 38 to 62 kHz RF field, plus some safety margin, about 35 to 65 kHz RF field on the proton ramp. For  $^{119}\text{Sn}$  we need to apply 50 kHz RF field. Since the RF field is proportional to the amplitude in a shape (RF-voltage output is proportional to shape amplitude value), the shape power must range from 65 kHz to 35 kHz, from 100 to about 50% amplitude. Use **calcpowlev** to calculate the changes in dB to achieve the calculated RF fields (enter reference RF-field to calculate required RF field instead of pulse lengths). In our case, the proton contact pulse power **sp0** is calculated at + 3.74 dB (65 kHz compared to 100 kHz), the power level for  $^{119}\text{Sn}$  is calculated at +1.94 dB (50 kHz compared to 62.5 kHz). Be sure to add the calculated number for a desired RF-field lower than the reference field, subtract the number if the desired RF-field is higher.
3. If such a table is not available, but an oscilloscope is, one can measure the RF- voltage for the X contact pulse of the known ( $^{13}\text{C}$ ) HH condition, calculate the pp-voltage for the unknown HH condition from the NMR-frequencies of the two nuclei, and set this voltage for the unknown HH condition.

### Hints, Tricks, Caveats for Multi-nuclear (CP-)MAS Spectroscopy

5.5

1. Since  $T_1$  relaxation tends to be slow in solids, direct observation of hetero-nuclei is usually time consuming, so CP is widely used because the proton  $T_1$  is usually bearable. However, CP can only be used if the hetero-nucleus is coupled to protons (or whatever nucleus the magnetization is drained from). Whereas  $^{13}\text{C}$  and  $^{15}\text{N}$  usually bear directly bonded protons, this is not the case for many other spin  $1/2$  hetero-nuclei. So the magnetization must come from more remote substitutes. More remote they may also be because atomic radii increase as one goes to nuclei with higher atomic mass. In short: HH conditions may be very sharp,  $T_{1,S}$  may be long, but proton  $T_{1,p}$  may still be short.
2. Chemical shift ranges and chemical shift anisotropies increase with nuclei of higher order number and number of electrons in the outer shell. Therefore one may be confronted with two problems:
  - to find the signal somewhere within the possible chemical shift range
  - to find the signal within a “forest” of spinning sidebands
3. Ease of setup therefore depends largely on the availability of a setup sample with decent  $T_1$ , efficient CP, and known chemical shift for referencing. Chapter 2 lists some useful setup samples together with known parameters.

### Setup for Standard hetero-nuclear Samples $^{15}\text{N}$ , $^{29}\text{Si}$ , $^{31}\text{P}$

5.6

1.  $^{15}\text{N}$  on  $\alpha$ -glycine: calculate HH condition as described above. Else:

Load  $\alpha$ -glycine  $^{13}\text{C}$  reference spectrum, set observe nucleus N15 in **edasp**

- add 2 dB to **sp0 (spnam0=ramp.100)**
- subtract 2 dB from **p11** (more is not required since the transmitter will usually put out 50% more power at  $^{15}\text{N}$  frequency)
- set **p15 = 3 ms**

- acquire 4-8 scans
  - optimize HH condition, acquire reference spectrum with **aq**=25-35 ms
2.  $^{29}\text{Si}$  on DSS
- load  $\alpha$ -glycine  $^{13}\text{C}$  reference spectrum
  - set observe nucleus to  $^{29}\text{Si}$  in **edasp**
  - add 2 dB to **spo**
  - acquire 4 scans with **aq** = 35 ms
  - optimize HH condition, acquire reference spectrum
3.  $^{31}\text{P}$  on ADP (ammonium dihydrogen phosphate  $\text{NH}_4 \text{H}_2 \text{PO}_4$ )
- load  $\alpha$ -glycine  $^{13}\text{C}$  reference spectrum
  - set observe nucleus to  $^{31}\text{P}$  in **edasp**
  - add 6 dB to **pl1**
  - optimize HH condition, acquire 2 scans, reduce **rg** appropriately.



# Basic CP-MAS Experiments

# 6

## Introduction

6.1

The following experiments can be run by calling a  $^{13}\text{C}$  CPMAS standard parameter, data set, or data, loading the appropriate pulse program and loading the pulse parameters obtained previously during the setup (see "[Basic Setup Procedures](#)"). Some attention needs to be paid to special experimental parameters. Most of those parameters are explained in the header section of the pulse programs.

The CPPI experiment series in [6.5](#) requires measuring the HH match using a constant amplitude contact pulse. This can be accomplished using a rectangular shape **square.100**, or using the pulse program **cplg**.

## Pulse Calibration with CP

6.1.1

Pulse calibration for  $^{13}\text{C}$  pulses after cross polarization using a flip back pulse.

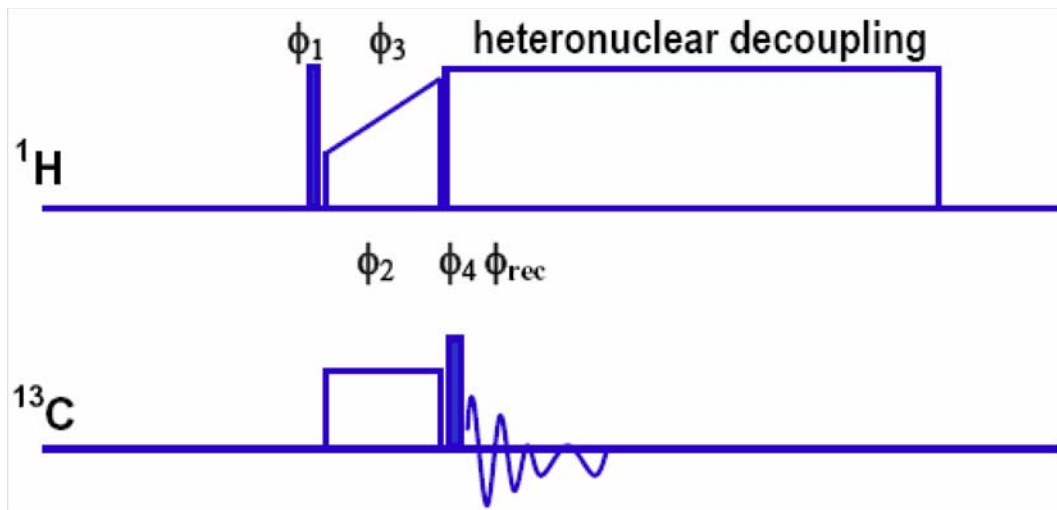


Figure 6.1. Pulse Program for CP with Flip-back Pulse

The experiment can be done directly after the CPMAS setup procedure. Loading the pulse program **cp90** and setting **p11=p11** allows one to measure the X nucleus spin nutation frequency at the HH contact power. Of course, the experiment allows nutation frequencies to be measured at other power levels as well. The typical nutation pattern has a cosine form, so a 90 degree pulse gives null signal. Use glycine spinning at N kHz as before. When using POPT for such measurements the optimization type is "ZERO" so that the program looks for a zero

crossing at the automatic data evaluation. To get nutation patterns without phase distortions, 90° pulses should always be executed close to the observed resonance. Larger offsets give different (shorter) p90 values and phase distortions for pulse lengths close to 180° and multiples thereof.

Table 6.1. Acquisition Parameters

Parameter	Value	Comments
<b>pulprog</b>	cp90	AVIII, cp90.av for older instruments
<b>nuc1</b>	13C	Nucleus on f1 channel
<b>nuc2</b>	1H	Nucleus on f2 channel
<b>sw</b>	300 ppm	Spectral width for Glycine
<b>o1p</b>	45	Close to C- $\alpha$
<b>td</b>	2048	Number of points sampled

Fine adjustment of the  $\pi$  pulse on  $^{13}\text{C}$  can also be done using the TOSS experiment, see next chapter.

### Total Sideband Suppression TOSS

### 6.2

The TOSS sequences permit complete suppression of spinning sidebands (SSB) in CPMAS experiments. The TOSS sequence consists of the basic CP sequence plus a 2 rotor period sequence with four specially spaced 180° pulses. As is the case for all extra pulses on the X channel in CPMAS experiments (with the exception of symmetry based sequences, see further below), these 180° pulses are set with **pl11**.

This experiment can be optimized for minimum spinning sideband intensity either by variation of the 180° pulse width or the associated power level **pl11**.

Two variations of the TOSS sequence exists, the default is TOSS A, which is appropriate for lower spinning speeds. TOSS B, for higher spinning speeds, is selected by setting **ZGOPTNS** to **-Dtossb**. The maximum spinning speed is either determined by common sense – if all sidebands are spun out, TOSS is not needed (low field instruments) – or by the shortest delay, which is **d26** in both cases. For TOSS B, **d26 = 0.0773s/cnst31-p2**, with **cnst31** the rotation rate in Hz and **p2** the 180° pulse width in  $\mu\text{s}$ . For TOSS A, **d26 = 0.0412s/cnst31-p2**, so the maximum spinning rate is lower.

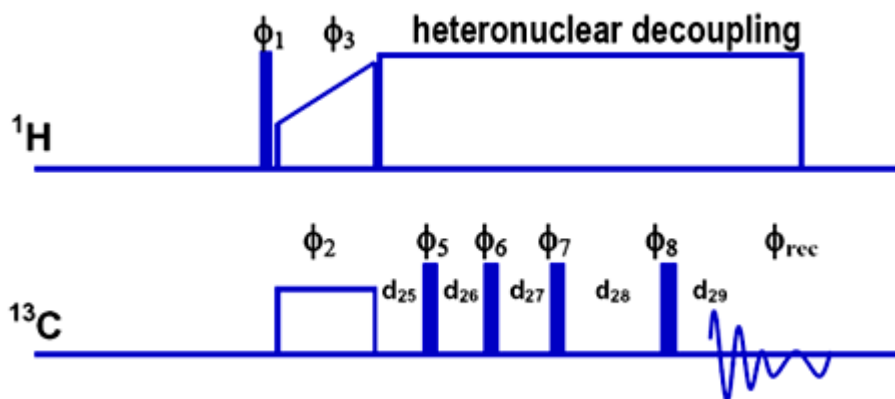


Figure 6.2. Pulse Program for CPTOSS.

If the timing becomes a problem, alternative TOSS schemes need to be found (see e.g. O.N. Antzutkin, *Sideband manipulation in magic-angle-spinning nuclear magnetic resonance*; Progress in Nuclear Magnetic Resonance Spectroscopy 35 (1999) 203-266.). The SELTICS sequence is an alternative.

Set up the experiment using glycine or tyrosine-HCl at a moderate spinning speed. Get a good CPMAS spectrum first then run a TOSS spectrum.

Table 6.2. Acquisition Parameters

Parameter	Value	Comments
<b>pulprog</b>	cptoss <b>cptoss243</b>	
<b>p2</b>		180° pulse on X nucleus
<b>pl11</b>		Power level driving P2 on X-channel
<b>cnst31</b>		Spinning speed in Hz e.g. 5 kHz the entry would be 5000
<b>zgoptns</b>	-Dtossb	Tossb if needed because of high spinning speed or long p2

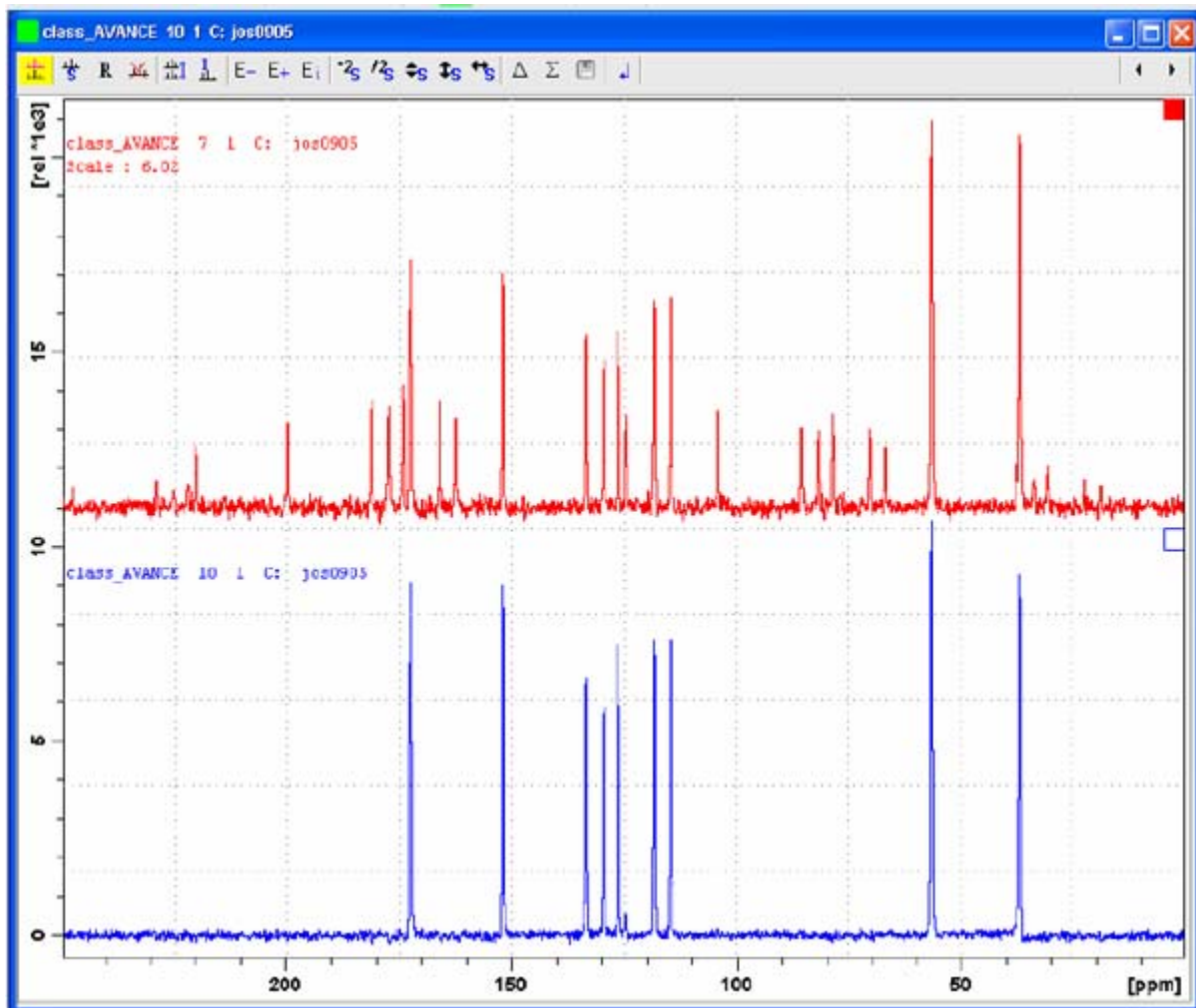


Figure 6.3. Comparison of a CPTOSS and CPMAS Experiment

**Figure 6.3.** compares a CPTOSS experiment (lower spectrum) to a CPMAS experiment (upper spectrum) on tyrosine HCl at 6 kHz sample rotation using a 4 mm CPMAS double resonance probe at 500 MHz with 16 accumulated transients.

The sequence is not perfectly compensated for experimental artifacts and if perfect suppression of SSB is required, one can use a 5 pulse sequence with a long phase cycle, requiring a minimum of 243 transients for complete artifact suppression using the pulse program ***cptoss243***, where the extension.av is added in case of the AV2 console. **Figure 6.4.** shows the advantage of the well compensated TOSS sequence with its 243 phase cycle steps over the above 4 pulse sequence. Besides the better compensation, the ***cptoss243*** pulse sequence is also shorter and uses only 1 instead of 2 rotor cycles. This pulse program can be used with fairly high spinning speeds, up to about 12.5 kHz sample rotation, depending, of course, on the width of the employed  $\pi$  – pulses. **Figure 6.5.** shows for a comparison the results obtained with the 4 pulse sequence with 256 scans.

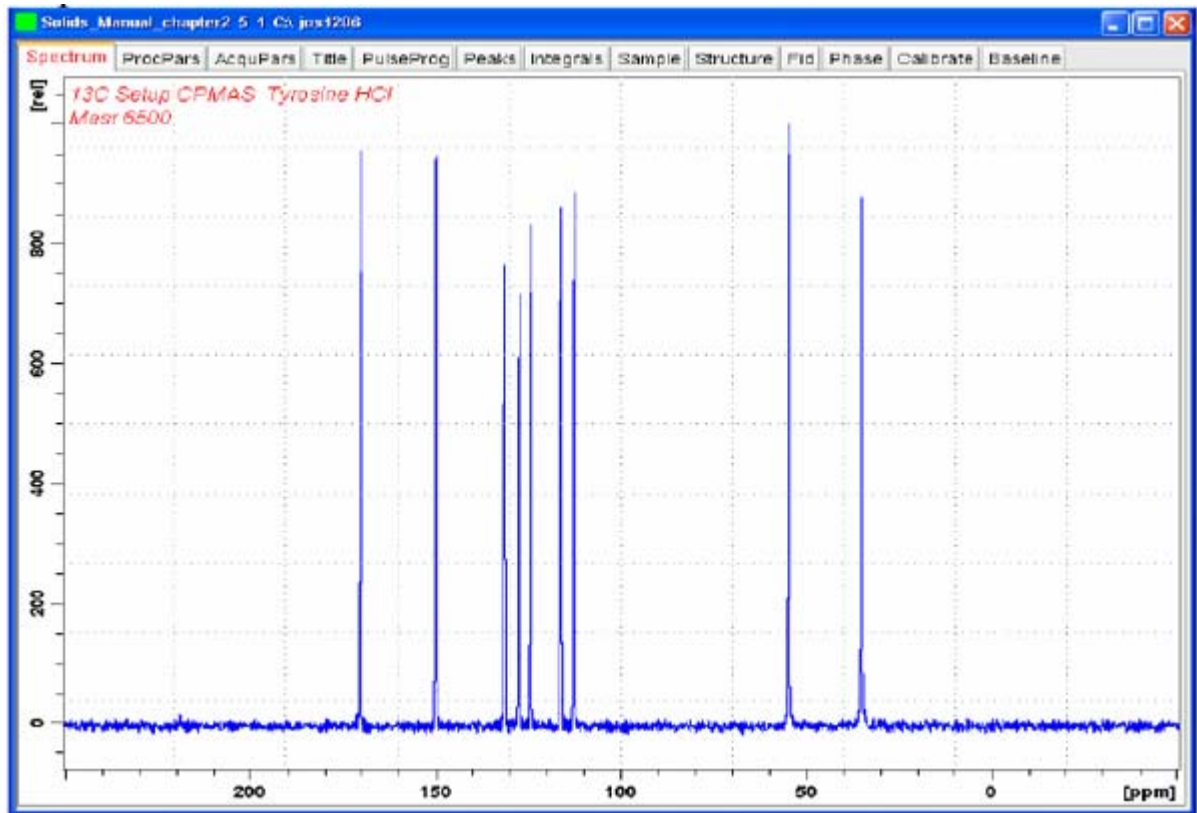


Figure 6.4. CPTOSS243 Experiment on Tyrosine HCl at 6.5 kHz

**Figure 6.4.** is a CPTOSS243 experiment on tyrosine HCl at 6.5 kHz sample rotation using a 4 mm CPMAS triple resonance probe at 500 MHz with 243 accumulated transients. No spinning sideband residuals can be observed, with a noise level below 2% peak to peak compared to the highest peak intensity.

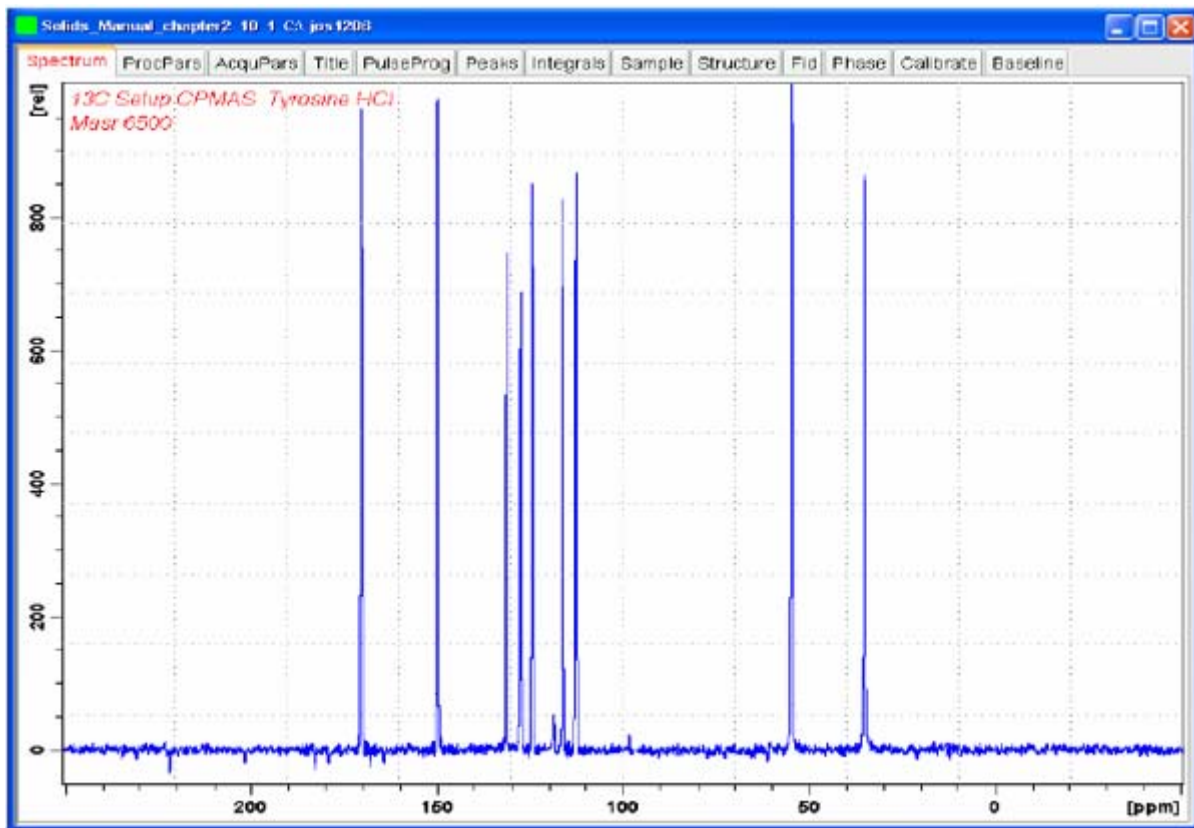


Figure 6.5. CPTOSS Experiment on Tyrosine HCl at 6.5 kHz

**Figure 6.5.** is a CPTOSS experiment on tyrosine HCl at 6.5 kHz sample rotation using a 4 mm CPMAS triple resonance probe at 500 MHz with 256 accumulated transients. Spinning sideband residuals can be observed outside a noise level of approximately 2% peak to peak compared to the highest intensity. The residual sidebands have up to 5% intensity compared to the highest resonance.

### SELTICS

### 6.3

Like the TOSS experiment, SELTICS (Sideband ELimination by Temporary Interruption of the Chemical Shift) is an experiment for spinning sideband suppression. Pulses on the  $^{13}\text{C}$  channel are driven with *p11* and pulse times are rotor synchronized. For optimum suppression, the shortest pulse ( $\tau/24$ ) of the sequences, where  $\tau_r$  is the rotor period, should be a  $\pi/2$  pulse or stronger. Choose *p11* accordingly. Unlike TOSS, SELTICS is only 0.5 rotor periods long.

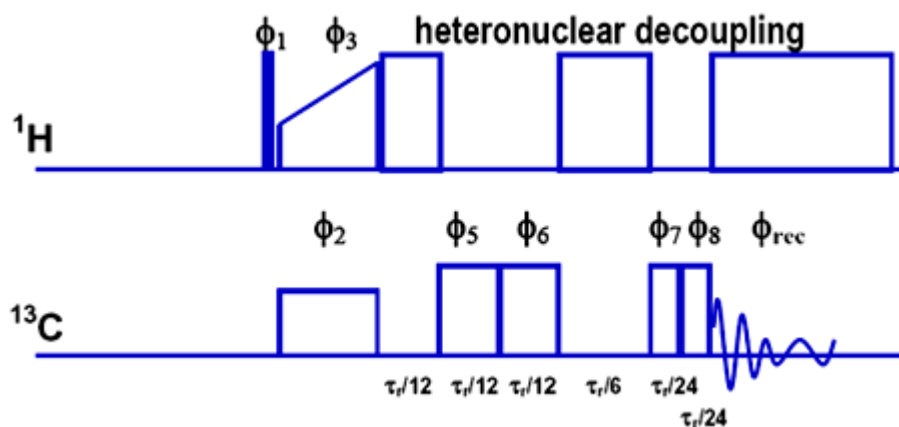


Figure 6.6. Pulse Program for SELTICS.

In **Figure 6.6**, one can see that the SELTICS experiment takes only  $\frac{1}{2}$  rotor period compared to the 2 rotor periods required in the TOSS experiment.

Use glycine or tyrosine.HCl at reasonable spinning speed.

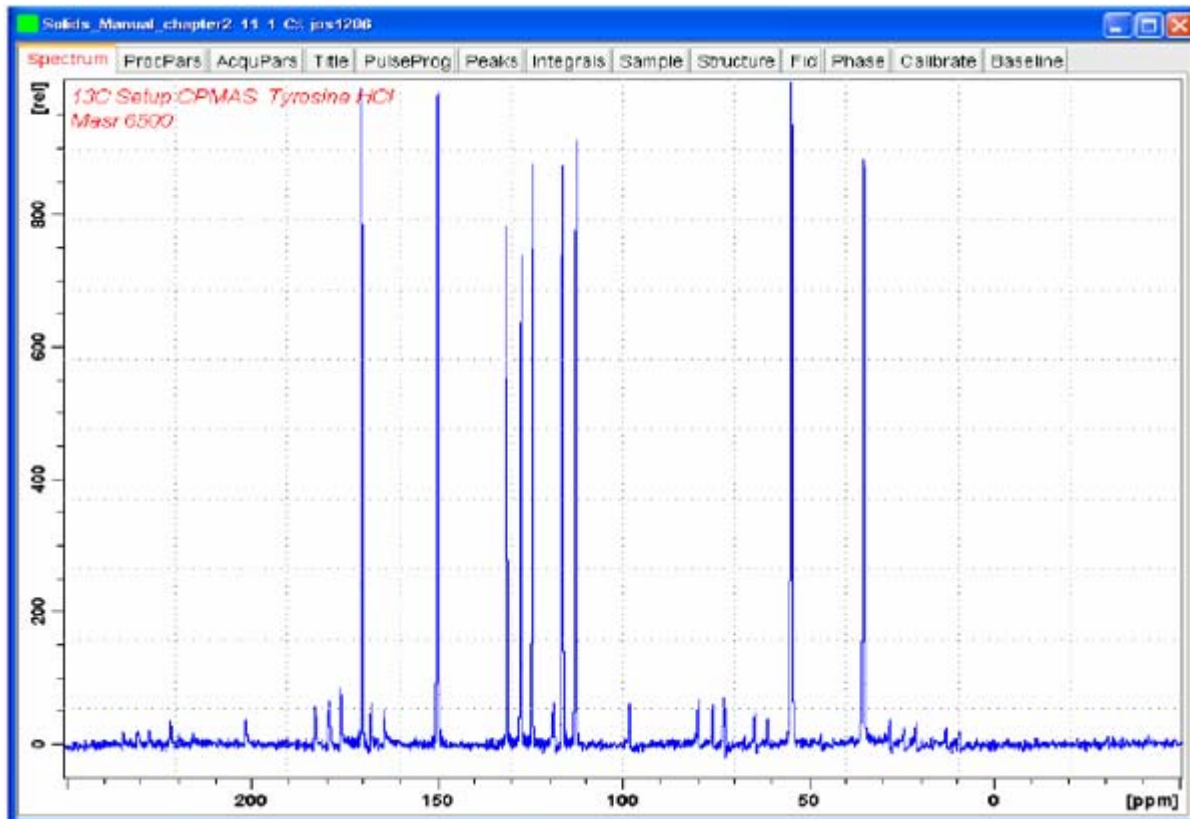


Figure 6.7. SELTICS at 6.5 kHz Sample Rotation on Tyrosine HCl.

## Basic CP-MAS Experiments

In **Figure 6.7.** the amplitude of the spinning sidebands are reduced to more than 10% compared to the original spectrum without sideband suppression. 256 transients were recorded.

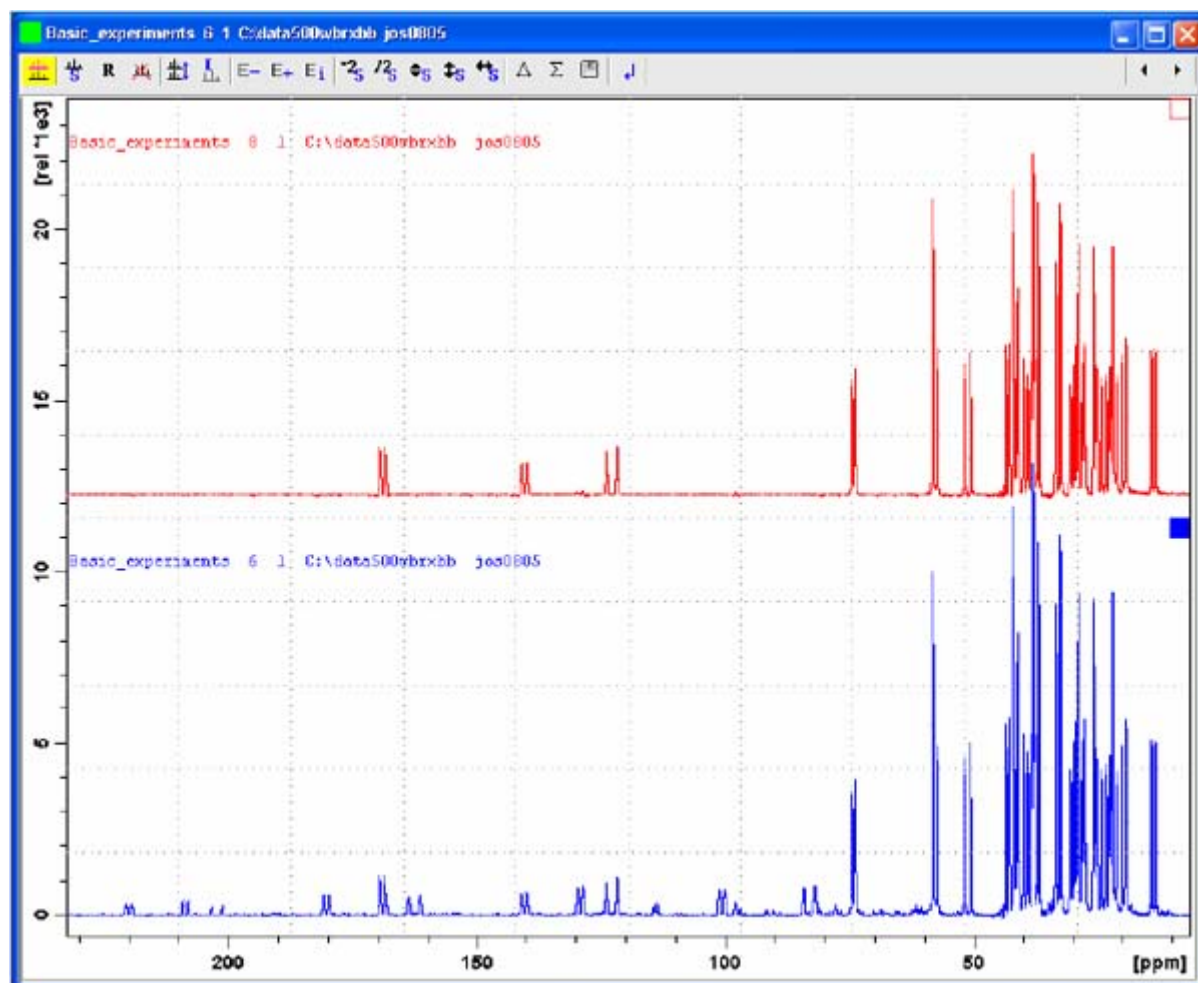


Figure 6.8. Cholesterylacetate Spectrum Using Sideband Suppression

**Figure 6.8.** is a cholesterylacetate spectrum using sideband suppression with the SELTICS sequence at 5 Hz sample rotation (upper spectrum). The lower spectrum is the CPMAS spectrum at 5 kHz sample rotation.

**Non-Quaternary Suppression (NQS)**

6.4

The NQS experiment is a simple spectral editing experiment. It relies on the fast dephasing of rare spins coupled to  $^1\text{H}$  spins through the hetero-nuclear dipolar interaction. For the dephasing delay  $d_3$  one uses between 30 and 80  $\mu\text{s}$ .

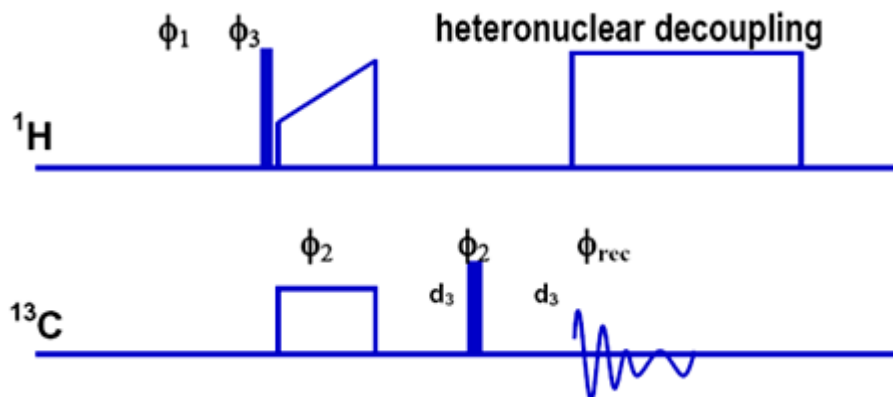


Figure 6.9. Block Diagram of the Non-quaternary Suppression Experiment

The **non-quaternary suppression** experiment is also called the **dipolar dephasing** experiment.

Use glycine or tyrosine spinning at 11 kHz as before.

Table 6.3. Acquisition Parameters

Parameter	Value	Comments
<b>pulprog</b>	cpnqs, cptoss_nqs	
<b>p2</b>		180° pulse on X nucleus.
<b>p11</b>		Power level driving P2 on X-channel.
<b>d3</b>	30 – 80 $\mu\text{s}$	Dephasing delay.

CP 5 kHz sample rotation  
dipolar dephasing



Current Data Parameters  
NAME: class2004\_sep  
EXPNO: 10  
PROCNO: 1

F2 - Acquisition Parameters  
Date: 20040920  
Time: 12:19  
DMECH3D: 4000 Hz  
PRGRND: 6 mm MAS 90/90  
PULPROG: cpmrg3vaw  
TD: 2048  
TELLV: 10 ms  
SF: 0  
DR: 0  
FID: 37878.769 Hz  
AQ: 18.495502 Hz  
RG: 0.027000 sec  
TDZ: 128  
IM: 13,200 usec  
EW: 4.00 usec  
DW: 2.00 K  
CR3T31: 5000.000000 sec  
D1: 5.00000000 sec  
D2: 0.0004000 sec  
d3: 0.00019200 sec  
LS: 1  
d13: 0.00015200 sec

CHANNEL f1  
PC1: 13C  
P15: 2000.00 usec  
P2: 0.00 usec  
P61: 2.20 dB  
P611: 2.20 dB  
RF01: 125.7693058 MHz

CHANNEL f2  
CPDP02: spinal64  
M0C0: 1W  
M1: 2.00 usec  
p30: 4.40 usec  
P11: 4.00 usec  
P612: 3.30 dB  
P62: 5.50 dB  
P622: 500.00078500 MHz  
RF0A00: 125.7693058 MHz  
RF0A10: 0.500  
RF0F00: 0.00 Hz

F2 - Processing parameters  
SI: 4096  
SF: 125.7477310 MHz  
WDW: No  
SSB: 0.00 Hz  
LB: 0.00 Hz  
GB: 0  
PC: 0.20

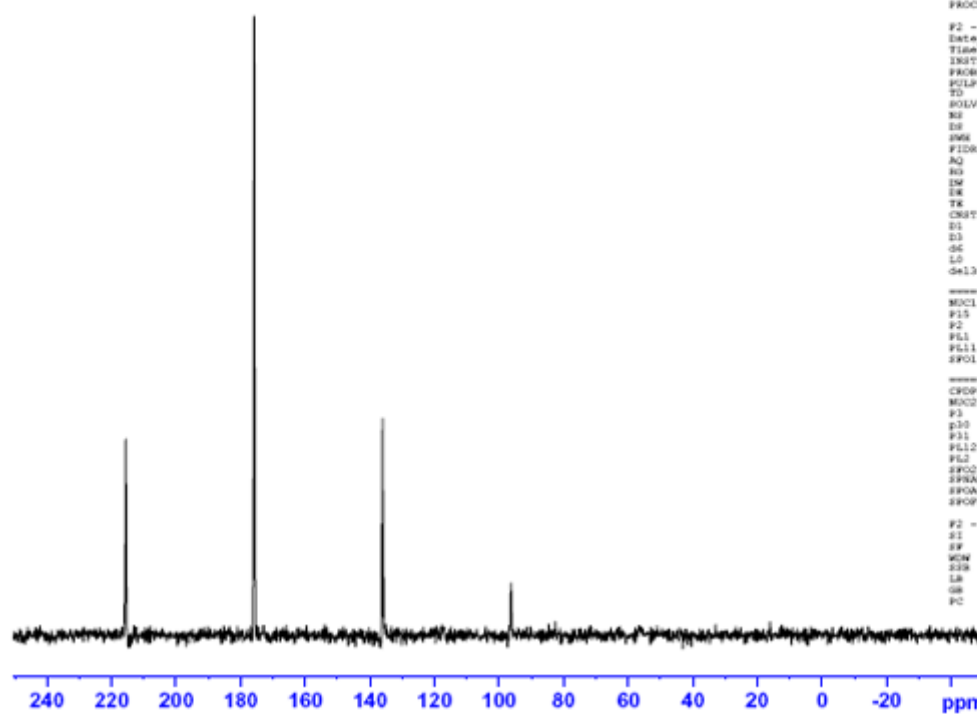


Figure 6.10. Glycine  $^{13}\text{C}$  CPMAS NQS Experiment with a Dephasing Delay

**Figure 6.10.** is a glycine  $^{13}\text{C}$  CPMAS NQS experiment with a dephasing delay  $d3 = 40 \mu\text{s}$  so that the total dephasing time is  $80 \mu\text{s}$ . Spinning sidebands are still visible.

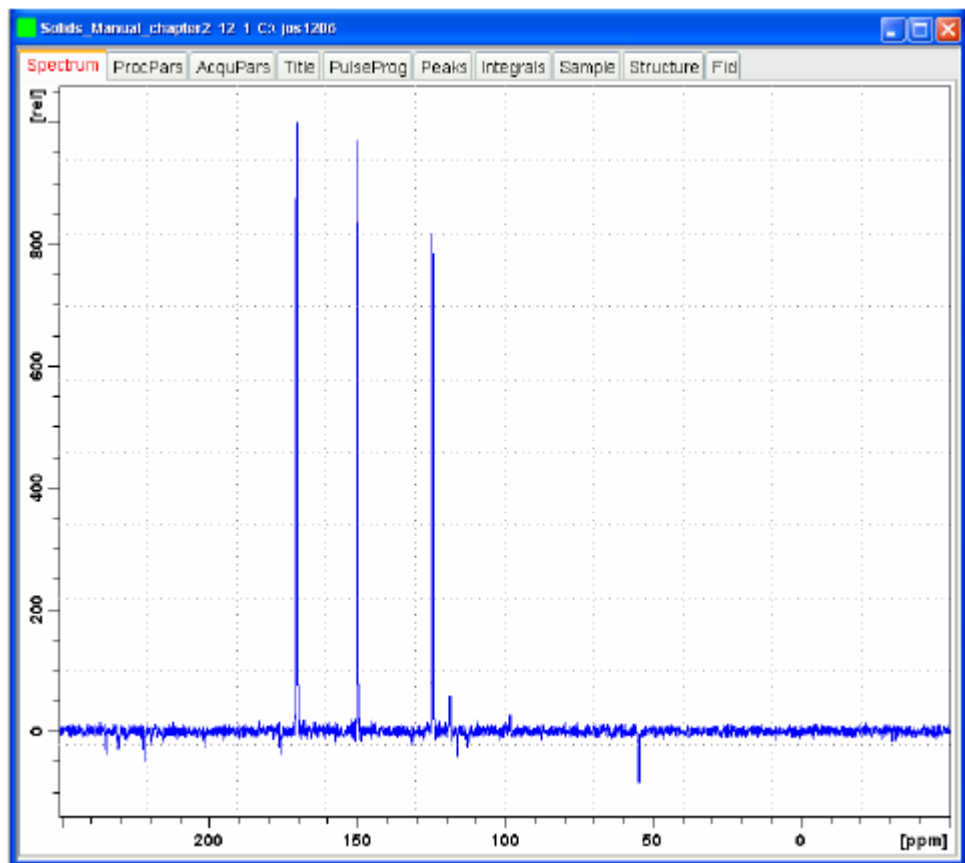


Figure 6.11. Tyrosine  $^{13}\text{C}$  CPMAS NQS Experiment with TOSS

**Figure 6.11.** is a tyrosine  $^{13}\text{C}$  CPMAS NQS experiment with TOSS using a dephasing delay  $d3 = 60 \mu\text{s}$ . Spinning sidebands are suppressed for a clean spectrum. In this experiment the total dephasing time is 20  $\mu\text{s}$  shorter than that used for the CPNQS experiment on glycine in **Figure 6.10.**

These spectral editing sequences help to distinguish CH, CH<sub>2</sub>, CH<sub>3</sub> and quaternary carbons in <sup>13</sup>C spectra. Common to all are various polarization and depolarization times, which properly mixed and combined give a series of spectra, which can be added and subtracted in order to obtain the various sub-spectra. All these sequences use constant-amplitude CP, which should be adjusted for maximum signal intensity. For the CPPI and CPPISPI sequences, the only parameter needed in addition to the CP parameters is **p16**, for which a good starting value is 40  $\mu$ s to give null signal for CH, negative signal for CH<sub>2</sub>, and positive signal for C and CH<sub>3</sub>. If necessary, this value can be optimized on a sample similar to the sample of interest for better editing. **p17**, for the repolarization step in the CPPIRCP experiment, is about 10 – 20  $\mu$ s.

For this experiment to succeed reliably, one should use moderate spinning speeds around (up to) 10 kHz. At slow rotation rates, no advantage was found in measuring the exact HH match. Running the experiment at constant amplitude CP, optimized for maximum signal, proved to be sufficient.

### References for these experiments

1. X. Wu, K. Zilm, *Complete Spectral Editing in CPMAS NMR*, J. Magn. Reson. A 102, 205-213 (1993);
2. X. Wu, K. Zilm, *Methylene-Only Subspectrum in CPMAS NMR*, J. Magn. Reson. A 104, 119-122 (1993);
3. X. Wu, S.T. Burns, K. Zilm, *Spectral Editing in CPMAS NMR. Generating Subspectra Based on Proton Multiplicities*, J. Magn. Reson. A 111, 29-36 (1994);
4. R. Sangill, N. Rastrup-Andersen, H. Bildsoe, H.J. Jakobsen, and N.C. Nielsen, *Optimized Spectral Editing of <sup>13</sup>C MAS NMR Spectra of Rigid Solids Using Cross-Polarization Methods*, J. Magn. Reson. A 107, 67-78 (1994).

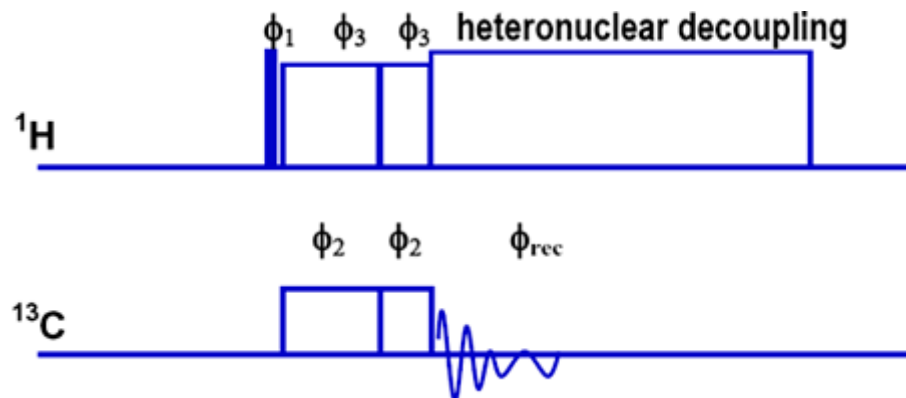


Figure 6.12. Block Diagram of the CPPI Experiment.

Typical pulse widths for the second part of the CP pulse with the phase inversion are 40  $\mu$ s.

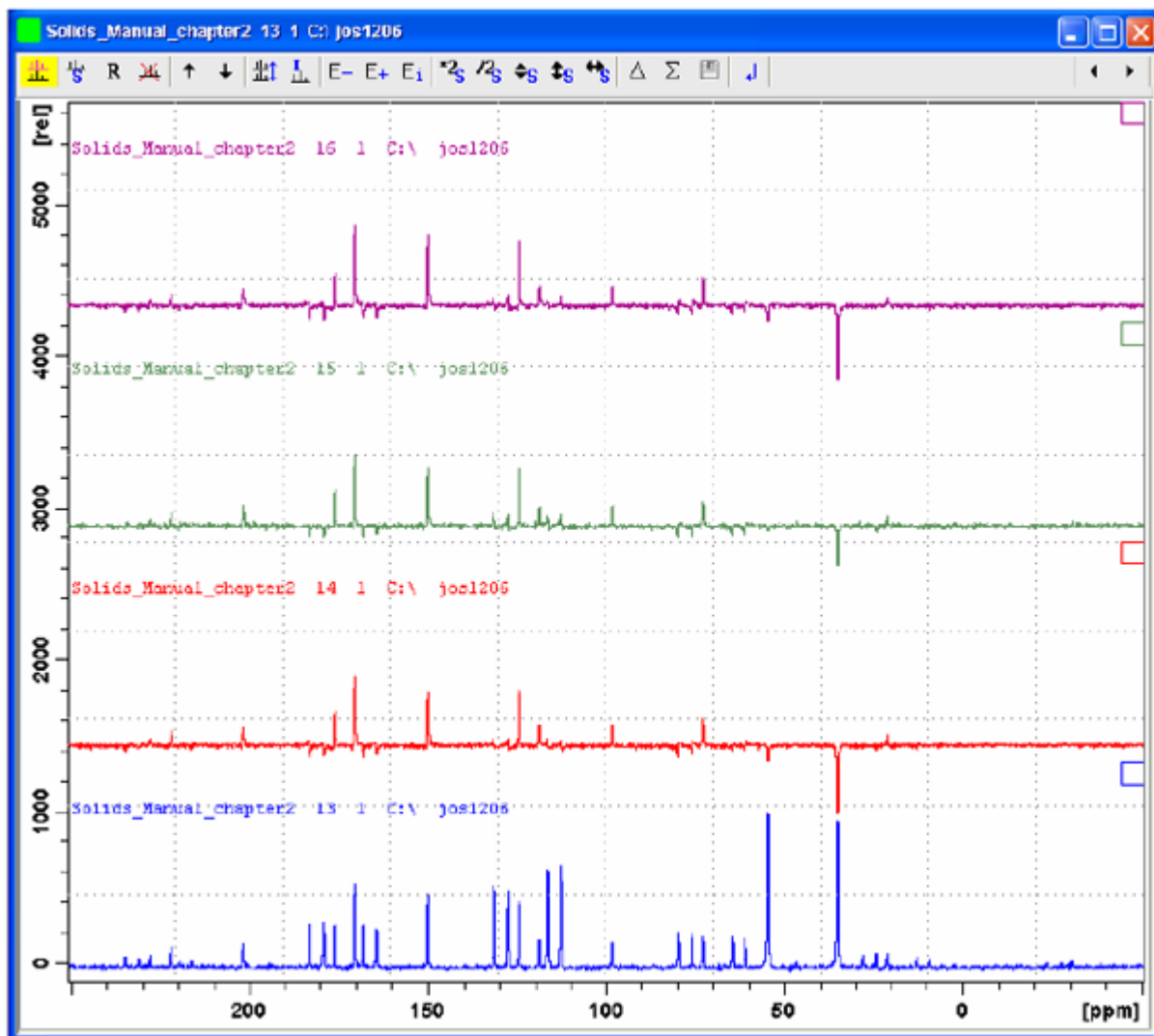


Figure 6.13. CPMAS Spectrum of Tyrosine.HCl at 6.5 kHz

CPMAS spectrum of tyrosine.HCl at 6.5 kHz sample rotation obtained on a 500 WB spectrometer using a 4 mm CPMAS double resonance probe. The red (third) spectrum is a CPPI spectrum where we see the  $\text{CH}_2$  resonance at 35 ppm with a negative intensity. The aromatic CH resonances are clearly suppressed, where the  $\text{C}_a$  shows a slightly negative intensity. The polarization inversion pulse  $p_{16}$  was 40  $\mu\text{s}$  long. The green (second) spectrum is a CPPIRCP experiment with  $p_{16}=40 \mu\text{s}$  and  $p_{17}=10 \mu\text{s}$  for better nulling of CH resonances, but in this case the aromatic CH resonances gained some intensity back. The purple (first) spectrum is a CPPISPI experiment with a similar performance as for the CPPI spectrum. Our experience is that one can adjust  $p_{15}$  (= 1 ms in this spectrum),  $p_{16}$  (= 30  $\mu\text{s}$  in the purple spectrum) and so edit for pure CH resonances for example. Such tuning needs to be done of course on a known sample, which behaves similarly to the one under investigation, for the editing to be conclusive and correct.

**Note:** For more editing experiments consider the **Solid State Attached Proton Test** experiment, using the *sostapt* pulse program name, or look at 2D editing sequences, based on the FSLG HETCOR experiment.



## Introduction

7.1

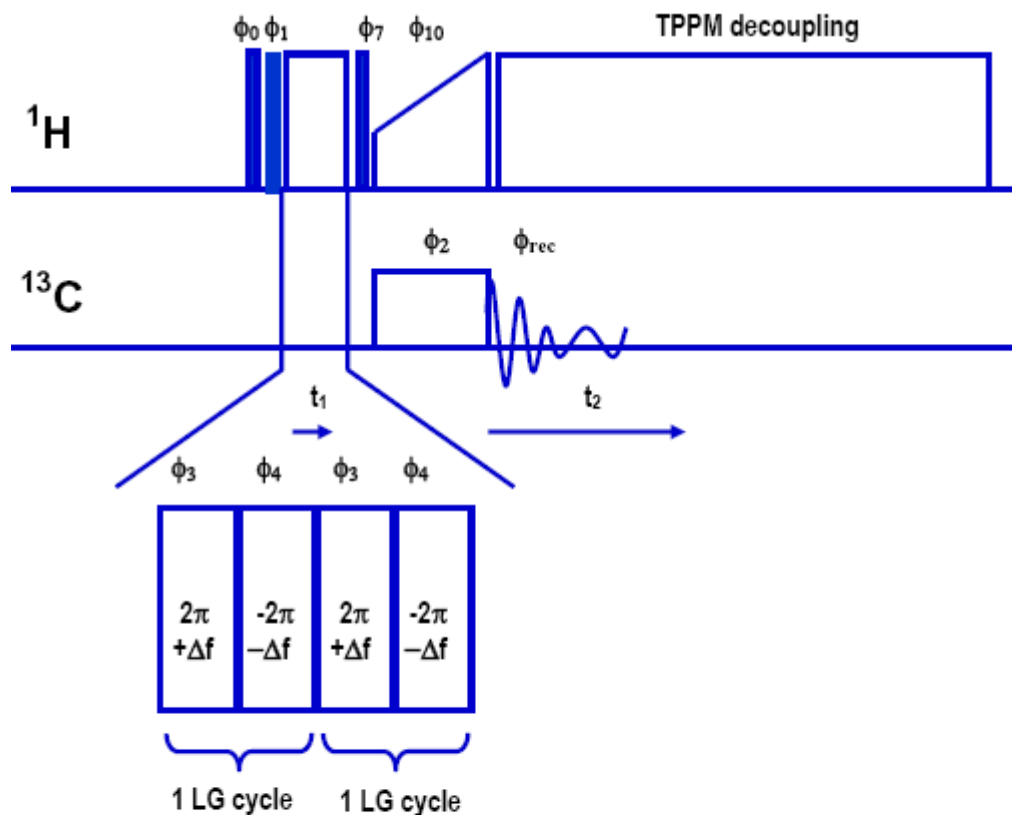
This chapter discusses setup and use of the Frequency Switched Lee Goldburg **hetero-nuclear Correlation** (FSLG HETCOR) experiment.

The FSLG Hetcor experiment correlates  $^1\text{H}$  chemical shifts with X-nuclei (e.g.  $^{13}\text{C}$ ,  $^{15}\text{N}$ ) chemical shifts. The experiment provides excellent  $^1\text{H}$  resolution in the indirect dimension. Homonuclear decoupling in the  $^1\text{H}$  evolution period is achieved with an FSLG pulse train. FSLG permits relatively high spinning speeds and makes this experiment available for high field systems, requiring high spinning speeds in order to move spinning sidebands out of the spectral region. Decoupling the protons from the coupled X-nucleus during evolution is not essential, since the high spinning speed already achieves that. One can however improve the hetero-nuclear decoupling by a  $\pi$ -pulse in the middle of the evolution period (see A. Lesage et. al.).

Mixing is achieved during the cross polarization contact time. Since magnetization transfer from protons to X (e.g.  $^{13}\text{C}$ ) occurs rapidly, contact times should be kept short in order to avoid long range transfer, leading to unspecific cross peak patterns since the magnetization then has time to flow from any proton to any X-nucleus. A modification of the basic sequence uses cross polarization under a LG frequency offset for the protons. In this case, the proton magnetization detected by the X-nucleus comes from close protons only, since the proton spin lock at an LG offset interrupts the “communication” between the proton spins. A third modification of the basic sequence uses phase modulated pulses instead of frequency shifts. These three modifications to the basic sequence are described in [\*\*“Modifications of FSLG HETCOR”\*\*](#).

## References:

- H.J.M. deGroot, H. Förster, and B.-J. van Rossum, *Method of Improving the Resolution in Two-Dimensional hetero-nuclear Correlation Spectra of Solid State NMR*, United States Patent No 5,926.023, Jul. 20, 1999.
- B.-J. van Rossum, H. Förster, and H.J.M. deGroot, *High-field and high-speed CP-MAS  $^{13}\text{C}$  NMR hetero-nuclear dipolar-correlation spectroscopy of solids with frequency-switched Lee-Goldburg Homo-nuclear decoupling*, J. Magn. Reson. A 120, 516-519 (1997).
- B.-J. van Rossum, *Structure refinement of photosynthetic components with multidimensional MAS NMR dipolar correlation spectroscopy*, Thesis, University of Leiden, Holland; (2000).
- B.-J. van Rossum, C.P. deGroot, V. Ladizhansky, S. Vega, and H.J.M. deGroot, *A Method for Measuring hetero-nuclear ( $^1\text{H}$ - $^{13}\text{C}$ ) Distances in High Speed MAS NMR*, J. Am. Chem. Soc. 122, 3465-3472 (2000).
- D.P. Burum and A. Bielecki, *An Improved Experiment for hetero-nuclear-Correlation 2D NMR in Solids*, J. Magn. Res. 94, 645-652 (1991).
- A. Lesage and L. Emsley, *Through-Bond hetero-nuclear Single-Quantum Correlation Spectroscopy in Solid-State NMR, and Comparison to Other Through-Bond and Through-Space Experiments*, J. Magn. Res. 148, 449-454 (2001).



$\phi_0 = 13 + \text{STATES-TPPI } (t_1)$	$\phi_1 = 1$	$\phi_{10} = 0$
$\phi_2 = 00221133$	$\phi_4 = 2 \text{ (-LG)}$	$\phi_3 = 0 (+LG)$
$\phi_7 = 3$	$\phi_{rec} = 02201331$	

Figure 7.1. The FSLG Hetcor Experiment

The FSLG Hetcor experiment consists of 3 basic elements, the Homo-nuclear decoupling sequence during which the <sup>1</sup>H chemical shifts evolve, the cross polarization sequence, during which the information of the <sup>1</sup>H spin magnetization is transferred to the X-spins, followed by observation of the X-spins under proton decoupling.

1. This experiment requires a probe of 4mm spinner size or smaller. One can run it on a 7 mm probe, but the results will not be very convincing.
2. Start from a data set with well adjusted cross polarization and proton decoupling at fairly high RF-fields. Unlike standard multiple pulse decoupling, which only works well at very high RF-fields, FSLG requires only moderately high RF fields. Decent performance is achieved at 80-100 kHz proton field. At lower magnetic fields (200-300 MHz proton frequency) lower RF-fields are adequate, RF fields of 100 kHz and higher perform better at higher magnetic fields (500 MHz and up).
3. Insert a suitable test sample, spin at a suitable speed. We recommend  $^{13}\text{C}$  labeled tyrosine hydrochloride, since it has a wide spread (2.5-12ppm) of proton shifts, a short proton  $T_1$ , a well resolved  $^{13}\text{C}$ -spectrum with quite many lines, and it is readily available. The unlabeled sample can also be used, but requires a few more scans (8-32).
4. Optimize the spin rate such that no overlap occurs between center- and sidebands (especially with the labeled sample, in order to avoid rotational resonance broadening). Re-optimize decoupling and HH-condition. Check the proton RF-field via the proton 90° pulse **p3**. Set **pl13 = pl12**, set **cnst20** to RF-field in Hz as calculated from **p3**.
5. Generate a new data set with **edc, new**. Set pulprog **Ighetfq** and change to a 2D parameter set using the “123” button in **eda**. Set **FnMode** to STATES-TPPI. Type **ased** or click the pulse symbol in **eda**.



Figure 7.2. The “12..” icon, and the **ased** icon in **eda**.

6. Performing **ased** will show all parameters which are essential for the acquisition, not all available parameters. In addition, it performs calculations which are specified in the pulse program. Note that all parameters which are calculated are not editable, and will show only, if explicitly used during the main pulse program between ze and exit. In this sequence, the proton chemical shift evolution is influenced by the RF field (**cnst20**) under which the shifts evolve and the type of Homo-nuclear decoupling sequence (FSLG in this case) which scales chemical shifts (by about 0.578 in this case). In order to obtain proton chemical shifts at the standard scale, both parameters are taken into account and an increment along F1 is calculated which yields correct chemical shifts for protons. Transfer this increment to **IN\_F1** in **eda** (**A** button in **ased**). This will set the sweep width along F1. Note that the time increment here is generated by a loop counter, counting the periods of FSLG. The loop counter **I3** is used to multiply this increment. Usually, I3 is set to 2-4 in order to reduce the F1 sampling width to a reasonable value. **Cnst24** is usually set to -1000 - -2000 in order to move the spectrum away from the center ridge in F1.

		Installed probe: 4 mm MAS BB1H H13762/0001	
General	▼ General		
Channel f1	PULPROG	lghetfq	... E Pulse program for acquisition
Channel f2	TD	1594	Time domain size
	NS	4	Number of scans
	DS	0	Number of dummy scans
	SWH [Hz]	50000.00	Sweep width in Hz
	AQ [s]	0.0169300	Acquisition time
	RG	128	Receiver gain
	DW [ $\mu$ s]	10.000	Dwell time
	DE [ $\mu$ s]	10.00	Pre-scan-delay
	CNST11	1.0000000	To adjust t=0 for acquisition, if digmod = base
	CNST20	100000.0000000	LG-RF field as adjusted, in Hz used to calculate
	CNST24	-2000.0000000	Offset for proton evolution under LG, usually 0
	D1 [s]	2.0000000	Recycle delay
	in0 [s]	0.00005664	$in0=(0.578713747294/360)*cnst20$
	ID	0	L0=0
	L3	3	For dwell in t1 = $4\pi pS^2 \cdot 10^{-6} \cdot 0.578$
	count	64	Count=tD1/2
	dwellf1 [s]	0.00005664	Dwellf1=in0
▼ Channel f1			
	blktr1 [ $\mu$ s]	2.00	Blktr1=2u
	NUC1	13C Edit...	Nucleus for channel 1
	P15 [ $\mu$ s]	300.00	Contact pulse - short 50 - 200 us
	PL1 [dB]	4.50	For X contact pulse
	PL1W [W]	104.27685968	For X contact pulse
	SFO1 [MHz]	150.9220830	Frequency of observe channel
▼ Channel f2			
	blktr2 [ $\mu$ s]	1.00	Blktr2=1u
	cnst21	0.000000	Cnst21=0
	cnst22	68710.679688	Cnst22=cnst20/sqrt(2)+cnst24
	cnst23	-72710.679688	Cnst23=-cnst20/sqrt(2)+cnst24
	CPDPRG2	spinal64	... E Tppm15, SPINAL64
	NUC2	1H Edit...	Nucleus for channel 2
	P3 [ $\mu$ s]	2.20	90 degree 1H pulse excitation
	p5 [ $\mu$ s]	8.17	$P5=((294/360)\cdot(cnst20))^2 \cdot 10^{-6}$
	PCPD2 [ $\mu$ s]	4.20	Pulse length in decoupling sequence
	PL2 [dB]	7.00	=120dB, not used
	PL2W [W]	47.41231155	=120dB, not used
	PL12 [dB]	6.00	For decoupling and excitation 1H
	PL12W [W]	59.68856430	For decoupling and excitation 1H
	PL13 [dB]	6.00	For homonuclear decoupling
	PL13W [W]	59.68856430	For homonuclear decoupling
	pul54 [ $\mu$ s]	1.34	$Pul54=(p3^2 \cdot 547) \cdot 900$
	SFO2 [MHz]	600.1500000	Frequency of observe channel
	SP0 [dB]	6.10	Proton power level during contact
	SP0W [W]	56.32986739	Proton power level during contact
	SPNAM0	Ramp70100.100	... E Shape for contact pulse ramp.100
	SPOAL0	0.500	Phase alignment of freq. offset in SPO
	SPOFFSO [Hz]	0.00	Offset frequency for SPO

Figure 7.3. The aed Display

In the figure above the frequency offsets for the FSLG part are shown as ***cnst22***, ***cnst23***. They are different because ***cnst24*** shifts the center frequency by 2000 Hz.

Table 7.1. Acquisition Parameters for FSLG-HETCOR (on tyrosine-HCl)

Parameter	Value	Comments
<b>pulprog</b>	lghetfq	FSLG program.
<b>nuc1</b>	13C	
<b>o1p</b>	100 ppm	
<b>nuc2</b>	1H	
<b>cnst20</b>	70-100000	Proton spin nutation frequency with PL13.
<b>cnst24</b>	0 - -2000	Place carrier off during evolution.
<b>pl1</b>		Power level channel 1 for contact pulse.
<b>pl12</b>		Power level channel 2 TPPM/SPINAL decoupling.
<b>pl13</b>		Power level channel 2 FSLG decoupling.
<b>sp0</b>		Power level channel 2 for contact pulse.
<b>spnam0</b>	ramp.100 or simil.	Shape for contact pulse channel f2.
<b>p3</b>	2.5 – 3 $\mu$ sec	90° pulse channel 2 at pl12.
<b>p15</b>	50 -500 $\mu$ sec	Contact pulse width.
<b>pcpd2</b>	$\approx 2*p3-0.2$	SPINAL64 /TPPM decoupling pulse.
<b>cpdprg2</b>	SPINAL64/TPPM15	Decoupling sequence.
F1 1H indirect		
<b>I0</b>	0	Start value 0, incremented during expt..
<b>I3</b>	2- 4	Multiples of FSLG-periods, increment per row.
<b>in_f1</b>	=in0 as calculated	Set according to value calculated by ased.
F2 13C acquisition		
<b>d1</b>	2s	Recycle delay.
<b>sw</b>	310ppm	Sweep width direct dimension.
<b>aq</b>	16-20 msec	
<b>masr</b>	10-15000 Hz	At 100 kHz RF, 15 kHz is ok.

Table 7.2. Processing Parameters for FSLG-HETCOR (on tyrosine-HCl)

Parameter	Value	Comment
F2 direct dim 13C		
<i>si</i>	2-4 k	
<i>wdw</i>	QSINE	SSB 2, 3 or 5
<i>ph_mod</i>	pk	
F1 indirect 1H		
<i>si</i>	256-1048	
<i>mc2</i>	STATES-TPPI	
<i>wdw</i>	QSINE	
<i>ssb</i>	3, 5	
<i>ph_mod</i>	pk	

A full plot of a FSLG-HETCOR on labeled tyrosine-HCl is shown in the next figure.

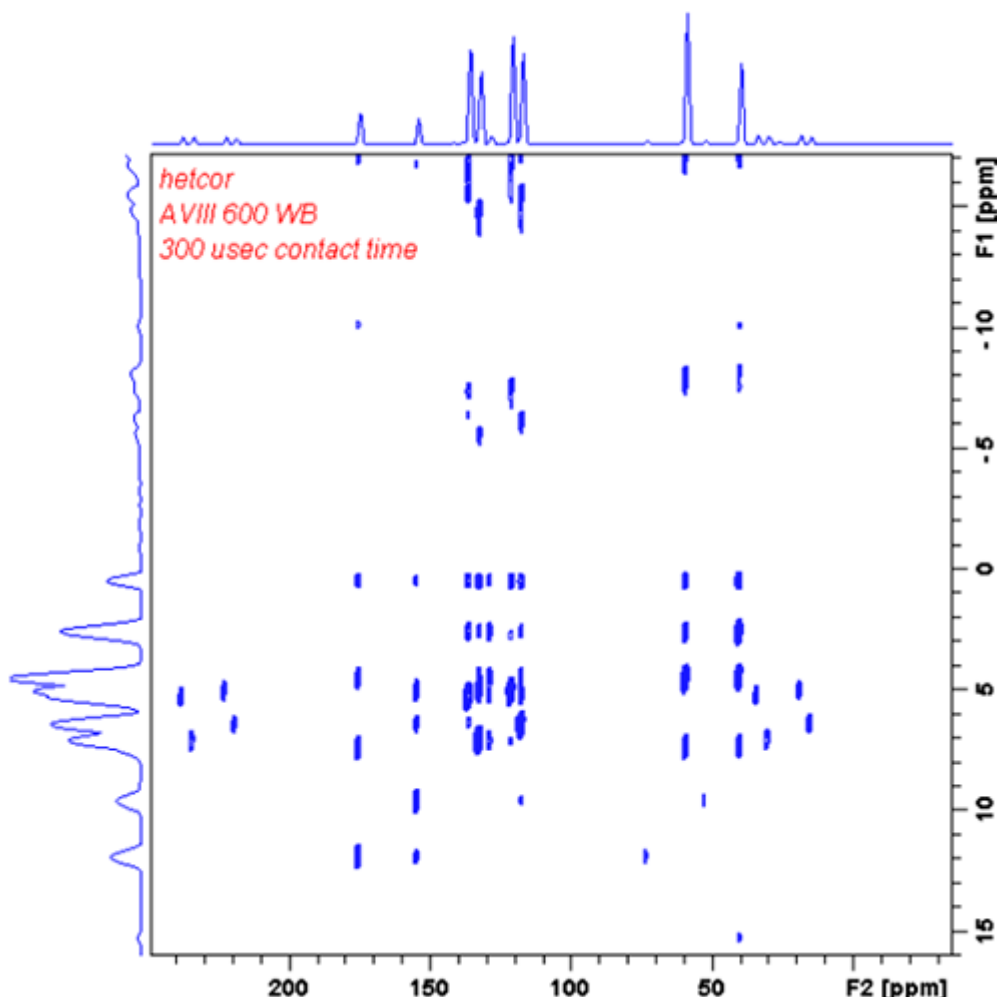


Figure 7.4. FSLG Hetcor Spectrum Tyrosine HCl

The figure above shows a FSLG Hetcor Spectrum Tyrosine HCl with parameters as shown in [Table 7.1](#)/[Table 7.2](#). Full transform with slight resolution enhancement,  $qsine/SSB=3$ . Proton shifts calibrated as 2.5 and 12 (most high field/low field peak). Center ridge at 0 ppm along F1 is spin locked signal which does not follow the FSLG-evolution. **Cnst24** is used to separate the proton spectrum from this ridge. The contact time of 300  $\mu$ sec shows many long range couplings. The next figure shows the region of interest excluding the center ridge and the spinning sidebands.

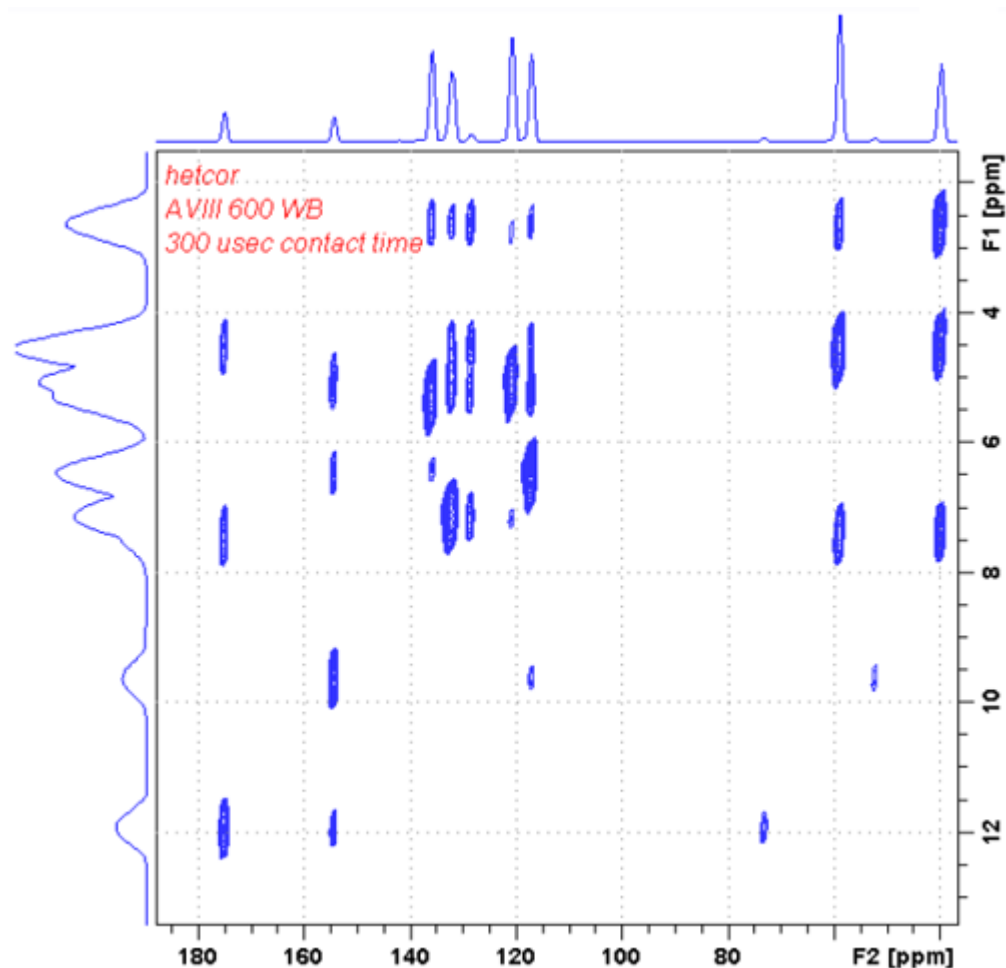


Figure 7.5. FSLG Hetcor Spectrum Tyrosine HCl

The figure above shows a FSLG Hetcor Spectrum Tyrosine HCl with parameters as shown in [Table 7.1](#)/[Table 7.2](#). Full transform with slight resolution enhancement, qsine/SSB=3. Proton shifts calibrated as 2.5 and 12 (most high field/low field peak). Expansion plot.

# **Modifications of FSLG HETCOR**

**8**

The basic HETCOR sequence can be improved in several respects. The protons which are observed are all coupled to  $^{13}\text{C}$  carbons (since we observe these). So the proton shifts evolve also under the residual dipolar coupling and the J-coupling to  $^{13}\text{C}$ . This can be refocused by a  $^{13}\text{C}$   $\pi$ -pulse in the middle of the proton evolution. The pulse program ***Ighettqpi*** will serve this purpose.

Furthermore, it may be desirable to compare the proton shift spectrum obtained with X-observation (HETCOR) with the proton spectrum obtained by CRAMPS techniques (see chapters 22, 23, and 24), observing the protons directly. Usually, these experiments use phase modulated shapes (PMLG or DUMBO). In order to make both experiments comparable, it is favored to use the same type of proton shift evolution in both sequences. The pulse programs which use phase gradient shapes to achieve Homo-nuclear proton dipolar decoupling are ***pmlghet*** and ***wpmIghet***. If DUMBO decoupling is desired, the pulse programs are **dumbohet** or **edumbohet**. These pulse programs use either windowless pulse trains, or windowed pulse trains which can be timed in exact analogy to the CRAMPS-type sequences **wpmIg\*2** and **dumbo\*2**. These sequences also suppress the center ridge efficiently so that the carrier frequency need not be shifted out of the proton range during evolution (**cnst24=0**). In contrary, it is possible to shift the carrier to the proton shift range center.

A third modification addresses the problem of poor discrimination between sites which are strongly and weakly coupled to protons. In the standard sequence this is solely achieved setting contact times short. Of course, this reduces cross peaks from remote couplings more than it reduces cross peaks from directly bonded protons. However, the remote couplings are always present through the Homo-nuclear coupling between all protons. These couplings can however be suppressed by executing the contact with a Lee-Goldburg proton offset. Then the protons are Homo-nuclear decoupled, and the transfer from protons to X only follows the hetero-nuclear dipolar coupling between those. The pulse program ***Ighetfqlgcp*** works completely in analogy to ***Ighetfq***, but executes the contact at a proton offset calculated from the proton RF field during the spin lock contact pulse. This modifies the HH condition, which must be reestablished using the pulse program **lgcp**.

In the following sections, the specifics of these modified sequences are discussed.

***Carbon Decoupling During Evolution***

The only difference between ***Ighetfq*** and ***Ighetfqli*** is the decoupling  $\pi$ -pulse at the center of the evolution period. All what needs to be set in addition is the X-  $\pi$ -pulse ***p2*** at power level ***p1***. At fast spin rates and in fully labeled samples, the narrowing effect on the proton spectrum may be small or not noticeable, but on samples with natural abundance it may be noticeable. At long contact times and transfer from many different protons, the line width in the proton spectrum may also be insensitive. In fig. 1, two columns through the most up field aliphatic peak in tyrosine-HCl are shown. The  $\pi$ -decoupled trace (red) is clearly narrower.

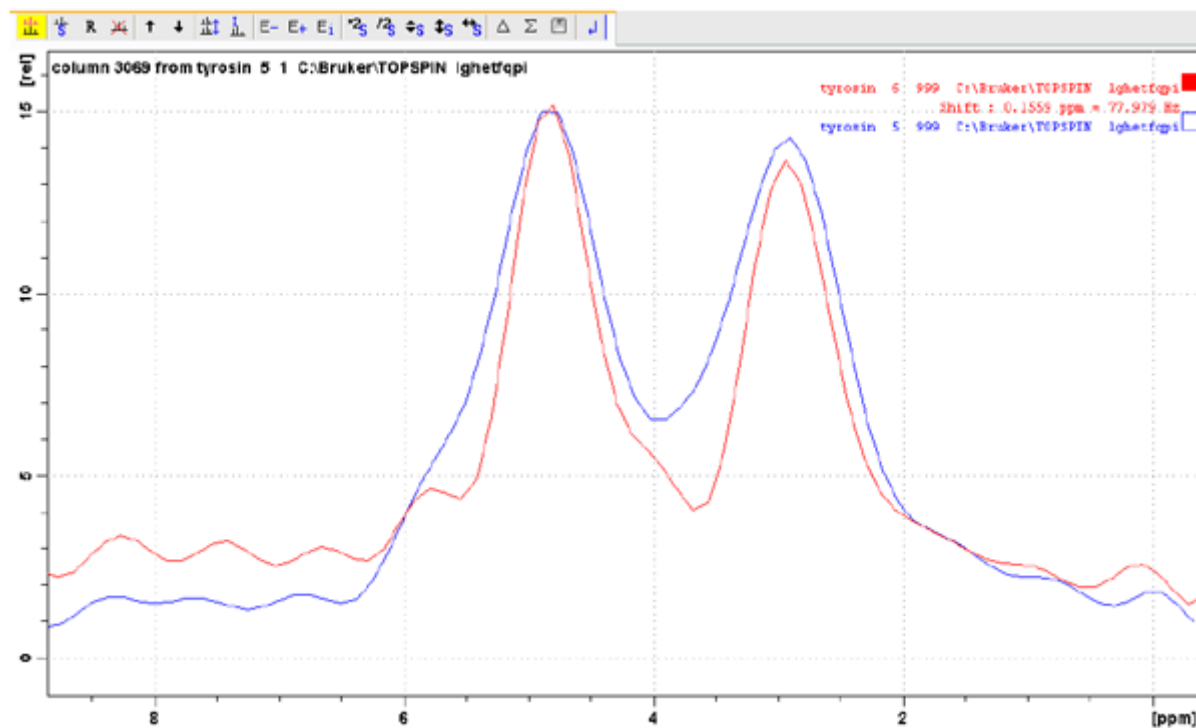


Figure 8.1. Comparison of HETCOR with and without  $^{13}\text{C}$ -decoupling

The figure above shows a comparison of HETCOR with and without  $^{13}\text{C}$ -decoupling. Natural abundance tyrosine-HCl was run with 50  $\mu\text{sec}$  contact time.

**Reference:**

- A. Lesage and L. Emsley, *Through-Bond hetero-nuclear Single-Quantum Correlation Spectroscopy in Solid-State NMR, and Comparison to Other Through-Bond and Through-Space Experiments*, J. Magn. Res. 148, 449-454 (2001).

**HETCOR with DUMBO, PMLG or w-PMLG, Using Shapes****8.2**

These sequences use phase modulated shapes for Homo-nuclear proton decoupling. Apart from some smaller differences, the sequences are in complete analogy to the HETCOR sequence using frequency shifts.

The only differences between these sequences lie in the length and type of shape used for Homo-nuclear decoupling. DUMBO and e-DUMBO (Emsley et al.) use principles known from multiple pulse NMR operating on resonance, whereas pmlg and w-pmlg (Vega et al.) use phase ramps which act like frequency offsets and are therefore derivatives of FSLG.

**References:**

- D. Sakellariou, A. Lesage, P. Hodgkinson and L. Emsley,  
*Homo-nuclear dipolar decoupling in solid-state NMR using continuous phase modulation*, Chem. Phys. Lett. 319, 253 (2000).
- Vinogradov, E.; Madhu, P. K.; Vega, S., *High-resolution proton solid-state NMR spectroscopy by phase-modulated Lee-Goldburg experiment*, Chem. Phys. Lett. (1999), 314(5,6), 443-450.
- E. Vinogradov, P.K. Madhu and S. Vega, *Proton Spectroscopy in Solid State NMR with Windowed Phase Modulated Lee-Goldburg Decoupling Sequences*, Chem. Phys. Lett. (2002), 354, 193.
- Leskes, Michal; Madhu, P. K.; Vega, Shimon, *A broad banded z-rotation windowed phase-modulated Lee-Goldburg pulse sequence for  $^1\text{H}$  spectroscopy in solid state NMR*, Chem. Phys. Lett. (2007), 447, 370-374.
- Leskes, Michal; Madhu, P. K.; Vega, Shimon, *Supercycled Homo-nuclear decoupling in solid state NMR: towards cleaner  $^1\text{H}$  spectrum and higher spinning rates*, J. Chem. Phys. (2007) in press.

**The Sequence pmlghet****8.2.1**

This sequence uses windowless phase ramped shapes. One can write these shapes as multiples of FSLG cycles to manipulate the length of the  $T_1$ -increment. Usually, 2 FSLG cycles make sense. The pulse program calculates the required shape pulse length from the RF-field during the FSLG-evolution. In pmlghet, a shape with 2 cycles is assumed in the calculation. The sequence is optimized for a simple twofold linear phase ramp (supplied as *Igs-2*). The carrier may be placed in the middle of the proton spectrum during evolution which may allow using fewer increments and therefore saving time. However, one should be aware of the presence of proton spinning sidebands along F1 which may inappropriately fold in if the spectrum window along F1 is chosen too small.

Processing is done in complete analogy to the FSLG-experiment, as for all following sequences.

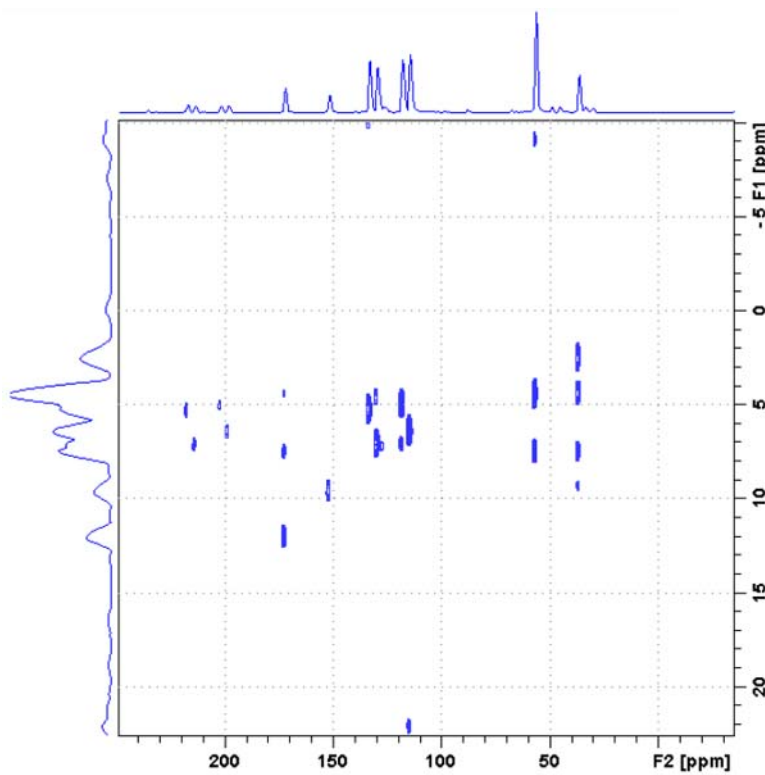


Figure 8.2. HETCOR Using Windowless Phase Ramps

The figure above shows the HETCOR using windowless phase ramped shapes for proton Homo-nuclear decoupling during evolution. The carrier was placed in the middle of the proton spectrum and the usual carrier ridge was suppressed by phase cycling (Leskes et al., Chem. Phys. Lett.). This allows reduced measurement times. Pmlghet, wpmlghet, dumbohet and edumbohet should give rather similar spectra.

Table 8.1. Acquisition Parameters for pmlg-HETCOR (on tyrosine-HCl)

Parameter	Value	Comments
<b>pulprog</b>	pmlghet	Using phase ramps.
<b>nuc1</b>	13C	
<b>o1p</b>	100 ppm	
<b>nuc2</b>	1H	
<b>cnst20</b>	80-100000	Proton spin nutation frequency with PL13.
<b>cnst24</b>	1000-3000	Place carrier within proton spectrum for evolution.
<b>pl1</b>		Power level channel 1 for contact pulse.
<b>pl12</b>		Power level channel 2 TPPM/SPINAL decoupling.
<b>pl13</b>		Power level channel 2 PMLG decoupling.

Table 8.1. Acquisition Parameters for pmlg-HETCOR (on tyrosine-HCl)

<b>sp0</b>		Power level channel 2 for contact pulse.
<b>spnam0</b>	ramp.100 or similar	Shape for contact pulse channel f2.
<b>sp1</b>	set to pl13	To match cnst20.
<b>spnam1</b>	lgs-2	To match ppg calculation of in0, in_f1.
<b>p3</b>	2.5 – 3 $\mu$ sec	90° pulse channel 2 at pl12.
<b>p15</b>	50 -500 $\mu$ s	Contact pulse width.
<b>pcpd2</b>	$\approx 2*p3$	SPINAL64 /TPPM decoupling pulse.
<b>cpdprg2</b>	SPINAL64/TPPM15	Decoupling sequence.
F1 $^1\text{H}$ indirect		
<b>I0</b>	0	Start value 0, incremented during expt.
<b>I3</b>	2- 4	Multiples of FSLG-periods, increment per row.
<b>in_f1</b>	=in0 as calculated	Set according to value calculated by <b>ased</b> .
F2 $^{13}\text{C}$ acquisition		
<b>d1</b>	2s	Recycle delay.
<b>sw</b>	310ppm	Sweep width direct dimension.
<b>aq</b>	16-20 msec	
<b>masr</b>	10-15 kHz	15 kHz ok at 100 kHz RF-field.

Table 8.2. Processing Parameters for pmlg-HETCOR (as for FSLG on tyrosine-HCl)

Parameter	Value	Comment
F2 direct dim $^{13}\text{C}$		
<b>si</b>	2-4 k	
<b>wdw</b>	QSINE	SSB 2, 3 or 5.
<b>ph_mod</b>	pk	
F1 indirect $^1\text{H}$		
<b>si</b>	256-1048	
<b>mc2</b>	STATES-TPPI	
<b>wdw</b>	QSINE	
<b>ssb</b>	3, 5	
<b>ph_mod</b>	pk	

If one wants to compare a solids proton spectrum, acquired via  $^{13}\text{C}$  detection (using HETCOR) and a direct detect proton spectrum (using w-pmlg), it is useful to do this using exactly the same parameters (power levels and timings) in both experiments. If w-pmlg is used and optimized for the direct detect experiment, the same parameters will work with w-pmlghet, provided that both experiments are done with the same probe.

*Table 8.3. Acquisition Parameters for wpmlg-HETCOR (on tyrosine-HCl)*

Parameter	Value	Comments
<b>pulprog</b>	wpmlghet	Phase ramp allows detection window.
<b>nuc1</b>	$^{13}\text{C}$	
<b>o1p</b>	100 ppm	
<b>nuc2</b>	1H	
<b>cnst20</b>	usually $\geq 100$ kHz	As prepared with wpmlgd proton detect exp.
<b>cnst24</b>	1000-3000	Place carrier within proton spectrum for evolution.
<b>pl1</b>		Power level channel 1 for contact pulse.
<b>pl12</b>		Power level channel 2 TPPM/SPINAL decoupling.
<b>pl13</b>		Power level channel 2 w-PMLG decoupling.
<b>sp0</b>		Power level channel 2 for contact pulse.
<b>spnam0</b>	ramp.100 or similar	Shape for contact pulse channel f2.
<b>sp1</b>	set to pl13	To match cnst20.
<b>spnam1</b>	m5m or m5p	Both include one FSLG cycle.
<b>p3</b>	2.5 – 3 $\mu\text{sec}$	90° pulse channel 2 at pl12.
<b>p15</b>	50 -500 $\mu\text{sec}$	Contact pulse width.
<b>pcpd2</b>	$\approx 2^*p3$	SPINAL64 /TPPM decoupling pulse.
<b>cpdprg2</b>	SPINAL64/TPPM15	Decoupling sequence.
F1 $^1\text{H}$ indirect		
<b>I0</b>	0	Start value 0, incremented during expt.
<b>I3</b>	2- 4	Multiples of FSLG-periods, increment per row.
<b>in_f1</b>	=in0 as calculated	Set according to value calculated by <b>ased</b> .
F2 $^{13}\text{C}$ acquisition		
<b>d1</b>	2s	Recycle delay.
<b>sw</b>	310ppm	sweep width direct dimension.
<b>aq</b>	16-20 msec	

DUMBO decoupling is as efficient as PMLG decoupling. As discussed in chapters 22 and 23, it requires to spin a bit slower (up to 12-13 kHz) and to place the carrier closer to resonance. The library of AU-programs in TopSpin includes **dumbo**, which calculates the desired shapes for windowed and windowless DUMBO shapes. If the windowless version is desired, the e-dumbo shape is preferred. Typing xau dumbo starts a dialog, in which e (for e-dumbo 22), 1 for the number of cycles, 64 for the number of steps, and 0 for an added angle (this value would be added to all phases in the shape). The program sets **p20** to 32  $\mu$ sec as default. This is appropriate for an RF field of 100 kHz. **Spnam2** is set to edumbo22\_1+0.

Table 8.4. Acquisition Parameters for e-DUMBO-HETCOR (on tyrosine-HCl)

Parameter	Value	Comments
<b>pulprog</b>	edumbohet	windowless dumbo shape.
<b>nuc1</b>	13C	
<b>o1p</b>	100 ppm	
<b>nuc2</b>	1H	
<b>cnst24</b>	1000-3000	Place carrier within proton spectrum for evolution.
<b>pl1</b>		Power level channel 1 for contact pulse.
<b>pl12</b>		Power level channel 2 TPPM/SPINAL decoupling.
<b>pl13</b>	for 100 kHz	Power level channel 2 DUMBO decoupling.
<b>sp0</b>		Power level channel 2 for contact pulse.
<b>spnam0</b>	ramp.100 or similar	Shape for contact pulse channel f2.
<b>sp2</b>	set to pl13	100 kHz for default duration 32 $\mu$ s.
<b>spnam2</b>	edumbo22_1+0	Both include one e-DUMBO cycle.
<b>p3</b>	2.5 – 3 $\mu$ sec	90° pulse channel 2 at pl12.
<b>p15</b>	50 -500 $\mu$ s	Contact pulse width.
<b>p20</b>	32 $\mu$ s	32 $\mu$ s for 100 kHz field, set by xau dumbo.
<b>pcpd2</b>	$\approx 2 \cdot p3$	SPINAL64 /TPPM decoupling pulse.
CPDPRG2	SPINAL64/TPPM15	Decoupling sequence.
F1 $^1$ H indirect		
<b>I0</b>	0	Start value 0, incremented during expt.
<b>I3</b>	2- 4	Multiples of e-DUMBO period, increment per row.
<b>in_f1</b>	=in0 as calculated	Set according to value calculated by <b>ased</b> .
F2 $^{13}$ C acquisition		
<b>d1</b>	2s	Recycle delay.

## Modifications of FSLG HETCOR

*Table 8.4. Acquisition Parameters for e-DUMBO-HETCOR (on tyrosine-HCl)*

<b>sw</b>	310 ppm	Sweep width direct dimension.
<b>aq</b>	16-20 msec	
<b>masr</b>	12000-13000	

**dumbohet**

**8.2.4**

This is the windowed version of the previous experiment, analogous to wpmighet. Run **xau dumbo**, select d (for dumbo), 1 (for 1 cycle), 0 (for added angle). The calculated shape, dumbo\_1+0 will be entered as spnam1, p10 will be set to 32  $\mu$ sec. The projection of this experiment can be compared to the result of a direct proton detected CRAMPS experiment, using dumbod2. At higher fields, p10 may have to be set to 24 rather than 32  $\mu$ sec for better resolution. The same pulse length p10, the same shape, the same window (p9) and the same power level should be used in both experiments.

The resolution along the proton dimension is comparable for all these experiments. The FSLG experiment is the most forgiving, requiring just the knowledge of the RF power level for decoupling at a certain RF field. Setting cnst20 to this RF-field (+ 5 or 10%) is all that needs to be set, if the  $^{13}\text{C}$  observe parameters are well adjusted.

*Table 8.5. Acquisition Parameters for DUMBO-HETCOR (on tyrosine-HCl)*

Parameter	Value	Comments
<b>pulprog</b>	dumbohet	Windowless dumbo shape.
<b>nuc1</b>	$^{13}\text{C}$	
<b>o1p</b>	100 ppm	
<b>nuc2</b>	$^1\text{H}$	
<b>cnst24</b>	1000-3000	Place carrier within proton spectrum for evolution.
<b>p11</b>		Power level channel 1 for contact pulse.
<b>p12</b>		Power level channel 2 TPPM/SPINAL decoupling.
<b>p13</b>		Power level channel 2 DUMBO decoupling.
<b>sp0</b>		Power level channel 2 for contact pulse.
<b>spnam0</b>	ramp.100 or similar	Shape for contact pulse channel f2.
<b>sp1</b>	set to p13	100 kHz for default duration 32 $\mu$ s.
<b>spnam1</b>	dumbo_1+0	Both include one DUMBO cycle.
<b>p3</b>	2.5 – 3 $\mu$ sec	90° pulse channel 2 at p12.
<b>p15</b>	50 -500 $\mu$ s	Contact pulse width.
<b>p10</b>	32 or 24 $\mu$ s	32 $\mu$ s for 100 kHz field, 24 $\mu$ s for better resolution at high magnetic fields (>500 MHz).
<b>pcpd2</b>	$\approx 2^*p3$	SPINAL64 /TPPM decoupling pulse.

Table 8.5. Acquisition Parameters for DUMBO-HETCOR (on tyrosine-HCl)

<b>cpdprg2</b>	SPINAL64/TPPM15	Decoupling sequence.
F1 $^1\text{H}$ indirect		
<b>I0</b>	0	Start value 0, incremented during expt.
<b>I3</b>	2- 4	Multiples of DUMBO-periods, increment per row.
<b>in_f1</b>	=in0 as calculated	Set according to value calculated by <b>ased</b> .
F2 $^{13}\text{C}$ acquisition		
<b>d1</b>	2s	Recycle delay.
<b>sw</b>	310ppm	Sweep width direct dimension.
<b>aq</b>	16-20 msec	
<b>masr</b>	12000-13000	

**HETCOR with Cross Polarization under LG Offset****8.3**

Usually, the cross polarization step is executed at less power than what is used for the initial excitation pulse and decoupling during observe. Therefore, a second LG condition must be set for the power level during contact. Furthermore, the HH condition must be re-established, since the proton spin lock pulse now must be a square pulse, not a ramp. The ramp can be transferred to the carbon (F1) side.

The following steps are involved:

1. The RF field for protons during contact must be measured and adjusted. With linearized transmitters, the required power level can be calculated from a known reference pulse width.
2. The LG frequency offset must be calculated from the RF field ( $\text{RF}/\sqrt{2}$ ).
3. The HH condition must be reestablished, varying the F1 ( $^{13}\text{C}$ )-RF field.

As the effective field, required to match for both nuclei at the HH condition, is the vector sum of RF-field and frequency offset, a higher power pulse is required on F1 with increasing offset. So it is recommended not to set the proton power higher than to 50 kHz RF field. For the setup, the pulse program Igcp is used. It contains an include file Igcalc2.incl which will calculate the LG offset from a given RF field specified as **cnst17**. It will set the calculated offset as **cnst19** during contact. In **ased**, it will calculate also **cnst16**, which shows the effective field under **cnst17** RF field and **cnst18**, **cnst19** offset. The X contact pulse is executed as (ramp)-shape. Any standard ramp is possible, but a flat ramp (70-100% or 90-100%) is preferred. Usually, calculating the required RF field for the HH match can be done in the following way:

1. Load the pulse program Igcp into a standard CP/MAS data set with all parameters set and optimized. Set p14 to about 54° flip angle. Use tyrosine \*HCl or the sample of interest.
2. From p3, calculate the power level **pI2** for 50 kHz RF field, using calcpowlev.
3. Enter **cnst17= 50000**, type **ased**. Read the value of **cnst16** (=effective field under **cnst18**, **cnst19** offset (about 61000 Hz). Add or subtract the spin rate used, for instance spinning at 13 yields 74000 or 48000 Hz. If a 30% ramp is used, and **sp0** is set to 74000 (with a safety

margin of 1000), the HH condition will cover 75000 down to 45000 Hz RF field. This includes both HH sidebands  $n=\pm 1$ .

4. Optimize the HH-condition varying ***sp0***, and ***p14, phcor1*** for maximum signal.
5. Run a variation of ***p15*** between 20 and 5000 ms on your sample (or tyrosine  $^3\text{HCl}$ ). One should see intensity variations (“dipolar oscillations”) which are normally smeared out by extensive Homo-nuclear dipolar couplings between protons.
6. Set up a 2D data set with the pulse program **Igcphetfq**. **Fig.3** and **fig.4** compare spectra taken with and without LG-offset during cp.

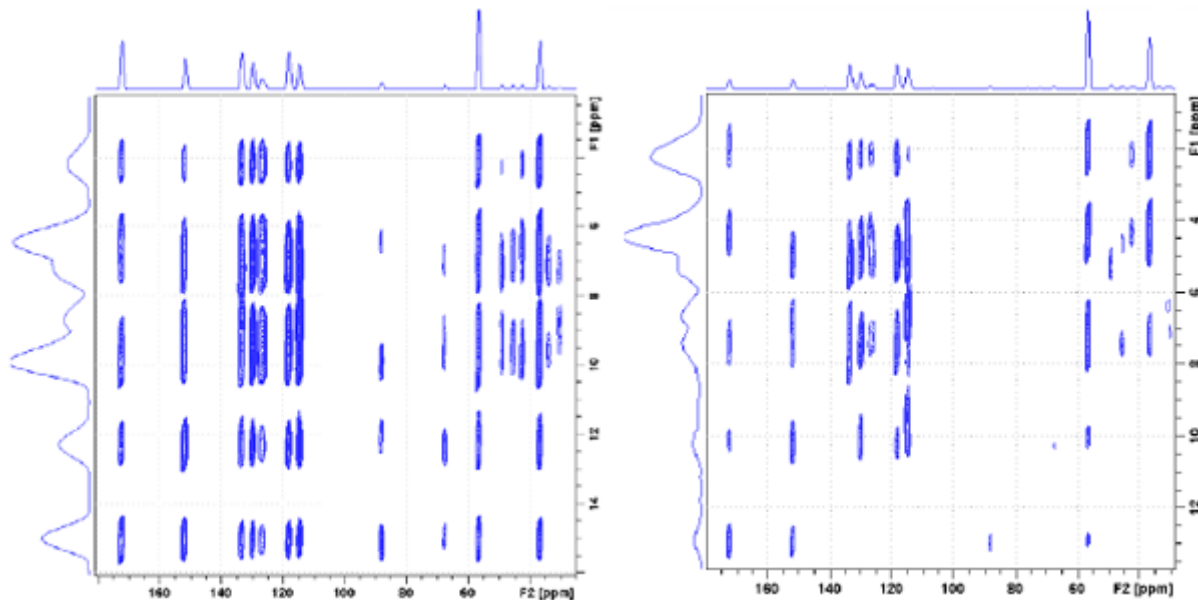


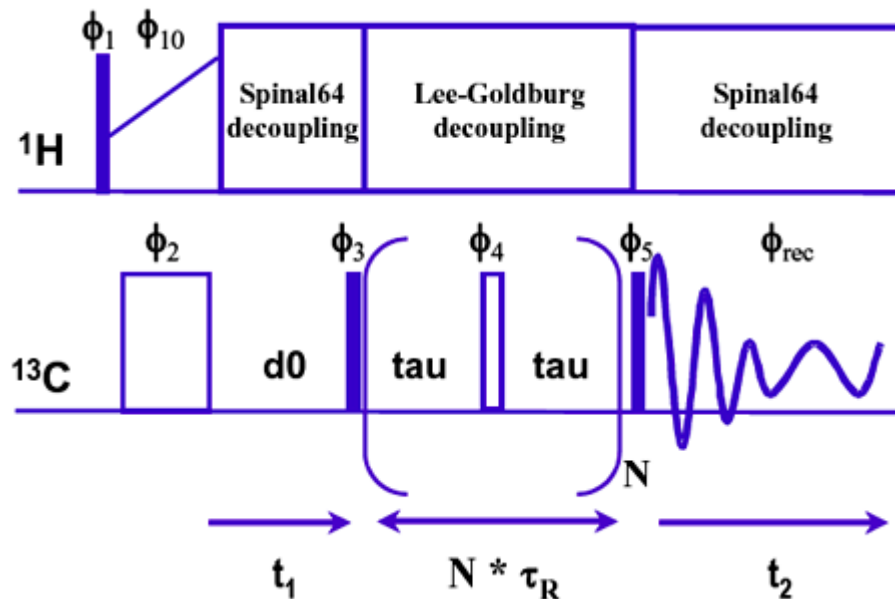
Figure 8.3. HETCOR on tyrosine  $^3\text{HCl}$  without (left) and with LG contact (1msec contact)

Radio Frequency-Driven Recoupling (RFDR) with longitudinal magnetization exchange is a Homo-nuclear dipolar recoupling experiment. This easy setup technique is a zero-quantum recoupling sequence that achieves chemical shift correlation under MAS conditions. The time-dependence of the cross peak amplitudes can be employed to determine inter-nuclear distances. With short dipolar recoupling times, only spins in close spatial proximity lead to cross peak facilitating assignment of  $^{13}\text{C}$  resonances in uniformly labelled peptides for instance. RFDR may also be used in order to correlate chemical shifts and crystallographic sites on materials samples.

The Homo-nuclear dipolar recoupling is implemented via the application of rotor-synchronised 180-degree pulses (one inversion pulse per rotor period). The phases of the 180-degree pulses are cycled with Gullion's compensated XY-8 echo sequence in order to achieve efficient recovery of single spin magnetization and to generate an effective dipolar recoupling Hamiltonian during the mixing period. The critical experimental point is to avoid  $^1\text{H}$ -X recoupling induced by interference between the  $^1\text{H}$  decoupling rf field and  $^{13}\text{C}$  rf recoupling field. This effect can be removed using a  $^1\text{H}$  decoupling rf field 3 times as strong as the  $^{13}\text{C}$  rf field used for recoupling or by using Lee-Goldburg  $^1\text{H}$  decoupling during the mixing period.

## References:

- T. Gullion, D. B. Baker and M. S. Conradi, *New, compensated Carr-Purcell sequences*, J. Magn. Reson. 89, 479-484 (1990).
- A. E. Bennett, J. H. Ok, R. G. Griffin and S. Vega, *Chemical shift correlation spectroscopy in rotating solids: Radio frequency-driven dipolar recoupling and longitudinal exchange*, J. Chem. Phys. 96, 8624-8627 (1992).
- A. E. Bennett, C. M. Rienstra, J. M. Griffith's, W. Zhen, P. T. Lansbury and R. G. Griffin, *Homo-nuclear radio frequency-driven recoupling in rotating solids*, J. Chem. Phys. 108, 9463-9479 (1998).
- B. Heise, J. Leppert, O. Ohlenschläger, M. Görlach and R. Ramachandran, *Chemical shift correlation via RFDR: elimination of resonance offset effects*, J. Biomol. NMR 24, 237-243 (2002).



$\phi_1 = 1$	$\phi_4 = 0101\ 1010$	
$\phi_2 = 1$	$\phi_5 = 0303\ 0303, 1010\ 1010$	
$\phi_3 = 0123\ 0321$	$\phi_{10} = 0$	$\phi_{rec} = 0220\ 0220, 1331\ 1331$

Figure 9.1. RFDR Pulse Sequence for 2D CPMAS Exchange Experiment.

**Sample:**  $^{13}\text{C}$  fully labelled histidine.

**Experiment time:** Less than 1 hour.

### Experiment Setup

First setup the  $^1\text{H}$ - $^{13}\text{C}$  cross polarization and the Hartmann-Hahn match according to the procedures described in ["Basic Setup Procedures" on page 13](#).

An important experimental consideration of the RFDR experiment is that the r.f. field strengths used in the recoupling channel (**pl11**) and the r.f. field on the  $^1\text{H}$  decoupling channel must be sufficiently different, *ca.* a factor of 3, to avoid rapid de polarization of the carbon signal during the mixing time. This is usually not achievable, so it should be set as high as possible, using a LG-offset.

During the mixing period (**cpds3=cwlq**), as shown in [Figure 9.1](#), the Gullion compensated echo sequence used for the mixing period is a XY-8 phase cycling ( $f_4 = \text{XYXY YXYX}$ ). Consequently, the number of rotor periods for the mixing time (**L1**) must be a multiple of 8.

**Sample:**  $^{13}\text{C}$  fully labelled histidine.

**Experiment time:** Several hours.

### Set-up 2D Experiment

9.3.1

After 1D parameter optimization as previously described, type **iexpno** to create a new data file and switch to the 2D mode using the “123” button. Set the appropriate **FnMode** parameter in **eda**. Pulse program parameters are indicated below ([Figure 9.1](#), shows the pulse sequence).



Figure 9.2. The “123” icon in the Menu Bar of the Data Windows Acquisition Parameter Page

The “123” icon in the menu bar of the data windows acquisition parameter page is used to toggle to the different data acquisition modes, 1D, 2D and 3D if so desired. is used to toggle to the different data acquisition modes, 1D, 2D and 3D if so desired.

Table 9.1. Acquisition Parameters

Parameter	Value	Comments
<b>pulse program</b>	cprfdr.av	Pulse program.
<b>nuc1</b>	$^{13}\text{C}$	Nucleus on f1 channel.
<b>o1p</b>	100 ppm	$^{13}\text{C}$ offset, to be optimized.
<b>nuc2</b>	$^1\text{H}$	Nucleus on f2 channel.
<b>o2p</b>	2-3 ppm	$^1\text{H}$ offset, to be optimized.
<b>pl1</b>		Power level for contact time on f1 channel.
<b>pl11</b>		Power level for f1 recoupling and excitation.
<b>pl2</b>		Power level for contact time on f2 channel.
<b>pl12</b>		Power level decoupling f2 channel and excitation.
<b>pl13</b>		Power level LG decoupling f2 channel.
<b>p1</b>		90° excitation pulse on f1 channel.
<b>p2</b>		180° excitation pulse on f1 channel.
<b>p3</b>		90° excitation pulse on f2 channel.
<b>p15</b>		Contact pulse on f1 and f2 channel.
<b>d0</b>	3u	t1 evolution period.

Table 9.1. Acquisition Parameters

<b>d1</b>		Recycle delay.
<b>cpdprg2</b>	Spinal64	Spinal64 decoupling on f2 channel.
<b>cpdprg3</b>	<b>cwlg</b>	cwlg decoupling on f2 channel.
<b>ns</b>	16	Number of scans.
<b>cnst20</b>	$\approx 100000$	Proton rf field in Hz to calculate LG parameters.
<b>cnst21</b>	0	f2 channel offset.
<b>cnst24</b>		Additional Lee-Goldburg offset.
<b>cnst31</b>		Spinning speed in Hz.
<b>I1</b>	for 2-40 msec	Number of rotor cycles for mixing time.
F2 direct $^{13}\text{C}$		Left column.
<b>td</b>	4k	Number of complex points.
<b>sw</b>	200 ppm	Sweep width direct dimension.
F1 indirect $^{13}\text{C}$		Right column.
<b>td</b>	256	Number of real points.
<b>sw</b>		Rotor synchronized sweep width.
<b>nd0</b>	1	Number of in0 in pulse program.
FnMode	TPPI or STATES	Or STATES-TPPI.

**Spectral Processing****9.4**

Table 9.2. Processing Parameters

Parameter	Value	Comment
F1 acquisition $^{13}\text{C}$		Left column.
<b>si</b>	4k	Number of points and zero fill.
<b>ph_mod</b>	pk	Phase correction if needed.
<b>bc_mod</b>	quad	DC offset correction.
F2 indirect $^{13}\text{C}$		Right column.
<b>si</b>	256	Zero fill.
<b>mc2</b>	TPPI or STATES	Or STATES-TPPI.
<b>ph_mod</b>	pk	Phase correction if needed.
<b>bc_mod</b>	no	Automatic baseline correction.

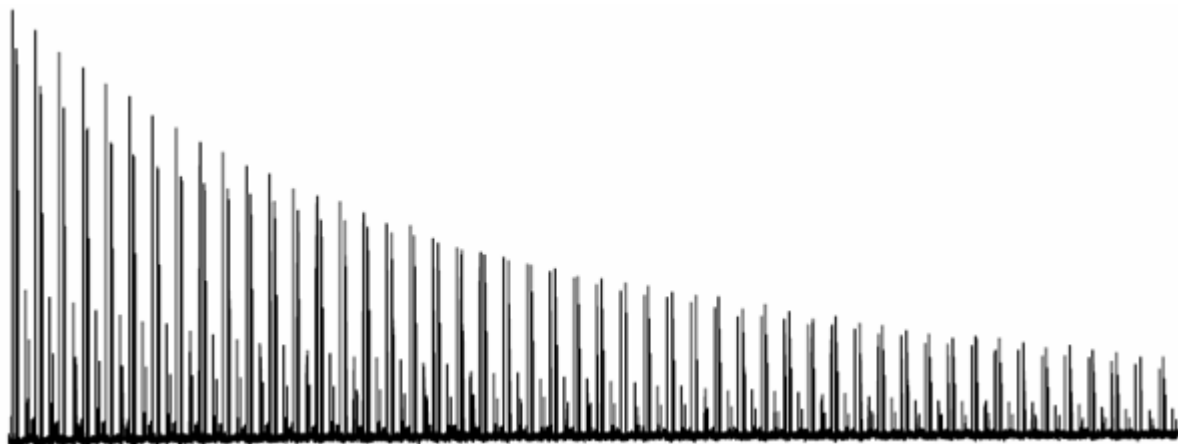


Figure 9.3.  $^{13}\text{C}$  Histidine Signal Decay as a Function of the RFDR Mixing Time

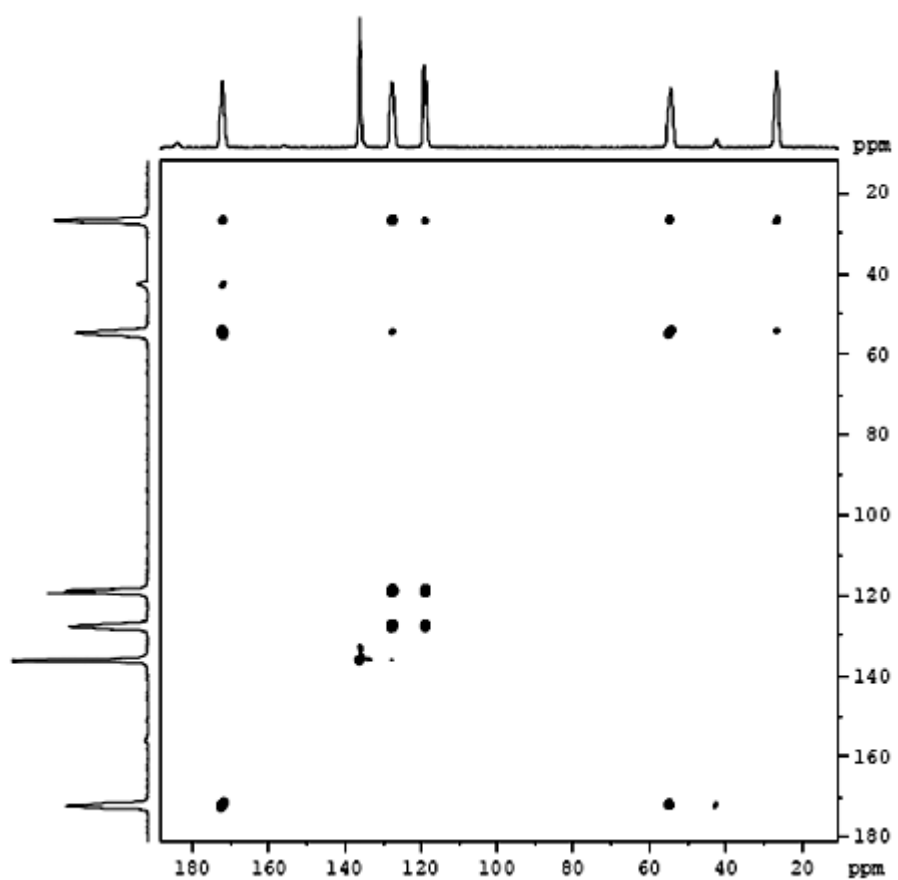


Figure 9.4. 2D RFDR Spectrum of  $^{13}\text{C}$  fully Labelled Histidine (RFDR mixing time 1.85 ms).



# **Proton Driven Spin Diffusion (PDSD)**

# **10**

PDSD is a 2D experiment that correlates a spin 1/2 nucleus to another spin of the same species via Homo-nuclear dipolar coupling or chemical exchange. The experiment resembles the NOESY (Nuclear Overhauser Effect SpectroscopY) pulse sequence in the liquid state by replacing the initial 90° pulse with a cross polarization scheme. Since spin diffusion between X-nuclei is measured, cross peak intensities depend on the probability of interaction between different sites, which is low with low natural abundance of NMR-active nuclei. Therefore, these experiments usually require enrichment for nuclei like  $^{13}\text{C}$  or  $^{15}\text{N}$  in order to allow sensible measurement times.

The pulse program **cpspindiff** allows to run several types of PDSD experiments. The *CP preparation* period excites the X nuclei. During the *evolution* time the X magnetization evolves under the effect of the chemical shift interaction. The *evolution* time ends with an X 90° pulse that stores the chemical shift information along the z axis and marks the beginning of the *mixing* time. The X spins communicate through chemical exchange or spin diffusion, depending on the properties of the material and the duration of the *mixing* time. At the end of the *mixing* period, another X 90° (read) pulse and the data *acquisition* follow. The usually strong  $^1\text{H}$ -X dipolar interaction is removed by high power  $^1\text{H}$  decoupling during the *preparation* and the *acquisition* time. The  $^1\text{H}$  decoupling is switched off during the *mixing* to dephase the residual X transverse magnetization. Spin diffusion between X-nuclei is usually very slow and requires very long mixing times since the dipolar coupling between all X-nuclei is small. However, turning the proton decoupling field off during the mix period allows another process to take place: spin diffusion via the proton spin system. Since the rare nuclei are strongly coupled to protons and all protons are strongly coupled to each other, the flip flop transition rate is high along the  $\text{X}_1\text{-H}_1\text{-H}_2\text{-X}_2$ -pathway. In fact, the spin exchange is almost solely due to proton mediated mechanisms except when chemical exchange is present. At high spin rates, spin diffusion may however still be slow since the X-H spins are decoupled. A simple procedure to recouple the X-H interaction is to irradiate the protons at an RF field of n times the spin rate. These modified sequences are DARR (Dipolar Assisted Rotational Resonance, T. Terao et al.) or RAD (Rf Assisted Diffusion, see C.R. Morcombe et al.).

The setup for all these sequences is rather robust, requiring only the  $^1\text{H}$  to X Hartmann-Hahn condition and the X 90° hard pulse to be set. For RAD and DARR, it is usually sufficient to calculate an RF power level corresponding to n times the spin rate, which is then applied during the mixing period. Rotor synchronization of the *mixing* period is recommended in some cases, where cross peaks due to sidebands need to be suppressed (de Jong et al.) or where spin diffusion is enhanced by matching the spin rate with the chemical shift difference between the sites to be correlated (M. Ernst et al.). PDSD is typically applied to high abundance nuclei or labeled materials to detect through space proximity between spins. This experiment has been often used on proteins as an alternative to Radio Frequency DRiven spin diffusion (see "[RFDR](#)" [on page 93](#)). RFDR provides similar information to PDSD but with a different *mixing* period. Here the term "frequency driven" relates to recoupling pulses on the X channel, whereas in DARR or RAD the radio frequency that drives the recoupling is the proton RF.

An important aspect of this experiment is that the *mixing* time is a simple delay and no pulse, or only weak rf irradiation (DARR, RAD) is required. Therefore it can be made very long because no technical or experimental problems can arise. So the effects even of small dipolar couplings

(requiring long spin diffusion times) can be observed. However the information from this experiment may be ambiguous, because a rather non-selective transfer (within the proton spin system) is utilized.

Nevertheless, even complex molecules like proteins can be surprisingly well characterized by PDSD experiments with different *mixing* times. The buildup of cross peak intensities can be studied and correlated, for instance, to the structure of a macromolecule in the solid state. The same approach has been used to compare different states of a protein, i.e. bound to a membrane or free, as can be found in the recent literature on solid state NMR applied to protein studies.

More elaborate derivatives of PDSD are also known in bio-molecular NMR, where the unspecific spin diffusion within the proton spin system is filtered through a double quantum selection (Lange et al.).

### References:

1. N.M. Szeverenyi, M.J. Sullivan, and G.E. Maciel, Observation of Spin Exchange by Two-Dimensional Fourier Transform  $^{13}\text{C}$  Cross Polarization Magic Angle Spinning, *J. Magn. Reson.* **47**, 462-475 (1982).
2. A.F. de Jong, A. P. M. Kentgens, and W. S. Veeman, Two-Dimensional Exchange NMR in Rotating Solids: a technique to study very slow molecular motions, *Chem. Phys. Lett.* **109**, 4, 337 (1984).
3. Matthias Ernst and Beat H. Meier, "*Spin Diffusion*" in Isao Ando and Tetsuo Asakura, Eds., "Solid-State NMR of Polymers", pp. 83-122, Elsevier Science Publisher (1998).
4. Matthias Ernst, Arno P.M. Kentgens, and Beat H. Meier, Pure-Phase 2D-Exchange NMR Spectra under MAS, *Journal of Magnetic Resonance* **138**, 66-73 (1999), and references cited therein.
5. K. Takegoshi, Shinji Nakamura and Takehiko Terao,  $^{13}\text{C}$ - $^1\text{H}$  dipolar-assisted rotational resonance in magic-angle spinning NMR, *Chem. Phys. Lett.* **2001**, 344, 631.
6. F. Castellani, B. van Rossum, A. Diehl, M. Schubert, K. Rehbein and H. Oschkinat, Structure of a protein determined by solid-state magic-angle-spinning NMR spectroscopy, *Nature* **420**, 98-102 (2002).
7. C.R. Morcombe, V. Gapenchenko, R.A. Byrd, and K. W. Zilm, Diluting Abundant Spins by Isotope Edited Radio Frequency Field Assisted Diffusion, *J. Am. Chem. Soc.* **126**, 7196-7197 (2004).
8. S.G. Zech, A.G. Wand and A.E. McDermott Protein Structure Determination by High-Resolution Solid-State NMR Spectroscopy: Application to Microcrystalline Ubiquitin, *J. Am. Chem. Soc.* **127**, 8618-8626 (2005).
9. W. Luo, X. Yao and M. Hong Large Structure Rearrangement of Colicin Ia channel Domain after Membrane Binding from 2D  $^{13}\text{C}$  Spin Diffusion NMR), *J. Am. Chem. Soc.* **127**, 6402-6408 (2005).
10. A.Lange, S. Luca, and M. Baldus, Structural constraints from proton-mediated rare spin correlation spectroscopy, *J. Amer. Chem. Soc.*, **124**, 9704-9705 (2002).

**Pulse Sequence Diagram**

10.1

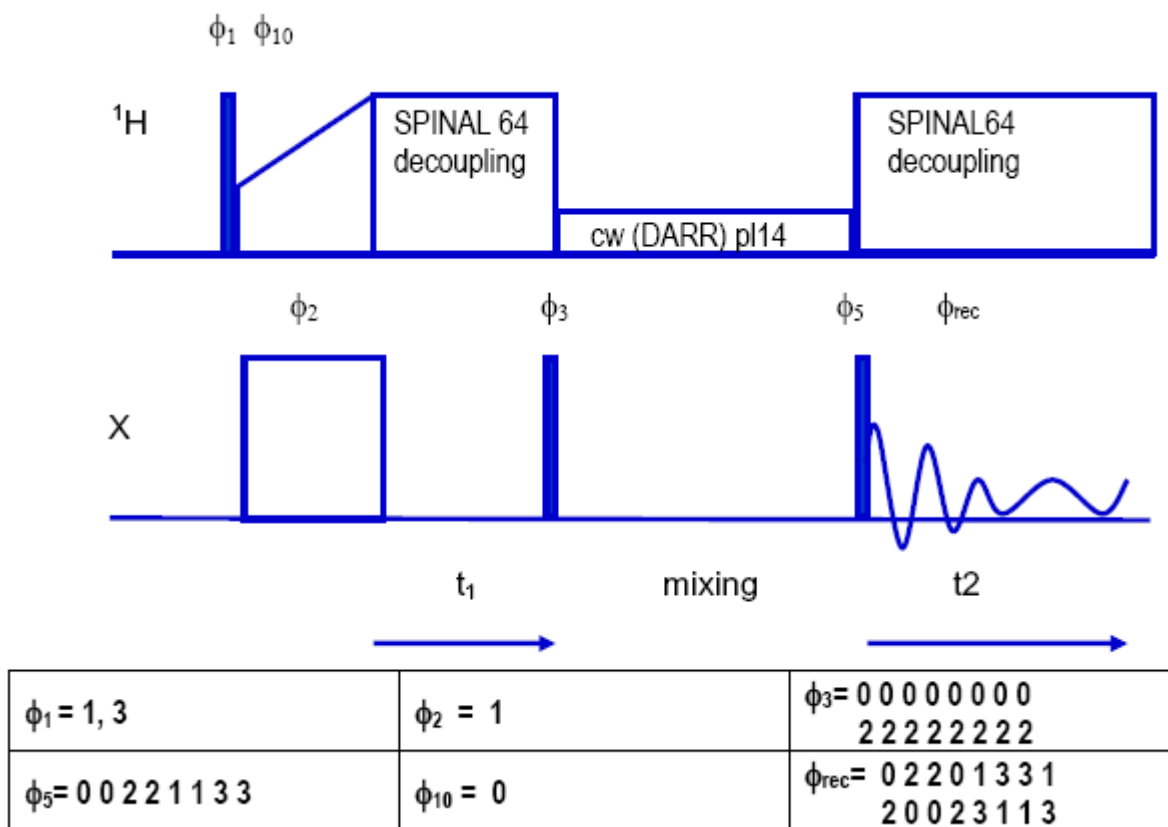


Figure 10.1. CPSPINDIFF Pulse Sequence

**Basic Setup**

10.2

1. On a standard sample (i.e. glycine) determine HH match and decoupling parameters.
2. Check the X 90° hard pulse with *cp90* on the standard sample.
3. If the real sample does tune and match very differently than the setup sample, verify the HH conditions briefly and eventually the X 90° hard pulse.
4. Set the spin rate as high as possible, make sure to avoid rotational resonance conditions (overlap between center bands and sidebands), recheck the HH condition. Set *cst31*=spin rate.
5. Optimize contact time, o1 and o2 on a <sup>13</sup>C 1D CP experiment if necessary.
6. Create a new experiment with either *iexpno* or *edc*.
7. Change to a 2D data set.

**2D Experiment Setup**

10.2.1

8. Type *iexpno* to create a new data file and switch to the 2D mode using the “123” button. Load the pulse program *cpspindiff*.

## Proton Driven Spin Diffusion (PDSD)

9. Recheck pulse widths and power levels, using `ased`.
  10. Go into `eda` and set parameters for sampling in the indirect dimension, the spectral width  $1\text{ swh}$ . Note, that in TopSpin 2.1 or later the parameter `IN_F1` replaces the parameters `in0` and `nd0`. Usually,  $1\text{ swh}$  equals  $\text{swh}$ . Choose a suitable spin rate such that no RR condition occurs and sidebands do not overlap with peaks, if possible set the sweep width in F1  $1\text{ swh}$  equal to the spin rate or such that sidebands folding in along F1 do not interfere.
  11. Make sure the correct nucleus is selected in the F1 dimension; make sure to choose an appropriate quadrature detection mode in `FnMode` (usually STATES-TPPI).
  12. Choose the appropriate sampling time (`td1`) so that the required resolution (`FIDRES`) in the indirect dimension is achieved.
  13. Set the desired mixing time as **`d8`**. The required multiple of spin periods (from `cnst31`) is calculated as **`I1`**, the real mixing time may deviate by fractions of a rotor period. The required mixing time may vary widely depending on the sample properties, from a few milliseconds to hundreds of milliseconds, if long distance correlations in a mobile sample need to be observed. Note that longer mixing times will result in S/N deterioration, as the mixing time approaches the  $T_1$  of the observed nuclei.

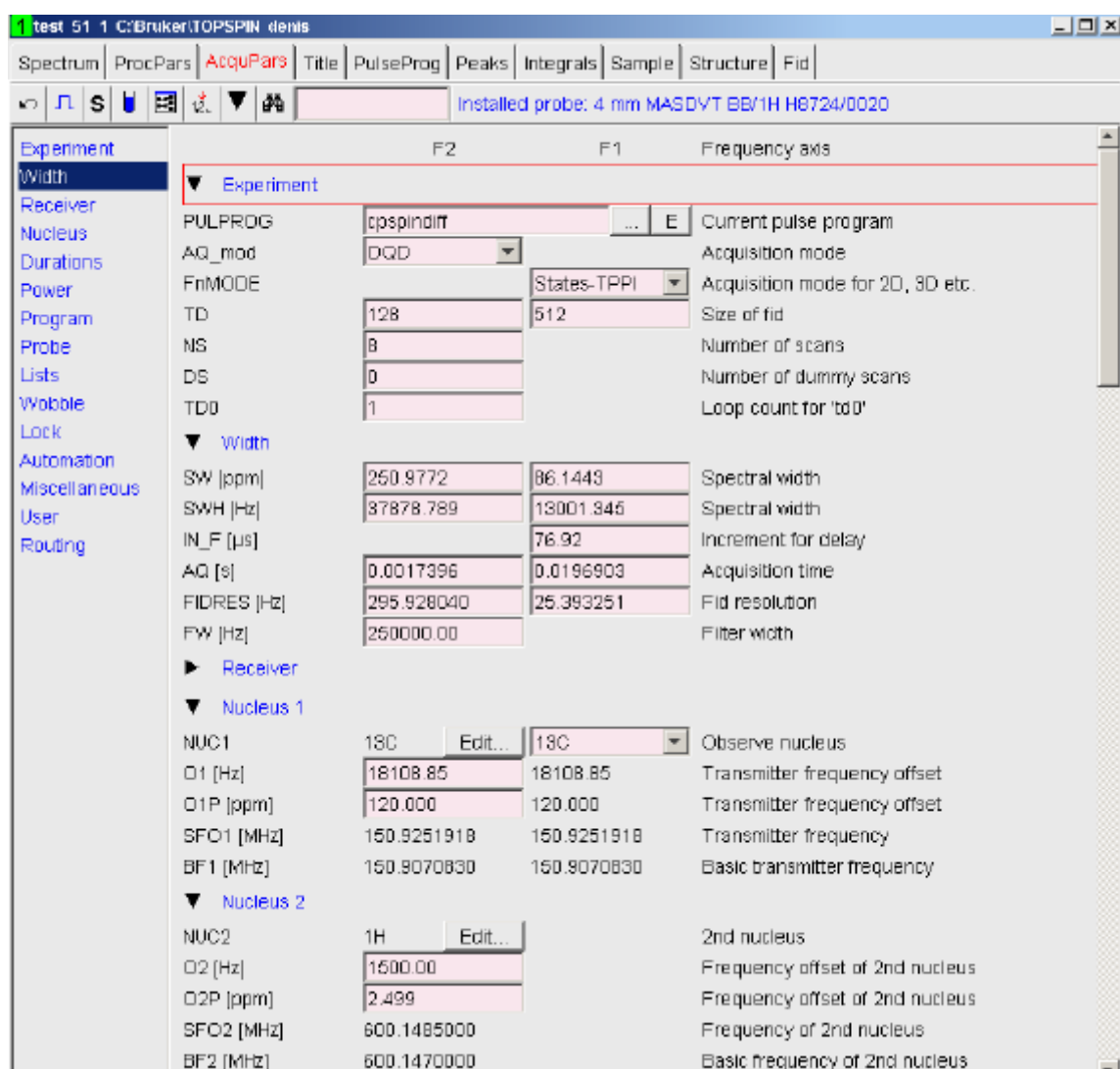


*Figure 10.2. The Acquisition Parameter Window (eda)*

14. Set  $p/14$ , if DARR/RAD is desired, else make sure  $p/14 = 120 \text{ dB}$ . For DARR/RAD calculate the required power level using calcpowlev, or use the setup procedure shown in 11.7.
15. Start the experiment.

**Acquisition Parameters****10.3**Sample:  $^{13}\text{C}$  labelled histidine (labelled tyrosine-HCl)

Experiment time: 90 min. (20 min.)

*Table 10.1. Acquisition Parameters*

<b>Parameter</b>	<b>Value</b>	<b>Comments</b>
PULPROG	cpspindiff (old: cpnoesy)	Pulse program.
NUC1	$^{13}\text{C}$	Set $^{13}\text{C}$ in both F2 and F1 column.
SW	250 ppm	To be optimized.
O1P	120 ppm	To be optimized.
NUC2	$^1\text{H}$	For CP/decoupling only.
O2P	3 ppm	To be optimized for dec.
PL1		For $^{13}\text{C}$ contact.
PL11		For $^{13}\text{C}$ flip pulses.
PL12		For $^1\text{H}$ excitation and decoupling.
PL14	for n*spin rate (DARR) or 120	Recoupling.
SP0		For $^1\text{H}$ contact using shape.
SPNAM0	ramp.100 or ramp70100.100	For $^1\text{H}$ - $^{13}\text{C}$ contact.
CPDPRG2	SPINAL64	At PL12.
P1		$^{13}\text{C}$ excitation (flip) pulse.
P3		$^1\text{H}$ excitation pulse.
P15		$^{13}\text{C}$ - $^1\text{H}$ Contact pulse .
PCPD2		Decoupling pulse for spinal64.
D1		Relaxation delay.
D8	5-500 msec	Depending on sample.
CNST31	MAS speed	Used to calculate d31 (rotation period).
L1	calculated from cnst31 and d8	Number of rotor cycles for mixing time.
AQ_MOD	DQD	
TD {F1}	512	Number of points.

## Proton Driven Spin Diffusion (PDSD)

Table 10.1. Acquisition Parameters

SW{F1}	usually = SW	=MASR if possible.
NUC1{F1}	=NUC1	
TD {F2}	128	Number of points.
ND0	1	Not required in TopSpin 2.1..
NS	4*n	
FnMode	TPPI/States/States-TPPI	

### Processing Parameters

10.3.1

Process with *xfb*.

Table 10.2. Processing Parameters

Parameter	Value	Comment
F2 acquisition $^{13}\text{C}$	*****	Left column.
SI	1k	Number of complex points in direct dimension.
WDW	QSINE	Apodization in t2.
SSB	2-3	
PH_mod	pk	
F1 indirect $^{13}\text{C}$	*****	Right column.
SI	512	Number of complex points in indirect dimension.
WDW	QSINE	Apodization in t1.
SSB	2-3	
PH_mod	pk	

### Adjust the Rotational Resonance Condition for DARR/RAD

10.4

1. Load the Adamantane sample, spin at the same speed as desired for your sample, match and tune, use a suitable cp setup (same as in section [10.3](#))
2. Set **CPDPRG2** to **cw**
3. Use the au program calcpowlev to calculate the power level required for a proton decoupling RF field of  $n \times \text{masr}$ , using p3 and pl12 as reference values. Refer to chapter "[Basic Setup Procedures](#)" on page [13](#) for more information).

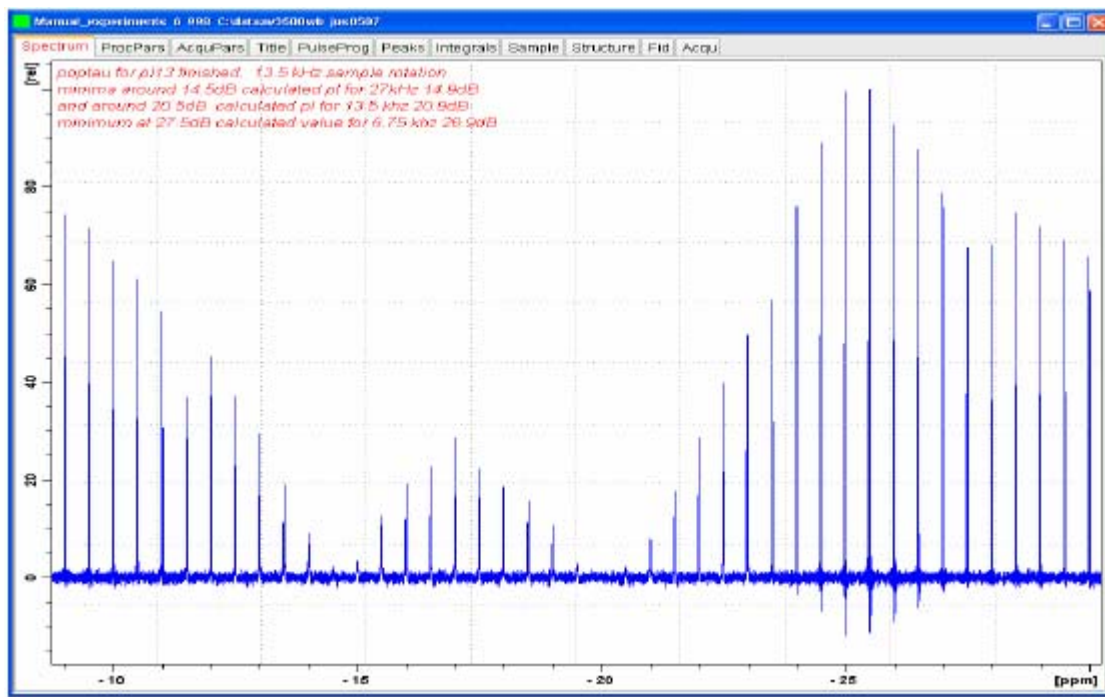


Figure 10.3. POPT Result for the cw Decoupling Power Variation

The figure above shows the POPT result for the cw decoupling power variation from about 50 kHz RF field to about 5 kHz RF field, spinning the adamantane sample at 13 kHz. The minima at 14.5 and 20.5 dB indicate the  $n = 2$  and  $n = 1$  RR conditions (26 and 13 kHz RF field).

4. Vary the decoupler power level ***pl12*** used with cw decoupling as indicated in [\*\*Figure 10.3.\*\*](#) from a power level value ***pl12*** 1 dB below the calculated  $n = 1$  condition to 1 dB above the calculated  $n = 2$  condition. Bandwidth considerations favor the  $n = 2$  condition, sample heating considerations favor the  $n = 1$  condition. An RF field of  $2 \times$  proton chemical shift range is on the safe side.
5. Enter the power level determined above as ***pl14*** recoupling power for DARR or RAD.
6. Using DARR or RAD shorter mixing times are possible.

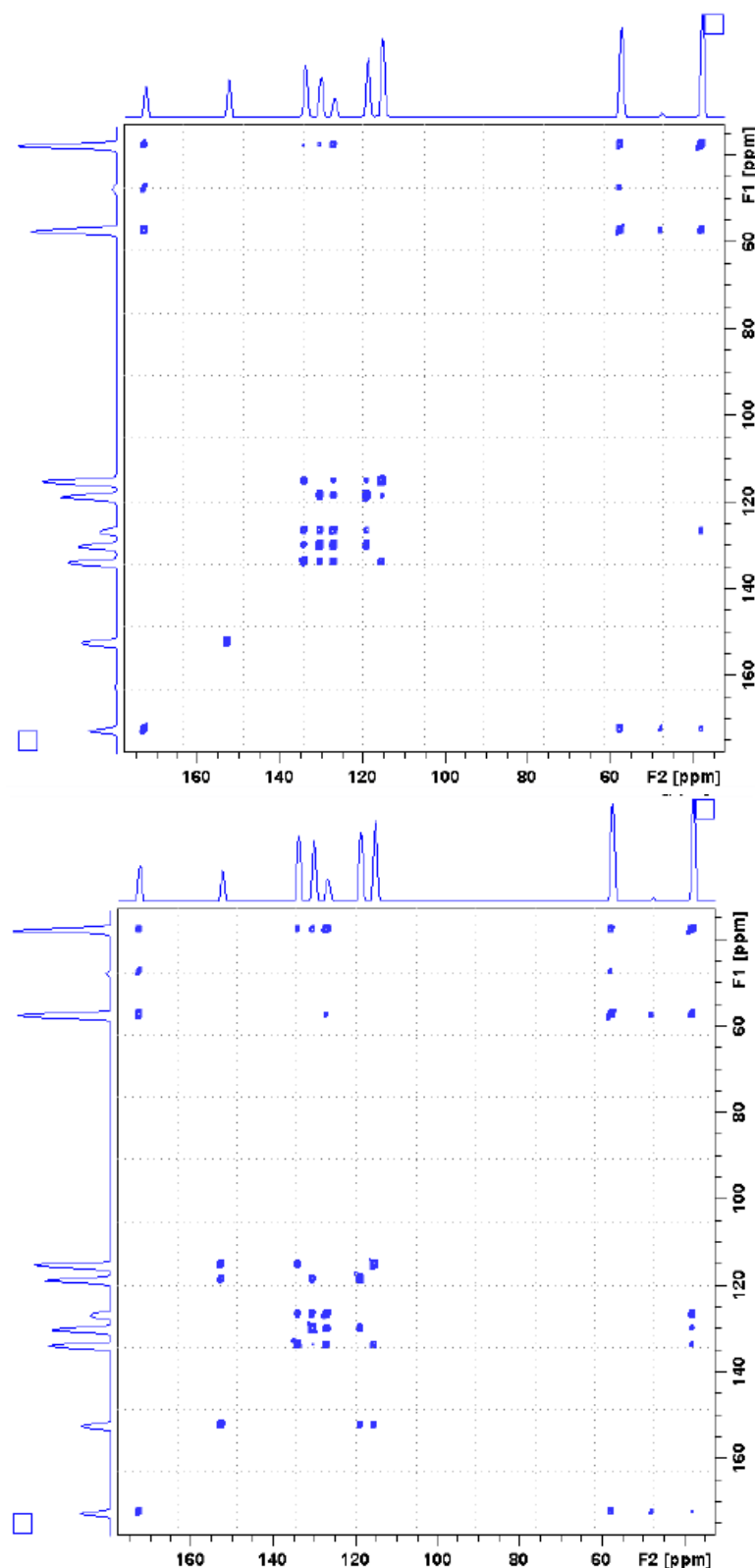


Figure 10.4.  $^{13}\text{C}$  CPSPINDIFF of fully labeled tyrosine\*HCl, spinning at 22 kHz, 4.6 msec mix.  
Upper: PDSD, lower: DARR

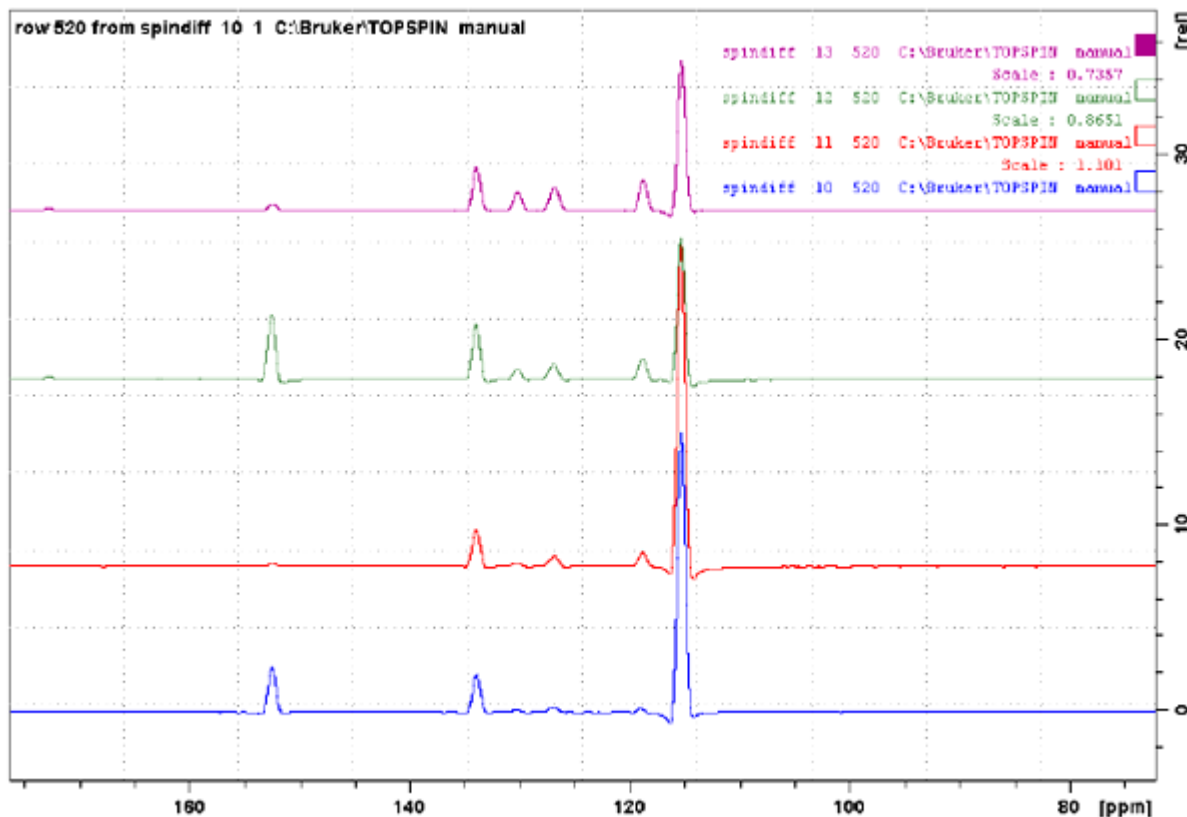


Figure 10.5. Comparison of DARR/PDSD

The figure above is a comparison of DARR/PDSD, with 4.6 and 20 msec mixing time, sample tyrosine-HCl spinning at 22 kHz. Traces through peak at 115 ppm, most high field aromatic carbon. Traces from below: DARR at 4.6 msec mix, PDSD at 4.6 msec mix, DARR at 20 msec mix, and PDSD at 20 msec mix. Note that some cross peak intensities differ substantially!

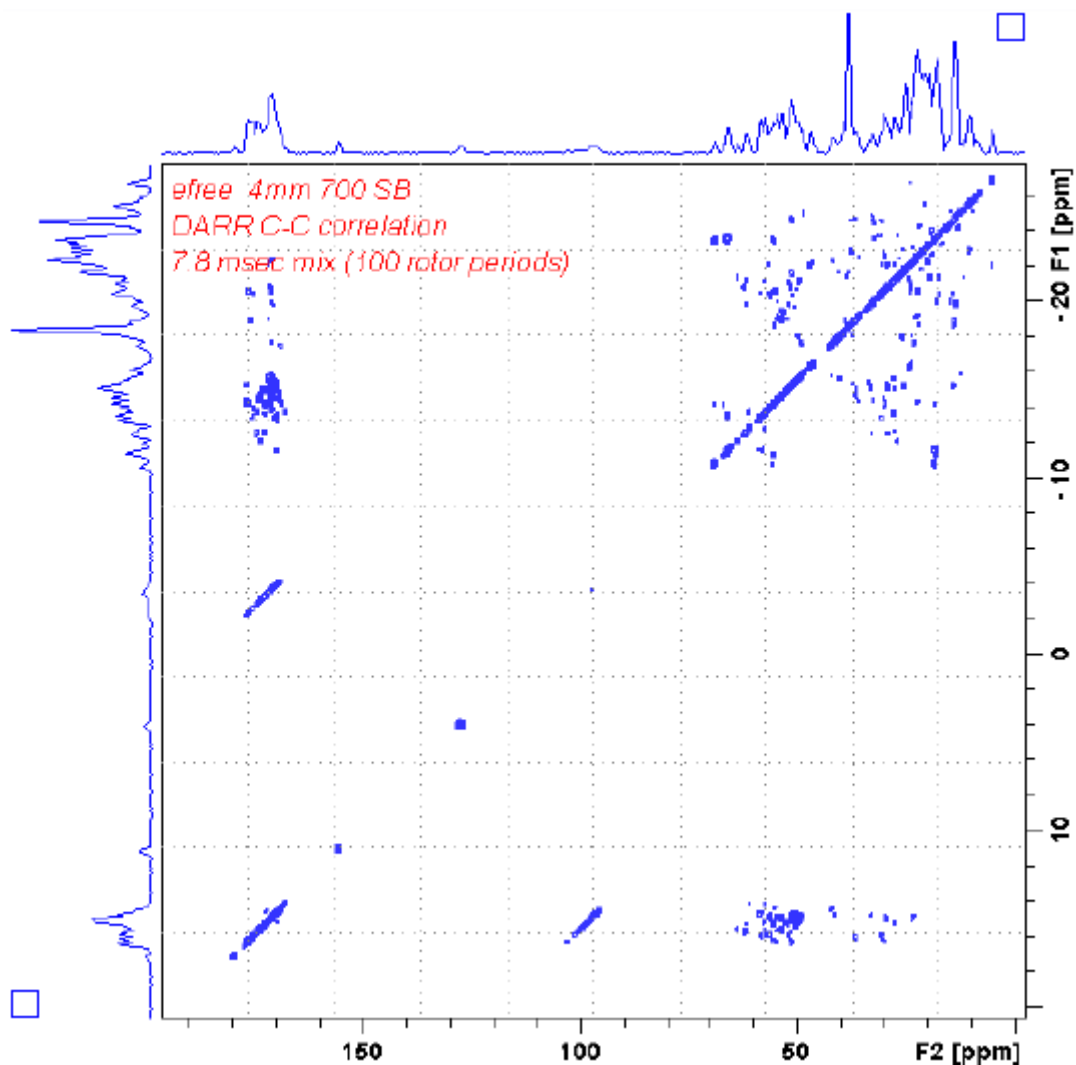


Figure 10.6. <sup>13</sup>C DARR of Fully Labelled Ubiquitine Spinning at 13 kHz

Separation of Undistorted Chemical-Shift Anisotropy Powder patterns by Effortless Recoupling (SUPER) correlates CSA powder patterns in the F1 dimension with the isotropic chemical shift in the F2 dimension. The SUPER experiment is based on Tycko's CS – CSA correlation experiment, but provides better compensation for experimental imperfections such as  $B_1$  in-homogeneities and pulse imperfections. Also, both experiments produce scaled powder patterns in F1, and the scaling factor is more favorable in SUPER than the factor 0.39 in Tycko's version. As a consequence, the SUPER experiment does not require high spinning speeds (to fit the F1 line-shape into the rotor-synchronized spectral window) or very strong  $^{13}\text{C}$  pulses.

SUPER has several advantages. First of all, it covers a large bandwidth for the isotropic chemical shift. Secondly, no requirements exist for  $^1\text{H}$  decoupling during the recoupling pulses, because it uses  $360^\circ$  pulses instead of the  $180^\circ$  pulses in Tycko's experiment. Exact  $360^\circ$  pulses automatically decouple the hetero-nuclear dipolar interaction so that no or only weak  $^1\text{H}$  decoupling is required during the recoupling pulses. The scaling factor is normally 0.155 so that a spectral width over 40 kHz can be achieved in the indirect dimension. As a consequence, moderate spinning speeds of up to 6.5 kHz can be chosen so that experiments can be performed without serious problems on high field instruments. The limiting factor in the choice of the spinning speed is the rotor synchronization requirement of the recoupling  $360^\circ$  pulses:

$$\nu_{RF} = 12.12\nu_{rot}$$

### References

1. S-F. Liu, J-D Mao, and K. Schmidt-Rohr, *A Robust Technique for Two-Dimensional Separation of Undistorted Chemical-Shift Anisotropy Powder Patterns in Magic-Angle-Spinning NMR*, *J. Magn. Reson.* 155, 15-28 (2002).
2. R. Tycko, G. Dabbagh, and P.A. Mirau, *Determination of Chemical-Shift-Anisotropy Line-shapes in a Two-Dimensional Magic-Angle-Spinning NMR Experiment*, *J. Magn. Reson.* 85, 265-274 (1989).

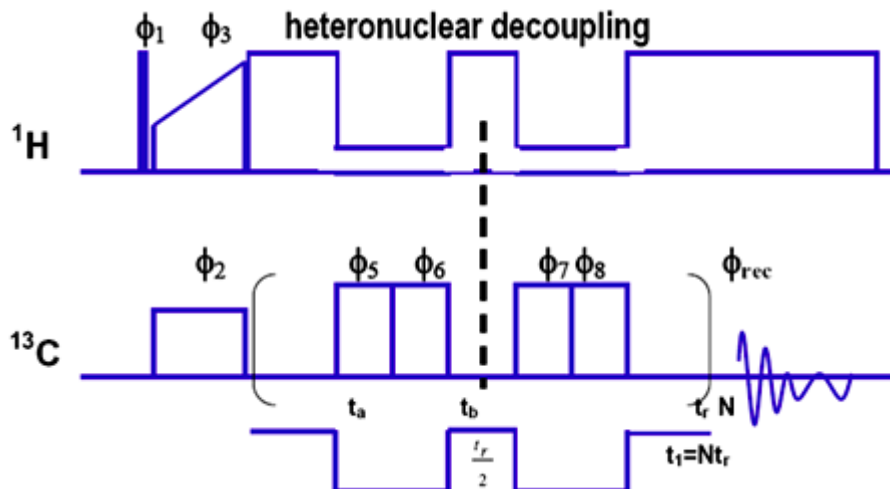


Figure 11.1. Pulse Sequence for 2D CPMAS exchange experiment

## Experiment Setup

## 11.3

**Sample:** Tyrosine HCl natural abundance.

**Experiment time:** Less than 1 hour

## Experiment setup

## 11.3.1

1. In order to setup the experiment, determine  $^1\text{H}$ - $^{13}\text{C}$  and parameters with variable amplitude on  $^1\text{H}$  according to "[Basic Setup Procedures](#)" on page 13.
2. Verify the pulse parameters on the  $^{13}\text{C}$  channel (see "Pulse Calibration Techniques with CP" on page 66) and calculate the power level required for the recoupling pulses, i.e.  $f_{\text{rf}} = 12.2 \times f_{\text{rot}}$ .
3. Verify pulse width.
4. Calculate power level required for hetero-nuclear decoupling during the recoupling pulses, **pl23**, i.e. 20 – 30 kHz or  $> 25 \times f_{\text{rot}}$ . Low power decoupling during the recoupling pulses is permitted because the 360 degree pulses act like hetero-nuclear decoupling pulses. **pl22** during delays should be high.
5. The experiment requires at a minimum accumulation of 64 transients to complete the phase cycle. Between 32 and 64 experiments are needed for a 2D data set. Depending on the choice for the gamma integral, more transients per slice may be required. The recommended value is 4, which increases the number of required transients per experiment to 256.
6. Run 1D experiment and make sure everything is set properly
7. Create a new experiment with either **iexpno** or **edc**.
8. Change to 2D data set:

After 1D parameter optimization as previously described, type **iexpno** to create a new data file and switch to the 2D mode using the “123” button. Set the appropriate **FnMode** parameter in **eda**. Pulse program parameters are detailed as follows ([Figure 11.1](#), shows the pulse sequence).



Figure 11.2. The “123” icon in the Menu Bar of the Data Windows Acquisition Parameter Page.

The “123” icon in the menu bar of the data windows acquisition parameter page is used to toggle to the different data acquisition modes, 1D, 2D, and 3D if so desired.

9. Make sure the correct nucleus is selected in F1 dimension, make sure an appropriate quadrature detection mode is selected in **FnMode** (TPPI, STATES-TPPI or STATES).
10. Choose the appropriate sampling time (**td1**) so that the required resolution (**FIDRES**) in the indirect dimension is achieved.
11. Set **p11** to give a pulse nutation frequency of 12.12\* rotation rate (see chapter 1).
12. Set **d4** the z-filter delay to about 1 ms (integer number of rotor periods if possible).
13. Set **p2** to be a 180° pulse at **p11** for the TOSS sequence.
14. Set **I5** for the gamma integral, typically = number of spinning sidebands normally 4.
15. Start the experiment.

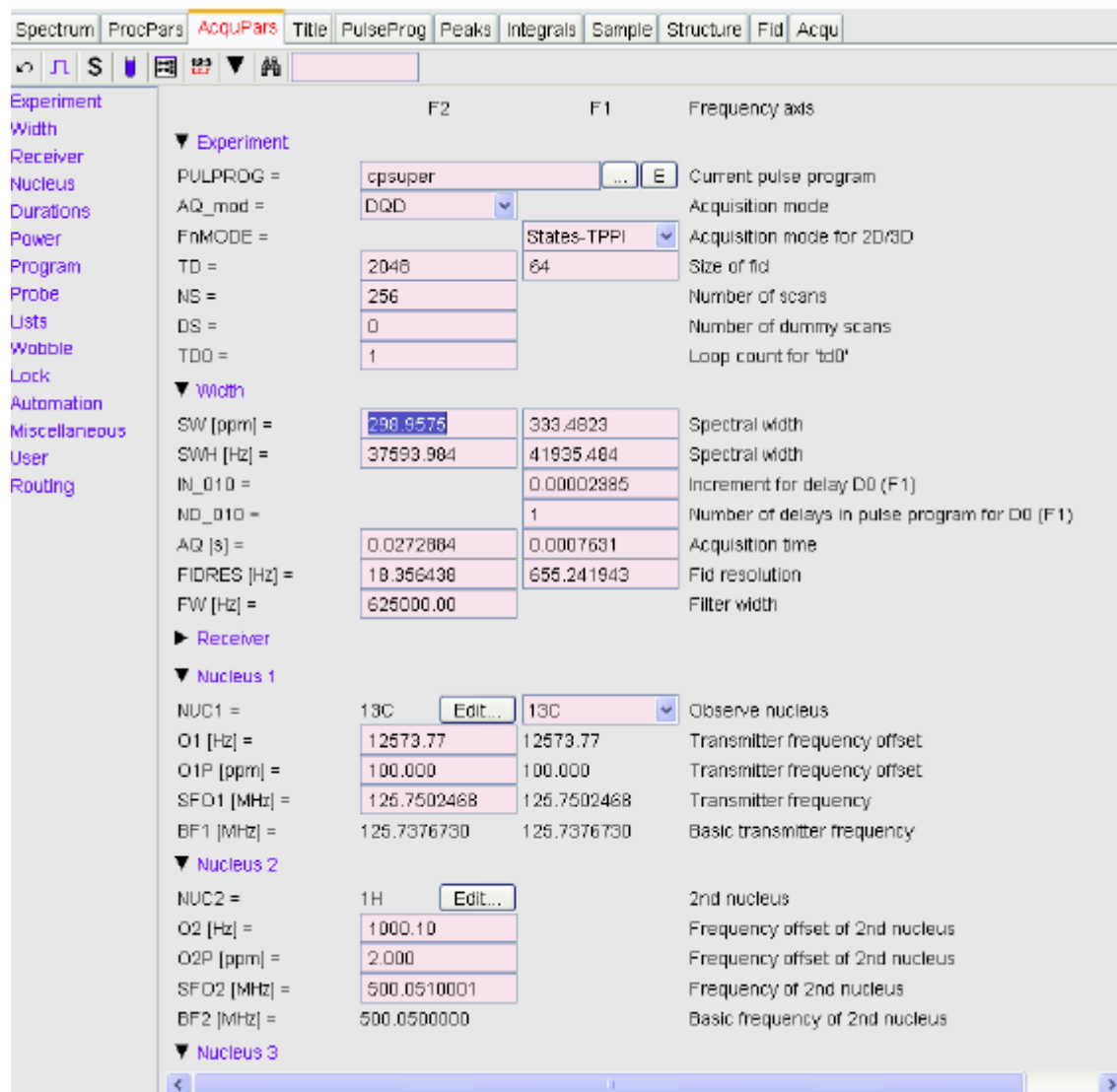


Figure 11.3. The Acquisition Parameter Window (eda)

**Data Acquisition****11.4****Sample:** Tyrosine HCl**Experiment time:** several hours*Table 11.1. Acquisition Parameters*

Parameter	Value	Comments
Pulse program	cpsuper	Pulse program.
NUC1	$^{13}\text{C}$	Nucleus on f1 channel.
O1P	100 ppm	$^{13}\text{C}$ offset.
NUC2	$^1\text{H}$	Nucleus on f2 channel.
O2P	0 ppm	$^1\text{H}$ offset (can be optimized for best decoupling).
PL1		Power level for f1 channel.
PL11		Power level for f1 recoupling.
P2		180° pulse on F1 during TOSS with PL1.
PL2		Power level for f2 channel.
PL12		Power level decoupling f2 channel and excitation.
P3		Excitation pulse f2 channel.
P15		Contact pulse – first contact.
CPDPRG2		TPPM or SPINAL64.
NS	$64*\text{n}*\text{l5}$	Number of scans.
CNST31		Spinning speed in Hz.
L5		L5/cnst31 counter for increment in t1 and number of gamma integral – typically number of SSB's.
F2 direct $^{13}\text{C}$		(left column).
TD	2048	Number of complex points.
SW	300 ppm	Sweep width direct dimension.
F1 indirect $^{13}\text{C}$		Right column.
TD	32 - 64	Number of real points.
FnMode		TPPI, STATES or STATES-TPPI.

Table 11.2. Processing Parameters

Parameter	Value	Comment
F1 acquisition $^{13}\text{C}$		Left column.
SI	4096	Number of points and zero fill.
WDW	QSINE	Squared sine bell.
SSB	2	90° shifted sine bell.
PH_mod	pk	Phase correction if needed.
BC_mod	quad	DC offset correction.
Alpha	-1	For shearing the spectrum.
F2 indirect $^{13}\text{C}$		Right column.
SI	128	Zero fill.
MC2	STATES-TPPI	
WDW	QSINE	Squared sine bell.
SSB	2	90° shifted sine bell.
PH_mod	pk	Phase correction if needed.
BC_mod	no	Automatic baseline correction.

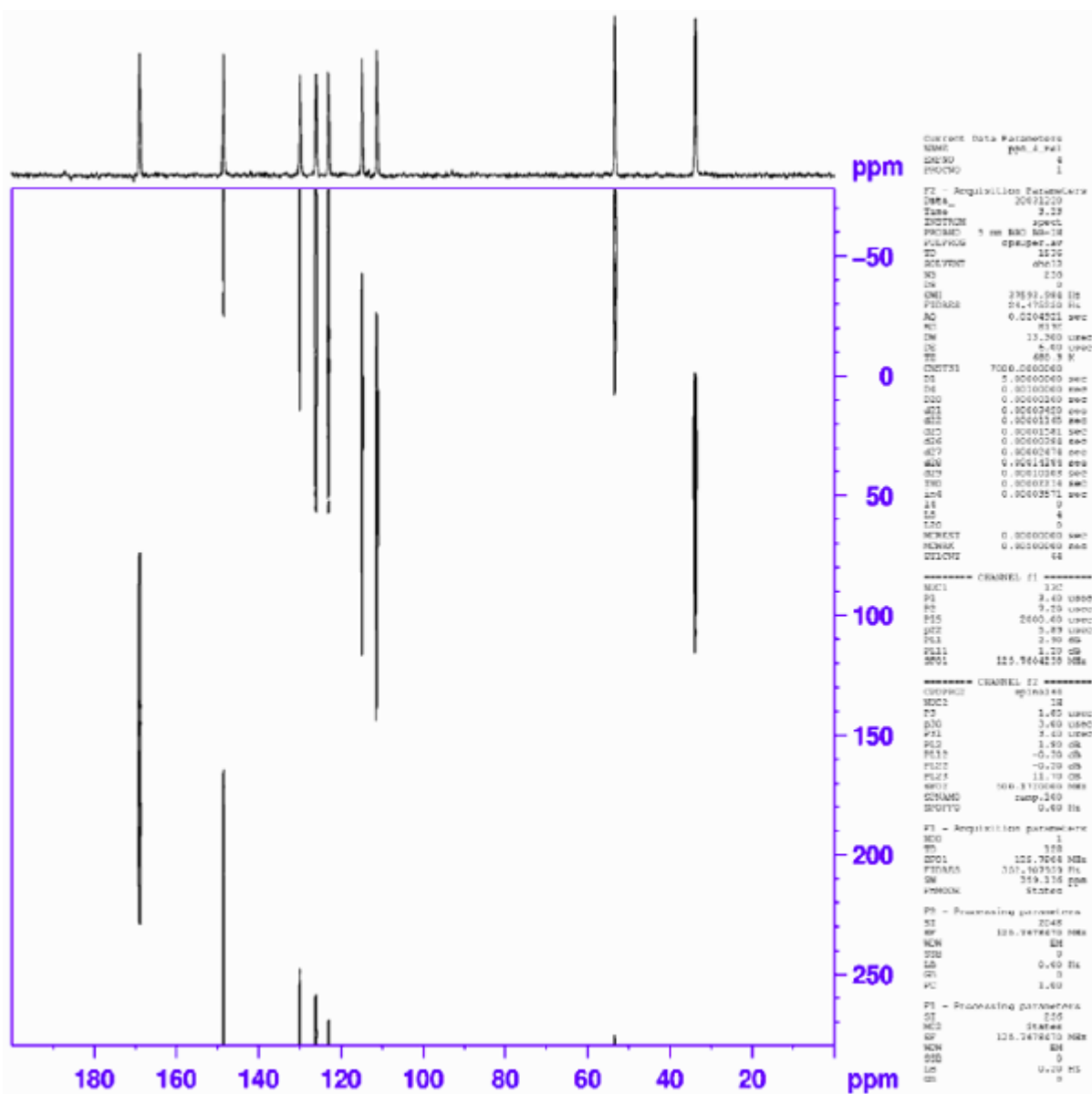


Figure 11.4. The SUPER Spectrum of Tyrosine HCl After Processing Using "xfb"

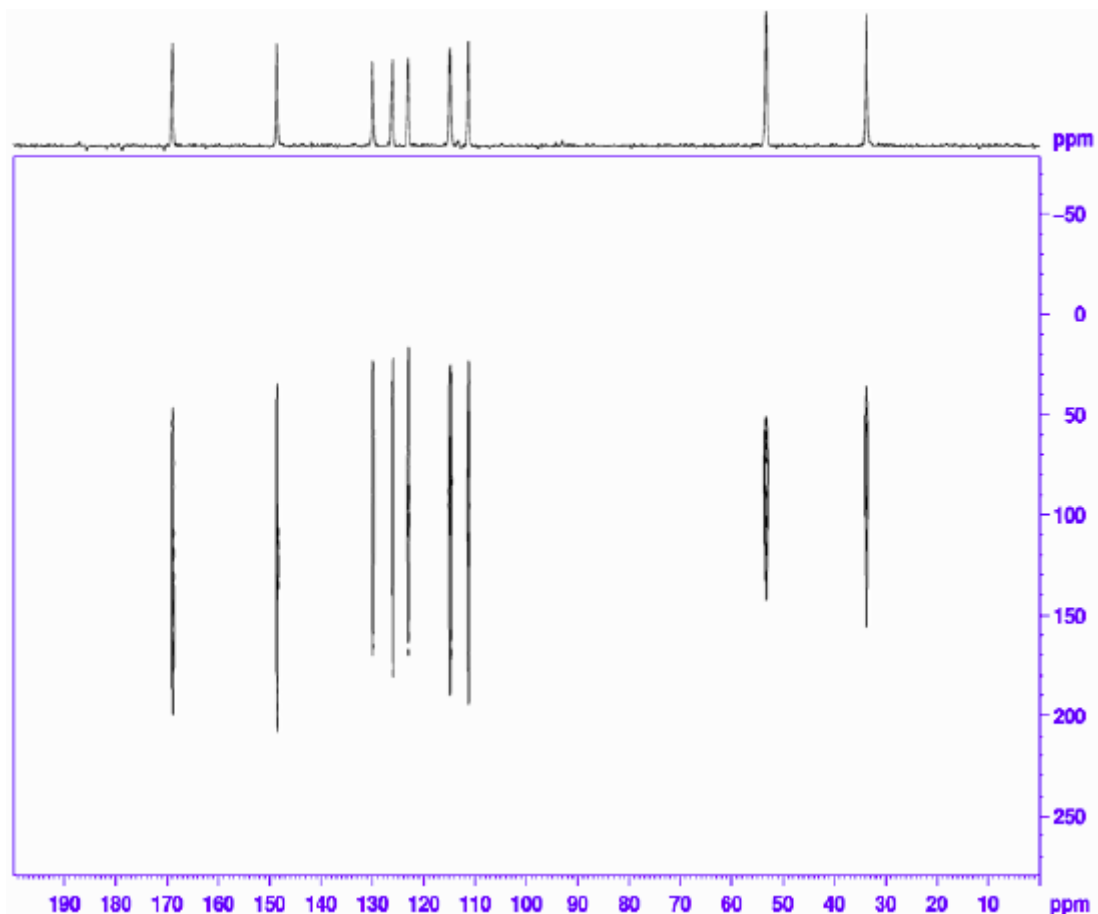


Figure 11.5. SUPER spectrum after tilting the spectrum setting “1 alpha” = -1

**Figure 11.5.** SUPER spectrum after tilting the spectrum setting “1 alpha” = -1 and using the command “ptilt1” repeatedly until the CSA lines are within the spectral range.

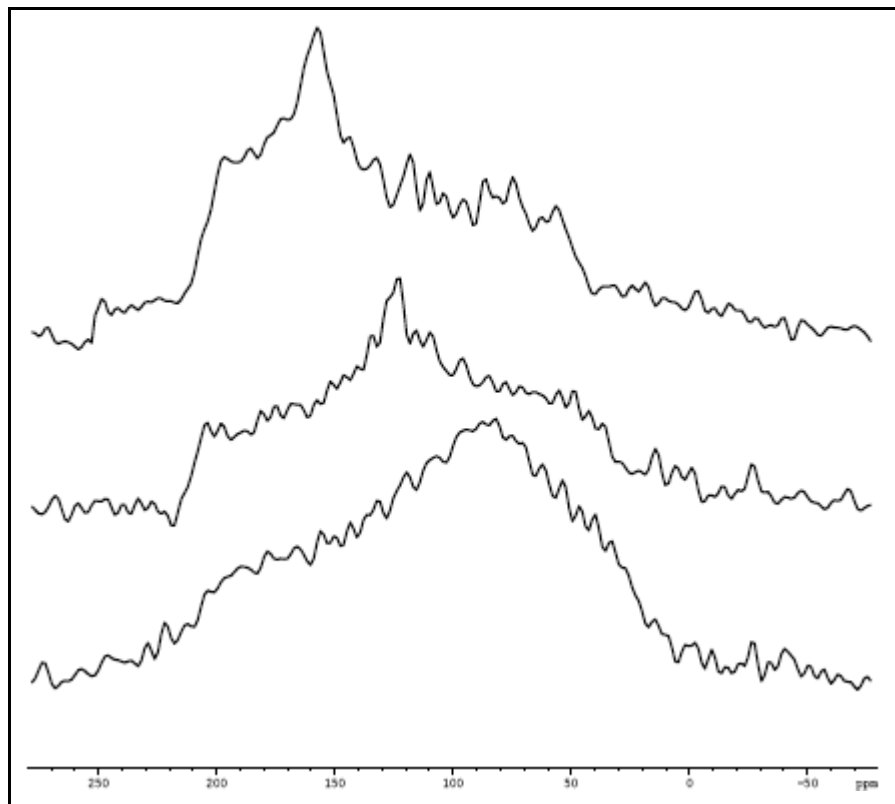


Figure 11.6. Various Cross Sections from the Upper 2D Experiment

**Figure 11.6.** illustrates various cross sections from the upper 2D experiment, from which CSA parameters can be determined.

**SUPER**

# Symmetry Based Recoupling

12

Sample rotation averages most anisotropic interactions, and therefore removes the information available from them. Therefore, selective recoupling of anisotropic interactions is desired for structural analysis (re-coupling, reintroduction of anisotropic interactions, like e.g. dipolar coupling), in order to regain specific information. The topic has been thoroughly reviewed, by E.A. Bennett et al, and by S. Dusold et al. One strategy is the use of symmetry based recoupling sequences; see M. Hohwy et al (1998) et al. and A. Brinkmann et al. (2000). In these sequences, double quantum coherence are excited via the dipolar Homo-nuclear dipolar coupling. Single quantum coherence are suppressed by phase cycling. The size of the dipolar coupling can be determined from the build-up rate of DQ signal intensity, measured after reconversion into SQ coherence. It should also be mentioned that there are recoupling sequences that do not generate double quantum coherence (DRAWS, DRAMA, and MELODRAMA).

Symmetry-based recoupling sequences recouple specific spin interactions, using cyclic sequences composed of N phase-shifted repetitions of either  $2\pi$  (C sequences) or  $\pi$  (R sequences) rotation elements. Which interaction(s) are recoupled by a given sequence is determined by the relationship between the sample rotation rate, the spin rotation rate, and the rate of phase shift between the elements. The sequences are denoted as e.g., where N is the number of elements in the cycle, n is the number of rotor periods spanned by the N elements, and the total phase rotation between the elements is  $2\pi/v$ . In the simplest implementation of a C sequence, the  $2\pi$  rotation element is simply a  $2\pi$  pulse, but other elements are possible. Thus the sequence C $7^1_2$  consists of 7 consecutive  $2\pi$  pulses, with the phase of each pulse shifted by  $2\pi/7$  from the previous one. The whole sequence takes two rotor periods, each  $2\pi$  pulse thus takes  $2/7^{\text{th}}$  rotor period. The spin nutation frequency and sample rotation frequency are thus related by  $v_{RF} = (7/2)*v_{rotor}$ . **In practice, the original C7 sequence uses an additional  $\pi$ -phase alternation for every second pulse, so that 14 pulses are executed during 2 rotor periods, requiring  $v_{RF} = 7*v_{rotor}$**

For all C and R sequences, the spin nutation frequency must be accurately matched to the sample rotation rate. Since X-X dipolar couplings are usually small, long mixing times are required to reintroduce the dipolar coupling. When  $^1\text{H}$  decoupling is required, it is important to avoid any transfer of magnetization to or from the proton spin system (HH condition), which would destroy the desired information. This means that the effective fields on X and H must be very different. However, proton decoupling must still be efficient as well. It has been shown that the two RF fields should differ by a factor of 3, which in practice is extremely difficult to meet. It has also been shown that at very high spin rates ( $>16$  kHz) decoupling is not necessary at all. A possible trick is also to use off-resonant LG decoupling during the recoupling sequence. This enhances the effective proton field (vector sum of RF field and offset), and sharpens the HH condition since the Homo-nuclear couplings are suppressed.

Another important parameter to observe is the required excitation bandwidth of these sequences. Naturally, going to higher magnetic fields, the higher chemical shift spread requires higher RF fields for the recoupled X-nuclei, requiring even higher RF fields for protons. So the tendency is going to high spin rates (also desired to get rid of spinning sidebands) and turning the decoupling off during recoupling, which represents a much lower RF load to the probes and increases experimental stability substantially.

## Symmetry Based Recoupling

Table 1 shows the sample rotation rate and the required spin nutation frequencies for the X-nucleus. The spin nutation frequency must be 7 times the sample rotation rate for C7, 5 times the sample rotation rate for SPC5 and 3.5 times the sample rotation rate for SC14. Be careful to obey the maximum allowed spin nutation frequencies for the hardware in use.

It is essential that all these parameters are considered carefully in context with the properties of your sample before the experiment is started, so that the appropriate hardware is used. Especially the choice of the MAS-probe is essential for achieving a sensible setup. [Table 12.1](#) shows the selection parameters for three standard recoupling sequences.

### References:

- E.A. Bennett, R.G. Griffin, and S. Vega, *Recoupling of homo- and hetero-nuclear dipolar interaction in rotating solids*, NMR Basic Principles and Progress **33**, 3-77 (1994).
- S Dusold and A. Sebald, *Dipolar Recoupling under Magic-Angle Spinning Conditions*, Annual Reports on NMR Spectroscopy **41**, 185-264 (2000).
- M. Hohwy, H.J. Jakobsen, M. Eden, M.H. Levitt, and N.C. Nielsen, *Broadband dipolar recoupling in the nuclear magnetic resonance of rotating solids: A compensated C7 pulse sequence*, J. Chem. Phys. **108**, 2686 (1998).
- M. Hohwy, C.M. Rienstra, C.P. Jaroniec, and R.G. Griffin, *Fivefold symmetric Homo-nuclear recoupling in rotating solids: Application to double quantum spectroscopy*, J. Chem. Phys. **110**, 7983 (1999).
- M. Hong, "Solid-State Dipolar INADEQUATE NMR Spectroscopy with a Large Double-Quantum Spectral Width", J. Magn. Reson. **136**, 86-91 (1999).
- A. Brinkmann, M. Edén, and M.H. Levitt, *Synchronous helical pulse sequences in magic-angle spinning nuclear magnetic resonance: Double quantum recoupling of multiple-spin systems*, J. Chem. Phys. **112**, 8539 (2000).
- M. Hohwy, C.M. Rienstra, and R.G. Griffin, *Band-selective Homo-nuclear dipolar recoupling in rotating solids*, J. Chem. Phys. **117**, 4974 (2002)
- C. E. Hughes, S. Luca, and M. Baldus, RF driven polarization transfer without hetero-nuclear decoupling in rotating solids, Chem. Phys. Letters, **385**, 435-440 (2004).

## Pulse Sequence Diagram, Example C7

12.1

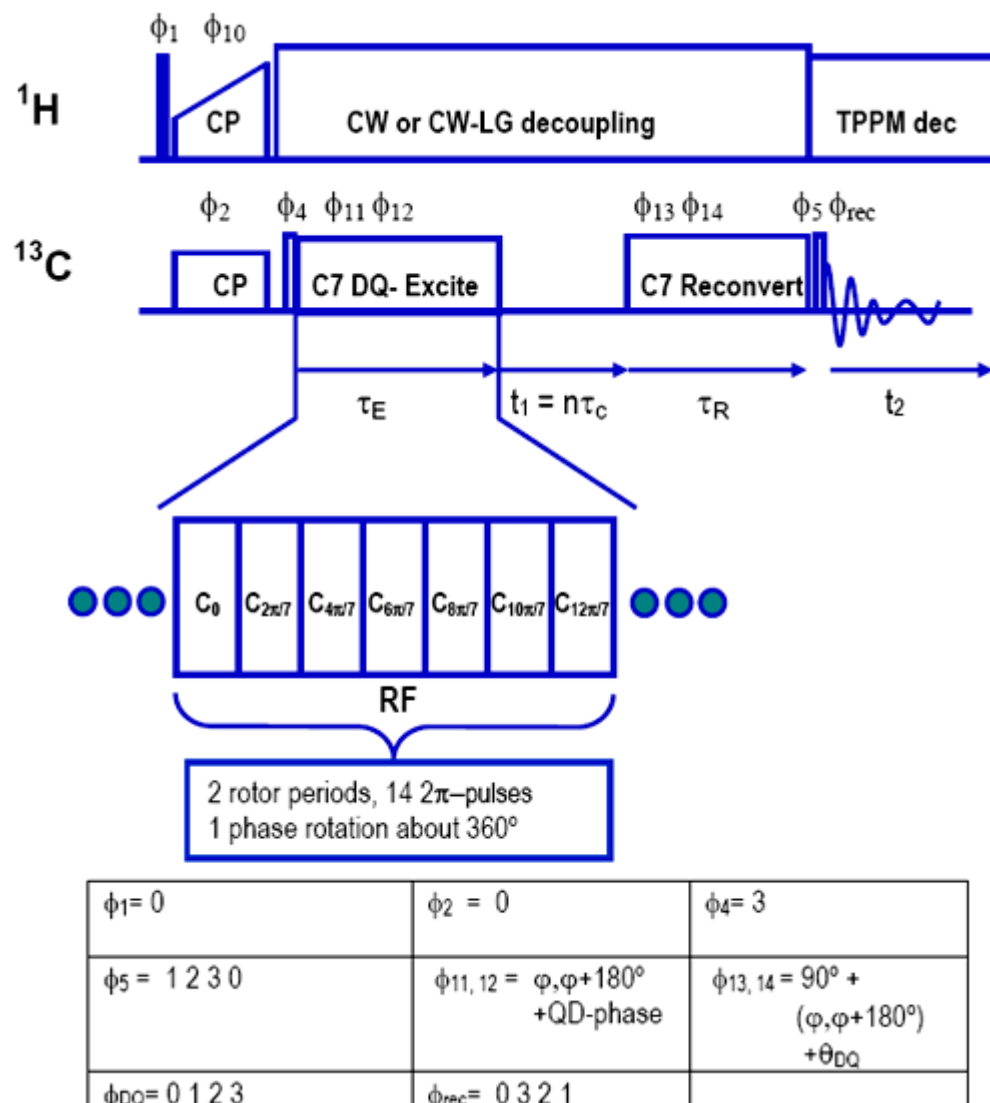


Figure 12.1. C7 SQ-DQ Correlation Experiment

## Setup

12.2

As mentioned before, it is essential that the parameters of your sample of interest are considered before the experiment is started. **Table 12.1.** illustrates the proper choice of hardware for the observe nucleus  $^{13}\text{C}$ . Obviously, observation of DQ coherence requires samples with reasonable dipolar couplings and reasonable probability of coupled species. So, running this experiment on  $^{13}\text{C}$  samples requires reasonable enrichment. Usually, fully enriched samples are used, sometimes diluted in natural abundance samples to reduce nonspecific long range interactions. As always, rotary resonance conditions (overlap of side- and center bands) should be avoided unless specifically desired.

Running the experiment on enriched  $^{15}\text{N}$  samples is of course possible, but one should consider that most samples will not have nitrogen atoms directly attached to each other, so small cou-

plings will prevail, requiring long DQ-excitation and -reconversion times, with a nucleus that requires high RF power levels to achieve a certain RF-field. On the other side, the shift range is not large, allowing relatively slow spinning. Considering a nucleus like  $^{31}\text{P}$ , there is no need for enrichment, but cases with directly bonded  $^{31}\text{P}$ -atoms are rare. Phosphates are usually easy, since the shift range is small (couplings are also rather small). If however a large shift range (possible with  $^{31}\text{P}$ ) needs to be covered, there may be a substantial problem.

*Table 12.1. Recommended Probe/Spin Rates for Different Experiments and Magnetic Field Strengths*

Sequence	n= ( $\nu_{\text{RF}} / \text{masr}$ )	rotor diameter/ <i>masr max.</i>	<i>masr max.</i> rec. <sup>4</sup> (Hz)	$\nu_{\text{RF}}(^{13}\text{C}) \text{ max.}$ (kHz/ $\mu\text{s}$ ) <sup>5</sup>	$\nu_{\text{RF}}(\text{H}) \text{ max.}$ (kHz/ $\mu\text{s}$ ) <sup>6</sup>	$B_0 \text{ max.}$ (MHz) <sup>8</sup>
POST-C7 <sup>1</sup>	7	7/6000	5000	35 / 7.15	70 / 3.5 +LG	300
		4/15000	9000	63 / 4	100 / 2.5 +LG <sup>7</sup>	500
		3.2/24000	12000	84 / 3	110 / 2.27 +LG <sub>7</sub>	600
		2.5/35000	14000	100 / 2.5	130 / 1.95 +LG <sub>7</sub>	800
SPC5 <sup>2</sup>	5	7/6000	5000	25 / 10	70 / 3.5	300
		4/15000	13000	65 / 3.85	100 / 2.5 +LG <sup>7</sup>	500
		3.2/24000	17000	85 / 3	none	700
		2.5/35000	20000	100 / 2.5	none	900
SC14 <sup>3</sup>	3.5	7/6000	6000	21 / 12	70 / 3.5	200
		4/15000	15000	52.5 / 4.75	100 / 2.5 +LG <sup>7</sup>	500
		3.2/24000	22000	77 / 3.25	none	700
		2.5/35000	28000	100 / 2.5	none	950

1. C7 is not recommended due to restricted excitation bandwidth.
2. SPC5 can be recommended as a standard sequence for 4mm probes and not too high fields.
3. SC14 or sequences with similar RF-field requirements are recommended for small spinners/high fields
4. Maximum speed results from max. possible RF-field
5. Maximum  $^{13}\text{C}$  RF fields taken from  $^{13}\text{C}$  RF field specification, or  $^1\text{H}$  RF field specification, considering the requirement of an off HH condition.
6. Maximum RF field for decoupling
7. +LG means cw decoupling with optimized LG-offset frequency at the given RF field in order to avoid HH contact.
8. Maximum magnetic field as proton resonance frequency in MHz. This results from spin rate requirements for  $^{13}\text{C}$  observation (to avoid rotary resonance conditions) as well as excitation bandwidth considerations.

**Spectrometer Setup for  $^{13}\text{C}$** **12.2.1**

1. Load a CPMAS parameter set for  $^{13}\text{C}$ .
2. Load a uniformly labeled glycine sample and rotate at the desired rotation rate (see table 1), depending on the recoupling experiment planned and the sample under investigation. Consider possible rotational resonance conditions in the sample of interest!
3. Tune and match the probe, optimize the  $^{13}\text{C}$  and  $^1\text{H}$  pulse parameters for excitation and decoupling.
4. Use the *cp90* pulse program with ***p11= p11*** to measure the nutation frequency for  $^{13}\text{C}$ , in order to calculate the recoupling conditions (see chapter .... Basic Setup Procedures). Calculate the power levels required by the spin speed (see table 1) using ***calcpowlev***.
5. Set ***p11*** back to 120 dB (***p1*** to zero) and run 1 experiment with 16 (4) scans as a reference.

**Setup for the Recoupling Experiment****12.2.2**

1. Create a new experiment and load the appropriate pulse program (***spc5cp1d***), use the same routing. Set the appropriate sample rotation rate, as required for step 14, set ***cns31*** equal to the rotation rate.
2. Load the power level calculated for the necessary  $^{13}\text{C}$  recoupling  $B_1$ -field into ***p11***, set ***p1*** as determined in step 4.
3. Set ***I0=15*** (should be, but need not be, a multiple of 5 for SPC5 or of 7 for PC7, SC14). This determines the DQ-build-up time (DQ generation). The reconversion time is usually also controlled by ***I0***, it may however be written such as to be independently controlled by a different loop counter. For glycine, about 5msec will be the optimum.
4. Set the decoupling program ***cpdprg1*** to ***cwlg***. Set ***p13*** such as to yield the desired decoupler RF field during the DQ generation/ reconversion, or set it to 120 if the spin rate suffices to omit decoupling. Set ***cns20*** = corresponding decoupling RF field.
5. Optimize ***p11*** for maximum signal intensity.
6. Optimize ***I0*** for optimum signal intensity. In a multi-site spectrum the optima may differ for different spin pairs.

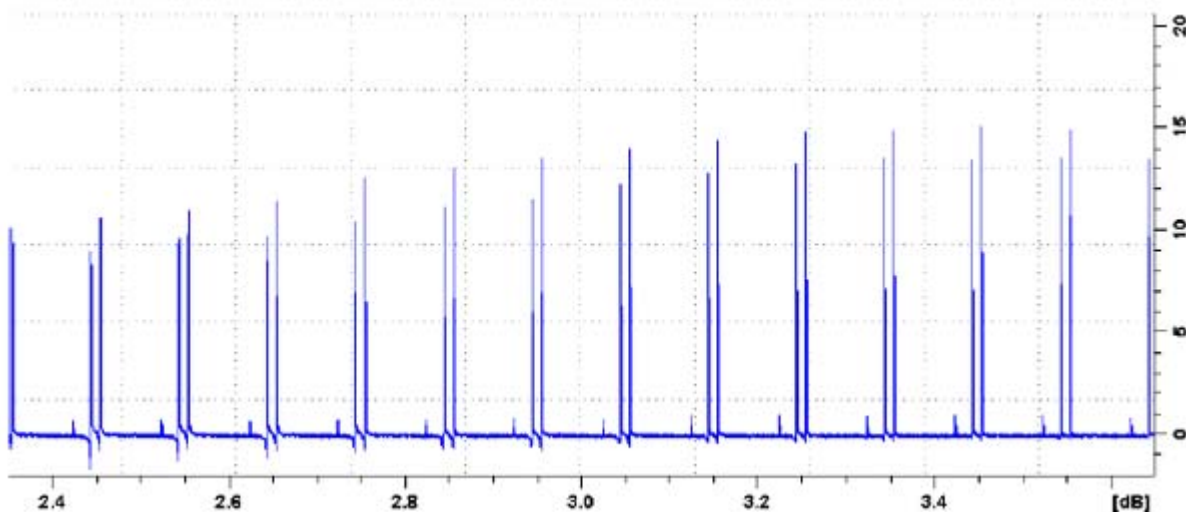


Figure 12.2. Optimization of the RF power level for DQ generation/reconversion on glycine.

## Symmetry Based Recoupling

In principle, both peaks must grow together as one approaches the RF=7\*MASR condition, but the resonances are differently influenced by non-ideal off-HH conditions. The glycine  $\alpha$ -peak is usually hard to get off HH, so it is frequently too small. Optimise the LG-decoupling condition on the glycine  $\alpha$ -peak (step 12).

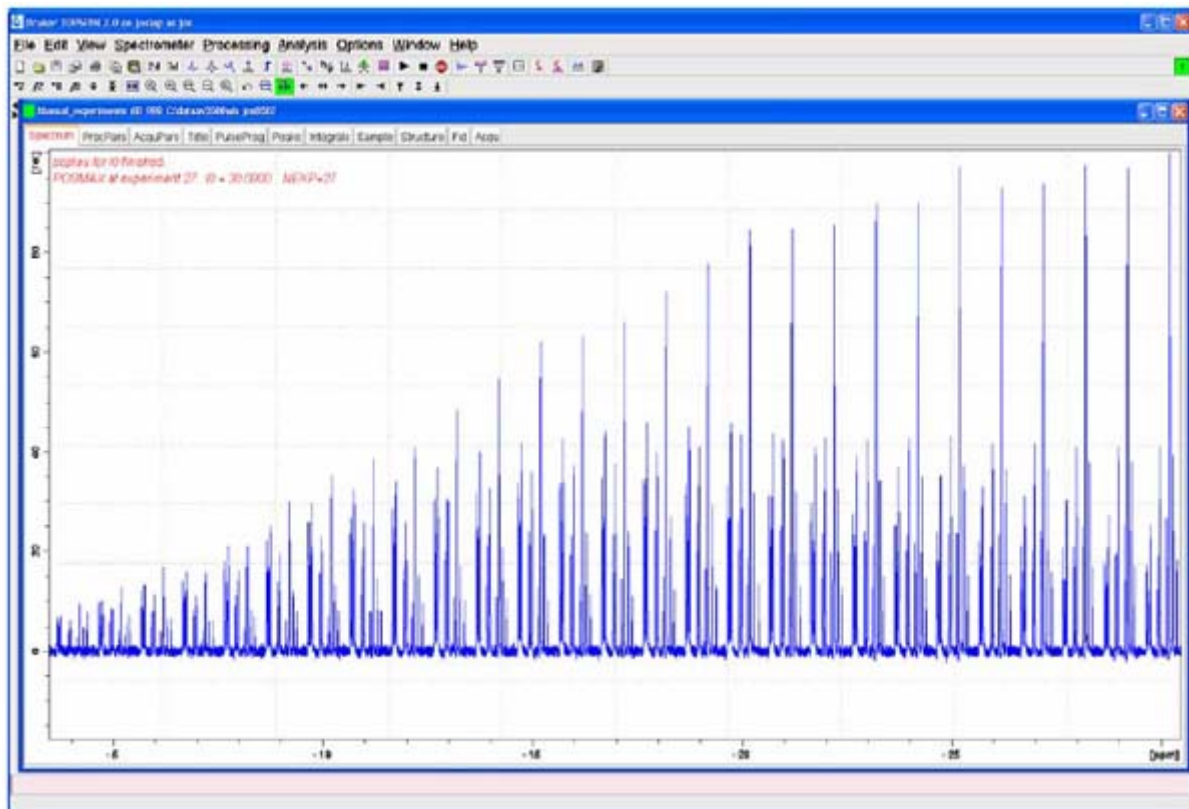


Figure 12.3. Variation of DQ-generation/reconversion time on a uniformly  $^{13}\text{C}$  labeled peptide (fMLF).

Both times were incremented in units of 2 rotation periods. One can clearly see the different maxima for the  $\text{C}_\alpha$ , the aliphatic carbons and the mobile  $\text{CH}_3$ -groups. Spinning speed was 13 kHz.

7. Optimize the **cwlg** decoupling if needed by variation of **cnst20** in increments of 5000 and check whether a different offset condition helps improving the signal intensity.
8. Run one experiment and compare with the direct CP experiment to measure the DQ recoupling yield.

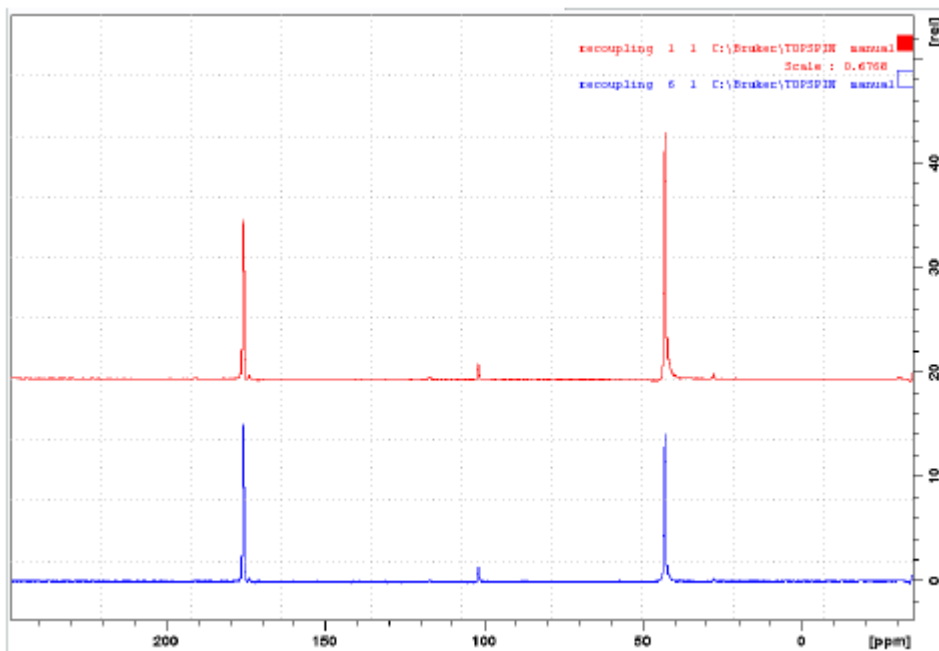


Figure 12.4. PC7 Recoupling Efficiency at a Spinning Speed of 13 kHz

**Figure 12.4.** illustrates PC7 recoupling efficiency at a spinning speed of 13 kHz (about 100 kHz RF field), using a 2.5 mm probe. LG decoupling at 125 kHz was used during DQ generation/reconversion. Quite a noticeable loss on the glycine  $\alpha$ -peak due to insufficient HH suppression is noticeable. Efficiency is 67% on the carboxyl peak (AVIII 700 SB).

#### Setup of the 2D SQ-DQ Correlation Experiment

#### 12.2.3

9. Running such a correlation experiment on glycine makes little sense, so insert a sample with more  $^{13}\text{C}$  sites (fully labelled tyrosine-HCl, or histidine or any other suitable labelled sample). Optimize **I0** for the best compromise in signal intensities.
10. Generate a new data set, set the mode to 2D using the 123 button in **eda**. Load the pulse program **spc5cp2d**.
11. Make sure  $^{13}\text{C}$  is selected as **nuc1** in the F1 dimension, set **FnMode =STATES-TPPI**.
12. Set the spectral window along F1. It is desirable to synchronize sampling along F1 with the rotor spin rate in order to eliminate spinning sidebands (fold back onto center band). This may however lead to peak fold over, since achievable spin rates are usually smaller than the spread of DQ-frequencies along F1. This does however not necessarily mean that the spectra are crowded and uninterpretable, because frequently the folding does not lead to cross peak overlap. Of course, the synchronization to the spin rate need not be used, **cnsf31** can be set equal to the sweep width along F2 which will normally produce spectra free of folding, but of course, spinning sidebands along F1 will occur and signal intensity will be spread over a larger number of cross peaks. An intermediate sampling rate along F1 can be achieved by incrementing the evolution period synchronised to the phase shifted blocks of the sequence (one PC7-block being  $2\pi/7$ ,  $\tau$ =rotor period). This will also not generate sidebands along F1, but provide a larger sweep width and less fold over (M. Hong 1999). Fold over can often be tolerated, **xfshear rotate** may be used to shift the spectrum suitably along F1.

13. Set the acquisition time along F1 to about 10 msec for a start. Lines along the double quantum dimension may be narrower than along the single quantum dimension, so a compromise between experiment time and digital resolution along F1 must be found.
14. Start the experiment.

**Data Acquisition****12.3**

**Sample:** Fully  $^{13}\text{C}$  labelled tyrosine-HCl, or a suitable fully labelled small peptide

**Spinning speed:** 5 – 20 kHz, depends on experimental requirements, see [Table 12.1.](#)

**Experiment time:** 1-4 hours.

*Table 12.2. Acquisition parameters for DQ-SQ correlation experiments using symmetry based recoupling sequences*

Parameter	Value	Comments
Pulse program	spc5cp2d spc5cp2dlsw sc14cp2d r14cp2d pc7cp2d .....	See <a href="#"><u>Table 12.1.</u></a> for hints which sequence to prefer. Rule of thumb: high field: fast spinning, sc14 low field, slow spinning, pc7. Intermediate: spc5. N.b.: sc14 usually has low DQ yield (35%), but that may not matter
NUC1	$^{13}\text{C}$	Nucleus on f1 channel
O1P	100 ppm	$^{13}\text{C}$ offset
NUC2	$^1\text{H}$	Nucleus on f2 channel
O2P	2-3 ppm	$^1\text{H}$ offset
PL1	for > 50 kHz $\nu_{\text{RF}}$	Power level for f1 channel CP and p1
PL11	dep. on <b>masr</b>	Power level for f1 channel recoupling power
PL12	as specified	Power level decoupling f2 channel and excitation
PL13	$\approx$ pl12, optimize, or 120, fast spinning	Power level decoupling f2 channel during cw or cwlq decoupling
P3		Excitation pulse f2 channel
PCPD2		Decoupler pulse length f2 channel ( $^1\text{H}$ ) TPPM
P15		Contact pulse – first contact
D1		Recycle delay
CNST20		Spin nutation frequency at PL13 for cwlq decoupling
L0	for 0.5-10 msec ("mix" in <b>ased</b> )	Use multiples of 5, 7, or 16 (spc5, pc7, sc14) for full phase cycle.
SPNAM0		Ramp for 1 <sup>st</sup> CP step; e.g. ramp: 80 – 100%
SP0		Power level for proton contact pulse

*Table 12.2. Acquisition parameters for DQ-SQ correlation experiments using symmetry based recoupling sequences*

CPDPRG2	SPINAL64	SPINAL64 decoupling
CPDPRG1	cwlg	To avoid HH contacts during DQ-generation, reconversion
NS	4-32	Number of scans (see pulse program phase cycle)
F2 direct $^{13}\text{C}$		(left column)
TD	1024 or 2048	Number of complex points
SW		Sweep width direct dimension, adjust to experimental requirements
F1 indirect $^{13}\text{C}$		(right column)
TD	128 - 512	Number of experiments in indirect dimension
SW	see para. 17 above	Sweep width indirect dimension
ND0	1	STATES-TPPI, not required. In TS 2.1

## Spectral Processing

12.4

### Processing Parameters

*Table 12.3. Processing parameters for DQ-SQ correlation experiments using symmetry based recoupling sequences*

Parameter	Value	Comment
F1 acquisition $^{13}\text{C}$		(left column)
SI	2-4 k	Number of points and zero fill
WDW	QSINE	Sine bell squared
SSB	2-5	Shifted sine bell
PH_mod	pk	Phase correction if needed
F2 indirect $^{13}\text{C}$		(right column)
SI	256-1024	Zero fill
MC2	STATES-TPPI	
WDW	QSINE	Sine bell squared
SSB	2	90° shifted sine bell

*Processing parameters for DQ-SQ correlation experiments using symmetry based recoupling sequences. The AU program **xfshear** may be used with option **rotate** and argument (+/-  $\delta$  ppm) to shift the spectrum suitably along F1. Setting 1 **sr** = 2\***sr+o1** will set the referencing along F1 correctly (just type **sr**, and in f1 enter the value of **sr** for F2 and add \*2+o1).*

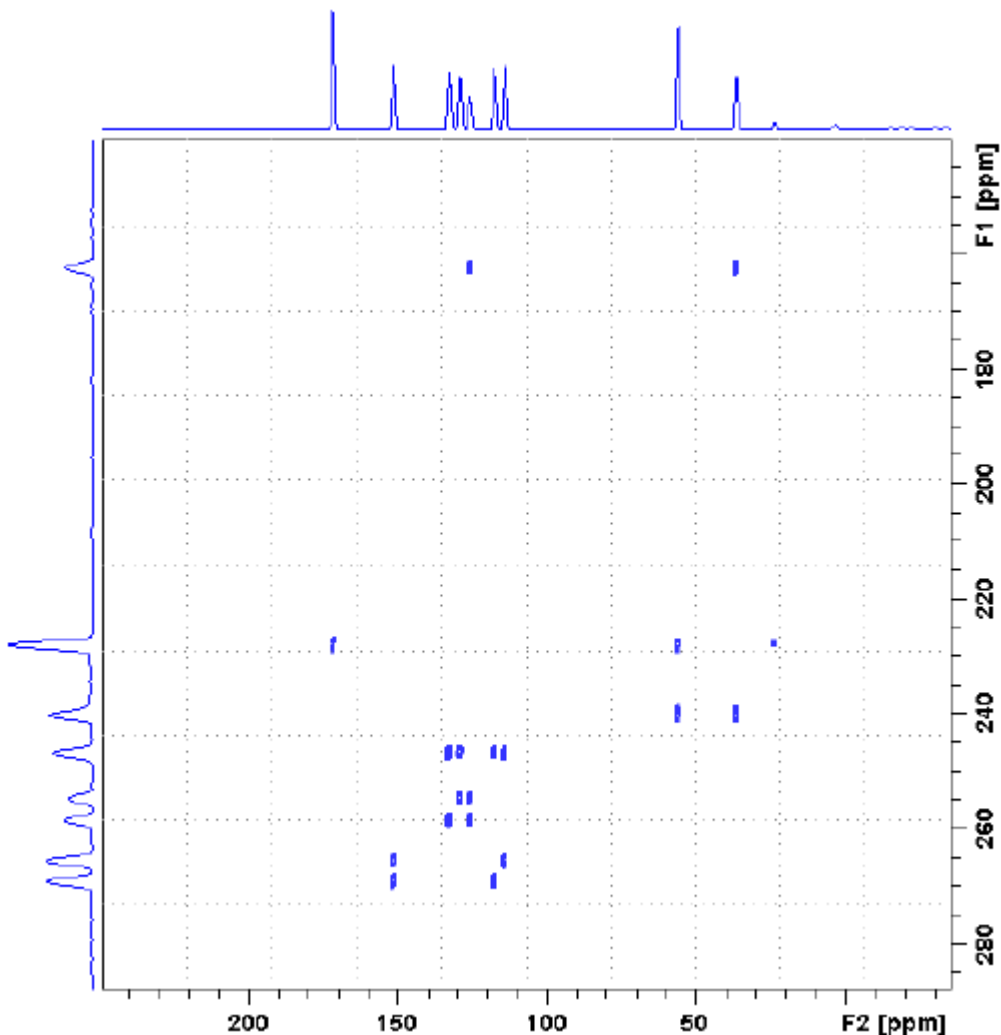


Figure 12.5. SC14 2d SQ-DQ correlation on tyrosine-HCl

SC14 2d SQ-DQ correlation on tyrosine-HCl, 56 rotor periods mixing at 26 kHz, 2.5 mm probe, AV III 700 SB. With the sampling window along F1= spin rate, only the  $\alpha$ - $\beta$ -correlation is folded.

### 13C-13C Single Quantum Correlation with DQ Mixing

### 12.5

Symmetry based DQ recoupling sequences may also be used as mixing periods in SQ-SQ correlation experiments. The experiment resembles the PDSD or RFDR experiments (see "[Proton Driven Spin Diffusion \(PDSD\)](#)" and "[RFDR](#)") as a NOESY-type correlation will be generated. Similarly, the MELODRAM (see Bennett et al., Dusold et al.) sequence with  $v_{RF} = 5 \cdot v_{rotor}$  may be used here.

Parameter	Value	Comments
Pulse program	pc7cp2dnoe	Any sequence may be used, make sure to use the correct timing.
NUC1	<sup>13</sup> C	Nucleus on f1 channel.
O1P	100 ppm	<sup>13</sup> C offset.
NUC2	<sup>1</sup> H	Nucleus on f2 channel.
O2P	2-3 ppm	<sup>1</sup> H offset.
PL1	for > 50 kHz v <sub>RF</sub>	Power level for f1 channel CP and p1.
PL11	dep. on <i>masr</i>	Power level for f1 channel recoupling power.
PL12	as specified	Power level decoupling f2 channel and excitation.
PL13	≈pl12, optimize, or 120, fast spinning	Power level decoupling f2 channel during cw or cwlq decoupling.
P3		Excitation pulse f2 channel.
PCPD2		Decoupler pulse length f2 channel ( <sup>1</sup> H) TPPM.
P15		Contact pulse.
D1		Recycle delay.
CNST20		Spin nutation frequency at PL13 for cwlq decoupling.
L0	for 0.5-10msec ("mix" in <i>ased</i> )	Use multiples of 5,7, or 16 (spc5,pc7,sc14) for full phase cycle.
SPNAM0		Ramp for 1 <sup>st</sup> CP step; e.g. ramp: 80 – 100%.
SP0		Power level for proton contact pulse.
CPDPRG2	SPINAL64	SPINAL64 decoupling.
CPDPRG1	cwlq	To avoid HH contacts during DQ-generation, reconversion.
NS	4-32	Number of scans (see pulse program phase cycle).
F2 direct <sup>13</sup> C		(left column)
TD	1024 or 2048	Number of complex points.
SW		Sweep width direct dimension, adjust to experimental requirements.
F1 indirect <sup>13</sup> C		(right column)
TD	128 - 512	Number of experiments in indirect dimension.
SW	usually = sw (F2)	Sweep width indirect dimension.
ND0	1	STATES-TPPI, not required in TS 2.1.

**Spectral Processing****Processing parameters:** as above

Parameter	Value	Comment
F1 acquisition $^{13}\text{C}$		(left column)
SI	2-4 k	Number of points and zero fill.
WDW	QSINE	Sine bell squared.
SSB	2-5	Shifted sine bell.
PH_mod	pk	Phase correction if needed.
F2 indirect $^{13}\text{C}$		(right column)
SI	256-1024	Zero fill.
MC2	STATES-TPPI	
WDW	QSINE	Sine bell squared.
SSB	2-5	90° shifted sine bell.

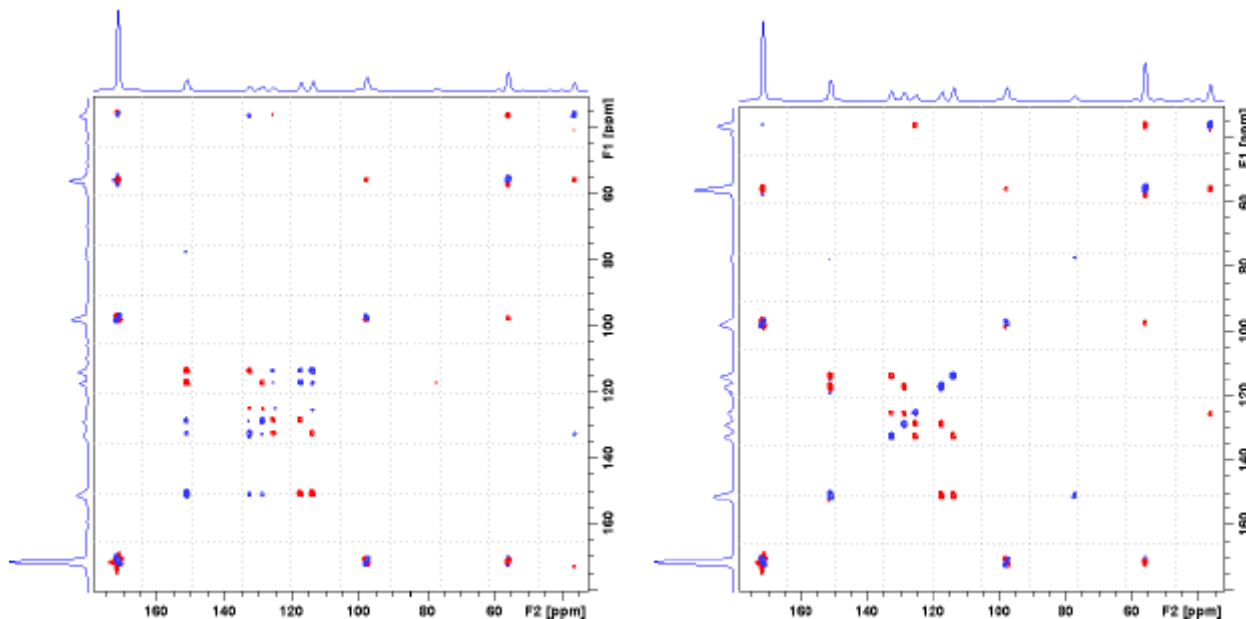


Figure 12.6. PC7 2d SQ-SQ correlation on tyrosine-HCl

PC7 2d SQ-SQ correlation on tyrosine-HCl, 56 rotor periods mixing at 13 kHz, 2.5 mm probe, AV III 700 SB. Left: 84 rotor periods DQ mixing, right: 56 rotor periods mixing. The 84 periods mixing time show relayed correlations (positive, blue) which are absent at 56 periods mixing (except for the SSB cross peaks). Direct correlations are negative (red).

**Introduction****13.1**

Polarization Inversion Spin Exchange at the Magic Angle is an experiment that correlates the chemical shift of a spin 1/2 X nucleus with the hetero-nuclear dipolar coupling to another spin 1/2 nucleus. Most of the applications so far reported have been in the field of structural biology, therefore, the X nucleus is normally  $^{13}\text{C}$  or  $^{15}\text{N}$  and the other heteronucleus  $^1\text{H}$ . The experiment provides orientation information on the vector connecting the  $^{13}\text{C}$  or  $^{15}\text{N}$  and the  $^1\text{H}$  nucleus. The achievable high resolution of the CS as well as the dipole coupling makes the experiment well suited for 3D NMR experiments on aligned systems or single crystals.

Unlike normal FSLG experiments, where the dipolar and CS interactions are scaled by,

$$\cos(\theta_m) = 0.577$$

the scaling factor for the hetero-nuclear dipolar interaction is

$$\sin(\theta_m) = 0.816$$

because the coupling takes place in the transverse plane of the rotating frame, the spin locked state. (The projection is from the tilted frame (locked  $^1\text{H}$  spin system) to the transverse plane of the rotating frame system (spin locked  $^{15}\text{N}$  spin system)).

Through the combination of spin exchange (dipolar flip flop term) and the Homo-nuclear decoupling using FSLG, PISEMA achieves a line width that is an order of magnitude better than its predecessor, the separated local field experiment.

The central line in the dipolar dimension can, among other things, be caused by a proton frequency offset introducing a constant term in the time domain signal. That offset frequency also makes the splitting larger. (See additional test procedures in A. Ramaamoorthy et.al., „*Experimental Aspects of Multidimensional Solid State Correlation Spectroscopy*“).

PISEMA is not very sensitive to the exact Hartmann-Hahn condition. A mismatch has only little effect on the dipolar coupling. The scaling factor in the indirect dimension depends of the  $^1\text{H}$  resonance offset and an incorrect  $^1\text{H}$  carrier frequency may cause some intensity loss and a zero frequency contribution. Diligent adjustment of the LG condition and the rf-carrier is critical for accurate measurement of the dipolar coupling as the splitting increases quadratically with increasing (proton) frequency offset.

Simulations of the spin dynamics show that the hetero-nuclear term in the Hamiltonian leads to a complicated spectrum for small hetero-nuclear dipolar couplings (usually introduced by remote protons), see Z. Gan's paper for more information.

**References**

1. C.H. Wu, A. Ramamoorthy, and S.J. Opella, *High-Resolution hetero-nuclear Dipolar Solid State NMR Spectroscopy*, J. Magn. Reson. A 109, 270-272 (1994).
2. A. Ramamoorthy, C.H. Wu, and S.J. Opella, *Experimental Aspects of Multidimensional Solid State NMR Correlation Spectroscopy*, J. Magn. Reson. 140, 131-140 (1999)
3. A. Ramamoorthy, and S.J. Opella, *Two-dimensional chemical shift / hetero-nuclear dipolar coupling spectra obtained with polarization inversion spin exchange at the magic-angle sample spinning (PISE-MAMAS)*, Solid State NMR 4, 387-392 (1995).
4. Zhehong Gan, *Spin Dynamics of Polarization Inversion Spin Exchange at the Magic Angle in Multiple Spin Systems*, J. Magn. Reson. 143, 136-143 (2000).

**Pulse Sequence Diagram**

13.2

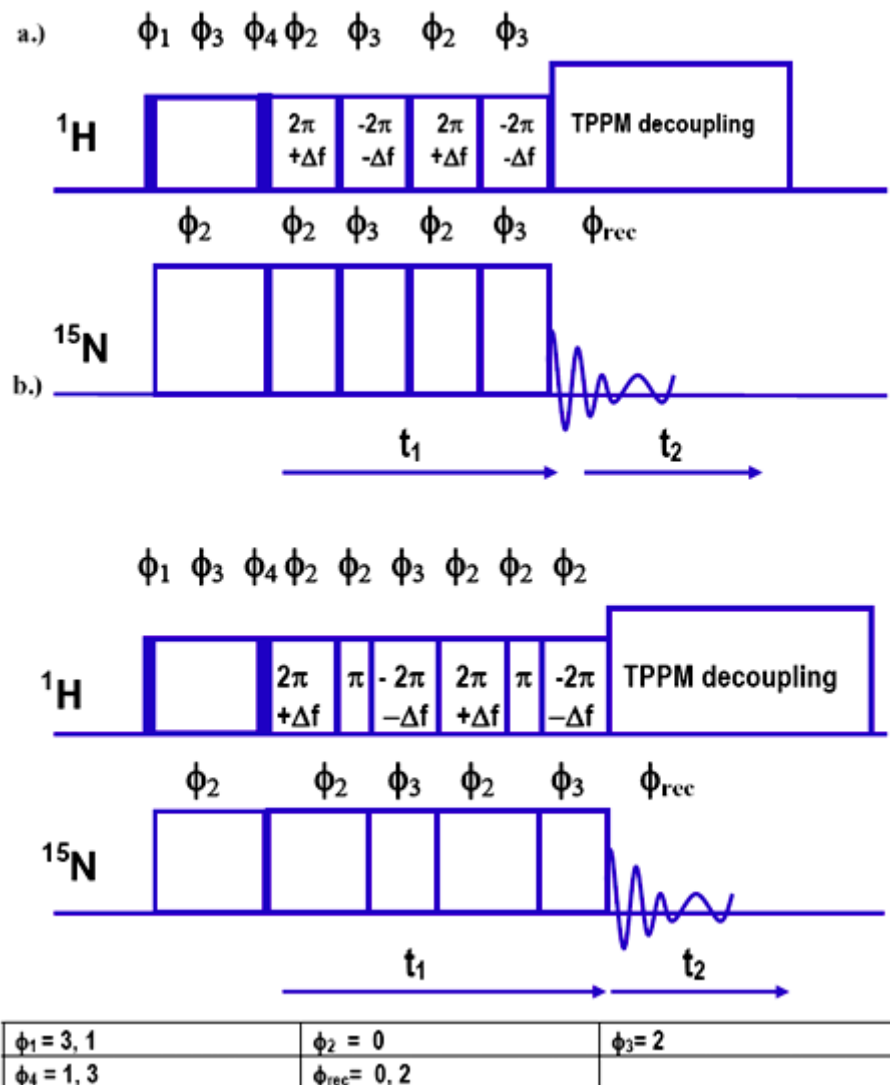


Figure 13.1. Pisema Pulse Sequence

**Figure 13.1:** Pisema pulse sequence a.) straight PISEMA, b.) “clean PISEMA” variation for further suppression of phase glitches (Ramamoorthy et al. Solid State NMR 4).

## Setup

## 13.3

1. Determine HH match of the static sample and the correct  $^1\text{H}$  offset frequency using the pulse program *cplg*.
2. Then, measure the nutation frequency for  $^1\text{H}$  in order to calculate the FSLG conditions.
3. For measuring the LGCP condition, create a new experiment and set the *cplg* pulse program into LGCP by setting the LG flag with **ZGOPTNS** set to **-Dlq**
4. Two possibilities exist to set the FSLG power levels and offset frequencies.
  - a. Either, use the appropriate offset frequency for the chosen contact power level of  $^1\text{H}$  and set **cnst20** accordingly to e.g. 50 kHz, i.e. **cnst20 = 50000.0**. This would give an offset frequency of approximately 35 kHz (**cnst22** should show this number in the **ased** display). Then adjust the  $^{15}\text{N}$  power level during the FSLG period to best HH match - which is at a power level of appropriately  $20 \cdot \log(\sin(54.7)) = 1.8$  dB higher than for the on resonance contact.
  - b. If that option is not adequate because of power limitations on  $^{15}\text{N}$ , one can also leave the on resonance contact levels of  $^{15}\text{N}$  and calculate the offset frequency and power level for  $^1\text{H}$ . That would reduce the required power by about 70% as compared to the power level for on resonance HH match. For the new nutation frequency (B1 field for LG condition):

$$B_{1LG} (^1\text{H}) = \sin(\theta_m) * B_{1on\_res} (^1\text{H}) = 0.82 * B_{1on\_res} (^1\text{H})$$

the offset frequency for the Lee-Goldburg condition is:

$$f_{LG} = \cos(\theta_m) * B_{1on\_res} (^1\text{H}) = 0.578 * B_{1on\_res} (^1\text{H})$$

with the inverse of a 360° pulse. Instead of raising the power level for

$$B_{1on\_res} = 1/(\tau_{2\pi})$$

$^{15}\text{N}$ , the power level for  $^1\text{H}$  is reduced by about 1.7 dB. Then the new  $2\pi$  pulse in the tilted frame is:

$$\tau_{2\pi_{LG}} = B_{1on\_res}^{-1} \sin^2(\theta_m) = 0.67 B_{1on\_res}^{-1}$$

In our example of a contact power level of 50 kHz on  $^{15}\text{N}$  one would then calculate for **cnst20 = 40 807.0**, giving an offset frequency of 28855 Hz for the LG frequency, which is calculated automatically.

5. In order to verify all calculated power levels and offset frequencies, optimize for the appropriate power level using the pulse program *cplg*.
6. If the sample does tune and match very differently than the setup sample, check the HH conditions briefly and verify that the found parameters are valid. Correct power levels or pulse parameters if needed. This is especially important for saline lipid water mixtures.
7. Create a new experiment and setup a 2D data set, as described in the previous chapter.

After 1D parameter optimization as previously described, type **iexpno** to create a new data file and switch to the 2D mode using the “123” button. Set in **eda** the appropriate **FnMode** parameter. Pulse program parameters are listed in [Table 13.1](#) in eda, set.



Figure 13.2. The “123” Icon in the Menu Bar of the Data Windows Acquisition Parameter Page.

The “123” icon in the menu bar of the data windows acquisition parameter page is used to toggle to the different data acquisition modes, 1D, 2D and 3D if so desired.

8. Go into **eda** and set parameters for sampling in the indirect dimension, the spectral width.
9. In order to set the  $t_1$  increment, go into the **ased** window and choose **I3** to be 1, 2 or 3. This sets the  $t_1$  increment and the parameter **in0** is updated. To get the calculated parameter **in0** such that one can inspect the appropriate spectral width in F1 which should be no less than 20 kHz, type **in0** and enter the value given behind **in0** in the **ased** window ([Figure 13.3](#)).
10. Make sure the correct nucleus is selected in Me dimension.
11. Choose the appropriate sampling time (**TD1**) so that the required resolution (**FIDRES**) in the indirect dimension is achieved.
12. Depending on the decision above, whether the rf power on the X or on the  $^1\text{H}$  channel are changed during the SEMA part of the experiment, set
  - a. either  $\text{PL13} = \text{PL2}$  (case 4b) and set  $\text{PL11}$  to the optimized value, higher power, i.e. a value of about 1.8 dB below  $\text{pl1}$ ;
  - b. or set  $\text{PL11} = \text{PL1}$  (case 4a above) and  $\text{PL13}$  to the obtained value in the cplg experiment, i.e. about 1.8 dB higher than  $\text{PL2}$ , which is less RF power.
13. Start the experiment.

<b>Channel F1</b>		<b>PULPROG =</b>	<b>pisemajos</b>	<input type="button" value="..."/> <input type="button" value="E"/>	Pulse program for acquisition
		<b>TD =</b>	<b>2048</b>		Time domain size
		<b>NS =</b>	<b>16</b>		Number of scans
		<b>DS =</b>	<b>0</b>		Number of dummy scans
		<b>SWH [Hz] =</b>	<b>37878.79</b>		Sweep width in Hz
		<b>AQ [s] =</b>	<b>0.0270036</b>		Acquisition time
		<b>RG =</b>	<b>32</b>		Receiver gain
		<b>DW [μs] =</b>	<b>13.200</b>		Dwell time
		<b>DE [μs] =</b>	<b>1.00</b>		Pre-scan-delay
		<b>CNST11 =</b>	<b>-1.0000000</b>		To adjust t=0 for acquisition, if digmod = base
		<b>CNST20 =</b>	<b>62500.0000000</b>		LG-RF field as adjusted, in Hz used to calculate offset
		<b>CNST24 =</b>	<b>1.0000000</b>		Offset for proton evolution under LG, usually 0
		<b>D1 [s] =</b>	<b>5.0000000</b>		Recycle delay
		<b>in0 [s] =</b>	<b>0.00004286</b>		$\text{In0}=2*\text{p513}^0.82$
		<b>I0 =</b>	<b>0</b>		$\text{I0}=0$
		<b>L3 =</b>	<b>2</b>		For dwell in t1 ( $=2*\text{p513}^0.82$ )
		<b>count =</b>	<b>32</b>		Count=t01/2
<b>▼ Channel F1</b>					
		<b>NUC1 =</b>	<b>13C</b>	<input type="button" value="Edit..."/>	Nucleus for channel 1
		<b>P15 [μs] =</b>	<b>2000.00</b>		Contact pulse
		<b>PL1 [dB] =</b>	<b>2.00</b>		For X contact pulse
		<b>PL11 [dB] =</b>	<b>120.00</b>		For X contact during SEMA
		<b>PL11W [W] =</b>	<b>0.0000000</b>		For X contact during SEMA
		<b>PL1W [W] =</b>	<b>158.48931885</b>		For X contact pulse
		<b>SFO1 [MHz] =</b>	<b>125.7502468</b>		Frequency of observe channel
<b>▼ Channel F2</b>					
		<b>cnst21 =</b>	<b>0.000000</b>		$\text{Cnst21}=0$
		<b>cnst22 =</b>	<b>44195.171875</b>		$\text{Cnst22}=\text{cnst20}/\sqrt{2}+\text{cnst24}$
		<b>cnst23 =</b>	<b>-44193.171875</b>		$\text{Cnst23}=-\text{cnst20}/\sqrt{2}+\text{cnst24}$
		<b>CPDPRG2 =</b>	<b>spinal64</b>	<input type="button" value="..."/> <input type="button" value="E"/>	$\text{Cw}, \text{tp1pm15}, \text{spinal64}$
		<b>NUC2 =</b>	<b>1H</b>	<input type="button" value="Edit..."/>	Nucleus for channel 2

Figure 13.3. ASE Display for the PISEMA Setup.

With  $L3 = 2$  and  $\text{cnst20} = 62500$ , an offset frequency of 44.2 kHz for the LG condition is calculated and consequently an  $\text{in0}$  of 42.86  $\mu\text{s}$ , which is already corrected for the scaling-factor of 0.82.

## Data Acquisition

## 13.4

**Sample:**  $^{15}\text{N}$  labeled glycine for power level determination and  $^{15}\text{N}$  labeled acetylated glycine or acetylated valine or leucine for running the PISEMA experiment

**Experiment time:** 15h

Table 13.1. Acquisition Parameters

Parameter	Value	Comments
PULPROG	Pisema, pisema-clean	Pulse programs.
NUC1	15N	
SW		Reasonable SW in F2.
O1P	90 – 160 ppm	For 15N labeled acetylated glycine.
NUC2	1H	
O2P	to be optimized	For 15N labeled acetylated glycine.
PL1		For 15N contact.
PL11		Or 15N evolution.
PL2		For 1H contact and excitation.
PL12		For 1H hetero-nuclear decoupling during t2.
PL13		For 1H Evolution under FLSG condition.
P3		1H excitation pulse.
P15		15N-1H Contact pulse.
P6		1H LG 294 degree pulse.
D3	1.4 $\mu$ s	For frequency & phase setting D*X only.
cnst20		1H spin nutation frequency achieved with PL13.
cnst21	0	Offset from o2 in Hz.
cnst22		+ LG frequency in Hz calculated.
cnst23		- LG frequency in Hz calculated.
L3	1 – 3	Loop counter for appropriate t1 increment.
F2 acquisition 15N	*****	(left column).
AQ_MOD	qsim	
TD	512	No of points.
DW		Dwell time in t2.
F1 indirect 1H	*****	(right column).
TD	64	Number of points.
ND0	1	
IN0	L3*2*p6*SF or L3*2.5*p6*SF	Scaling factor for PISEMA 0.82 = sin(54.7 deg.) calculated by pulse program.

1. Process the direct dimension with *xf2*.
2. Accommodate for the *cos* modulated signal by setting the imaginary part to zero using the au program *zeroim* by typing into the command line *zeroim*.
3. Process the indirect dimension with the command *xf1*.
4. For more automated processing one can write a short macro using the command *edmac* and the filename *2dft* for examples: write the following commands using the text editor:

*xf2*

*zeroim*

*xf1*

5. Save and close the *edmac* editor.
6. In future you can do then the processing by simply typing *2dft* into the command line or even creating your own icon in TopSpin for this purpose.

Table 13.2. Processing Parameters

Parameter	Value	Comment
F2 acquisition $^1\text{H}$	*****	Left column.
SI	1k	Number of complex points in direct dimension.
WDW	no	Apodization in t2.
F1 indirect $^{15}\text{N}$	*****	Right column.
SI	128	Number of complex points in indirect dimension.
MC2	QF	

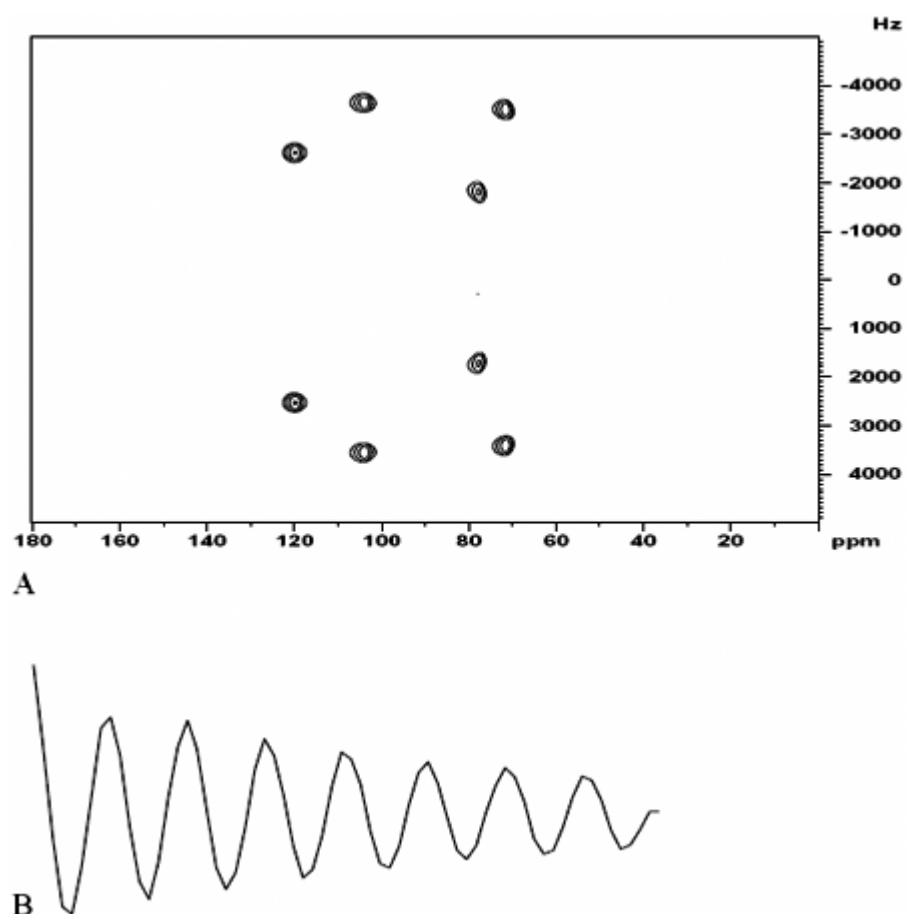


Figure 13.4. A) PISEMA Spectrum of  $^{15}\text{N}$  Labeled Acetylated Valine, B) FID in  $t_1$  over 3.008 ms 64 Data Points

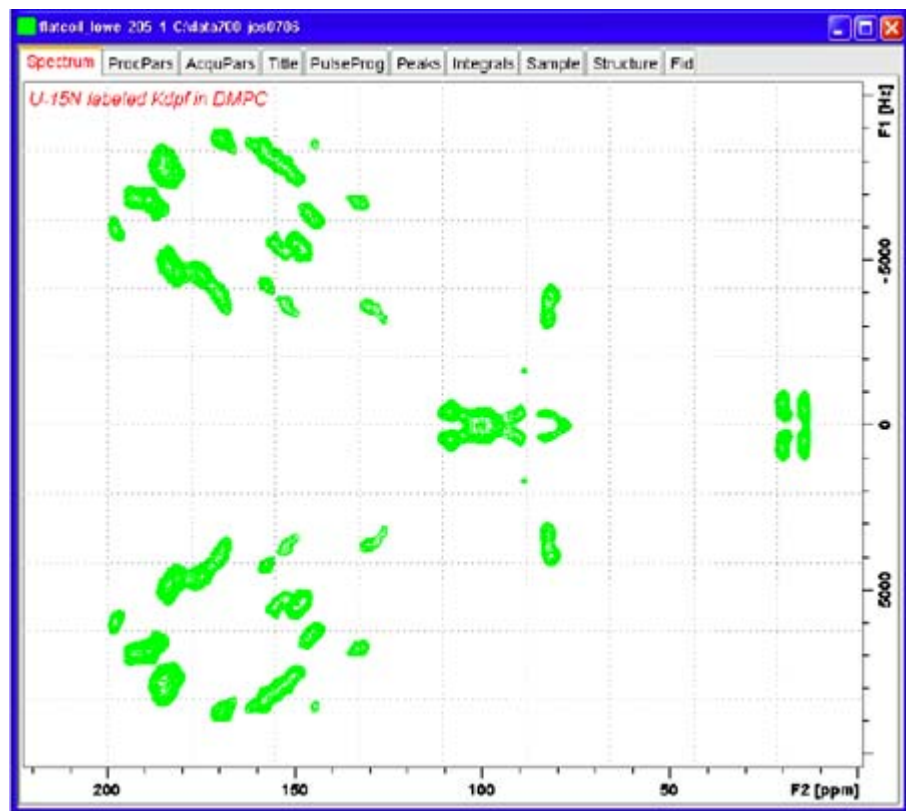


Figure 13.5. PISEMA Spectrum of  $^{15}\text{N}$  Labeled Kdpf Transmembrane Protein.

PISEMA spectrum of  $^{15}\text{N}$  labeled Kdpf transmembrane protein aligned in DMPC (courtesy NHMFL T Cross) membrane between glass plates using  $E^{\text{FREE}}$  700 MHz probe.



# Relaxation Measurements

# 14

In NMR experiments, one is generally concerned with measuring resonance frequencies, and relating these to the local molecular environment. To do this the state of the system of spins in the sample must be changed from equilibrium. At equilibrium, the net magnetization due to the spins is aligned along the magnetic field axis. By applying a radio frequency pulse the net magnetization is tilted away from the field axis, and the resulting precessing magnetization generates the observed signal. The pulse has disturbed the system from equilibrium, and over time the system will return to its equilibrium state. This process is called relaxation.

This chapter describes experiments used for measuring relaxation rates in solid-state NMR. A basic description of relaxation is provided in order to define terms and introduce the techniques involved, but discussion of the significance and use of relaxation data is outside the scope of this manual. Many textbooks provide more detail on the theory of relaxation: the classic is Abragam:

A. Abragam, *Principles of nuclear magnetism*, Oxford: Clarendon Press, (1961)

but simpler descriptions can be found in the books of Slichter and Levitt:

C.P. Slichter, *Principles of magnetic resonance*, Springer (1996, 3<sup>rd</sup> ed.)

M.H. Levitt, *Spin dynamics: Basics of nuclear magnetic resonance*, Wiley (2001)

Some discussion of  $T_{1r}$  relaxation, including effects of dipolar coupling to proton spins, can be found in:

D.L. VanderHart and A.N. Garroway,  $^{13}\text{C}$  NMR rotating frame relaxation in a solid with strongly coupled protons: polyethylene, *J. Chem. Phys.*, **71**:2773-2787, 1979

Details of the X  $T_1$  experiment with CP are in:

D.A. Torchia, The measurement of proton-enhanced  $^{13}\text{C}$   $T_1$  values by a method which suppresses artifacts, *J. Magn. Reson.*, **30**:613-616, 1978

The TOPSPIN software includes a tool for processing the data obtained in relaxation measurements, and this will be demonstrated for the different types of relaxation experiment.

---

## Describing Relaxation

14.1

Relaxation of the net magnetization can be described in terms of two processes. After a pulse, the state of the system differs from the equilibrium in two ways: the z-magnetization is not equal to the equilibrium value, and the net magnetization in the transverse plane is non-zero. The return of the z-magnetization to equilibrium is termed longitudinal relaxation, or spin-lattice relaxation, and the return of transverse magnetization to zero is termed transverse or spin-spin relaxation. Both the transverse magnetization and the difference between the current and equilibrium z-magnetization decay exponentially, with time constants denoted  $T_1$  for longitudinal relaxation and  $T_2$  for transverse relaxation. Relaxation also occurs while radio frequency pulses are being applied to the system. Normally this is ignored, but in the case of spin-locking pulses it is important. During cross-polarization, the magnetization on the dilute spins is increased by

transfer from another nucleus, but it will also decay, since the radio frequency field (weak compared to the static field  $B_0$ ) is insufficient to maintain the resulting transverse magnetization. If the pulse on the excitation nucleus is stopped, and only that on the detection nucleus continued, the transverse magnetization will decay exponentially, with a time constant denoted  $T_{1\rho}$ . This rate of decay will be strongly affected by the amplitude of the spin-locking pulse.

Both of these processes occur via spin energy level transitions. It turns out that the spontaneous transition rate is very low, and thus relaxation is dominated by stimulated transitions. Such transitions are stimulated by local magnetic fields, which fluctuate due to local molecular motion, and the transition rates depend on the strength, and details of the fluctuations, of these local fields. Since the fluctuations are random, the rate of fluctuation is defined by the correlation time of the motion. For efficient relaxation via a particular energy level transition, fields fluctuating with an inverse correlation time close to the frequency of the transition are required. Longitudinal relaxation occurs via transitions on a single spin, and thus requires fields fluctuating with inverse correlation times near to the Larmor frequency. Transverse relaxation occurs also via flip-flop transitions of pairs of spins, which have energies close to zero, and so local fields fluctuating very slowly will cause transverse relaxation.  $T_{1\rho}$  relaxation involves transitions at the nutation frequency of the spin-locking pulse, which can be chosen by the experimenter. Measurement of these relaxation rates can therefore provide information about local motions on a range of time scales.

### T1 Relaxation Measurements

14.2

Longitudinal relaxation can be measured using a number of methods – which method is appropriate depends on the sample involved. Here the experiments are demonstrated on glycine, which has a very simple spectrum and will give results using all the methods discussed. In general the only setup required is to calibrate pulses for the nucleus under observation, and to have some idea of the relaxation time constants involved.

#### Experimental Methods

14.2.1

The inversion-recovery method is the originally proposed method for measuring  $T_1$  values. The experiment proceeds as follows: firstly, the magnetization is inverted by a  $180^\circ$  pulse. Then, there is a delay during which the magnetization relaxes, and a  $90^\circ$  pulse converts the remaining longitudinal magnetization to transverse magnetization, and an FID is recorded. The intensity of a particular signal in the resulting spectrum depends on the initial intensity, the relaxation delay, and the relaxation time constant  $T_1$  as follows:

$$S(t) = S_E + (S(0) - S_E) \exp(-t/T_1) \quad (\text{Eq. 14.1})$$

where  $t$  is the relaxation delay,  $S_E$  is the maximum signal seen when  $t$  is infinite,  $S(0)$  is the signal measure with no relaxation delay, and  $T_1$  is the relaxation time constant for the spins giving rise to that signal. Measurement of  $S(t)$  for a number of relaxation delays allows determination of  $T_1$ .

The disadvantage of the inversion recovery experiment is that the delay between scans needs to be somewhat longer than the longest  $T_1$  of the slowest relaxing spins in the sample. If cross-polarization from protons is possible, the initial inversion pulse can be replaced by a cross-polarization step followed by a  $90^\circ$  pulse on the nucleus to be observed. Then, the required delay between scans  $d1$  becomes that for relaxation of the protons. *In most cases, the proton T1 is moderate so inversion recovery (Torchia method) is the method of choice.*

If the T<sub>1</sub> relaxation time is extremely long, the saturation-recovery experiment is preferred. Here, the transitions are saturated by a rapid sequence of hard pulses, such that no signal remains. There is then a variable delay, during which relaxation occurs, and then a 90° read-out pulse. If the relaxation delay is very short, no signal is seen, and at long relaxation times the maximum signal is seen. The advantage is that the saturation time required does not need to be many times the longest T<sub>1</sub> value. The state of the system at the start of the experiment is forced by the saturation pulses, so a long recycle delay is not required.

***The CP Inversion Recovery Experiment*****14.2.2**

**Sample:** Glycine

**Spinning speed:** 10 kHz

**Experiment time:** 20 minutes

Before starting the experiment, the spectrometer should be set up as described in the basic setup procedures chapter, including measurement of the carbon pulse lengths, and the CP spectrum of glycine should be acquired for reference. Since relaxation times are necessarily temperature dependent, control of the sample temperature is desirable. The data shown here were all acquired at an approximate temperature of 20° C. The form of the pulse program is shown in the following figure.

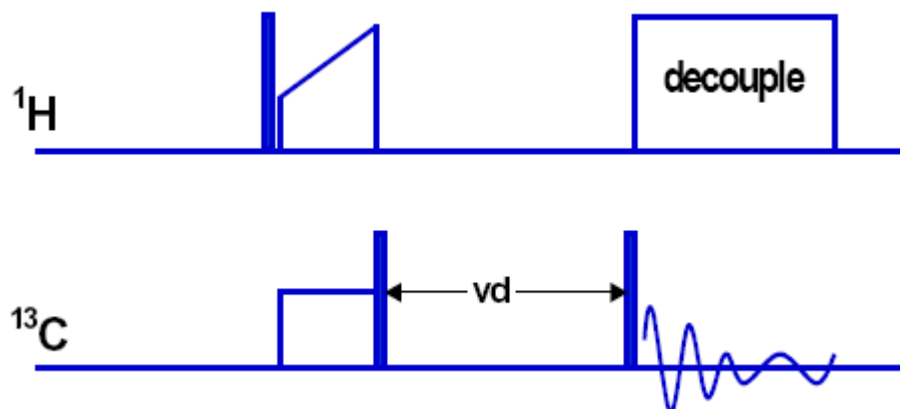


Figure 14.1. The CPX T1 Pulse Sequence

Starting from the glycine spectrum, create a new data set, set parameters according to [Table 14.1](#), and acquire a 1D spectrum. The relaxation delay after inversion is controlled by a variable delay list – this can be created using `edlist`, and the name of the list set as the parameter `vdlist`.

Table 14.1. Parameters for the 1D CP Inversion Recovery Experiment

Parameter	Value	Comments
Pulprog	cpxt1	
Vdlist	See text	Relaxation delays after inversion pulse. Short value – to set spectrum phase correctly.

## Relaxation Measurements

*Table 14.1. Parameters for the 1D CP Inversion Recovery Experiment*

d1	3s	Needs only to be 3x proton T1.
p11	Measured X pulse power.	
p1	Measured 90° X pulse length at p11.	
Ns	2	Should be enough to see a reasonable spectrum.

This pulse program uses the method of Torchia, in which the phase of the contact pulse, and the receiver, is inverted in alternate scans. In the first scan, the first 90° pulse creates  $-z$  magnetization, and in the second scan it creates  $+z$ . The phase cycling of the receiver means that the difference between the two scans is recorded. For short relaxation delays, neither relaxes significantly, and so the maximum signal is recorded. At longer relaxation delays, both the  $+z$  magnetization (which is larger than the equilibrium value as it is created by CP), and the  $-z$  magnetization relax, and the recorded signal decays exponentially as a function of the relaxation delay. At long times both have relaxed back to equilibrium, and the two scans yield a zero signal.

The resulting spectrum should be phased to give positive peaks – given the very short recovery delay, no appreciable relaxation will have occurred. Now we can set parameters for the 2D acquisition, as in [Figure 14.1](#). Since this is a pseudo-2D experiment, the only relevant parameter in F1 is the number of points, which should be the number of entries in the vd list. The most important setting is the range of relaxation delays set in the vd list. Ideally, the list should run from times short enough for no appreciable relaxation to occur, up to a few times the longest  $T_1$  value. Of course, the accurate relaxation time constants are not known in advance, but order of magnitude estimates can be obtained by running the 2D experiment with a small number of relaxation delays, and a small number of scans per slice. The relaxation delays should be approximately equally spaced in  $\log(\text{delay})$ , in order that decays with all time constants in the range are equally well characterized. Data can always be improved either by increasing the number of relaxation delays sampled, or by averaging more FIDs at each relaxation delay. For the glycine sample, a suitable list of times would be:

100ms, 220ms, 450ms, 1s, 2.2s, 4.5s, 10s, 22s, 45s.

*Table 14.2. Parameters for 2D Inversion Recovery Experiment*

Parameter	Value	Comments
Parmode	2D	
Vdlist	See text	
td(f1)	Number of entries in vd list	
FnMODE	QF	This is not a real 2D experiment.
NS	4, for the glycine sample	Sample dependent – need to see a reasonable spectrum, but must be an even number.

Once the pseudo-2D data has been recorded, the processing parameters must be set and checked before it can be evaluated using the T<sub>1</sub>/T<sub>2</sub> relaxation tool. **Table 14.3.** lists the relevant parameters. No processing is done in the indirect dimension (the relaxation dimension), but the size must still be set to a power of two for TOPSPIN to create a processed data file. The size should be next power of two larger than the number of relaxation delays used. The zero points appended are ignored by the relaxation analysis. In principle the line shape in the frequency dimension does not affect the analysis, so exponential multiplication with **Ib** of the order of the observed line width can be applied to improve the signal-to-noise ratio.

*Table 14.3. Processing Parameters for CP T1 Relaxation Experiment*

Parameter	Value	Comment
F2 – acquisition dimension		
SI	=TD	Zero fill.
LB		Matched to line width.
WDW	EM	
Ft_mod	FQC	
ABSF1	1000	Limits for baseline correction.
ABSF2	-1000	Should cover entire F2 width.
F1 – relaxation dimension		
SI	Smallest power of 2 greater than TD(F1)	Must be 2n, but any zeros will be ignored.

Once the parameters are set, process the data with **xf2**, to execute a Fourier transform in the f2 dimension only. The phase can be adjusted from within the relaxation analysis tool, but baseline correction should be carried out with **abs2**. Start the relaxation analysis guide with the command **t1guide**. The sequence of icons guides you through the analysis as follows:

**Extract slice:** The first spectrum row should be selected for phase correction, as this contains maximum signal. The spectrum should then be phased to give positive peaks.

**Define ranges:** Here you must define integral regions containing the peaks of interest. The fitting routine can either use the integral of the signal, or the intensity, in which case the maximum signal in each integral region is used. Regions can be defined via the cursor, or between specified limits via a dialogue box. The integral regions need to be saved to a special file, by clicking the disk icon towards the left of the integral window (not the standard save integrals button on the right), and selecting ‘export regions to relaxation module and.ret’.

**Relaxation window:** Here the intensity or area values from the first integral region are displayed. The icons at the top of this window allow you to move between the integral regions, exclude points from the calculation, display the data on a variety of axes, and start the fit for the displayed region or all regions. **Figure 14.1.** shows the decay of the a-carbon signal of glycine as a function of relaxation delay, along with the fit and calculated relaxation parameters. Note that any peaks with integrals or intensities too close to zero will be omitted from the analysis by

the software – if you see less points in the relaxation window than were actually recorded, this may be because they have insufficient intensity.

**Fitting function:** Here the parameters of the fitting calculation are set. The general parameters should be determined automatically, but ensure that the limits for baseline correction are set to cover the whole spectrum. The fitting function depends on the experiment, but in this case the signals decay exponentially, so the function ‘expdec’ should be chosen. The list filename should be ‘vd’ – this will take the specified **vdlist** from the data set. Note that when the experiment is run, the selected **vdlist** is written into the acquisition data directory as the file “vdlist”, so it is always available, even if the source list is edited. The fitting program can calculate multi exponential fits, but data with very good signal-to-noise is required for this to be accurate. Unless there is obvious overlap of peaks, the assumption is usually that each peak corresponds to a single nuclear site, and thus a single  $T_1$  value.

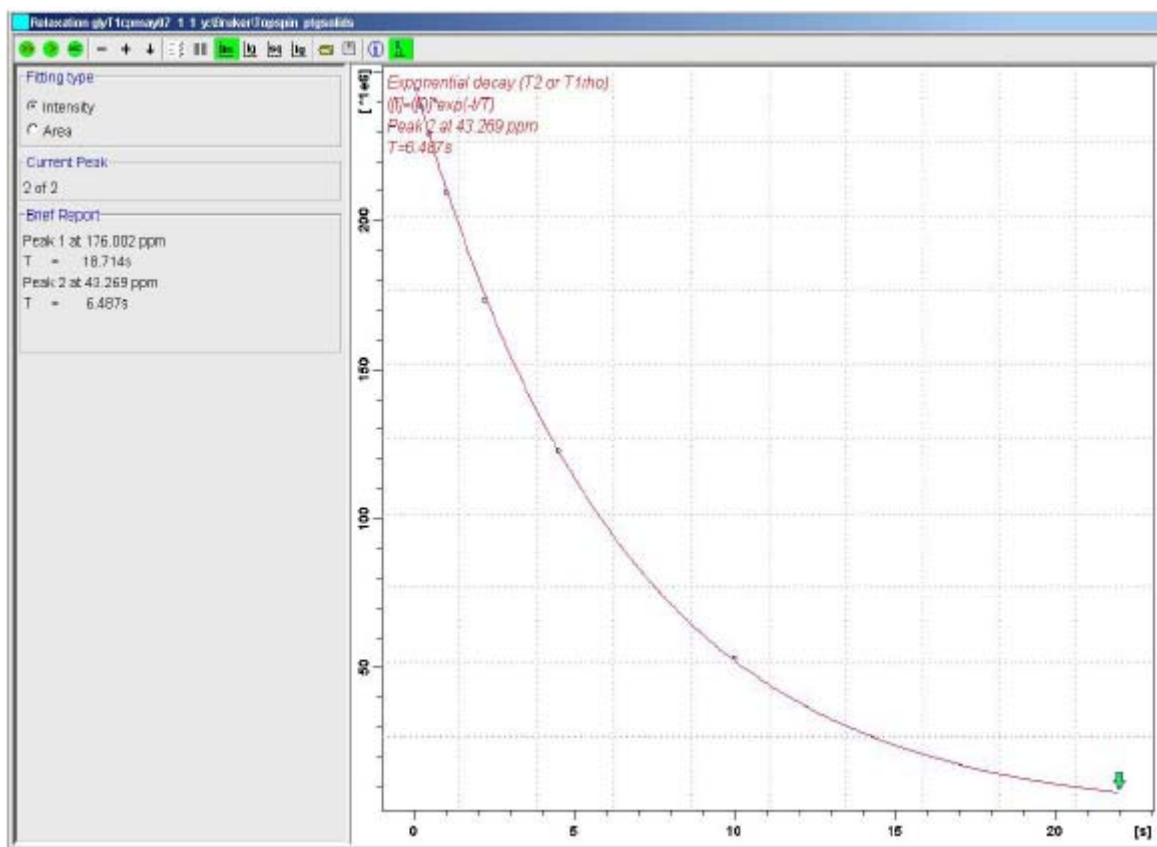


Figure 14.2. Relaxation of Alpha-carbon Signal in Glycine

**Start calculation:** This will perform the fitting procedure for all regions. The calculated function is displayed as a red line on the same axes as the data points. The plus and minus icons can be used to move through the different regions. If you wish to change whether the fit is based on the integral or the intensity, select the appropriate radio button, and repeat the fit using the icons immediately above. The >> icon will fit all the peaks, the > icon will fit just the current one.

**Display report:** This displays a text report of the results of the fit, including the details of the fit function, and the calculated values of the parameters in the function. The experimental and calculated data points are also displayed. Note that the experimental data is normalized such that the most intense point has a value of 1. This report file is also saved in the processed data di-

rectory when the fit is calculated. If fitting of a single peak is performed, only this result is written to the report. If the 'fit all peaks' option is used, all results will be stored.

The results for glycine at 500 MHz and room temperature should be approximately 18.5s and 6.4s for the carbonyl and alpha-carbon signals respectively - at other field strengths the numbers will be somewhat different. If the signals are really undergoing mono exponential relaxation, the curve should be a good fit to the measured data.

### ***The Saturation Recovery Experiment***

**14.2.4**

For samples where cross-polarization is not possible, the inversion recovery experiment would be very time consuming, as the recycle delay **d1** would need to be approximately 3x the longest  $T_1$  value. For glycine at room temperature, this would mean a delay of about 60s per scan, in addition to the variable relaxation delay. The saturation-recovery experiment removes the need for long **d1** by forcing the system into saturation at the beginning of each scan.

**Sample:** Glycine

**Spinning speed:** 10 kHz

**Time:** 20 minutes

#### **Experiment setup**

Start from standard carbon CP parameters, and set pulprog to **satrect1**.

Set **zgoptns** to –Ddec to turn on proton decoupling. If decoupling is not required on a real sample, this can be left blank to turn off the decoupling.

Set **p1** and **pl1** to the measured carbon 90-degree pulse parameters (as used in the CP T1 experiment, or see chapter Basic Setup Procedures). Set **d1** to a relatively long value for the preparation experiments.

Set the number of pulses in the saturation train, **I20**, to zero, and acquire a spectrum. This will give an idea of the amount of signal, and thus how many scans need to be acquired for each relaxation delay.

Create a new data set with **iexpno**, and set the saturation parameters, **I20** = 5-100 and **d20** = 1-50 ms respectively.

Acquire a spectrum, and verify that saturation is complete – there should be no signal at all.

#### **Setting up the 2D experiment**

Set the parameters for the 2D acquisition as detailed in [\*\*Table 14.4\*\*](#).

For the variable recovery delay, the same values can be used as for the inversion recovery experiment.

The recycle delay **d1** can be very short, but take care not to exceed the duty cycle limits: high-power pulsing should not exceed 5% of the total scan time. In the case of decoupling, the acquisition time comprises most of the pulsing, so **d1** should be >20x **aq** – 1 second is reasonable in this case. If the experiment is run without decoupling, then the saturation period is the only significant period of high-power pulsing, and **d1** can be shorter.

Acquire the 2D spectrum with **zg**.

*Table 14.4. Parameters for the Saturation Recovery Experiment*

Parameter	Value	Comments
Parmode	2D	
Vdlist	See text	
td(f1)	Number of entries in vd list	
FnMODE	QF	This is not a real 2D experiment.
NS	16, for the glycine sample	More scans needed than for the CP experiment, due to reduced signal.

## Data Processing

The saturation-recovery data should be processed in the same way as the inversion-recovery data above (see [Table 14.3](#) for parameters). The only differences are that the fitting function should be satrec rather than expdec, and the slice selected for processing should be the last one (signal is maximum at long recovery times). The calculated relaxation time constants should be the same as those obtained by inversion-recovery.

## T1p Relaxation Measurements

### 14.2.5

Rotating-frame relaxation measurements, under a spin-locking rf field, can be used to probe motions on shorter timescales than  $T_1$  measurements, with inverse correlation times of the order of the spin-locking rf field strength.

To measure  $T_{1r}$  relaxation, after CP a variable length spin-locking pulse is applied to the X nucleus. The remaining X magnetization decays exponentially to zero, as a function of spin-lock time. The parameters of cross-polarization can also be determined from variable-contact-time CP experiments (the function cpt1rho is provided in the relaxation analysis tool for this purpose), but here only simple  $T_{1r}$  measurements will be discussed.

It should be noted that the relaxation in a  $T_{1r}$  experiment might result from processes other than true  $T_{1r}$  relaxation. For example, in glycine, the carbon spins are dipolar coupled to protons, and there is a possible fast relaxation pathway via the protons, which is not  $T_{1r}$  relaxation. This is inhibited by having a high spin-lock field strength, but at large field strengths care must be taken over the length of the spin-lock pulse. If apparently non exponential decay is observed, this may result from such alternative relaxation processes.

## Experiment setup

**Sample:** Glycine

**Spinning speed:** 10 kHz

**Time:** 20 minutes

1. Start from standard CP parameters. The only additional calibration required is the carbon RF field strength of the spin-lock pulse. This can be set independently of the field strength for the cross-polarization. In principle, the strength of this field can be set to any value (with-

in probe limits) to probe motions on a range of time scales. However, only at relatively large field strengths is true  $T_{1r}$  relaxation the only significant relaxation pathway.

2. Set **pulprog** to *cp90* and measure the required power level for a 70 kHz RF field (3.57  $\mu$ s 90 degree pulse).
3. Make a new data set with **iexpno**, change **pulprog** to *cpxt1rho* and set this measured power as **pl11**.
4. Set up a variable pulse list for the incrementation of the spin-lock, with the command **edlist vp**. Check that this list is set as the parameter **vplist**. Remember that this is a high-power pulse, so the duration should not be too long. For the glycine sample, a possible set of times would be: 1ms, 2ms, 5ms, 10ms, 15ms, 20ms, 25ms, 30ms, 40ms, 50ms. This will not allow the signals to decay completely, so is not ideal, but should not place undue stress on the probe. Often a compromise must be reached between recording an ideal decay curve and avoiding the risk of probe damage.
5. Change **parmode** to 2D and set other 2D parameters as for the other relaxation experiments.
6. Acquire spectrum with **zg**.

### Data Processing

The data can be processed in the same way as the other relaxation experiments. The slice with shortest spin-lock time contains most signal, so this slice should be used for processing. The fitting function should be set to *expdec*, and **vplist** should be selected as the list file name, in the fitting function dialogue.

At 500 MHz, with a 60 kHz spin-lock field, the  $T_{1p}$  values should be approximately 400 ms and 48 ms for the carbonyl and alpha carbons respectively. The data for the alpha carbon does not give a perfect fit to a single exponential, but this may result from the relatively low spin-lock field allowing non- $T_{1p}$  relaxation.

### Indirect Relaxation Measurements

14.3

If proton relaxation measurements are desired, the considerable broadening of the proton resonances seen at even high spinning speeds can make resolution of individual components impossible. In such cases, indirect observation of proton relaxation by X-nucleus observation can be used. A typical example would be attempting to observe the proton relaxation of two components of a mixture or multi phase material. In general, the proton spins within a single molecule are sufficiently strongly coupled by the Homo-nuclear dipolar coupling that different relaxation is not seen for the different sites. If the experiments are set up with short contact times, the individual carbon signals will be derived only from directly bonded protons, and thus any differences in proton relaxation within a molecule could be isolated.

Such indirect observation can be implemented conveniently for both  $T_1$  and  $T_{1p}$  relaxation. For  $T_1$ , a proton saturation-recovery step is inserted prior to the cross-polarization step in a standard CP sequence. The proton magnetization immediately prior to CP, and thus the observed carbon signal, depends on the extent of recovery after the saturation, so the carbon signal as a function of recovery delay gives the proton  $T_1$  value. For  $T_{1p}$ , a variable length proton only spin-lock pulse is applied after the 90-degree pulse in the CP experiment. The proton magnetization after this pulse, and thus the carbon signal after CP, depends on the proton  $T_{1p}$  relaxation.

**Sample:** Glycine

**Spinning speed:** 10 kHz

**Time:** 20 minutes

Start from standard CP parameters, as for the X T<sub>1</sub> measurement with CP, and set **pulprog** to *cph+1*. Set the saturation loop **I20** to zero, and acquire a spectrum, to check signal intensity. Signal to noise should be comparable with the standard CP experiment, so a similar number of scans to that used for the carbon T<sub>1</sub> experiment should suffice.

Saturation parameters can be set as for carbon saturation previously: **I20** = 5-100 and **d20** = 1-50 ms. Acquire a spectrum with these parameters and verify that there is again no signal.

Make a new data set with **iexpno** and set parameters for 2D acquisition, as for the previous experiments. D1 can be short, with the same proviso about duty cycle as the X saturation-recovery experiment. A reasonable set of delays for the vdlist would be: 10 ms, 22 ms, 45 ms, 100 ms, 220 ms, 450 ms, 1 s, 2.2 s, 4.5 s, 10 s.

#### Data processing

The data should be processed in the same way as for the X saturation recovery experiment. Both the carbonyl and alpha-carbon peaks derive their carbon polarization from the same proton spins, and so analysis of the two peaks should give the same result. If you have a sample containing some gamma-glycine (gives peaks at slightly lower shifts than the more common alpha-glycine form), this should show different T<sub>1</sub> values for the two sets of peaks.

At 500 MHz, the proton relaxation time should be approximately 520 ms at room temperature.

# Basic MQ-MAS

# 15

## Introduction

15.1

The MQMAS experiment for half integer quadrupole nuclei is a 2D experiment to separate anisotropic interactions from isotropic interactions. In the NMR of half integer quadrupole nuclei the dominant anisotropic broadening of the central  $+1/2 \leftrightarrow -1/2$  transition (CT), and symmetric multiple-quantum (MQ) transitions, is the 2<sup>nd</sup> order quadrupole interaction which can only partially be averaged by MAS. The satellite transitions (ST, e.g. the  $\pm 3/2 \leftrightarrow \pm 1/2$  transitions) however, are broadened by a 1<sup>st</sup> order interaction, which is several orders of magnitude larger than the 2<sup>nd</sup> order broadening. Under MAS the 1<sup>st</sup> order interaction of the ST can be averaged but since the spinning cannot be fast compared to the first order broadening (of the order of MHz), a large manifold of spinning side bands remains. The 2<sup>nd</sup> order broadening of the CT can only be narrowed by a factor of 3 to 4 by MAS so a signal is observed that still reflects this 2<sup>nd</sup> order broadening, which may be of the order of kHz. Lineshapes resulting from nuclei in different environments are thus likely to be unresolved in a simple 1D spectrum.

The 2D MQMAS experiment exploits the fact that the 2nd order broadening of the symmetric MQ transitions (e.g.  $+3/2 \leftrightarrow -3/2$  in a spin 3/2), is related to the 2nd order broadening of the CT by a simple ratio. A 2D spectrum is recorded which correlates e.g. a  $+3/2 \leftrightarrow -3/2$  3Q coherence involving the satellite transitions and the  $+1/2 \leftrightarrow -1/2$  single quantum coherence of the central transition. This spectrum shows a ridge line shape for each site, with slope given by the ratio of the second order broadening of the two transitions (-7/9 in the case of the 3Q transition). A projection of the 2D spectrum perpendicular to this slope yields an isotropic spectrum free from quadrupolar broadening.

## Pulse sequences

15.2

**Figure 15.1.** and **Figure 15.2.** show two of the basic sequences, a 3-pulse and a 4-pulse sequence with z-filter. Both sequences start with an excitation pulse **p1** that creates 3Q coherence which is allowed to evolve during the evolution period **d0**. In the 3-pulse sequence the subsequent conversion pulse **p2** flips magnetization back along the z-axis, which after a short delay **d4** (to allow dephasing of undesired coherency) is read out with a weak CT selective 90° pulse **p3**. In the 4-pulse sequence, however, the conversion pulse **p2** changes 3Q coherency to 1Q coherency which then passes through a Z-filter of two CT selective 90° pulses in a **p3-d4-p3** sequence.

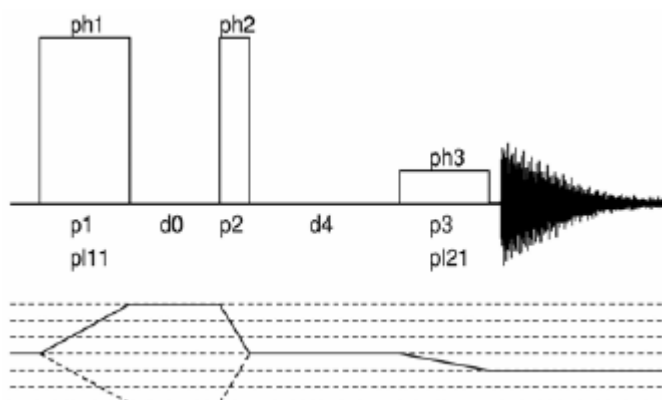


Figure 15.1. A 3-Pulse Basic Sequence with Z-Filter.

Three pulse sequence and coherence transfer pathway for the 3Q MAS experiment with z-filter (mp3qzqf.av). The ratio for pulses  $p_1$  and  $p_2$  is approximately 3. The corresponding power level  $p_{11}$  should be set to achieve at least 150 kHz RF field amplitude.  $p_3$  should be some tens of  $\mu\text{s}$ , corresponding to an RF field amplitude of a few kHz. Delays  $d_0$  and  $d_4$  are the incremented delay for  $t_1$  evolution and 20  $\mu\text{s}$  for z-filter, respectively. Phase lists are as follows, for phase sensitive detection in F1 the phase of the first pulse must be incremented by 30° in States or States-TPPI mode:

```

ph1 = 0
ph2 = 0 0 60 60 120 120 180 180 240 240 300 300
ph3 = 0 180
receiver = + - - +.

```

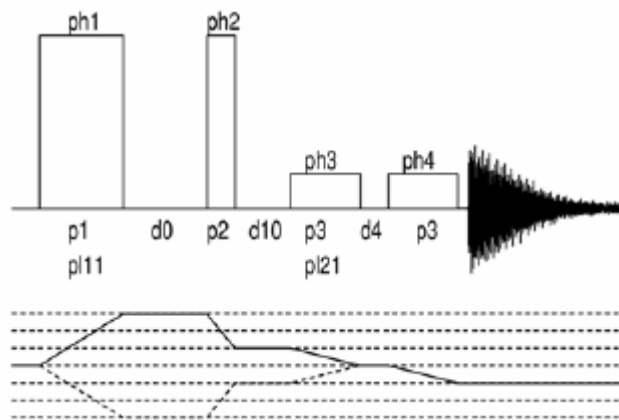


Figure 15.2. A 4-Pulse Basic Sequence with Z-Filter.

Four pulse sequence and coherence transfer pathway for the 3Q MAS experiment with z-filter (mp3qzfil.av).  $p_1$  is the same,  $p_2$  is usually somewhat shorter than in the three pulse sequence. Corresponding power level  $p_{11}$  should be set to achieve at least 150 kHz RF field amplitude.  $p_3$  should be some tens of  $\mu\text{s}$ , corresponding to an RF field amplitude of a few kHz. Delays  $d_0$  and  $d_4$  are the incremented delay for  $t_1$  evolution and 20  $\mu\text{s}$  for z-filter, respectively.

Delay  $d10$  initially is 0 and can be incremented proportional to  $d0$  ( $d10 = d0 * 7/9$ ), if the observe nucleus has spin  $I=3/2$ . Phase lists are as follows, for phase sensitive detection in F1 the phase of the first pulse must be incremented by  $30^\circ$  in States or States-TPPI mode:

```

ph1 = 0 60 120 180 240 300
ph2 = 0*24 90*24 180*24 270*24
ph3 = 0
ph4 = 0*6 90*6 180*6 270*6
receiver = {0 180}*3 {90 270}*3 {180 0}*3 {270 90}*3 {180 0}*3 {270 90}*3{0 180}*3 {90 270}*3.

```

Of course, the sequence with more pulses has slightly inferior sensitivity; however, it is the basic sequence to improve sensitivity by FAM or DFS. The 3-pulse sequence itself can be used directly to enhance sensitivity by soft-pulse added mixing (pulse program *mp3qspam.av*). In ["MQ-MAS: Sensitivity Enhancement" on page 169](#) some of the sensitivity enhancement techniques will be described.

Note that pulse programs suitable for AV and AVII spectrometers have the extension.*av*, pulse programs for the AVIII have no extension.

## Data Acquisition

## 15.3

Before the 2D experiment on your sample of interest can be started, two set-up steps must be done as described in detail below. All set-up steps should be done on a sample with a) a known MAS spectrum, b) with sufficiently good sensitivity to facilitate the set-up and c) a 2<sup>nd</sup> order quadrupole interaction in the order of the one expected for your sample of interest. In the first step a low power selective pulse must be calibrated in a single pulse experiment. With this the MQMAS experiment can be optimized using the 2D pulse sequence for  $t_1=0$ .

### Setting Up the Experiment

### 15.3.1

**Sample:** There are a large number of crystalline compounds which can be used to set up the experiment. Please refer to table 1 to select a suitable sample. For the general procedure described here the spin  $I$  of the nucleus is not important, of course obtained pulse widths will depend on the spin  $I$ , and the Larmor frequency. You can use any arbitrary sample showing a considerable broadening by the 2nd order quadrupole interaction to adjust the experiment, however, reasonable 1D MAS spectra should be obtained quickly for sensitivity reasons.

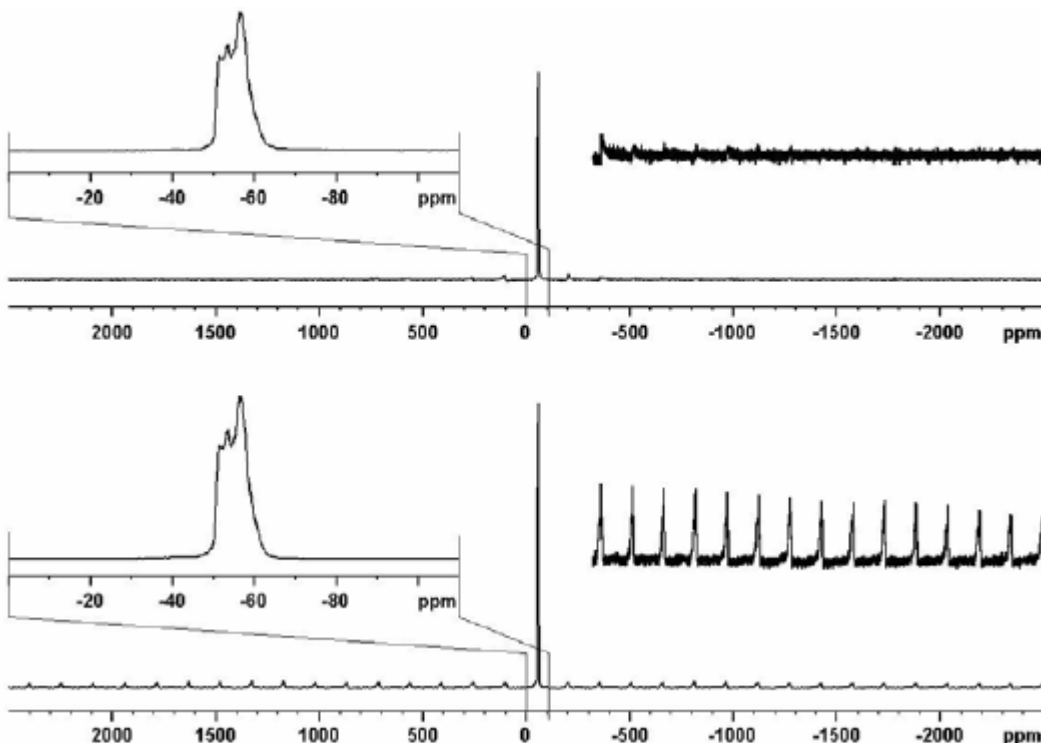
The set-up must be done in two steps; in the first step a central transition selective pulse that merely excites the central transition must be calibrated. This pulse must be weak enough so that only this transition is affected and it must be short enough so that the central transitions of all sites in the spectral range are excited. As an example, the sinc shape excitation profile of a 20  $\mu$ s pulse has its zero-crossings at  $1/20 \mu\text{s} = \pm 25 \text{ kHz}$  which means that the central transition signals must not extend beyond this range, otherwise severe line shape distortions will be observed. On the other hand the corresponding RF field amplitude of a 20  $\mu\text{s}$  90° pulse will be  $1/(80 \mu\text{s}*(I+1/2)) = 12.5 \text{ kHz}/(I+1/2)$ . This means that  $w_{RF} < w_Q$  as a prerequisite for a CT selective pulse is most likely to be fulfilled. For the calibration of this pulse a power level around 30 dB with 500 W and 1 kW amplifiers and around 20 dB with 300 W amplifiers should be expected. The pulse program *zg* (which uses *p1* and *p11*) or *zgsel.av* (which uses *P3* and *PL21*) can be used.

Table 15.1. Some Useful Samples for Half-integer Spin Nuclei

Nucleus	Spin	Spectrometer Frequency <sup>*1)</sup>	d1 [s] <sup>*3)</sup>	Sample	Comments
<sup>17</sup> O	5/2	67.78	2	NaPO <sub>3</sub>	> 10% enriched
<sup>11</sup> B	3/2	160.42	>5	H <sub>3</sub> BO <sub>3</sub>	
<sup>23</sup> Na	3/2	132.29	10	Na <sub>2</sub> HPO <sub>4</sub> <sup>*2)</sup>	
<sup>27</sup> Al	5/2	130.32	5	YAG	
<sup>27</sup> Al	5/2	130.32	0.5	Al <sub>2</sub> O <sub>3</sub>	
<sup>27</sup> Al	5/2	130.32	0.5	VPI-5	
<sup>27</sup> Al	5/2	130.32	0.5	AlPO <sub>4</sub> -14	
<sup>11</sup> B	3/2	160.46	5	H <sub>3</sub> BO <sub>3</sub>	
<sup>87</sup> Rb	3/2	163.61	0.5	RbNO <sub>3</sub>	
<sup>93</sup> Nb	9/2	122.25	1	LiNbO <sub>3</sub>	

<sup>\*1)</sup> In MHz at 11.7 T (i.e. 500.13 MHz proton frequency)  
<sup>\*2)</sup> Alternatively Na<sub>2</sub>HPO<sub>4</sub> \* 2H<sub>2</sub>O can be used. For anhydrous Na<sub>2</sub>HPO<sub>4</sub> the sample should be dried at 70° C for a couple of hours before packing the rotor in order to eliminate crystal water completely  
<sup>\*3)</sup> Recycle delays at 11.7 T, longer delays may be required at higher fields

**Figure 15.3.** shows a comparison of a spectrum excited by a short non-selective pulse with a spectrum that has been obtained by a weak selective pulse. Note that in the latter the spinning sidebands from the satellite transition are no longer visible which is used as an indication that it is not excited.



*Figure 15.3. Comparison of  $^{87}\text{Rb}$  MAS spectra of  $\text{RbNO}_3$  excited with selective and non-selective pulses.*

The lower trace is a spectrum excited with a  $1\ \mu\text{s}$  non-selective pulse corresponding to a small flip angle. Above is a spectrum excited with a  $20\ \mu\text{s}$  selective  $90^\circ$  pulse. Note that in the latter no spinning side bands from the satellite transition are observed. Spectra are taken on AV500WB at a Larmor frequency of  $163.6\ \text{MHz}$  with a  $2.5\ \text{mm}$  CP/MAS probe spinning at  $25\ \text{kHz}$ .

**Figure 15.4.** shows the nutation profiles of a non-selective and a selective pulse, respectively. Note that for the selective pulse a fairly precise  $180^\circ$  pulse of a length of  $2\tau_{90^\circ}$  can be determined whereas for a non-selective pulse this is not the case.

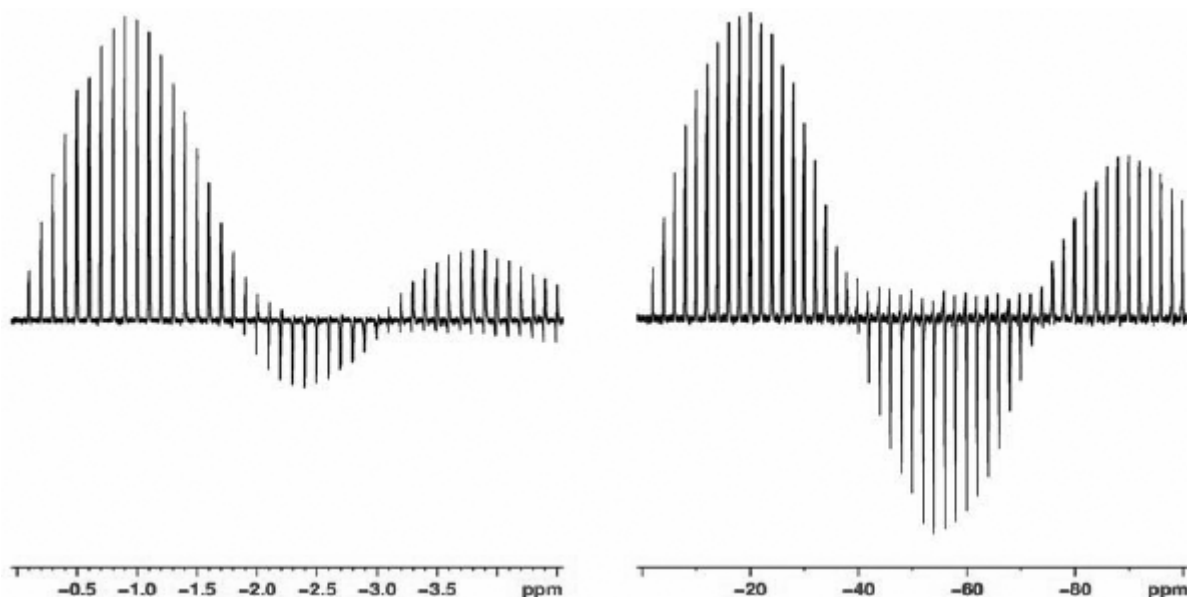


Figure 15.4. Nutation profiles of selective and non-selective pulses.

Left diagram shows signal intensity of  $^{87}\text{Rb}$  resonances in  $\text{RbNO}_3$  as a function of a non-selective pulse at approx. 150 W RF power, the right diagram shows the signal intensity as function of a selective pulse at less than approx. 0.5 W. Spectra are taken on AV500WB at a Larmor frequency of 163.6 MHz with 2.5 mm CP/MAS probe spinning at 25 kHz. Note the different scaling of x-axis, which is displayed as "ppm" but corresponds to the used pulse lengths in  $\mu\text{s}$  (apart from the sign).

Once the central transition selective  $90^\circ$  pulse is calibrated the parameters can be copied to a new data set with **iexpno**, and the MQMAS pulse program can be loaded. Available pulse programs are *mp3qzqf* and *mp3qzfil*. The first is a 3-pulse sequence, the second a 4-pulse sequence. The sequence with fewer pulses will be slightly more sensitive, whilst the 4-pulse sequence can be used as an initial set-up for experiments with sensitivity enhancement methods like DFS or FAM (see ["MQ-MAS: Sensitivity Enhancement" on page 169](#) describing sensitivity enhancement methods).

In [Table 15.2](#), the starting parameters for the set-up are displayed. This table gives typical values for the pulses and powers that should be close to the final values confirmed by the optimization procedure. Parameters like **O1**, **TD**, **SWH**, **RG**, should already be set in the standard 1D spectrum. For 4 mm probes these pulse lengths are about the limit of what can be achieved, for 2.5 mm probes somewhat shorter pulses can be obtained. For  $I = 3/2$  and  $I = 5/2$  nuclei the ratio of  $p1/p2 \approx 3$ .

For **p11** an initial value that corresponds roughly to 300 W can be used. Optimization will be done on the first increment of the 2D sequence, i.e. **d0** = 1  $\mu\text{s}$ . Two strategies for the optimization procedure can be followed; either the pulse lengths **p1** and **p2** or the power level **p11** can be optimized for maximum signal amplitude. However, the latter can be disadvantageous because a power level above the probe limit might be applied, in order to clearly determine the optimum power. In the case of 300 W amplifiers the maximum signal amplitude may not be obtained even at full power, with the chosen pulse lengths.

Table 15.2. Initial Parameters for Setup

Parameter	Value	Comments
Pulprog	mp3qzqf.av or mp3qzfil.av	Pulse program.
NS	12*n (zqf) 96*n (zfil)	Full phase cycle is important.
D0	1u	Or longer, $t_1$ -period.
D1	5 * $T_1$	Recycle delay, use dummy scans if shorter.
D4	20 $\mu$ s	Z-filter delay.
P1	3.6 $\mu$ s	Excitation pulse at pl11.
P2	1.2 $\mu$ s	Conversion pulse at pl11.
P3	20 $\mu$ s	90° selective pulse at pl21 taken from previous pulse calibration.
PL1	=120 dB	Not used.
PL11	start with $\approx$ 300 W	Power level for excitation and conversion pulses.
PL21		Power level for selective pulse, approx. pl11+30 dB taken from previous pulse calibration.

Hence, it is always better to optimize the pulse lengths **p1** and **p2**. In this case **p2** should be optimized before **p1** because the signal intensity is much more sensitive to this pulse length. A suitable set-up for the parameter optimization procedure **popt** is shown in following figure.

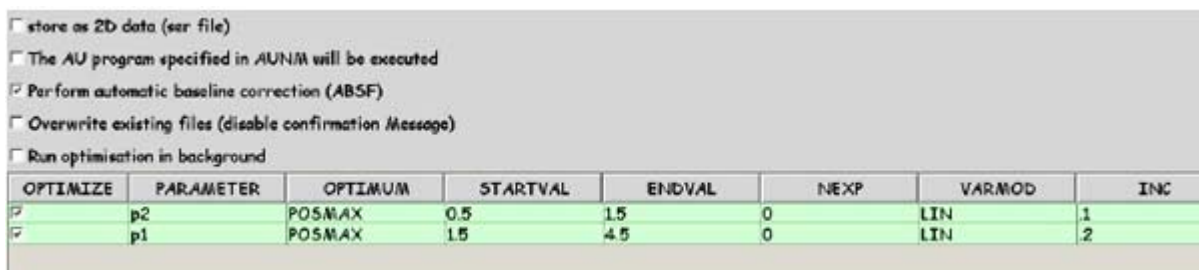


Figure 15.5. Example for popt Set-up for Optimization of p1 and p2.

In the first step **p2** is optimized to which the experiment is the more sensitive. In the second step **p1** is optimized using the optimum value found for **p2** in the first step.

For more details about using the **popt** procedure to optimize a series of parameters please refer to the manual. **Figure 15.6.** shows the signal amplitudes as functions of pulse lengths **p2** and **p1**.

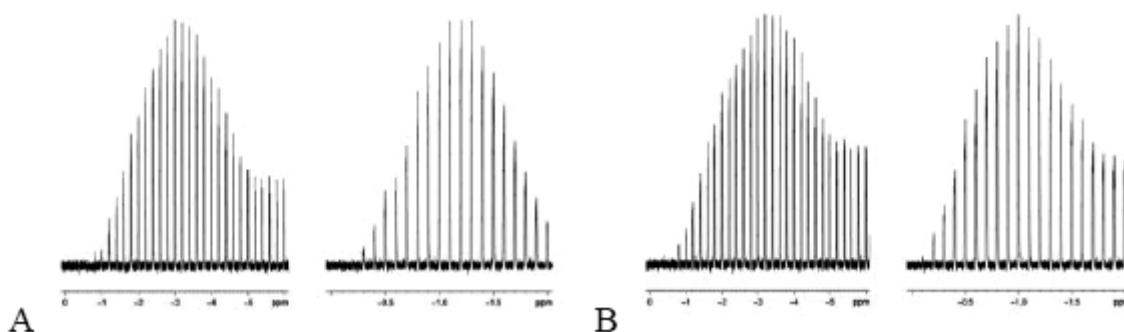


Figure 15.6. Signal Intensities of  $^{87}\text{Rb}$  Resonances in  $\text{RbNO}_3$  as Function of  $\mathbf{p1}$  and  $\mathbf{p2}$ .

Each pair of diagrams in A and B shows the signal intensities as function of the excitation pulse  $\mathbf{p1}$  and the conversion pulse  $\mathbf{p2}$ . In A the 3-pulse sequence and in B the 4-pulse sequence was used. Note that the signal intensity is much more sensitive to the proper length of the conversion pulse. Maximum intensities were  $3.0\ \mu\text{s}$  and  $1.2\ \mu\text{s}$  in A and  $3.2\ \mu\text{s}$  and  $1.0\ \mu\text{s}$  in B, respectively. This corresponds to approximate RF field amplitudes of  $160\ \text{kHz}$ . Spectra are taken on an AV500WB at a Larmor frequency of  $163.6\ \text{MHz}$  with a  $2.5\ \text{mm}$  CP/MAS probe spinning at  $25\ \text{kHz}$ . Note the different scaling of the x-axes, for  $\mathbf{p1}$  they range from 0 to  $6\ \mu\text{s}$ , for  $\mathbf{p2}$  from 0 to  $2\ \mu\text{s}$ .

## Two Dimensional Data Acquisition

### 15.3.2

Once the pulses are calibrated everything is ready for the 2D data acquisition. Create a new data set and change *parmode* to 2D. In the acquisition parameters for the (new) indirect F1 dimension the following parameters must be set according to the following table.

Table 15.3. F1 Parameters for 2D Acquisition

Parameter	Value	Comments
FnMode	States or States-TPPI	Acquisition mode for 2D.
TD	see text	Number of FID's to be acquired.
ND_010	1	There is only 1 d0 delay in the sequence.
SWH	"masr"	Equals spinning frequency for rotor synchronization, from this IN_010 is calculated correctly, if ND_010 is already set.
NUC1		Select the same nucleus as for F2 so that transmitter frequency offset is correctly set (important for referencing). <sup>1</sup>
D10	0	Used in mp3qzfil.av only.
IN10	=in0*7/9	Used in mp3qzfil.av for nuclei with spin I=3/2 only, so that no shearing FT is required.

<sup>1</sup> Note the difference in increment handling in Topspin 2.1 and higher.

Some further comments and explanations on the parameters listed above:

**FnMode** must be States or States-TPPI so that the shearing FT can be performed for processing. If the pulse program *mp3qzfil.av* is used, no shearing is required in case of nuclei with spin I=3/2 if **in10** is set correctly in which case a split-t<sub>1</sub> experiment is performed. **td** determines the number of FID's to be accumulated in the indirect dimension. This value is determined by the line width and resolution that can be expected in the indirect MQ dimension (F1) and which depend on the properties of the sample. In crystalline material fairly narrow peaks can be expected so a maximum acquisition time in F1 of 2 to 5 ms is expected. In disordered materials where the line width is broader and determined by chemical shift distribution a total acquisition time in F1 of 1 ms may be sufficient. The total acquisition time **aq** in F1 equals (**td/2**)\***in\_010**.

For rotor synchronized experiments **in\_010** = 1/spinning frequency so will typically be between 100 µs (10 kHz spinning) and 28.5 µs (35 kHz spinning), so only 10 to 40 experiments in amorphous samples but 50 to 200 experiments in crystalline samples might be required. The rotor synchronization means that the spectral range in F1 is limited. Depending on the chemical shift range, spinning frequency, and quadrupole interactions the positions of the peaks may fall outside this range. In such a case care must be taken when interpreting the spectrum. Acquisition with half-rotor synchronization to double the spectral window in F1 may help. However, in this situation one set of spinning sidebands appears and it must be avoided that the spinning side bands of one peak fall on top of other peaks. Some sort of rotor synchronization is always recommended because spinning side bands in the indirect dimension extend over a very wide range, which cannot be truncated by e.g. filtering. Therefore, rotor synchronization together with States or States-TPPI phase sensitive acquisition helps to fold spinning sidebands from outside back onto centre bands or other side bands.

**Data processing**

Processing parameters should be set according to the following table:

*Table 15.4. Processing Parameters for 2D FT*

Parameter	Value	Comments
F2 (acquisition dimension)		
SI		Usually set to one times zero filling.
WDW	no	Don't use window function.
PH_mod	pk	Apply phase correction.
BC_mod	no	No DC correction is required after full phase cycle.
ABSF1	1000 ppm	Should be outside the observed spectral width.
ABSF2	-1000 ppm	Should be outside the observed spectral width.
STSR	0	Avoid strip FT.
STS1	0	Avoid strip FT.
TDoff	0	Avoid left shifts or right shifts before FT.
F1 (indirect dimension)		
SI	256	Sufficient in most cases.
WDW	no	Don't use window function, unless F1 FID is truncated.
PH_mod	pk	Apply phase correction.
BC_mod	no	No DC correction is required after full phase cycle.
ABSF1	1000	Should be outside the observed spectral width.
ABSF2	-1000	Should be outside the observed spectral width.
STSR	0	Avoid strip FT.
STS1	0	Avoid strip FT.
TDoff	0	Avoid left shifts or right shifts before FT.

Data obtained with *mp3qzfil.av* from nuclei with spin  $I = 3/2$  can be processed with ***xfb***, if ***IN10*** has been set appropriately to run a split- $t_1$  experiment. If this is not the case data can be sheared in order to align the anisotropic axis along the F2 axis. This is done with the AU program ***xfshear***. The AU program checks the nucleus to determine the spin quantum number, checks the name of the pulse program and decides what type of experiment has been performed. In case the nucleus is unknown to the program, or the pulse program has a name that does not contain a string "nq" nor "nQ" (with n=3, 5, 7, 9), the required information is asked for by the program, in order to calculate the shearing correctly.

Note that using a user designed pulse program that contains e.g. a string "5q" but performs a 3Q experiment (and vice versa) will yield erroneous shearing. When started the AU program prompts for "Apply ABS2?" and "F1 shift in ppm:". It is advisable to calculate a baseline correction after F2 Fourier transform. Note that the range defined by ABSF1 and ABSF2 is used for this. You should make sure that the limits are at least as large as the spectral width to allow baseline correction of the whole spectrum. The "F1 shift in ppm" allows shifting the spectrum

(including its axis) in the vertical direction for cases where peaks are folded due to a limited spectral window in a rotor synchronized experiment. For the first processing both prompts are typically returned. At the end of the processing the AU program corrects the apparent spectrometer frequency of the indirect dimension by a factor  $|R-p|$ , where  $R$  is defined in equation [1] and  $p$  is the order of the experiment (e.g. 3 for 3QMAS):

$$(Eq. 15.1) \quad R = \frac{m(18I(I+1)-8.5m^2-5)}{18I(I+1)-3.5}$$

This ratio is calculated from the spin quantum number  $I$  of the nucleus and the magnetic spin quantum number  $m$ , which is determined by the experiment, e.g. 3/2 in case of a 3Q experiment of an order  $p=3$ . The program stores the “F1 shift” that was calculated and will prompt for it when data are processed next time. If the same F1 shift should be applied as before the AU program can be called with the option “lastf1”. Before giving some further explanations about the experiment, **Figure 15.7.** shows the 2D  $^{87}\text{Rb}$  3QMAS spectrum of  $\text{RbNO}_3$ .

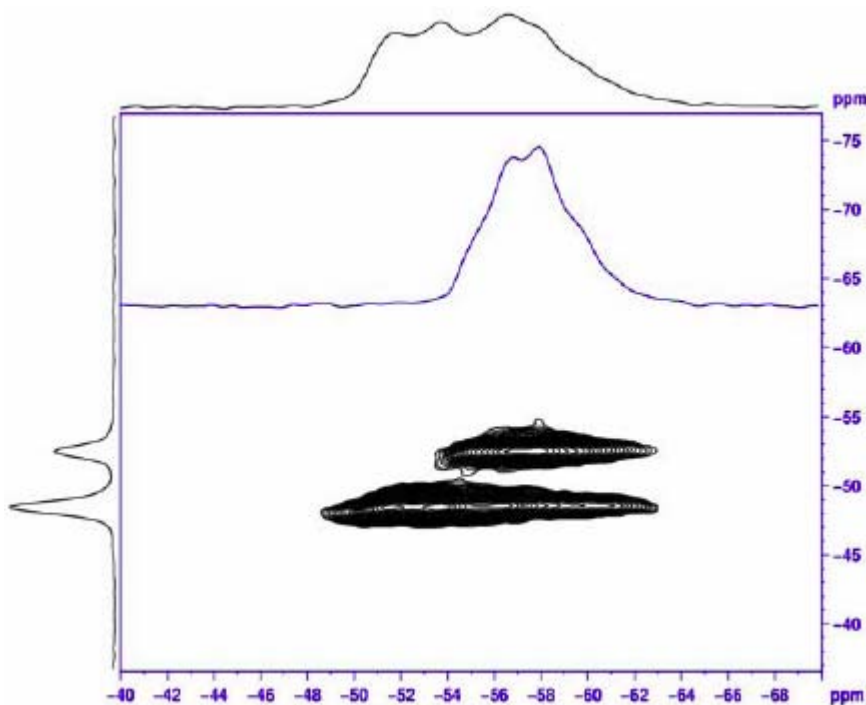


Figure 15.7. 2D  $^{87}\text{Rb}$  3QMAS Spectrum of  $\text{RbNO}_3$ .

*Top and left projections are the summations over the signal ranges. The spectrum included in the 2D map is a cross section through the resolved peak resonating at approximately 53 ppm. Note that at 11.7 T two of the three sites cannot be resolved in the 2D spectrum. The spectral range shown in F1 corresponds to the spinning frequency. Spectra are taken on AV500WB at a Larmor frequency of 163.6 MHz with a 2.5 mm CP/MAS probe, spinning at 25 kHz.*

Since the quadrupole parameters are usually unknown before performing the experiment the positions of the peaks in the indirect dimension cannot be predicted. Therefore, it may happen that a peak is positioned at the border of the spectral range in the F1 dimension or even folded. When using **xfshear** the prompt “F1 shift in ppm:” can be used to shift the spectrum including

its axis upfield (negative value) or low field (positive value) accordingly. For data which don't need a shearing transformation, the ppm axis in F1 can be correctly calibrated by running the AU program *xfshear* with the option „rotate”. It will calibrate the F1 axis and perform the 2D FT. **Figure 15.8** compares the same 2D 3Q MAS spectrum processed with no shift and an additional shift of 5 ppm, respectively. We see that without the additional shift, the uppermost peak is at the border of the spectral range and the projection shows that the edge of this peak reenters into the spectral range from the opposite side. In summary the AU program ***xfshear*** can be called with the following options:

- lastf1:** Use the F1 shift value from last processing
- abs:** Do abs2 after F2 Fourier transform of data
- noabs:** Don't do abs2 after F2 Fourier transform of data
- rotate:** don't calculate shearing, only use F1 shift to rotate spectrum along F1 axis
- ratio:** Use different value for ratio R, value can either be entered or passed.

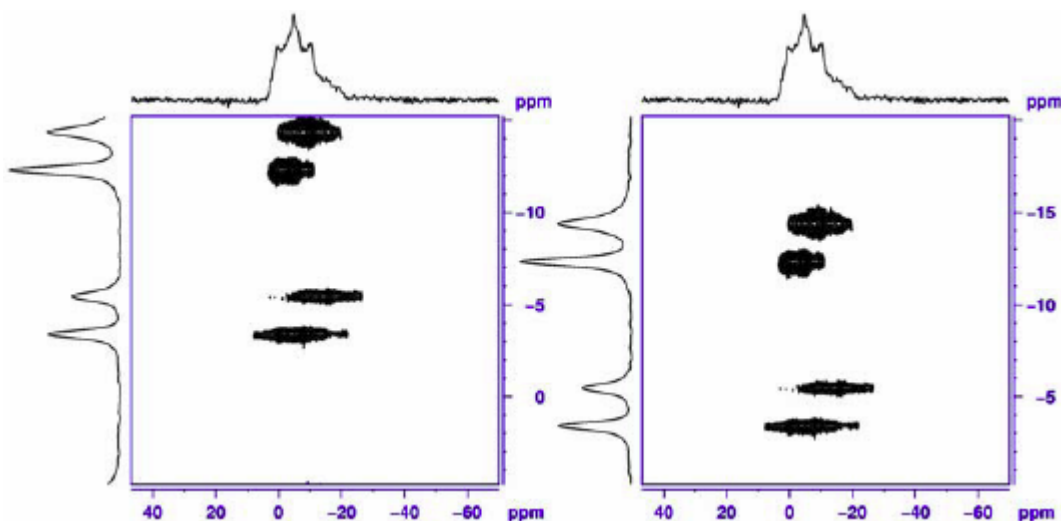


Figure 15.8. Comparison of Differently Processed 2D  $^{23}\text{Na}$  3Q MAS Spectra of  $\text{Na}_4\text{P}_2\text{O}_7$ .

The left spectrum was processed with an additional F1 shift of 0 ppm, the right spectrum with +5 ppm. Spectra are taken on an AV500WB at a Larmor frequency of 132.3 MHz with a 4 mm CP/MAS probe spinning at 10 kHz. Note that the F1 range equals the spinning frequency of 10 kHz in both cases.

**Obtaining Information from Spectra****15.5**

The referencing procedure in ***xfshear*** defines the axis in the MQ dimension such that:

$$\delta_{MQ} = \delta_{iso} - \frac{10}{17} \delta_{qis} \quad (\text{Eq. 15.2})$$

The value of  $\delta_{qis}$  is given by:

$$\delta_{qis} = -\frac{3(4I(I+1)-3)}{(4I(2I-1))^2} * \frac{Q_{cc}^2}{\omega_0^2} \left(1 + \frac{\eta^2}{3}\right) * 10^5 \quad (\text{Eq. 15.3})$$

In **(Eq. 15.3)**  $I$  is the spin quantum number,  $Q_{cc}$  the quadrupolar coupling constant,  $\omega_0$  the Larmor frequency, and  $\eta$  the asymmetry parameter. This makes  $\delta_{MQ} \propto \omega_0^{-2}$ , which causes the MQ positions to be field dependent. An interesting behavior results as one compares spectra at different fields. Plots of the function  $\delta_{MQ}$  over  $\omega_0^{-2}$  are shown in **Figure 15.9**, for an arbitrary sample with two sites. If the isotropic chemical shifts of the two sites are identical, then it is obvious that the separation of the two lines increases as the field decreases (plot A). In the opposite case of identical quadrupole couplings separation increases as the field is increased (plot B). In cases where a difference in isotropic chemical shift  $\delta_{iso}$  exists and the sites have different quadrupole couplings the relative positions depend on which site has the larger quadrupole coupling. The separation of the lines will always increase as the field decreases (plots C and D), but in some cases a crossover of the shift positions may be observed as the field  $B_0$  is altered (plot C).

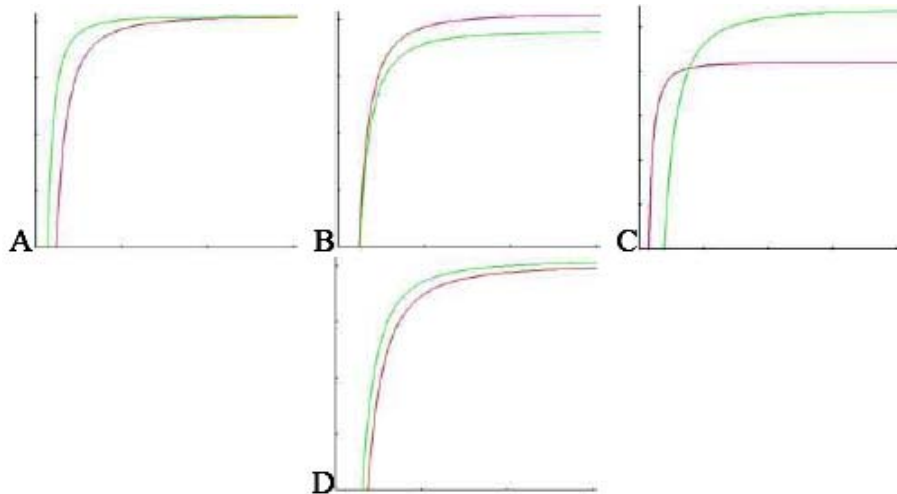


*Figure 15.9. Calculated Shift Positions  $\delta_{MQ}$*

*Calculated shift positions  $\delta_{MQ}$  as function of the static magnetic field  $B_0$  for two different sites with arbitrary  $\delta_{iso}$  and  $\delta_{qis}$ . The x axis in each plot is the static magnetic field  $B_0$  increasing from left to right; the y axis  $\delta_{MQ}$  increases from bottom to top. Plot A is for identical  $\delta_{iso}$ , plot B for identical quadrupole coupling and. In plots C and D shift positions for two sites with large and small  $\delta_{iso}$  and large and small  $\delta_{qis}$  and with large and small  $\delta_{iso}$  and small and large  $\delta_{qis}$  are plotted, respectively.*

This behavior is independent of the spin quantum number and of the order  $p$  of the experiment. Higher quantum order experiments are possible for half integer spin quantum numbers  $>3/2$ , however, corresponding pulse programs are not provided in the pulse program library. They can easily be derived from the 3Q pulse program by changing the phase cycle. In the 3-pulse sequence (*mp3qzqf*) e.g. ph2 should be changed for the 5Q experiment to:

```
ph2 = 0 0 36 36 72 72 108 108 144 144 180 180 216 216 252 252 288 288 324 324
```

An  $18^\circ$  phase increment of the phase ph1 of the first pulse is required for States or States-TPPI phase sensitive acquisition. For a full phase cycle a multiple of 20 scans must be used.

For the 4-pulse sequence (*mp3qzfil*) the phases should be changed to:

```
ph1 = 0 36 72 108 144 180 216 252 288 324
```

```
ph2 = 0*40 90*40 180*40 270*40
```

```
ph3 = 0
```

```
ph4 = 0*10 90*10 180*10 270*10
```

```
receiver = {0 180}*5 {90 270}*5 {180 0}*5 {270 90}*5 {180 0}*5 {270 90}*5 {0 180}*5 {90 270}*5.
```

Again an  $18^\circ$  phase increment of the first pulse for States or States-TPPI phase sensitive detection in F1 is needed. Thus a full phase cycle can be performed with a multiple of 160 scans.

The usefulness of such a 5Q experiment is limited, and there are several drawbacks: Firstly, the sensitivity is much inferior to the 3Q experiment because of the lower transition probability and a less efficient excitation. Secondly, the shift range (in ppm) in the indirect dimension is much smaller when a rotor synchronized experiment is performed. The factors  $|R-p|$  are listed in **Table 15.5**. The shift positions in the MQ dimension in a sheared spectrum are the same for all orders  $p$  and therefore, no additional information can be expected. However, the observed line widths are slightly reduced in the higher order experiments so in special cases some enhancement of resolution can provide additional information.

*Table 15.5. Values of  $|R-p|$  for Various Spins  $I$  and Orders  $p$*

Spin I	R(p=3)	$ R-p $ ( $p=\pm 3$ )	$ R-p $ ( $p=\pm 5$ )	$ R-p $ ( $p=\pm 7$ )	$ R-p $ ( $p=\pm 9$ )
3/2	-7/9	3.78	-	-	-
5/2	19/12	1.42	7.08	-	-
7/2	101/45	0.76	3.78	10.58	-
9/2	91/36	0.47	2.36	6.61	14.17

The spectral width in the MQ dimension of the sheared spectrum is given by spinning speed /  $|R-p|$  in a rotor synchronized experiment. A 5Q experiment e.g. gives a  $7.08/1.42 = 5$  times smaller spectral range in the indirect dimension than a 3Q experiment.

We see that a 5Q experiment has a 5 times smaller range than the 3Q experiment and therefore, folding of peaks will always occur even at fast spinning. For even higher quantum orders the shift ranges are 7 and 30 times smaller for 7Q and 9Q than for the 3Q experiment, respectively. **Table 15.6** summarizes ppm ranges for the maximum spinning frequencies of 2.5, 3.2, and 4 mm probes, respectively. A Larmor frequency of 100 MHz is assumed. One can see that the ranges become less than the typical chemical shift range for many nuclei. The expression  $|R-p|$  acts like a scaling factor that scales the frequency scale directly. Mathematically this is

solved in the AU program **xfshear** in such a way that the observe Larmor frequency is multiplied by the factor  $\Delta R \cdot p$  Å to redefine an apparent Larmor frequency in the MQ dimension.

Table 15.6. Chemical Shift Ranges for all MQ Experiments for All Spins I

Spin $I$ and MQ Experiment	15 kHz [4 mm probe]	25 kHz [3.2 mm probe]	35 kHz [2.5 mm probe]
3/2	39.6 ppm	66.0 ppm	92.4 ppm
5/2 3Q 5/2 5Q	105.6 ppm 26.1 ppm	176.0 ppm 35.2 ppm	246.4 ppm 49.3 ppm
7/2 3Q 7/2 5Q 7/2 7Q	197.4 ppm 39.5 ppm 14.1 ppm	329.0 ppm 65.8 ppm 23.5 ppm	460.6 ppm 92.1 ppm 32.9 ppm
9/2 3Q 9/2 5Q 9/2 7Q 9/2 9Q	319.2 ppm 63.2 ppm 45.6 ppm 10.6 ppm	532.0 ppm 160.4 ppm 76.0 ppm 17.7 ppm	744.8 ppm 144.9 ppm 106.4 ppm 24.8 ppm

Figures are calculated for a Larmor frequency of 100 MHz.

From the isotropic shift and the shift position in the MQ dimension the so-called SOQE parameter can be calculated,  $d_{qis}$  being given by equation 2:

(Eq. 15.4)

$$SOQE = Q_{cc}^2 \left( 1 + \frac{\eta^2}{3} \right) = \delta_{qis} f(I) \frac{\omega_0^2}{10^5}$$

with

(Eq. 15.5)

$$f(I) = -\frac{(4I(2I-1))^2}{3(4I(I+1)-3)}$$

$f(I)$  equals 4, 16.67, 39.2, and 72 for  $I=3/2, 5/2, 7/2$ , and  $9/2$ , respectively. So one can see that for a given value of  $Q_{cc}$  the second order quadrupole induced upfield shift  $d_{qis}$  decreases as the spin  $I$  increases. With  $d_{qis}$  always being negative this has a direct influence on the appearance of the sheared 2D spectra.

**Figure 15.10.** shows 2D  $^{17}\text{O}$  3QMAS spectra at 11.7 T and 18.8 T where the Larmor frequency of this nucleus is 67.8 and 108.4 MHz, respectively. The sample is sodium metaphosphate  $\text{NaPO}_3$  in the glassy state. The enrichment of  $^{17}\text{O}$  is approx. 30 to 33%. It contains 2 oxygen positions: there are bridging oxygen (P-O-P) and non-bridging oxygen (P-O-Na).

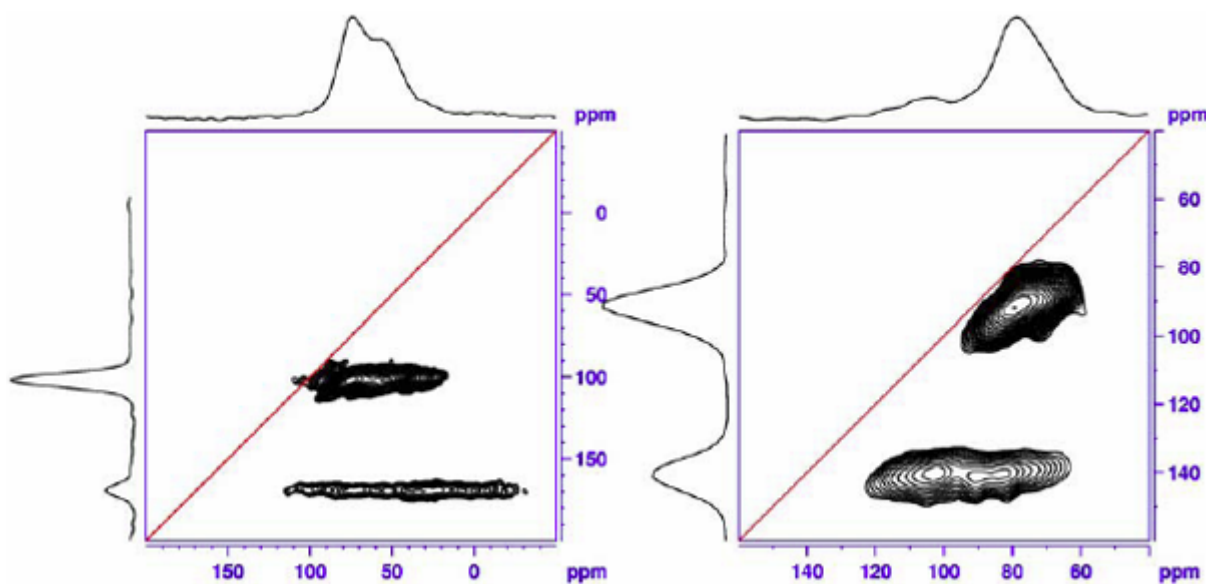


Figure 15.10.  $^{17}\text{O}$  MQMAS of  $\text{NaPO}_3$  at 11.7 T (67.8 MHz) on the left and 18.8 T (108.4 MHz) on the right.

The red lines in the spectra indicate the isotropic chemical shift axis. Approximate quadrupole parameters of the two sites are  $\text{Q}_{\text{cc}} \approx 7.7 \text{ MHz}$ ,  $h \approx 0.36$ ,  $\text{diso} \approx 125 \text{ ppm}$  for the lower peak and  $\text{Q}_{\text{cc}} \approx 4.5 \text{ MHz}$ ,  $h \approx 0.16$ ,  $\text{diso} \approx 85 \text{ ppm}$  for the upper peak (sample courtesy of Alexandre Flambard, LCPS, Univ. de Lille).

The bridging oxygen give rise to the lower peaks in the 2D spectra of [Figure 15.10](#), the non-bridging ones give rise to the upper peak. An additional red line is drawn into the spectrum which represents the diagonal, meaning  $d(F_2) = d(F_1)$ . One can see that all line positions must be below this diagonal because the negative quadrupole induced shift is scaled down and subtracted from the isotropic shift to give the MQ shift. In the example shown in [Figure 15.10](#) two sites are visible with distinct differences in their spectroscopic parameters. In the sheared spectra we find the lower peak at 170 ppm (11.7 T) and 140 ppm (18.8 T), respectively, in the 3Q dimension. This peak is dispersed parallel to the F2 axis which means that its line width is mainly due to second order quadrupole broadening. The upper peak at 100 ppm (11.7 T) and approx. 90 ppm (18.8 T) in the 3Q dimension has a much smaller quadrupole coupling which can immediately be recognized from the fact that the peak is much closer to the diagonal. It is very nice example where the second order broadening which is still the dominant interaction at 11.7 T is so much reduced at 18.8 T that the width of the peak is now determined by the distribution of chemical shift. This is expressed in the fact that the peak is dispersed along the diagonal.

[Figure 15.11](#). shows the results of the fitting with the solids line shape analysis package included in TopSpin. The spectra used for that have been extracted from rows of the 2D spectrum shown in [Figure 15.10](#).

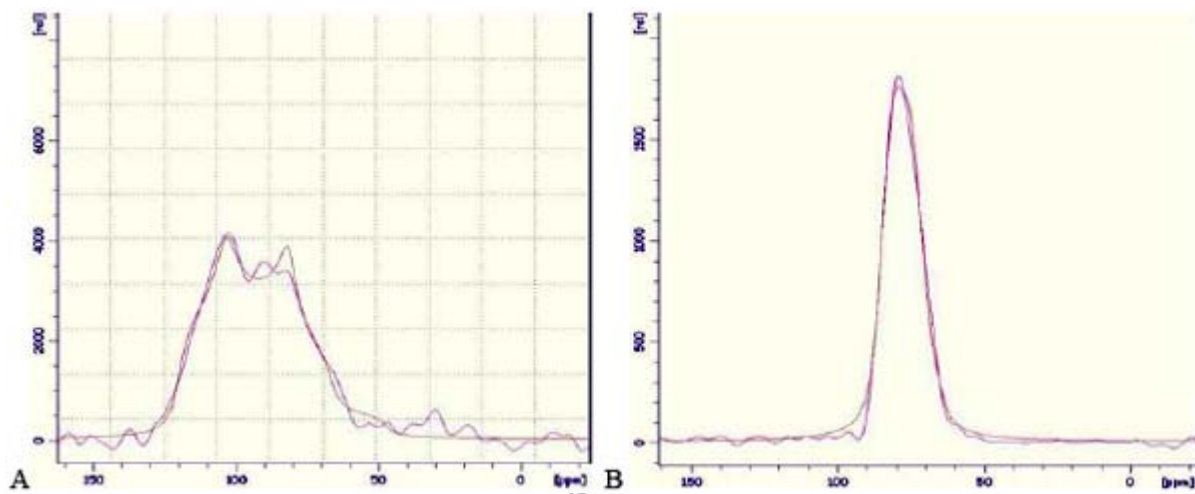


Figure 15.11. Slices and Simulations of the 18.8 T  $^{17}\text{O}$  MQMAS of  $\text{NaPO}_3$ .

Fitted parameters are A)  $\text{Qcc} \approx 7.7 \text{ MHz}$ ,  $h \approx 0.36$ ,  $\text{diso} \approx 125 \text{ ppm}$  and B)  $\text{Qcc} \approx 4.5 \text{ MHz}$ ,  $h \approx 0.16$ ,  $\text{diso} \approx 87 \text{ ppm}$  for the upper peak (sample courtesy of Alexandrine Flambard, LCPS, Univ. de Lille).

Spectra that are sheared can be evaluated graphically as follows, as shown in [Figure 15.12](#). In addition to the (red) isotropic chemical shift axis indicated as “axis CS” with the slope  $\Delta\delta(\text{F2})/\Delta\delta(\text{F1}) = 1$  there are two more lines drawn. The (blue) axis indicated as “axis Qis” is the quadrupole induced shift axis with the slope  $\Delta\delta(\text{F2})/\Delta\delta(\text{F1}) = -17/10$ . This axis is identical for all different spins  $I$  and all orders  $p$  of the MQMAS experiments. This axis can be shifted, retaining the same slope, so that it intersects a spectral line in its centre of gravity. Through the intersection point of the Qis axis with the CS axis a third line can be drawn parallel to the F2 axis. This is the dotted black line in [Figure 15.12](#). The shift value that is read from the F1 axis at this position is the isotropic chemical shift of that particular site, and the Qis is then given by [\(Eq. 15.2\)](#).

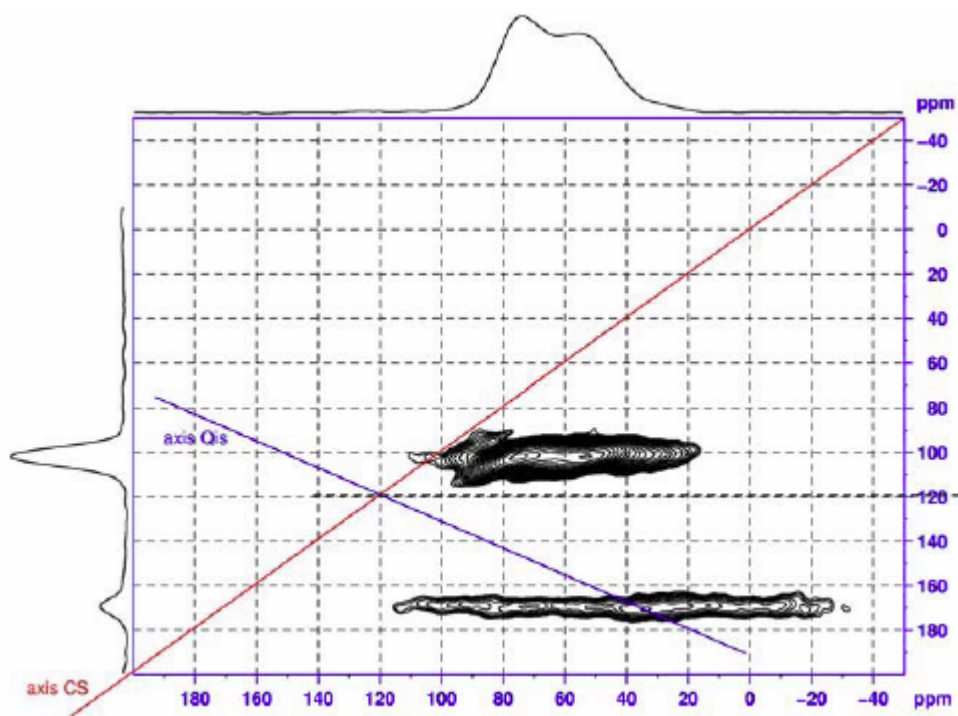


Figure 15.12. Graphical Interpretation of the Spectrum from [Figure 15.10.](#)

In the 11.7 T spectrum this gives quadrupole induced shifts  $\delta_{qis}$  of  $\approx -75$  ppm and  $\approx -20$  ppm for the two sites, respectively. At 18.8 T the  $\delta_{qis}$  of the lower peak in the 2D spectrum decreases to  $\approx -30$  ppm, whereas it cannot be determined graphically anymore for the upper peak since the chemical distribution broadens the peak in the F1 dimension more than the theoretical  $\delta_{qis}$  of  $\approx -5$  ppm.

# **MQ-MAS: Sensitivity Enhancement**

# **16**

The MQMAS experiment on half integer quadrupole nuclei is an extremely insensitive experiment. This is due to the low efficiencies of both the excitation of 3Q coherence and their conversion to observable magnetization. Several approaches have been taken to enhance the efficiency of the excitation and conversion, mainly focusing on the conversion, as this is the least efficient step. Adiabatic pulses can be used for the conversion instead of a single high power CW pulse, and alternative phase cycling schemes have also yielded improvements. Improving the efficiency of the MQ excitation pulse has been tried but no generally applicable scheme exists so far. Before describing the optimization procedures, some experimental approaches used in combination with these enhancement techniques are introduced.

## ***Split-t<sub>1</sub> Experiments and Shifted Echo Acquisition***

**16.1**

The excitation pulse in the MQMAS experiment creates 3Q coherence that can be refocused into an observable SQ echo by the conversion pulse. As the  $t_1$  period is incremented in successive slices of the 2D experiment this echo position relative to the conversion pulse changes as a function of the duration of the actual  $t_1$  delay. If this observable (SQ) magnetization can be refocused again, by a central transition selective 180° pulse, a shifted echo acquisition can be implemented. The delay between the conversion pulse and the 180° pulse or the delay prior to the start of the acquisition must be incremented proportional to  $t_1$ . This results in a split- $t_1$  experiment where the top of the shifted echo appears at a constant position after the final pulse throughout the entire 2D experiment. The position of the echo top depends on the spin  $I$  of the observed nucleus. If the delay before the selective 180° pulse is long enough, the signal will have decayed and the full build up and decay of the echo can be recorded. By this method a phase modulated data set is acquired with a full echo that contains twice the intensity of the simple MQMAS experiment (if transverse relaxation can be neglected). At the end of the  $t_1$  period of the split- $t_1$  experiment, there is no net evolution under the second order quadrupole broadening. This is the case because the evolution of the MQ coherence in the first part of  $t_1$  is cancelled out by the evolution of the SQ coherence in the part of  $t_1$  after the conversion pulse (the lengths of the two periods are related by the ratio of the second order broadening of the MQ and SQ coherence). The resulting 2D spectrum thus requires no shearing transformation to make  $f_2$  the isotropic dimension.

Whether this experimental trick is useful for your sample of interest can easily be determined by running a simple Hahn-echo experiment, where the delay  $\tau$  in the 90°- $\tau$ -180° sequence is adjusted so that the FID of the signal is decayed before the 180° pulse is applied. This is shown in [Figure 16.1](#). The FID generated by the initial 90° pulse is not sampled, but after it is decayed it is refocused with a 180° pulse into a so-called shifted echo, meaning that the position of the echo can be shifted by adjusting the delay **d6**.

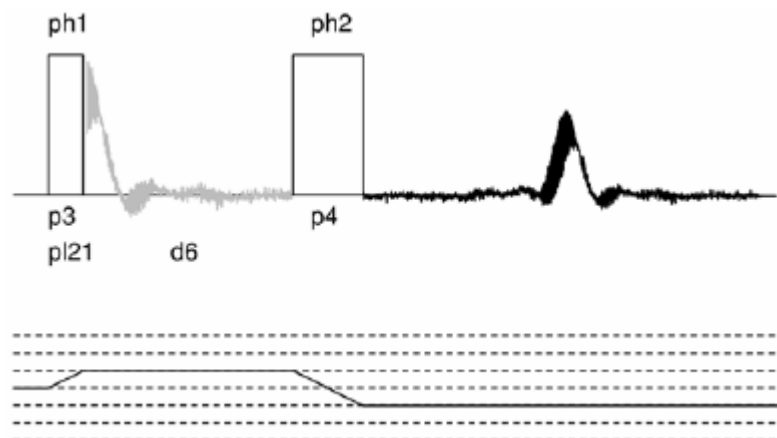


Figure 16.1. Hahn Echo Pulse Sequence and Coherence Transfer Pathway.

After the initial  $90^\circ$  pulse **p3** the magnetization dephases and is refocused by the  $180^\circ$  pulse **p4**. If the  $\tau$  delay **d6** is long enough a full echo can be acquired.

If data acquisition starts immediately after the second pulse the whole echo will be acquired. The integrated intensity of the echo will be almost twice the intensity of the single FID; it is just  $T_2$  relaxation during  $\tau$  that leads to attenuation. In MAS experiments it is advisable to synchronize the echo with the sample rotation i.e. make  $\tau$  an integer multiple of rotor periods. For FT of the shifted echo FID there is a slight “inconvenience” as shown in [Figure 16.2](#), because after a normal FT the signal looks quite unconventional. To obtain the usual spectrum a magnitude calculation can be done on 1D spectra, with the loss of phase information. Alternatively, and in particular in 2D spectra it is possible to apply a large 1<sup>st</sup> order phase correction **phc1** to compensate for the time delay before the echo top. The value of this is:

$$phc1 = -\frac{d6}{dw} \cdot 180^\circ \quad (\text{Eq. 16.1})$$

This value can be entered into the processing parameters and a phase correction **pk** can be performed. After this the 0<sup>th</sup> order phase correction still needs to be adjusted interactively. The best method is to phase the spectrum to give minimum signal intensity and add or subtract  $90^\circ$  to the obtained value (click 90 or -90 in the TopSpin phasing interface).

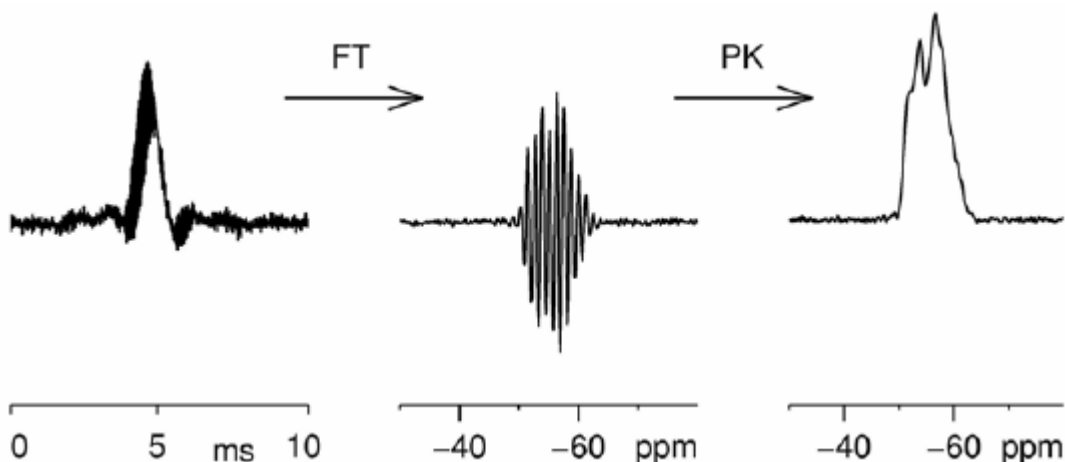


Figure 16.2. Processing of Hahn Echo. Left is the Shifted Echo.

The middle shows the spectrum after FT. On the right is the spectrum with the correct first order phase correction.

## Implementation of DFS into MQMAS experiments

## 16.2

Two pulse sequences are available to implement a double frequency sweep (DFS). [Figure 16.3](#). shows the 4-pulse sequence with z-filter, *mp3qdfs.z*.av. The principle of this sequence is already described in the chapter "[Basic MQ-MAS](#)" on page 151, with a CW pulse instead of a DFS for conversion. [Figure 16.4](#). shows a 3-pulse sequence with a shifted echo acquisition in a split- $t_1$  experiment, *mp3qdfs.z*.av. In both sequences the same sweep is used. Both sequences start with an excitation pulse **p1** that creates 3Q coherence which is allowed to evolve during the evolution period **D0**. The sweep during **P2** is used to change (non-observable) 3Q coherency to observable SQ coherency. In the 4-pulse sequence they pass through a z-filter by a sequence of CT selective 90°-90° pulses **P3-D4-P3**. In the 3-pulse sequence a delay **D6** is introduced so that the obtained signal can first dephase and then be refocused with a 180° CT selective pulse.

### Optimization of the Double Frequency Sweep (DFS)

### 16.2.1

At this point it is assumed that the pulses **p1**, **P3**, and **P4** together with their corresponding power levels **PL11** and **PL21** are already calibrated as described in the chapter "[Basic MQ-MAS](#)" on page 151. Starting from this set-up a data set should be created into which either of the two DFS pulse programs is loaded.

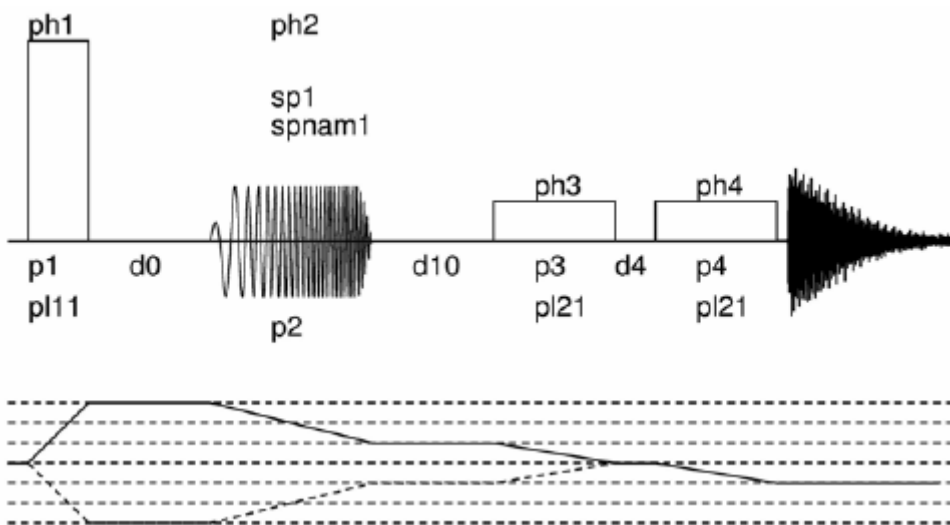


Figure 16.3. Four Pulse Sequence and Coherence Transfer Pathway for the 3Q MAS Experiment

Four pulse sequence and coherence transfer pathway for the 3Q MAS experiment with z-filter (*mp3dfsz.av*) and double frequency sweep (DFS). Excitation pulse *p1* and selective pulses *P3* are the same as for *mp3qzfil.av*. Delays *D0* and *D4* are the incremented delay for *t<sub>1</sub>* evolution and 20  $\mu$ s for z-filter, respectively. Delay *D10* can be incremented for spin *I* = 3/2 nuclei proportional to *D0*. Power level and duration of the sweep *P2* must be optimized. Phase lists are as follows, for phase sensitive detection in *F1* the phase of the first pulse must be incremented by 30° in States or States-TPPI mode:

*ph1* = 0 60 120 180 240 300

*ph2* = 0\*24 90\*24 180\*24 270\*24

*ph3* = 0

*ph4* = 0\*6 90\*6 180\*6 270\*6

*receiver* = {0 180}\*3 {90 270}\*3 {180 0}\*3 {270 90}\*3

{180 0}\*3 {270 90}\*3 {0 180}\*3 {90 270}\*3.

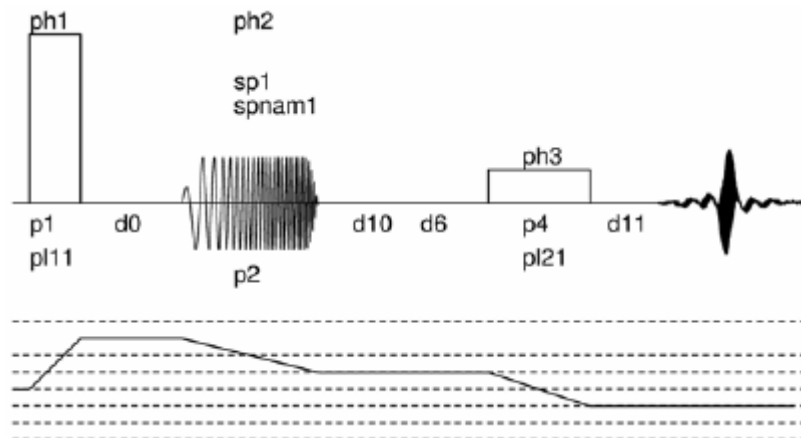


Figure 16.4. Three Pulse Sequence and Coherence Transfer Pathway

*Three pulse sequence and coherence transfer pathway for the 3Q MAS experiment with z-filter (mp3qdfs.av). Excitation pulse **p1** is the same as for mp3qzfil.av, **P4** is a central transition selective 180° pulse (usually 2\*p3). Delays **D0** is the incremented delay for  $t_1$  evolution. Delays **D10** or **D11** must be incremented proportional to **D0**. Power level and duration of the sweep **P2** must be optimized. Phase lists are as follows, 2D data are acquired in QF mode, which means that no phase incrementation is required:*

```
ph1 = 0 30 60 90 120 150 180 210 240 270 300 330
```

```
ph2 = 0
```

```
ph3 = 0*12 90*12 180*12 270*12
```

```
receiver = {0 270 180 90}*3 {180 90 0 270}*3
```

Initial parameter values are listed in [Figure 16.1](#). A few of these parameters need further explanation:

**D6**: Is calculated as  $(1s * L1 / CNST31) - (P4/2) - (P2/2)$ . This ensures that the delay from the centre of the sweep to the middle of the 180° pulse is an integer multiple of the rotor period. **L1** must be set so that **D6** becomes long enough for a full echo to build up. If we assume the FID has decayed after 3 ms, spinning frequency is 25 kHz, and the 90° pulse is 20  $\mu$ s, then **L1** should be between 70 and 80 so that **D6** is between 2.77 and 3.17 ms.

**P2**: Is calculated as  $1s / (CNST31 * L0)$ . The duration of the sweep can be adjusted depending on  $T_2$  of the sample. The sweep should not be longer than one rotor period, for many samples you may find that a quarter of a rotor period or even less is sufficient.

In **ased** the values of the two parameters **D6** and **P2** are greyed, because they cannot be set anymore. They are calculated in the pulse program from the parameters explained below, which must be set accordingly:

**L0**: Defines the fraction of a rotor period for the duration of the sweep **P2**, usually between 1 and 8.

**L1**: Defines **D6** to be an integer number of rotor periods.

The sweep will be defined by further parameters:

**CNST1**: Start frequency (in kHz) of the sweep; the sweep should start slightly off resonance, usually 30 to 50 kHz from the resonance of the central transition.

**CNST2**: End frequency (in kHz) of the sweep; the sweep should cover the satellite transition, but this is often broader than the band width of the probe of approximately 1 MHz. Therefore, it does not make sense to have this value bigger than 1000.

Table 16.1. Initial Parameters for the DFS Experiment

Parameter	Value	Comments
pulprog	mp3qdfs.av or mp3qdfsz.av	Pulse program.
NS	48*n (dfs) 96*n (dfsz)	Full phase cycle is important.
D0	3 $\mu$ s	Or longer, $t_1$ -period.
D1	5 * $T_1$	Recycle delay, use dummy scans if shorter. If d1 is too short artefacts in the 2D spectrum may show up.
D4	20 $\mu$ s	Z-filter delay, mp3qdfsz.av only.
D6	see text	Calculated in pulse program mp3qdfs.av only.
D10	=4u	
D11	=0	Used in mp3qdfs.av only.
P1	$\leq$ 3.6 $\mu$ s	Excitation pulse at pl11.
P2	see text	Calculated in pulse program.
P3	20 $\mu$ s	90° selective pulse at pl21 used in mp3qdfsz.av only.
P4	40 $\mu$ s	180° selective pulse at pl21 used in mp3qdfs.av only.
PL1	=120 dB	Not used.
PL11		Power level for excitation pulse, use value from standard MQMAS optimization.
PL21		Power level for selective pulse, approx. pl11+30 dB taken from previous pulse calibration.
spnam1	dfs	Set by AU program zg_dfs.
sp1	to be optimized	Power level for dfs.
aunm	zg_dfs	AU program to calculate sweep.
L0	see text	Fraction of rotor period for sweep.
L1	see text	Number of rotor cycles for synchronization used in mp3qdfs.av only.
cnst1	see text	Start frequency of sweep (in kHz).
cnst2	see text	End frequency of sweep (in kHz).
cnst3	50	(in ns) timing resolution for sweep
cnst31	“masr”	Spinning frequency

**CNST3:** (in ns) = 50. This is the maximum timing resolution that can be obtained on a shaped pulse, with AV or AVII hardware. However, if **cortab** is defined for that nucleus, 100 ns is the maximum timing resolution possible in a shaped pulse.

**CNST31:** Magic angle spinning frequency, used for the calculation of the duration of the sweep and the echo delay.

The calculation of the sweep is done via an AU program called **zg\_dfs**. It calculates the sweep according to the parameters given above and stores it as a shape file, which is called **dfs**. After the calculation the AU program starts the acquisition. In order to ensure that the correct sweep is always used, it is advisable to enter the name of this AU program into the parameter **aunm**, and start all acquisitions using the command **xaua**. All that needs to be optimized now is the appropriate RF power level for the sweep, defined as parameter **sp1**. As a first guess a value of 3 dB less RF power than for the excitation pulse should be used (i.e. **SP1 = PL11 + 3 dB**). You may use **popt** for the optimization, where **SP1** is decremented by 1 dB up to the same power level used for the excitation pulse (e.g. from 20 dB to 0 dB). Initially a sweep of one whole rotor period (i.e. **L0 = 1**) can be used. The optimization of **SP1** can be repeated e.g. for half a rotor period, a quarter of a rotor period and so on. With a shorter sweep you will find that higher RF power will be needed.

OPTIMIZE	PARAMETER	OPTIMUM	STARTVAL	ENDVAL	NEXP	VARMOD	INC
<input checked="" type="checkbox"/>	sp1	POSMAX	20	0	0	LIN	-1
<input checked="" type="checkbox"/>	IO	POSMAX	2	2	1	LIN	null
<input checked="" type="checkbox"/>	sp1	POSMAX	20	0	0	LIN	-1
<input checked="" type="checkbox"/>	IO	POSMAX	4	4	1	LIN	null
<input checked="" type="checkbox"/>	sp1	POSMAX	20	0	0	LIN	-1
<input checked="" type="checkbox"/>	IO	POSMAX	8	8	1	LIN	null
<input checked="" type="checkbox"/>	sp1	POSMAX	20	0	0	LIN	-1

Figure 16.5. Example for **popt** to Set-up for Optimization of DFS.

Note that the option “The AU program specified in AUNM will be executed” is checked. This ensures that the sweep is recalculated for the variation of **IO** and stored in the shape file **dfs**. The initial value of **IO** is 1.

**Figure 16.5.** shows a **popt** window with successive optimization of **SP1** for several fractions of rotor periods **IO**. Note that the check mark for “The AU program specified in AUNM will be executed” MUST be set, in order to force recalculation of the shape for each step of the optimisation. In this case acquisition is run with the command **xaua**, which ensures that the correct sweep is stored in the shape file **dfs**. In the above example optimization proceeds such that in the first run **SP1** is varied from 20 to 0 in 21 steps. Then **L0** is set to 2 and **SP1** is again varied from 20 to 0. Then **IO** is set to 4 and so on. **Figure 16.6.** shows results of the variation of the RF power level of sweeps with different durations. Experiments have been run at 20 kHz and optimization procedures for 1, 0.5, 0.25, and 0.125 rotor periods corresponding to 50, 25, 12.5, and 6.25  $\mu$ s respectively have been run. One can see that as the duration of the sweep is reduced the required RF field amplitude is higher. This is true when the spinning frequency is kept constant and the sweep is a smaller fraction of a rotor period and when the sweep is kept at e.g. one rotor period and the spinning frequency is increased (and hence the rotor period decreased). On “real life” samples the differences between signal intensities at one rotor period compared to e.g.  $\frac{1}{4}$  rotor periods will be more pronounced than on a crystalline model compound. Since the spinning frequency is usually determined by the spectrum itself, the only de-

gree of freedom is the amplitude of the sweep. In the example chosen here any of the conditions will provide a good quality spectrum, and the condition with the biggest enhancement at the least power is to be preferred.

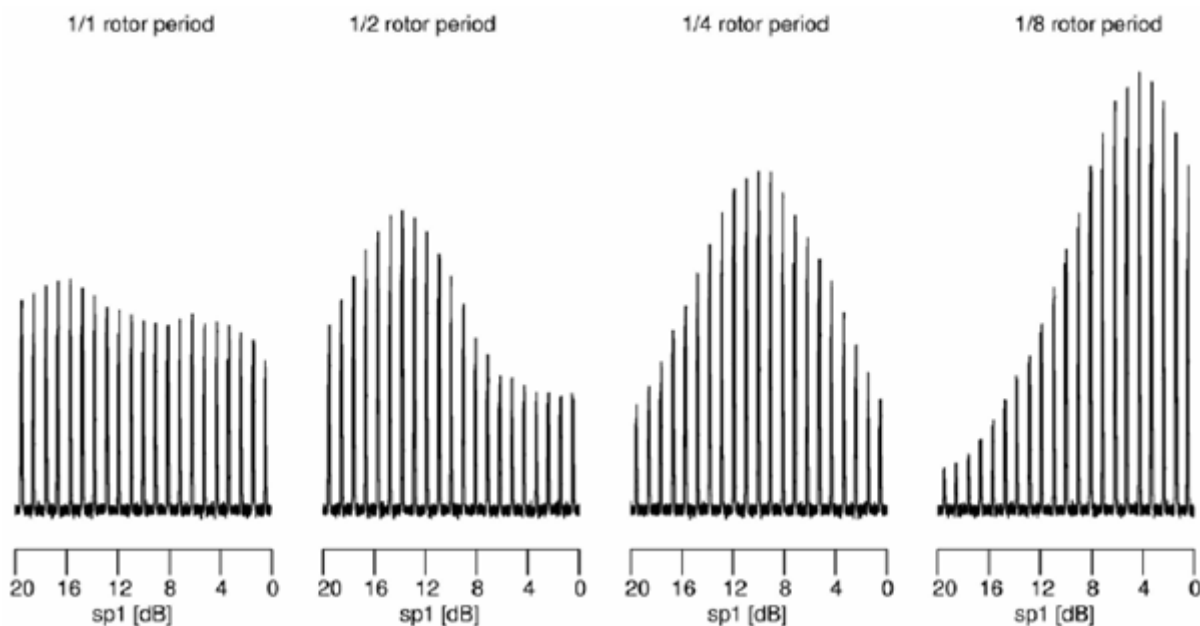


Figure 16.6. Signal Intensities of  $^{87}\text{Rb}$  in  $\text{RbNO}_3$

Signal intensities of  $^{87}\text{Rb}$  in  $\text{RbNO}_3$  as function of duration and RF field amplitude for double frequency sweeps.

## 2D Data Acquisition

### 16.2.2

After the parameters for the DFS are adjusted the 2D data acquisition can be prepared. In tables 2 and 3 the important parameters are listed for the two pulse sequences. Parameters are listed separately for F1 and for the pulse program relevant parameters which should be set in **eda** and **ased**, respectively.

The 3-pulse sequence used in *mp3qdfs.av* creates a phase modulated data set and therefore, FnMODE must be QF. However, since a whole echo acquisition is performed a pure absorption mode spectrum can be obtained. Increments for **D10** and **D11** must be set correctly so that a standard two-dimensional FT can be applied.

Using the 4-pulse sequence *mp3qdfsز.av* FnMode must be States or States-TPPI, so that the shearing FT can be performed for processing. However, no shearing is required in case of nuclei with spin I=3/2 where a split-t<sub>1</sub> experiment can be performed, in which case **IN10** must be set correctly.

For both sequences, TD in F1 determines the number of FID's to be accumulated in the indirect dimension. This value is determined by the line width and resolution that can be expected and which depend on the properties of the sample. In crystalline material fairly narrow peaks can be expected so that a maximum acquisition time in F1 of 2 to 5 ms is expected. In disordered material where the line width is broader and determined by distribution a total acquisition time in F1 up to may be 1 ms may be sufficient. The total acquisition time aq in F1 equals  $(\text{TD}/2)*\text{IN\_010}$ . For rotor synchronized experiments **IN\_010** = 1/spinning frequency so will typically

be between 100  $\mu$ s (10 kHz spinning) and 28.5  $\mu$ s (35 kHz spinning), so only 100 to 250 experiments might be required. The rotor synchronization immediately means that the spectral range in F1 is limited. Dependent on chemical shift range, spinning frequency, and quadrupole interactions the positions of the peaks may fall outside this range. In such a case care must be taken when interpreting the spectrum. Acquisition with half-rotor synchronization to double the spectral window in F1 may help. However, in this situation one set of spinning sidebands appears and it must be avoided that the spinning side bands of one peak fall on top of other peaks. Some sort of rotor synchronization is always recommended because spinning side bands in the indirect dimension extend over a very wide range, which cannot be truncated by e.g. filtering. Therefore, rotor synchronization together with States or States-TPPI phase sensitive acquisition helps to fold spinning sidebands from outside back onto centre bands or other side bands.

Table 16.2. Parameters for 2D Data Acquisition of 3-pulse Shifted Echo Experiment mp3qdfs.av.

Parameter	Value	Comments
pulprog	mp3qdfs.av	
F1 parameters:		In eda.
FnMode	QF	Acquisition mode for 2D.
TD	see text	Number of FID's to be acquired.
ND_010	1	There is only one d0 delay in the sequence.
SWH	"masr"	Equals spinning frequency for rotor synchronization, from this in0 is calculated correctly, if ND_010 must be set first.
NUC1		Select the same nucleus as for F2 so that transmitter frequency offset is set the same in both dimensions (essential for referencing).
pulse program parameters:		In ased.
D10	0	
IN10	=IN0*7/9 0	For spin $I = 3/2$ , for all other spin I.
D11	0	
IN11	0 =IN0*19/12 =IN0*101/45 =IN0*91/36	For spin $I = 3/2$ , For spin $I = 5/2$ , For spin $I = 7/2$ , For spin $I = 9/2$ .

Table 16.3. Parameters for 2D Data Acquisition of 4-pulse Z-filtered Experiment mp3qdfs.z.av.

Parameter	Value	Comments
pulprog	mp3qdfs.z.av	
F1 parameters:		In <i>eda</i> .
FnMode	States or States-TPPI	Acquisition mode for 2D.
TD	see text	Number of FID's to be acquired.
ND_010	1	There is only one d0 delay in the sequence.
SWH	"masr"	Equals spinning frequency for rotor synchronization, from this in0 is calculated correctly, ND_010 must be set first.
NUC1		Select the same nucleus as for F2 so that transmitter frequency offset is set the same in both dimensions (essential for referencing).
Pulse program parameters:		In <i>ased</i> .
D10	0	
IN10	=IN0*7/9 0	For spin I=3/2, so that no shearing FT is required. For all other spin I.

**Data Processing****16.2.3**

Processing parameters should be set according to [Table 16.4](#). Data obtained with mp3qdfs.av can be processed with **xfb** alone, if **IN10** or **IN11** have been set appropriately to run a split-t<sub>1</sub> experiment. Since a whole echo is accumulated FT along F2 from -Δ > t > +Δ is done which necessitates a large 1<sup>st</sup> order phase correction to compensate for the start of the acquisition before the echo top. This correction can easily be calculated as given in ([Eq. 16.1](#)) and should be stored into the parameter **PHC1**. This gives an approximate value, which can be precisely adjusted in the interactive phase correction routine. The phase of the spectrum must be corrected such that there is no signal in the imaginary part, as described above.

Table 16.4. Processing Parameters

Parameter	Value	Comments
F2 (acquisition dimension)		
SI		Usually set to one times zero filling.
WDW	no	Don't use window function.
PH_mod	pk	Apply phase correction.
BC_mod	no	No DC correction is required after full phase cycle.
ABSF1	1000 ppm	Should be outside the observed spectral width.
ABSF2	-1000 ppm	Should be outside the observed spectral width.
STSR	0	Avoid strip FT.
STSI	0	Avoid strip FT.
TDoff	0	Avoid left shifts or right shifts before FT.
F1 (indirect dimension)		
SI	256	Sufficient in most cases.
WDW	no QSINE	Don't use window function. Only use if FID in F1 is truncated.
SSB	2	$\pi/2$ shifted squared sine bell.
PH_mod	pk	Apply phase correction.
PHC1		$-(d_6/dw)^{*}180$ .
BC_mod	no	No dc correction is required after full phase cycle.
ABSF1	1000	Should be outside the observed spectral width.
ABSF2	-1000	Should be outside the observed spectral width.
STSR	0	Avoid strip FT.
STSI	0	Avoid strip FT.
TDoff	0	Avoid left shifts or right shifts before FT.

Data obtained with `mp3qdfszz.av` can be processed with the AU program `xfshear`, unless in case of nuclei with spin  $I = 3/2$  where a straight 2D FT can be used if a split- $t_1$  experiment has been recorded by setting **IN10** appropriately. The information obtained from the DFS enhanced spectra is the same as from the standard MQMAS experiments. Please refer to the chapter **"Basic MQ-MAS" on page 151** for further details regarding the shearing transformation and the information obtained from MQMAS spectra.

**Fast Amplitude Modulation - FAM****16.3**

It must be mentioned at this point that similar approaches have been made where the frequency of irradiation is established by a fast modulation of the amplitude of the pulses. This is realized by a repetitive train of either [pulse-delay-pulse-delay]<sub>n</sub> or [delay-pulse-pulse-delay]<sub>n</sub>. Pulses and delays in these trains are of the same length. The phases of the pulses are alternating +x and -x which creates a fast cosine type amplitude modulation. The frequency of this amplitude modulation appears to the spin system as an irradiated frequency.

Two pulse programs are available, *mp3qfamz.av* and *mp3qfam.av*. They correspond to the pulse sequences depicted in [Figure 16.3](#) and [Figure 16.4](#), but the shaped pulse realizing the DFS is replaced with a sequence **D2-P2-P2-D2** embedded in a loop repeated by loop counter **L2** and with power level **PL14** for the pulses. These sequences are only useful for spin  $I = 3/2$  nuclei. There are also sequences for higher spins, which are not included in the pulse program library. In those cases it is recommended to use DFS. The difference between FAM and DFS can be understood in such a way that FAM establishes the irradiation of a single distinct frequency whereas DFS continuously irradiates (sweeps) over a range of frequencies. These frequencies must lie in the range of the satellite transitions, therefore a single frequency irradiation is sufficient for spin  $I = 3/2$ . Higher spins have more satellite transitions and therefore, a correspondingly larger number of irradiation frequencies are required. DFS is here the most convenient solution.

Start values for the parameters determining FAM are listed in [Table 16.5](#).

*Table 16.5. Parameters for FAM*

Parameter	Value	Comments
PL14	PL11 + 3 dB	Less RF power than for a CW pulse is sufficient.
P2	0.8 $\mu$ s	
D2	= P2	Calculated in the pulse program.
L2	2	

All other parameters are in full analogy to the other MQMAS pulse programs, in particular for z-filtering and creating the shifted echo. What is left is to find the best conditions for FAM optimizing **PL14**, **P2**, and **L2** consecutively. This can conveniently be performed with the parameter optimization procedure **popt**, where two or three iterations can automatically be performed.

**Soft Pulse Added Mixing - SPAM****16.4**

A simple and ingenious experimental trick can immediately give a signal enhancement. Starting from the standard 3-pulse sequence the phase cycling of reconversion pulse **P2** and the CT selective 90° pulse **P3** is eliminated. This changes the coherence transfer pathway from 0 → ±3 → 0 → -1 to 0 → +3 → -1, 0, +1 → -1 and 0 → -3 → -1, 0, +1 → -1. It has been shown that this leads to a substantial gain in sensitivity. However, it requires that data are acquired in echo/anti-echo mode in order to store the two different coherence transfer pathways in consecutive FID's in the serial file.

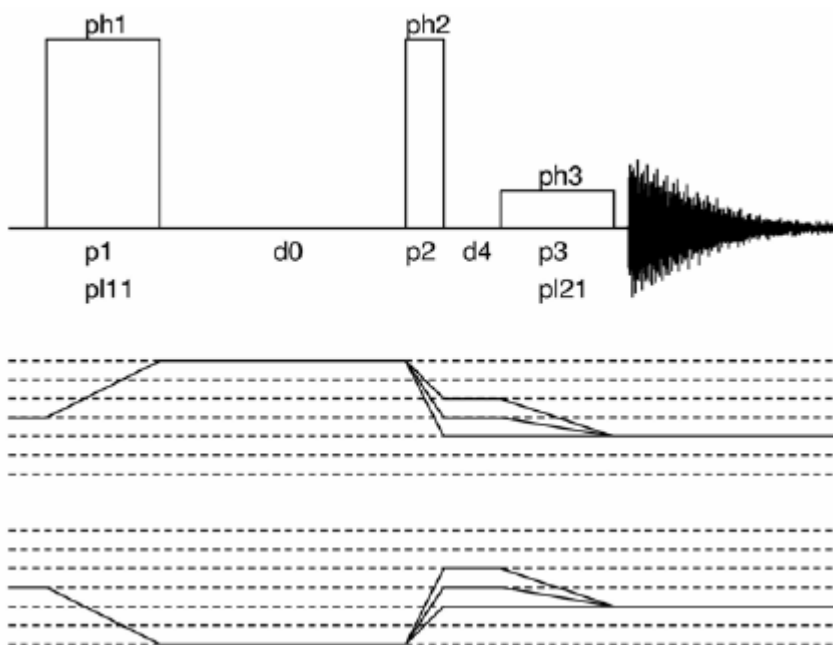


Figure 16.7. Pulse Sequence and Coherence Transfer Pathways for SPAM 3QMAS.

It is extremely convenient that the setup of the pulse lengths and power levels can be done with the pulse program *mp3qzqf.av*. The setup procedure is exactly the same as described for this experiment in the chapter "[Basic MQ-MAS](#)" on page 151. Before the start of the 2D data acquisition all that needs to be set is the pulse program, *mp3qspam.av*, and a small number of other parameters. These are listed in [Table 16.6](#):

*Table 16.6. Further Parameters for 2D Data Acquisition of SPAM MQMAS Experiment mp3qspam.av*

Parameter	Value	Comments
pulprog	mp3qspam.av	
Further F1 parameters:		In <i>eda</i> .
FnMode	Echo/Anti-echo	Acquisition mode for 2D.
Further pulse program parameters:		In <i>ased</i> .
D4	0.5 $\mu$ s	Not 20 $\mu$ s like in <i>mp3qzqf.av</i> .
I4	1	Set by the pulse program, internally used counter.
I5	see text	Number of anti-echos to be acquired 0 > I5 > td{F1}/2.
I6	3 1	For spin I = 3/2. For all other spins.

**FNMODE:** Even though this parameter is not evaluated by the pulse program it will be used by the processing AU program **xfshear**.

**D4:** A very short delay is used here, just to allow for amplitude and phase switching.

**I4:** This loop counter is internally used for checking if the echo or anti-echo is currently being acquired.

**I5:** In the acquisition of echo-anti-echo 2D spectra signals from the echo and anti-echo pathways are stored into consecutive FID's in the serial file. In MQMAS experiments these echos and anti-echos behave differently. For  $t_1 = 0$  both signals have their echo top immediately after the selective 90° pulse. As  $t_1$  is incremented the top of the echo appears at later point in time whereas the top of the anti-echo appears at an earlier point in time. It means that the contribution of the anti-echo becomes less and less until finally the signal fades out completely and only noise is sampled. It can be advantageous to terminate the acquisition of this noise in order to increase the overall S/N and save spectrometer time. However, in the processing of echo-anti-echo data two consecutive FID's are linearly combined in the following way:

$$\begin{aligned} re1 &= -im2 - im1 & re2 &= re2 - re1 \\ im1 &= re2 + re1 & im2 &= im2 - im1 \end{aligned} \quad (\text{Eq. 16.2})$$

Where *re* and *im* refer to the real and imaginary points of FID's 1 and 2. Hence, acquiring a smaller number of anti-echos than echos leads to the usual truncation effects (wiggles in the spectrum). Furthermore, since both signals contribute to the phase information care must be taken that the pure absorption line shape of the 2D peaks is not obscured. Therefore, in case of doubt it is probably the best idea to set **L5 = TD[F1]/2**. If less anti-echos are to be accumulated the question is how many anti-echos to acquire - this depends on the sample. In amorphous or disordered materials the FID decays rapidly and so does the anti-echo. In such a case 4 to 8 anti-echos may be sufficient. In the case of crystalline materials it takes many more  $t_1$  increments before the anti-echos decay. Hence, the number of anti-echos should be of the order of half the number of echos. It is always better to acquire more anti-echos than are really needed, because then you can be sure that you acquire a 2D spectrum with a reliable 2D absorption line shape. Never risk gaining sensitivity or saving experimental time at the expense of quality of lineshapes.

**I16:** the value of this loop counter is needed to set the phases of the soft pulses correctly and define what is an echo and what is an anti-echo (which are different for spin  $I = 3/2$  and all the other spin quantum numbers).

Processing of these spectra is done in analogy to spectra obtained with *mp3qzqf.av*. However, phase correction in the acquisition dimension F2 cannot be determined on the first FID. Therefore, **xf2** must be applied first and then F2 phase correction can be determined on either the first slice, in case of nuclei with spin  $I = 3/2$ , or the second slice for all other nuclei. 2D processing is then done with the AU program **xfshear**. Alternatively **xfshear** can be used first, with a subsequent 2D interactive phase correction.

**Introduction**

17.1

The STMAS experiment for half integer quadrupole nuclei is a 2D experiment to separate anisotropic interactions from isotropic interactions. In the NMR of half integer quadrupole nuclei the dominant anisotropic broadening of the central  $+1/2 \leftrightarrow -1/2$  transition (CT), and symmetric multiple-quantum (MQ) transitions, is the 2<sup>nd</sup> order quadrupole interaction which can only partially be averaged by MAS. The satellite transitions (ST, e.g. the  $\pm 3/2 \leftrightarrow \pm 1/2$  transitions) however, are broadened by a 1<sup>st</sup> order interaction, which is several orders of magnitude larger than the 2<sup>nd</sup> order broadening. Under MAS the 1<sup>st</sup> order interaction of the ST can be averaged but spinning cannot be fast compared to the first order broadening (of the order of MHz), a large manifold of spinning side bands remains. The 2<sup>nd</sup> order broadening of the CT can only be narrowed by a factor of 3 to 4 so a signal is observed that still reflects this 2<sup>nd</sup> order broadening.

The 2D STMAS experiment exploits the fact that the 2<sup>nd</sup> order broadening of the ST transitions (e.g.  $+ 3/2 \leftrightarrow + 1/2$  in a spin 3/2), is related to the 2<sup>nd</sup> order broadening of the CT by a simple ratio. A 2D spectrum is recorded which correlates a single quantum coherence of the satellite transitions (usually one of the inner transitions,  $\pm 3/2 \leftrightarrow \pm 1/2$ ), and the  $+ 1/2 \leftrightarrow - 1/2$  single quantum coherence of the central transition. The resulting 2D spectrum yields an isotropic projection where the 2<sup>nd</sup> order broadening has disappeared. The information content is in full analogy to the MQMAS experiment.

**Experimental Particularities and Prerequisites**

17.2

In contrast to the MQMAS experiment the first pulse in the STMAS experiment excites single quantum (SQ) coherency. The signal which is thus generated consists of contributions from both the CT and the ST. In **Figure 17.1**, the contribution of the CT shows up in the cosine curve starting at the (blue) filled rectangle resembling the initial pulse.

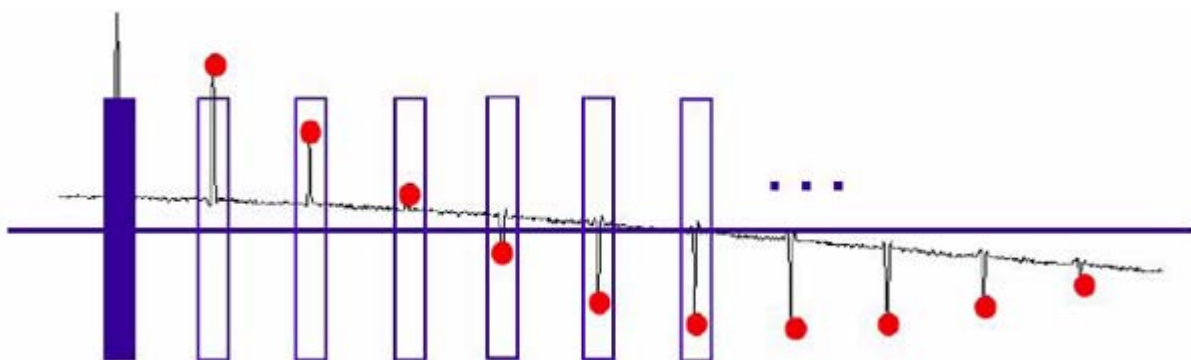


Figure 17.1. Principle of 2D Data Sampling in STMAS Experiments.

The (blue) filled rectangle on the left symbolizes the first pulse, which starts the evolution period  $t_1$ . After each revolution of the rotor, rotational echo's show up which are indicated by the

(red) filled circles. The open rectangles symbolize the second pulse (one pulse at the end of each individual  $t_1$  increment). They must always occur precisely on top of the rotational echo. For each increment the  $t_2$  data acquisition, which is not shown here, starts after the second pulse.

In the following discussion we will ignore this part completely. It showed up in the original experiments but can be completely suppressed by a double quantum filter. The contribution of the ST “rides” on top of the CT signal like spikelets. Since MAS efficiently averages the 1st order quadrupole interaction of the ST, the corresponding MHz broad signal is now narrowed into a huge number of spinning side bands. These coherency originating from the ST dephase rapidly and refocus into rotational echoes with each rotor cycle. A pulse precisely on top of such a rotational echo can transfer the SQ coherency from the ST to SQ coherency of the CT, the signal from which can then be acquired under standard MAS conditions. The evolution in the indirect dimension is achieved in such a way that the delay between the two pulses, which is the evolution period  $t_1$ , is incremented by integer multiples of the rotor period.

Two extremely important points must be considered for the experimental realization of the ST-MAS experiment. Firstly, the spinning frequency must be kept absolutely constant. The duration of the rotational echoes in the STMAS experiment is determined by the width of the satellite transition, giving a length of e.g. 1  $\mu$ s for a satellite transition of 1 MHz width. If the rotor period varies from that specified in the parameters, the calculated delay in the pulse program is incorrect and the pulse misses the echo top, so less or no signal intensity is obtained.

**Table 17.1.** summarizes the time deviation that occurs when the spinning frequency fluctuates by  $\pm 1$  Hz and  $\pm 10$  Hz at various desired spinning frequencies. One can see that when the  $t_1$  increment accumulates to as much as 100 rotor periods it is possible to miss an echo completely. For example, if the duration of the rotational echo is 1  $\mu$ s it will be missed when the deviation is larger, which is the case for a 1 Hz deviation at 10 kHz, but requires a fluctuation of 10 Hz at 30 kHz spinning.

*Table 17.1. Time deviation of the rotor period for spinning frequency variations of  $\pm 1$  and  $\pm 10$  Hz for various spinning frequencies.*

Fluctuation of ... Hz @ desired spinning frequency	Deviation from precise rotor period after 1 rotor period	Deviation from precise rotor period after 100 rotor periods
10 Hz @ 30 kHz	11 ns	1.1 $\mu$ s
1 Hz @ 30 kHz	1.1 ns	110 ns
10 Hz @ 20 kHz	25 ns	2.5 $\mu$ s
1 Hz @ 20 kHz	2.5 ns	250 ns
10 Hz @ 10 kHz	100 ns	10 $\mu$ s
1 Hz @ 10 kHz	10 ns	1 $\mu$ s

Typically the spinning frequency must be stable within  $\leq 1$  Hz throughout the entire 2D data acquisition. Secondly, the accuracy of the magic angle setting is extremely important. The sidebands resulting from the first order broadening are narrowed from the full first order line width by a factor of  $(3\cos^2\theta - 1)$ , hence for a deviation of  $d\theta$  from the magic angle the broadening is  $3\cos\theta\sin\theta d\theta$ , which close to the magic angle is  $\sqrt{2}d\theta$ . The magnitude of the interaction that must be narrowed in the present case is in the order of MHz so even a small deviation causes

a severe broadening in the STMAS spectrum. This can easily be understood as the rotational echoes decay much more rapidly when the magic angle is off. Experimentally it has been found that the precision for setting the angle must be  $\leq 0.002^\circ$ . The dependence on the accuracy is so important that the experiment itself must be used to find the most precise magic angle setting. It is obvious that this can only be done on a well-known sample, as we will see later in the chapter. In order to achieve the necessary precision for the adjustability of the angle a special goniometer screw with an adapted gear transmission ratio is provided for the magic angle setting knob as an upgrade for Bruker WB MAS probes. Once the best angle setting is found it is advisable to leave the probe in the magnet. Sample changes, however, on the WB probes doesn't change the setting noticeably.

## Pulse Sequences

## 17.3

**Figure 17.2.** and **Figure 17.3.** show two of the basic sequences, which are 4-pulse sequences with z-filter (*stmasdqfz.av* and *stmasdqfe.av*). Both sequences start with a non-selective excitation pulse **p1** that creates SQ coherency on the innermost ST which is allowed to evolve during the evolution period **D0**. Shortly before the end of the  $t_1$  period there is a selective 180° pulse **P4**. This provides a double quantum filter by which magnetization of the CT transition is eliminated which will otherwise give a strong diagonal signal from a CT  $\rightarrow$  CT coherence transfer pathway. The  $t_1$  period is terminated with the second non-selective pulse **P2**.

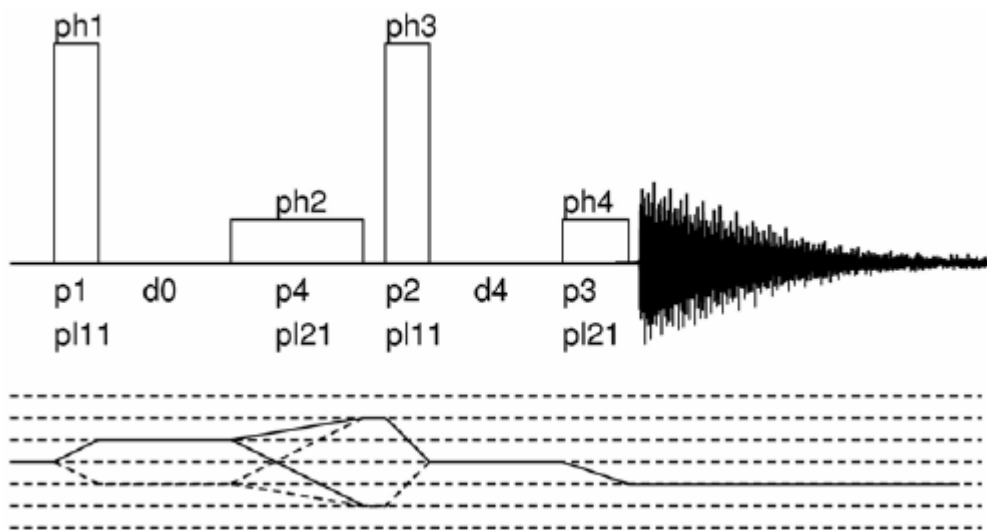


Figure 17.2. Four-pulse sequence and coherence transfer pathway for the double quantum filtered STMAS experiment with z-filter (*stmasdqfz.av*).

Pulses **p1** and **P2** are non-selective pulses. The corresponding power level **PL11** should be set to achieve around 100 kHz RF field amplitude. **P3** and **P4** are CT selective pulse 90° and 180° pulses of about 20 and 40  $\mu$ s, respectively, corresponding to an RF field amplitude of a few kHz. Delays **D0** and **D4** are the incremented delay for  $t_1$  evolution and 20  $\mu$ s for z-filter, respectively. Phase lists are as follows, for phase sensitive detection in F1 the phase of the first pulse must be incremented by 90° in States or States-TPPI mode:

ph1 = 0 2

ph2 = 0 0 2 2

ph3 = 0 0 0 1 1 1 1 2 2 2 2 3 3 3 3

```

ph4 = 0*8 1*8 2*8 3*8 4*8
receiver = 0 2 2 0 2 0 0 2 0 2 2 0 2 0 0 2 1 3 3 1 3 1 1 3 1 3 3 1 3 1 1 3
2 0 0 2 0 2 2 0 2 0 2 2 0 3 1 1 3 1 3 3 1 3 1 1 3 1 3 3 1.

```

In the *stmasdqfz.av* pulse sequence this pulse flips the magnetization back along the z-axis. After a short z-filter delay **D4** a CT selective 90° pulse **P3** creates transverse magnetization. In the *stmasdqfe.av* pulse sequence the non-selective pulse **P2** converts the ST SQ coherence into CT SQ coherence. This is allowed to evolve for another delay **D6** after which it refocuses into an echo by a CT selective 180° pulse. When either the **D6** before the 180° pulse or **D7** after the 180° pulse is incremented proportionally to the  $t_1$  period a split- $t_1$  experiment as described in chapters 16 and 17 for some MQMAS experiments will be performed.

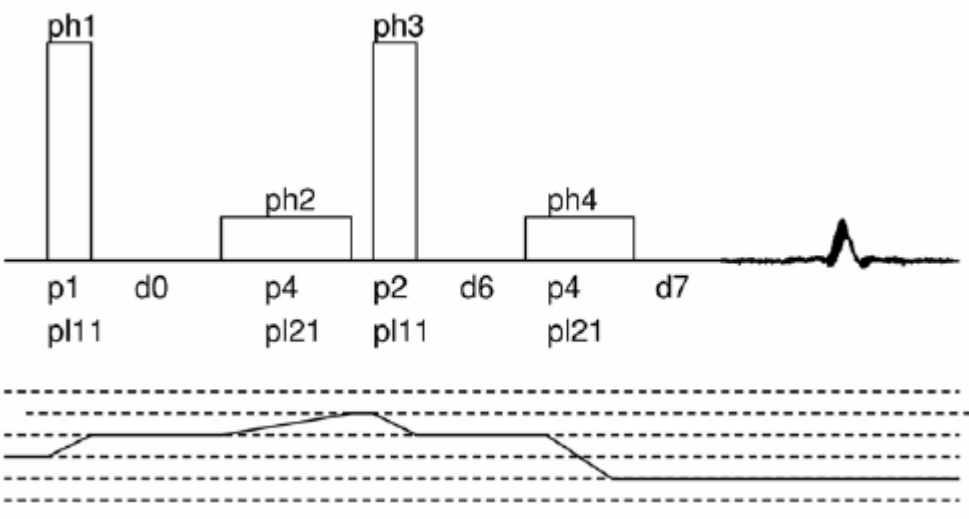


Figure 17.3. Four pulse sequence and coherence transfer pathway

Four pulse sequence and coherence transfer pathway for the double quantum filtered STMAS experiment with shifted echo acquisition (*stmasdqfe.av*). Pulses **p1** and **P2** are non-selective pulses. Corresponding power level **PL11** should be set to achieve around 100 kHz RF field amplitude. **P3** and **P4** are CT selective pulse 90° and 180° pulses of about 20 and 40  $\mu$ s, respectively, corresponding to an RF field amplitude of a few kHz. Delay **D0** is the incremented delay for  $t_1$  evolution, **D6** and **D7** can be incremented proportional to **D0** depending on the spin of the observed nucleus. Phase lists are as follows, incrementation of the phase of the first pulse is not required because a phase modulated data set is acquired with FnMODE being QF:

```

ph1 = 0 180 90 270
ph2 = 0*4 90*4 180*4 270*4
ph3 = 0*16 90*16 180*16 270*16
ph4 = 0
receiver = ph3-ph1-ph2

```

Before the 2D experiment on your sample of interest can be started some setup steps must be done as described in detail below. All setup steps should be done on a sample with:

- a. A known MAS spectrum,
- b. With sufficiently good sensitivity to facilitate the set-up, and,
- c. A 2<sup>nd</sup> order quadrupole interaction of the order of the one expected for your sample of interest.

In a first step, a low power selective pulse must be calibrated in a single pulse experiment. After this the STMAS experiment can be optimized using the 2D pulse sequence for the first  $t_1$  increment.

**Sample:** There are a large number of crystalline compounds that can be used to set-up the experiment. Please refer to **Table 17.2**, to select a suitable sample. For the general procedure described here the spin  $I$  of the nucleus is not important, of course the obtained pulse widths will depend on the spin  $I$ , and the Larmor frequency. For the STMAS experiment, in contrast to MQMAS, it is advisable to use a well-known sample for the setup because the accuracy of the magic angle setting is extremely critical.

Table 17.2. Some Useful Samples for Some Nuclei with Half Integer Spin

Nucleus	Spin	Spectrometer frequency * <sup>1)</sup>	$d_1$ [s] * <sup>3)</sup>	Sample	Comments
<sup>17</sup> O	5/2	67.78	2	NaPO <sub>3</sub>	> 10% enriched
<sup>11</sup> B	3/2	160.42	>5	H <sub>3</sub> BO <sub>3</sub>	
<sup>23</sup> Na	3/2	132.29	10	Na <sub>2</sub> HPO <sub>4</sub> * <sup>2)</sup>	
<sup>27</sup> Al	5/2	130.32	5	YAG	
<sup>87</sup> Rb	3/2	163.61	0.5	RbNO <sub>3</sub>	
<sup>93</sup> Nb	9/2	122.25	1	LiNbO <sub>3</sub>	

\*<sup>1)</sup> In MHz at 11.7 T (i.e. 500.13 MHz proton frequency).  
\*<sup>2)</sup> Alternatively Na<sub>2</sub>HPO<sub>4</sub> \* 2H<sub>2</sub>O can be used. For anhydrous Na<sub>2</sub>HPO<sub>4</sub> the sample should be dried at 70° C for a couple of hours before packing the rotor in order to eliminate crystal water completely.  
\*<sup>3)</sup> Recycle delays at 11.7 T, longer delays may be required at higher fields.

As for MQMAS the setup must be done in two steps; in the first step a central transition selective pulse that merely excites the central transition must be calibrated. This pulse must be weak enough so that only the central transition is affected and it must be short enough so that the central transitions of all sites in the spectral range are excited. These conditions are typically fulfilled by a 20  $\mu$ s pulse. For the calibration of this pulse a power level around 30 dB with 500 W and 1 kW amplifiers and around 20 dB with 300 W amplifiers should be expected. The pulse program zg (which uses **p1** and **p11**) or zgsel.av (which uses **P3** and **PL21**) can be used. For more details please refer to chapter 16.

Once the central transition selective 90° pulse is calibrated the STMAS pulse program can be loaded. Available pulse programs are *stmasdqfz.av* and *stmasdqfe.av*. Both are double quantum filtered 4-pulse sequences, the first with a z-filter, the second with a shifted echo. If this second sequence is to be used a proper setting of the timing for the shifted echo is required, to allow collection of the full echo signal. This is explained in chapter 17, where a shifted echo can be used in DFS enhanced MQMAS experiments.

In *Table 17.3* and *Table 17.4*, the starting parameters for the setup of the two sequences are given. Typical values for the pulses are entered so one should see some signal for further optimisation. Parameters like **O1**, **TD**, **SWH**, **RG**, should already be set in the standard 1D spectrum. Since the experiment is not as dependent on the pulse lengths or the applied RF field amplitude as MQMAS, pulse lengths between 1 and 2 µs, which can be achieved with every probe with 4mm or smaller rotor diameter, are sufficient.

*Table 17.3. Initial Parameters for the Set-up of stmasdfqz.av.*

Parameter	Value	Comments
pulprog	stmasdqfz.av	Pulse program.
NS	16*n	For set-up the full phase cycle is not so critical.
D0	see text	Calculated in pulse program.
D1	5 * T <sub>1</sub>	Recycle delay, use dummy scans if shorter.
D4	20 µs	Z-filter delay.
P1	1.5 µs	Excitation pulse at pl11.
P2	1.5 µs	Conversion pulse at pl11.
P3	20 µs	90° selective pulse at pl21 taken from previous pulse calibration.
PL1	=120 dB	Not used
PL11	start with ≈ 150 to 300 W	Power level for excitation and conversion pulses.
PL21		Power level for selective pulse, approx. pl11+30 dB taken from previous pulse calibration.

For **PL11** an initial value that corresponds to 150 to 300 W can be used. Optimization will be done on the first increment of the 2D sequence, which is calculated within the pulse program according to "**D0=(1s\*L0/CNST31)-P1/2-P4-0.3µ-P2/2**", because it is essential that the centres of the pulses **P1** and **P2** are exactly an integer number of rotor periods apart. In this formula **P1**, **P2**, and **P4** are the RF pulses as listed in table 2, **CNST31** must be set equal to the spinning frequency. This means that the first increment can last between 100 µs (10 kHz spinning) and 28.5 µs (35 kHz spinning). Since **P4** is the 180° selective pulse, which can be as long as 40 µs, **L0** must be set large enough to avoid the situation where the calculated **d0** is negative. Optimization of the pulses **P1** and **P2** can be done using **popt** in full analogy to the optimization of the pulses in MQMAS.

*Table 17.4. Initial Parameters for the Set-up of stmasdfqe.av.*

Parameter	Value	Comments
pulprog	stmasdqfe.av	Pulse program.
NS	16*n	For set-up the full phase cycle is not so critical.
D0	See text	Calculated in pulse program.
D1	5 * T <sub>1</sub>	Recycle delay, use dummy scans if shorter.
D6	See text	
D7	See text	
P1	1.5 μs	Excitation pulse at pl11.
P2	1.5 μs	Conversion pulse at pl11.
P3	20 μs	90° selective pulse at pl21 taken from previous pulse calibration.
PL1	=120 dB	Not used.
PL11	Start with ≈ 150 to 300 W	Power level for excitation and conversion pulses.
PL21		Power level for selective pulse, approx. pl11+30 dB taken from previous pulse calibration.

**Two Dimensional Data Acquisition****17.4.2**

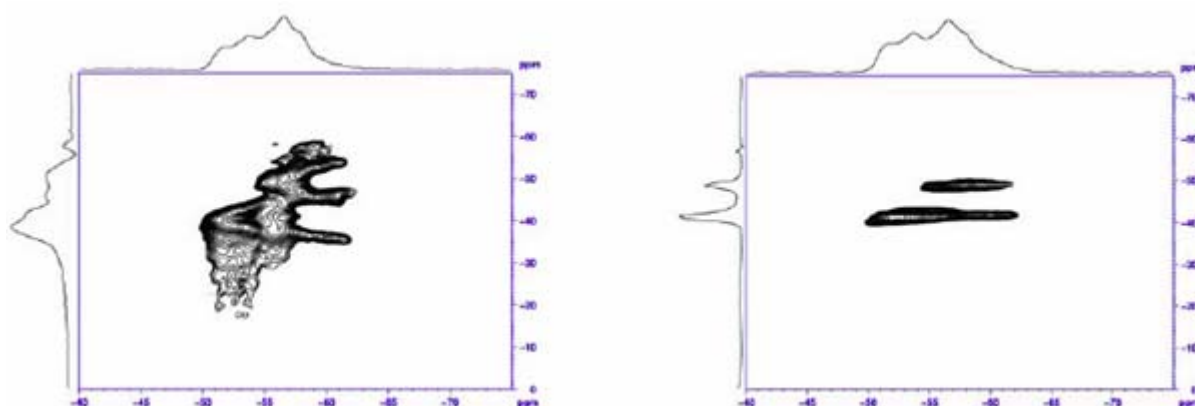
Once the pulses are calibrated the 2D data acquisition can be used to find the correct and precise magic angle setting. Create a new data set and change *parmode* to 2D. The acquisition parameters for the (new) indirect F1 dimension must be set according to [Table 17.5.](#)

Similar considerations for the maximum t<sub>1</sub> period, determined by the number of FID's to be acquired and the t<sub>1</sub> increment, can be made as for MQMAS. Because the shift range in ppm is twice as big as in 3QMAS a larger increment can be used to give an equivalent shift range, the increment being calculated from the spinning speed. Since the magic angle is probably not yet perfect 32 to 64 FID's will be sufficient initially. Processing parameters are described in the next section.

Table 17.5. F1 Parameters for the 2D Data Acquisition.

Parameter	Value	Comments
F1 parameters:		In <i>eda</i> .
FnMode	States-TPPI or States QF	2D acquisition mode for <i>stmasdqfz.av</i> . 2D acquisition mode for <i>stmasdqfe.av</i> .
TD	see text	Number of FID's to be acquired.
ND_010	1	There is only 1 D0 delay in the sequence.
SWH	"masr"	Equals spinning frequency for rotor synchronization, from this IN0 is calculated correctly, if ND_010 is already set.
NUC1		Select the same nucleus as for F2 so that transmitter frequency offset is correctly set (important for referencing).
Pulse program parameters:		In <i>ased</i> .
D6	0	Used in <i>stmasdqfe.av</i> only.
IN6	=IN0*8/9	Used in <i>stmasdqfe.av</i> for I = 3/2.
D7	0	Used in <i>stmasdqfe.av</i> only.
IN7	=IN0*7/24 =IN0*28/45 =IN0*72/55	Used in <i>stmasdqfe.av</i> for I = 5/2. Used for I = 7/2. Used for I = 9/2.

In **Figure 17.4**, two 2D plots of the  $^{87}\text{Rb}$  STMAS experiment on  $\text{RbNO}_3$  are compared. The spectrum on the left was obtained after the first execution of the experiment. The spectrum on the right was obtained after several iterations of resetting the angle and rerunning the spectrum. From this it is obvious that the spectrum of the sample for the setup must be known because otherwise it is impossible to judge whether a shoulder or a splitting is due to an incorrectly set angle or another signal from another site in the sample.

Figure 17.4.  $^{87}\text{Rb}$  STMAS Spectra of  $\text{RbNO}_3$ .

While the left spectrum has been obtained after adjusting the magic angle with KBr, the right spectrum can be obtained after several iterations of readjusting the angle and rerunning the 2Dspectrum.

## Data Processing

17.5

Processing parameters should be set according to the table below:

Table 17.6. Processing Parameters for the 2DFT

Parameter	Value	Comments
F2 (acquisition dimension)		
SI		Usually set to one times zero filling.
WDW	No	Don't use window function.
PH_mod	Pk	Apply phase correction.
BC_mod	No	No DC correction is required after full phase cycle.
ABSF1	1000 ppm	Should be outside the observed spectral width.
ABSF2	-1000 ppm	Should be outside the observed spectral width.
STSR	0	Avoid strip FT.
STS1	0	Avoid strip FT.
TDoff	0	Avoid left shifts or right shifts before FT.
F1 (indirect dimension)		
SI	256	Sufficient in most cases.
WDW	no	Don't use window function, unless F1 FID is truncated.
PH_mod	pk	Apply phase correction.
BC_mod	no	No DC correction is required after full phase cycle.
ABSF1	1000	Should be outside the observed spectral width.
ABSF2	-1000	Should be outside the observed spectral width.
STSR	0	Avoid strip FT.
STS1	0	Avoid strip FT.
TDoff	0	Avoid left shifts or right shifts before FT.

Data obtained with *stmasdqfe.av* can be processed with *xfb* only, if **IN6** or **IN7** have been set appropriately to run a split-t<sub>1</sub> experiment. Data acquired with the pulse program *stmasdqfz.av* should be processed with the AU program *xfshear*. For information about this program please refer to chapter 16. In an analogous way to MQMAS spectra the apparent Larmor frequency in the indirect dimension is recalculated by multiplying the real Larmor frequency with the corresponding value of |R-p|. The values for the different spin quantum numbers are summarized in **Table 17.7.**, for experiments using the inner ST ( $\pm 3/2 \leftrightarrow \pm 1/2$ ). R determines the shearing

ratio, i.e. the slope in a non-sheared spectrum,  $|R-p|$  is the scaling factor for referencing in the indirect dimension. Using this procedure the shift positions in the indirect dimension are identical (in ppm) to all MQMAS experiments, and the information obtained is the same. Refer to the chapter "[Basic MQ-MAS](#)" on page 151 for details about the information obtained from such spectra.

*Table 17.7. Values of R and |R-p| for the Various Spin Quantum Numbers Obtained in the ST-MAS Experiment*

Spin I	R	R-p  (p = ± 1)
3/2	-8/9	1.889
5/2	7/24	0.70833
7/2	28/45	0.3777
9/2	55/72	0.263111

# Double-CP

18

Double Cross Polarization (DCP) experiments use two consecutive cross polarization steps. Usually, the first step transfers from protons to one type of X-nucleus (to achieve high sensitivity), the second step transfers to a different (Y) nucleus in order to probe the dipolar coupling between X and Y. The sequence of transfers is in principle arbitrary, but usually sensitivity is an issue, so transfer from protons (to generate a large magnetization) and detection on the nucleus of higher sensitivity (to gain signal intensity) is the standard procedure. Detection of the most sensitive nucleus, protons, is also possible, but is difficult if the Homo-nuclear proton-proton dipolar coupling is strong (see "[CRAMPS: General" on page 207](#)).

In this chapter, the most popular double CP experiment is described. Here, the first CP step transfers magnetization from protons to  $^{15}\text{N}$ . Then, in a second cross polarization step, magnetization is transferred from  $^{15}\text{N}$  to  $^{13}\text{C}$ ; the signal is finally detected on  $^{13}\text{C}$  under suitable proton decoupling. The purpose of this experiment is to gain information about the C-N dipolar coupling which in turn provides special information.

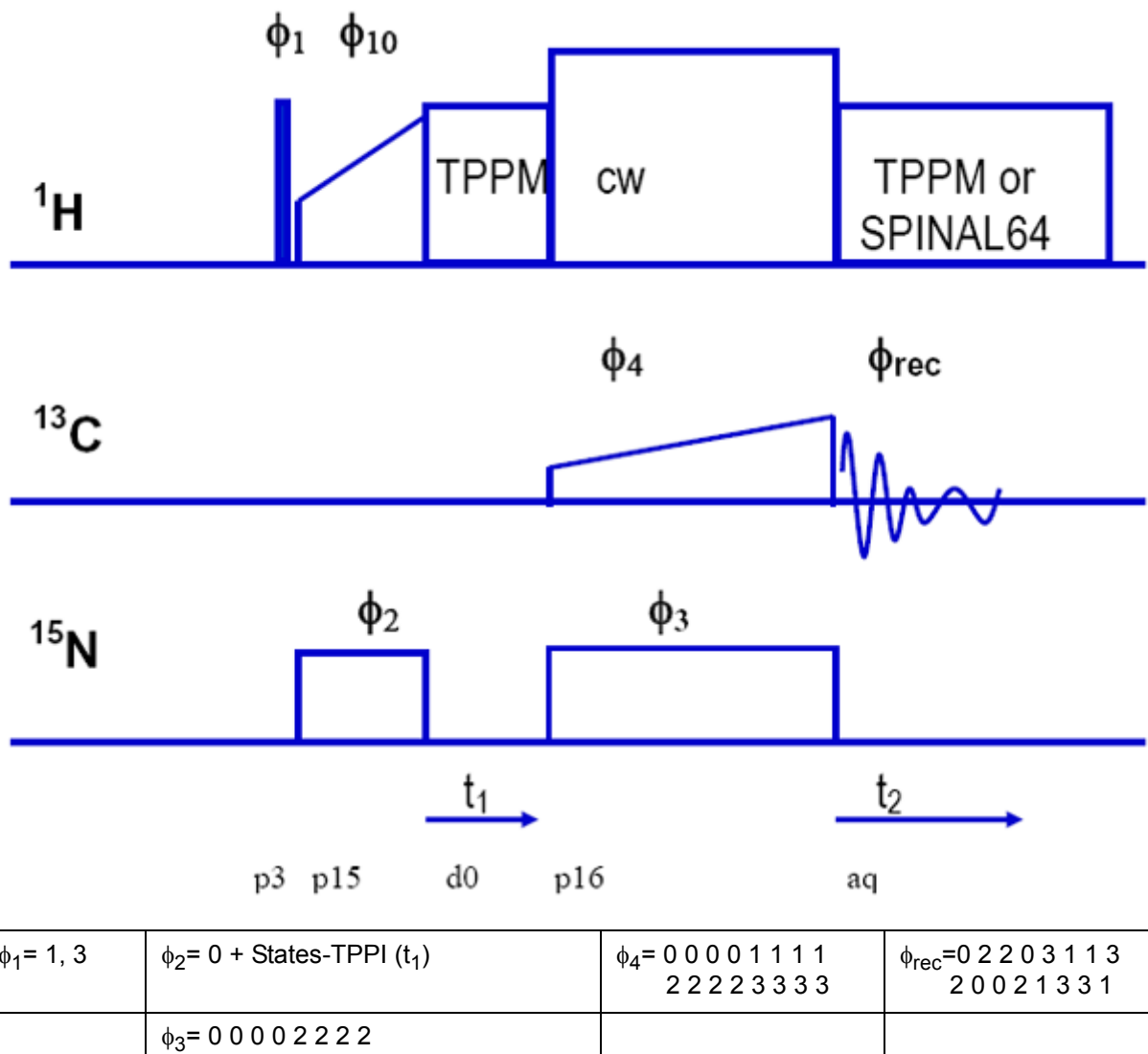
Naturally, the C-N-, or in general, the X-Y dipolar coupling is much smaller than any dipolar coupling involving protons. For C-N, it is <2.5 kHz. This has some experimental consequences:

1. There is no need to decouple  $^{15}\text{N}$  while observing  $^{13}\text{C}$ , since the coupling is spun out already at moderate spin rates.
2. The Hartmann-Hahn condition for this cross polarization is extremely sharp and must be adjusted very carefully for every spin rate.
3. The magnetization transfer is substantially slower than from protons, meaning that contact times are usually longer.
4. The transfer occurs (unlike CP from protons) not out of a bath of abundant spins, but behaves (especially at high spin rates) more like a transfer between spin pairs.
5. Labeled samples must be used so that an observable number of coupled spins is present.

Advanced experimental schemes use tangential pulses to provide adiabatic conditions during the cross polarization (S. Hediger et al.) or provide only selective polarization transfer, Specific CP (Baldus et al.).

## References:

- J. Schaefer, T.A. Skokut, E.O. Stejskal R.A. McKay, and J.E. Varner, Proc. Nat. Acad. Sci. USA **78**, 5978 (1981).
- J. Schaefer, E.O. Stejskal, J.R. Garbow, and R.A. McKay, Quantitative Determination of the Concentrations of  $^{13}\text{C}$ - $^{15}\text{N}$  Chemical Bonds by Double Cross-Polarization NMR, J. Magn. Reson. **59**, 150-156 (1984).
- M. Baldus, A.T. Petkova, J. Herzfeld, and R.G. Griffin, Cross Polarization in the tilted frame: assignment and spectral simplification in hetero-nuclear spin systems. Mol. Physics **5**, 1197-1207 (1998).

Figure 18.1. Pulse sequence diagram for 1D ( $t_1=0$ ) and 2D double CP experiments.

1. Prepare your probe for triple resonance applications H/C/N
2. Load a sample of glycine,  $^{15}\text{N}$  and  $\text{C}_1$ - $\text{C}_2$  (or only  $\text{C}_2$ )  $^{13}\text{C}$  labelled. Make sure the sample is  $\alpha$ -glycine, you will get nowhere with  $\gamma$ -glycine, since the proton  $T_{1\rho}$  is very short and CP just does not work with high efficiency. Rotate at 11 kHz. The sample may be fully labelled or diluted with natural abundance glycine. A restricted volume rotor is preferred. If a different spin rate is used, a different shape must be generated for the second CP step.

3. Check the **edasp** routing and set up 3 RF channels for C, H and N, such that the lower power amplifier (500W or less) is used for  $^{13}\text{C}$ . ( $^{15}\text{N}$  may require more than 500W). Set for  $^{13}\text{C}$  observation.
  4. Make sure the preamplifiers in use are set up for the appropriate frequencies. The following external RF filters are required: proton bandpass,  $^{13}\text{C}$  bandpass, and  $^{15}\text{N}$  low pass. The channel isolation required between X and Y (here  $^{13}\text{C}$  and  $^{15}\text{N}$ ) is usually sufficient with a bandpass on one of the channels, but a filter to remove the proton decoupling RF interference is required for X and Y. This means that one of the band pass filters on X or Y may be replaced by a proton reject, X low pass filter. If the channel isolation between X and Y is not adequate, the probe cannot be tuned.

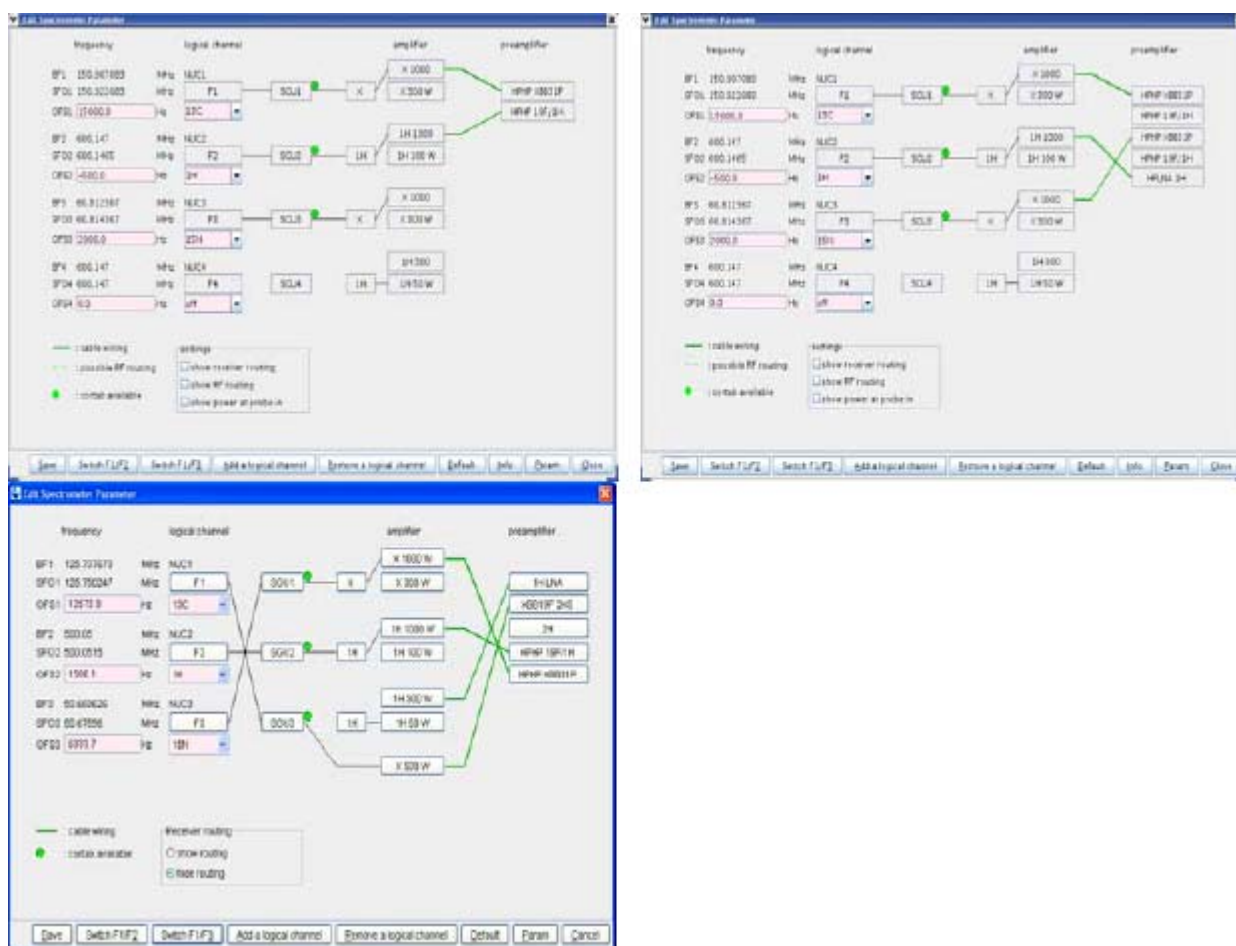


*Figure 18.2. The edasp routing tables for H-C-N double CP.*

Three examples are shown: Setup with only one X-HP-preamplifier (must be recabled for  $^{13}\text{C}$  and  $^{15}\text{N}$  setup), setup with 2 X-BB HP-preamplifiers and 2 HP transmitter, and setup with one HP transmitter and one 500W transmitter. The higher frequency nucleus is set for the lower power amplifier.

5. Set up for standard  $^{13}\text{C}$  CP operation in triple mode. Remember that a double tuned probe has better signal to noise and requires less power on X than a triple probe.
  6. Optimize decoupling and CP condition, run a reference  $^{13}\text{C}$  CP/MAS spectrum of the labelled glycine sample, using 16 scans. This reference spectrum will serve to measure the efficiency of the DCP magnetization transfer.

7. To set up the conditions for the N to C transfer, one must define the RF field at which the transfer is to take place, and find the appropriate power levels to achieve these RF fields. In order to minimize losses due to insufficient excitation bandwidths and  $T_{1p}$  relaxation, the contact should be executed at high power. However, there are limitations in terms of what the probe can take, and there are losses due to unwanted HH contact to the proton spin system. On the other hand, in many samples (bio-samples) the spread of chemical shifts that one wants to cover is not extremely wide or one even wants to execute the transfer selectively ("Specific-CP"). An RF field of 35 kHz is a decent compromise. So, using the **cp90** pulse program, and moving the carrier close to the  $C_\alpha$ -peak, determine a power level **p11** which corresponds to 35 kHz RF (7.14  $\mu$ sec 90 ° pulse). However, since the sample spins at 11 kHz, the HH condition will require 46 or 24 kHz on one nucleus and 35 kHz on the other nucleus. If you decide to account for the spin rate on the  $^{13}\text{C}$  side, calculate the required power levels for 24 and 46 kHz (= 35 kHz RF field +/- 11 kHz spin rate) RF field using **xau calcpowlev**. Now the  $^{13}\text{C}$  channel is set.

 **$^{15}\text{N}$  Channel Setup****18.2.2**

8. Create a new experiment using edc.
9. Setup the proper routing by going into **edasp**. Click the switch F1/F3 button to get  $^{15}\text{N}$  on channel 1.

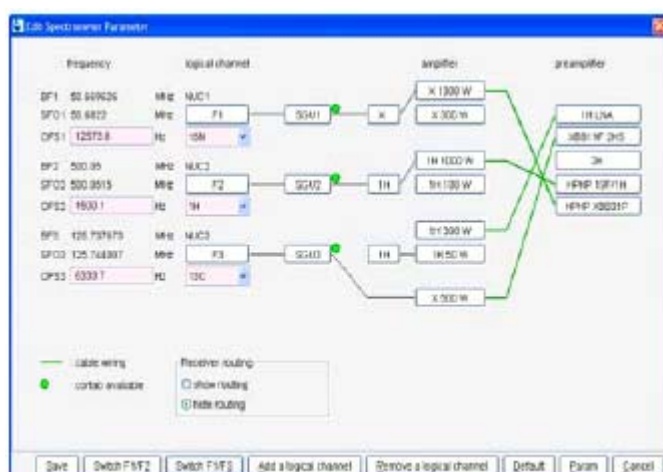


Figure 18.3. Routing table for triple resonance setup change for  $^{15}\text{N}$  pulse parameter measurement and CPMAS optimization.

10. If available, set **p11** and **sp0** for a proton/ $^{15}\text{N}$  HH condition in triple mode. On a labelled sample, even the previous settings for  $^{13}\text{C}$  should give a signal which allows optimizing the HH condition.
11. When the HH condition is optimized, find the power level to achieve a 35 kHz RF field (7.14  $\mu$ sec 90 ° pulse, carrier close to the  $^{15}\text{N}$ -resonance). It is essential to optimize the first proton to nitrogen HH contact. This is not as trivial as one might think, since the transfer efficiency depends strongly on the timing and RF fields of the HH match. The proton  $T_{1p}$  of the glycine NH<sub>2</sub> protons (from which the nitrogen is polarized) is fairly short, so the polarization transfer is not efficient. On a fully labelled sample, a maximum enhancement factor of 8.3 is possible (5 protons transfer to one nitrogen). Comparing the cross polarized  $^{15}\text{N}$  spectrum to the directly observed spectrum (using **hpdec** and 90 degree pulses at 4 sec repetition)

one can measure the enhancement factor rather easily. Without optimization, the enhancement factor may be as low a 5fold. It should be at least 6.5fold, more than 7.5fold is hard to achieve. To achieve a good result, the HH RF-fields should be set as high as possible with a contact time of 4 msec (higher proton RF fields yield a longer proton T1p and allow longer contact times). Of course, the RF field is limited by transmitter power and probe breakthrough limits. Note the optimum power levels (**sp0** and **p11**) and contact time (**p15**).

### Setup of the Double CP Experiment

### 18.2.3

1. Read the reference carbon data set and generate a new data set using **edc** or **iexpno**.
2. Select the pulse program **doubcp1d**. Set the optimum  $^{15}\text{N}$  cp parameters as found in the previous step (set **sp0**, **p15** and **p13** for proton to  $^{15}\text{N}$  cp). Set **o3** close to the  $^{15}\text{N}$  peak position.
3. Now we have to select the appropriate parameters for the nitrogen to carbon magnetization transfer. In the standard **doubcp1d** pulse program, **p16** is used as the second contact time, and shapes **sp1** and **sp2** are specified for the  $^{13}\text{C}$  and  $^{15}\text{N}$  contact, so **p16**, **p11** ( $^{13}\text{C}$  power level) and **p15** ( $^{15}\text{N}$  power level) are the relevant parameters. The C-N contact consists of a square pulse on one channel and a ramp or adiabatic shape on the other channel. Setting the square shape on the  $^{15}\text{N}$  channel is preferred if the transmitter for  $^{15}\text{N}$  does not have ample power and is operated close to the power limits.

Table 18.1. Recommended Parameters for the DCP Setup

Parameter	Value	Comments
Pulse program	doubcp1d	AVIII, Topspin 2.1 only, else use <b>doubcp</b> , <b>doubcp.av</b> .
NUC1	$^{13}\text{C}$	Nucleus on f1 channel.
O1P	100 ppm	$^{13}\text{C}$ offset.
NUC2	$^1\text{H}$	Nucleus on f2 channel.
O2P	2-4 ppm	$^1\text{H}$ offset, optimize.
NUC3	$^{15}\text{N}$	Nucleus on f3 channel.
O3P	$\approx$ 35 glycine $\approx$ 120 histidine $\approx$ 65 -130 protein	$^{15}\text{N}$ offset depending on sample.
PL1		Power level for f1 channel, NC contact pulse.
PL3		Power level for $^{15}\text{N}$ channel HN contact.
PL5		Power level for $^{15}\text{N}$ channel, NC contact pulse.
PL12		Power level decoupling f2 channel and excitation.
pl13		power level during second contact, cw dec.
cnst24		offset for cw decoupling during p16.
P3		Excitation pulse f2 channel.
PCPD2		Decoupler pulse length f2 channel ( $^1\text{H}$ ) TPPM.
P15	3-5 msec	Contact pulse – first contact.

Table 18.1. Recommended Parameters for the DCP Setup

P16	5-12 msec	Contact pulse – second contact f1 – f3 channel.
D1	5-10s histidine 4s $\alpha$ -glycine	Recycle delay.
SPNAM0		Ramp for 1 <sup>st</sup> CP step; e.g. ramp: 80 – 100%.
sp0		Power level for Ramp HN contact pulse 1H.
spnam1	ramp45-55, tcn5500, or square.100	Tangential contact pulse <b>tcn5500</b> on C, or square.
spnam2	square.100 or ramp45-55, tcn5500	Square on N, or ramp/tangential pulse.
CPDPRG2	SPINAL64	SPINAL64 decoupling.
NS	2,4 or 16	Number of scans.

4. Now we select the shape to use for the C-N contact. To find the HH contact more rapidly (it is a very narrow condition) it is recommended to start with a ramp shape. In order to find a HH condition independent of the type of shape, it is recommended to select shapes which are all centred around 50% amplitude, which allows arbitrary amplitude modulation without changing the HH condition. For a start, generate a ramp shape from 45 to 55% with 100 slices, using shape tool (**stdisp**). Store the ramp as ramp4555.100. Select this ramp as **spnam1** (or **spnam2**, if the shape should be executed on the Y channel).

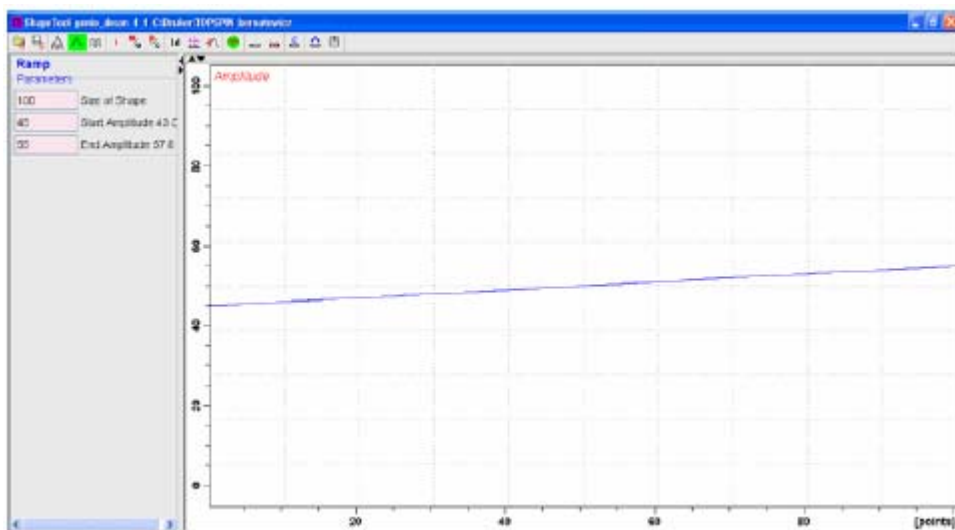


Figure 18.4. Shape Tool display with ramp shape from 45 to 55%.

The amplitude factor is 50%, corresponding to 50% RF field or a power level change of 6 dB, since the amplitude corresponds directly to the pulse voltage.

5. Since the shape is centred around 50%, the RF voltage here is down by a factor of 2 (= 6 dB in voltage), the power must be increased by 6 dB to get the same RF field as with a 100% square pulse.
6. Usually, the ramp shape is set on  $^{13}\text{C}$  (but it can also be used on  $^{15}\text{N}$ ). Set **spnam2** to **square.100**, **p15** to 46 or 24 kHz RF field on  $^{15}\text{N}$ . Set **spnam1** to **ramp4555.100**, **p1** to 35 kHz RF field on  $^{13}\text{C}$  - 6 dB. Set **p13=p12** for a start, set **p16** to 5 msec. Optimize the power level **p15**. A variation over -1 to +1 dB in steps of 0.2 dB should be ample. In order to be sure, one can optimize **p1** and **p15** as an array, **p1** in steps of 0.5 dB, **p15** in steps of 0.2 dB. Use a full phase cycle to avoid signal from a direct proton to carbon transfer (which is cancelled by the phase cycle). Optimize **p16** between 5 and 15 msec. See **fig. 6** for an optimization of **p15** ( $^{15}\text{N}$  square pulse power)
7. With a ramp shape for the N-C transfer, one should get 40-50% DCP efficiency (**fig.7**), compared to the reference direct  $^{13}\text{C}$  CP spectrum. If this cannot be achieved, even with careful HH matching, the following parameters should be checked:
8. Re-optimize **p16**, the optimum should be > 10 msec. If the signal gets worse with longer contact time, there is a loss due to direct  $^{13}\text{C}-^1\text{H}$  contact. Minimise this loss in the following way:
9. Never use a pulsed proton decoupling schemes during **p16**. Frequency shifted Lee-Goldburg decoupling is no alternative, since the signal will broaden and decay with shorter  $T_2$ . Use cw decoupling during **p16**, and carefully optimize the decoupling power (**p13**) for maximum signal. A slight offset may be set using **cnst24**.
10. Instead of a 45-55% ramp, a tangential amplitude modulation shape can be used. Since this shape provides 100% transfer efficiency on a spin pair system (compared to 50% of a standard rectangle or ramp shape), the DCP efficiency can be increased. With such a shape, one can get 50-70% DCP efficiency. To generate such a shape in **stdisp**, select TanAmp-Mod as a shape model, select solids notation, select 1000 points, set the spin rate to half the actual spin rate (5500), set the RF field to the actual RF field used on this channel, select 400 for the dipolar coupling, and 50% for the scaling factor. Save the shape as tcn5500 (if not already available), and select this name for **spnam1** (or **spnam2**). The efficiency should be noticeably better. Re-optimize the first HH contact, decoupling and **p16**. More than 50% should definitely be obtained.

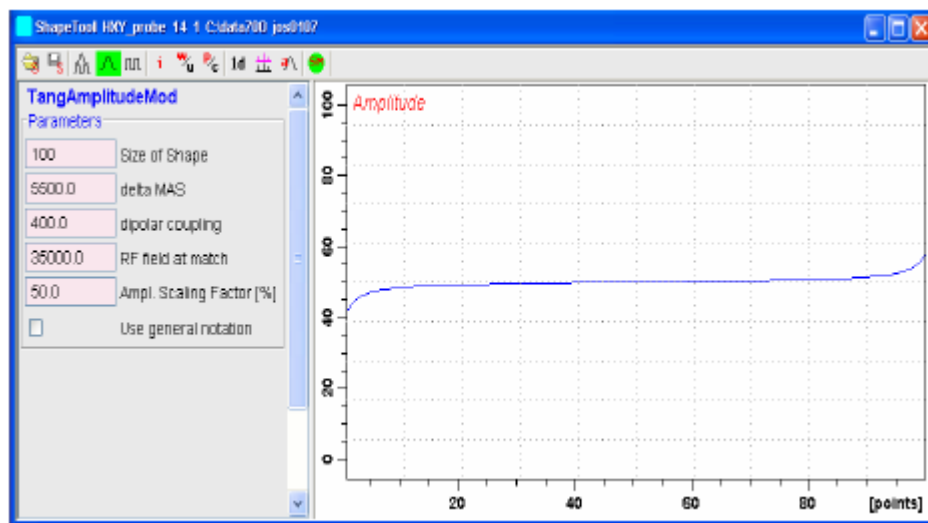


Figure 18.5. Shape Tool display with a tangential shape for adiabatic cross polarization.

The amplitude factor is 50%, corresponding to 50% RF field or a power level change of +6 dB, since the amplitude corresponds directly to pulse voltage.

11. Optimize the DCP condition on the rectangular pulse, using 0.1 dB steps over a range of +/- 1 dB around the optimum found with the ramp.

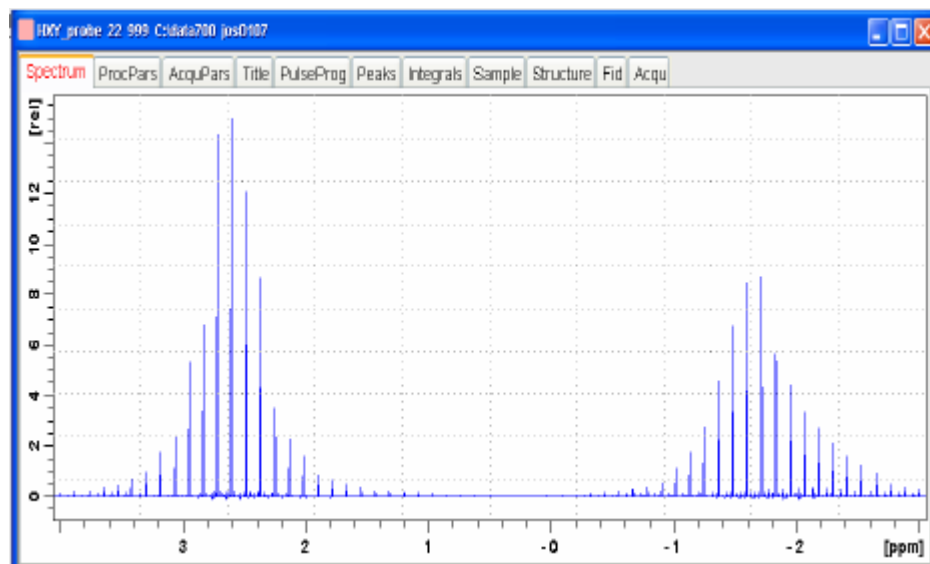
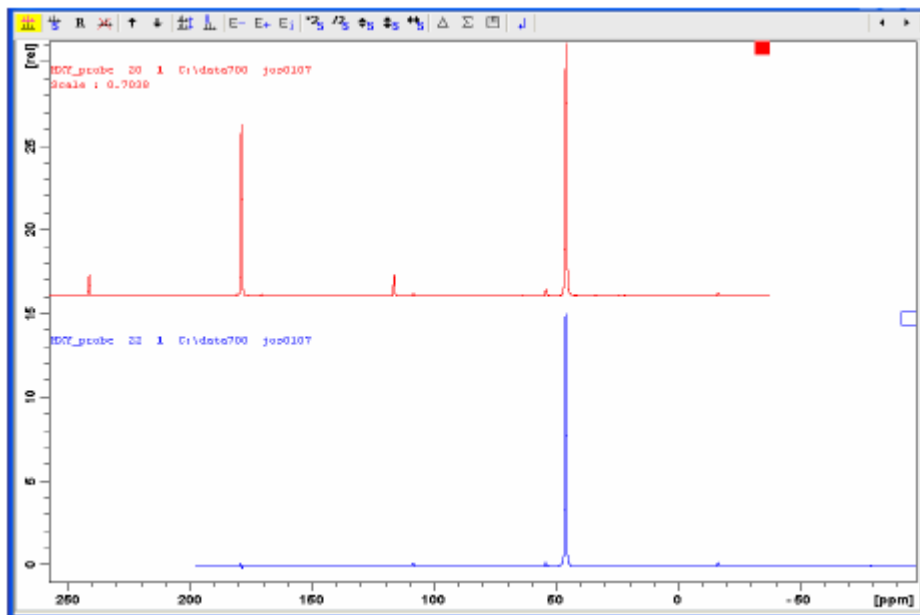


Figure 18.6. Double CP optimization of PL5 in increments of 0.1 dB.

Note how narrow the optimum DCP conditions are. However, with diligent preparation, one should be very close to the optimum with the first try.

12. Run an experiment with 16 scans and compare the signal amplitude with the signal intensity of the  $^{13}\text{C}$  CPMAS experiment with the same number of scans, using dual display. The intensity ratio of the aliphatic resonance of the CPMAS compared to the one obtained with the DCP experiment gives the DCP yield, see [Figure 18.7](#).



*Figure 18.7. Double CP yield, measured by comparing CPMAS and DCP amplitudes of the high field resonance.*

*Note that the C<sub>1</sub> carbon receives very little magnetization under these conditions, the transfer is rather selective.*

The setup for DCP can be rather much sped up and simplified by a python program named `dcpset.py`. This program will ask for the 90° pulse widths and associated power levels and for the spin rate and calculate the appropriate power levels for the HH condition for all pulses except for the proton channel.

Contact [solids@bruker.de](mailto:solids@bruker.de) to receive this python program and some instructions for use. This program serves as an example on how the experiment setup can be controlled by the high level script language.

#### Setup of the 2D Double CP Experiment

#### 18.2.4

1. Load a suitable sample, spin it up, set the desired temperature and match and tune the probe. As a simple setup sample, full <sup>13</sup>C, <sup>15</sup>N-histidine may be used (**d1**=10s, 2-4 scans, **p15**=1msec, **p16**=3msec). A labeled oligopeptide or small protein will of course provide a more interesting spectrum. With proteins, good results should only be expected if the preparation is micro-crystalline. In such a case, water, salt and cryo-protectant (glycol, glycerol) will very likely be present. This means that the probe proton channel will be detuned to lower frequency, and tuning may be difficult, if not impossible at high proton frequencies and salt contents. In such cases, E<sup>free</sup> probes are recommended.
2. Run standard 1D cp <sup>13</sup>C and <sup>15</sup>N experiments; determine the required offsets for all frequencies and the required sampling windows.
3. Re-optimize the H-N and N-C HH conditions.
4. Generate a new data set and switch to 2D data mode, using the “123”-icon in **eda**.
5. In **eda**, set the pulse program to **doubcp2d**. Set FnMode as desired, usually STATES-TP-PI.

6. Make sure the correct nucleus ( $^{15}\text{N}$ ) is selected in the F1 dimension.
7. Set the sampling windows for both dimensions from the previously acquired 1D spectra.
8. Both acquisition times in F2 and F1 should be considered with care, since the decoupler is on at high power during both periods. Especially for biological samples, where the RF heating may be high and the samples are temperature sensitive, it is essential not to use overly long acquisition times and high duty cycles. Remember that the heating effect is generated inside the sample where the temperature increases within milliseconds, whereas cooling requires transfer of the energy to the outside of the spinner, which takes seconds! E<sup>free</sup> probes eliminate these problems to a large extent.
9. The basic double-CP experiment can be extended into many different variations. One example is the double transfer N-C <sub>$\alpha$</sub> -C <sub>$\beta$</sub> , where the second transfer step is made selective so only  $\alpha$ -carbons are polarized from the nitrogen, then magnetization is transferred from the  $\alpha$ -carbons to the adjacent  $\beta$ -carbons. This can be done by a simple PDSD or DARR proton spin diffusion step, or by a  $^{13}\text{C}$ - $^{13}\text{C}$  Homo-nuclear recoupling step (HORROR, DREAM, or other). Likewise, the N-C <sub>$\alpha$</sub> -C<sub>X</sub> experiment transfers from the  $\alpha$ -carbons to all (X) carbons which are in close enough proximity to the  $\alpha$ -carbons. Check with your applications support for appropriate pulse programs.

**2D Data Acquisition****18.3**

**Sample:**  $^{15}\text{N}$ ,  $^{13}\text{C}$ -labeled histidine, peptide or protein.

**Spinning speed:** 10 – 15 kHz, depending on  $^{13}\text{C}$  spectral parameters (rotational resonance must be avoided)

**Experiment time:** 30 min. – several hours

**Acquisition Parameters:**

Table 18.2. Recommended Parameters for the DCP 2D Setup

Parameter	Value	Comments
Pulse program	doubcp2d	Pulse program.
NUC1	$^{13}\text{C}$	Nucleus on f1 channel.
O1P	100 ppm	$^{13}\text{C}$ offset.
NUC2	$^1\text{H}$	Nucleus on f2 channel.
O2P	2-4 ppm	$^1\text{H}$ offset, optimize.
NUC3	$^{15}\text{N}$	Nucleus on f3 channel .
O3P	65 – 150 ppm	$^{15}\text{N}$ offset depending on sample.
PL1		Power level for f1 channel, NC contact pulse.
PL3		Power level for $^{15}\text{N}$ channel HN contact.
PL5		Power level for $^{15}\text{N}$ channel, NC contact pulse.
PL12		Power level decoupling f2 channel and excitation.
P3		Excitation pulse f2 channel.

*Table 18.2. Recommended Parameters for the DCP 2D Setup*

PCPD2		Decoupler pulse length f2 channel ( $^1\text{H}$ ) TPPM.
P15	1-5 msec	First contact, optimize on $^{15}\text{N}$ cp spectrum.
P16	3-10 msec	Second contact f1 – f3 channel, optimize on 1D dcp spectrum.
D1	5-10s for histidine	Recycle delay, optimize on 1d.
SPNAM0		Ramp for 1 <sup>st</sup> CP step; e.g. ramp: 80 – 100%.
SP0		Power level for Ramp HN contact pulse 1H.
SPNAM1	tcn5500	Tangential or ramp contact pulse.
spnam2	square.100	Shape on $^{15}\text{N}$ channel.
CPDPRG2	SPINAL64	SPINAL64 decoupling.
NS	2 or 16	Number of scans.
F2 direct $^{13}\text{C}$		(left column)
TD	2k	Number of complex points.
SW	$\approx$ 200 ppm	Sweep width direct dimension, adjust to experimental requirements.
F1 indirect $^{15}\text{N}$		(right column)
TD	128-.512	Number of real points.
SW	$\approx$ 100-150ppm	Sweep width indirect dimension.

***Spectral Processing*****18.4****Processing parameters***Table 18.3. Recommended Processing Parameters for the DCP 2D*

Parameter	Value	Comment
F1 acquisition $^{13}\text{C}$		(left column)
SI	2-4k	FT-size.
WDW	QSINE	Squared sine bell.
SSB	2-5	Shifted square sine bell, >2: res. enhancement.
PH_mod	pk	Phase correction if needed.
F2 indirect $^{15}\text{N}$		(right column)
SI	512-1024	Zero fill.
MC2	STATES-TPPI	
WDW	QSINE	Squared sine bell.
SSB	2-5	

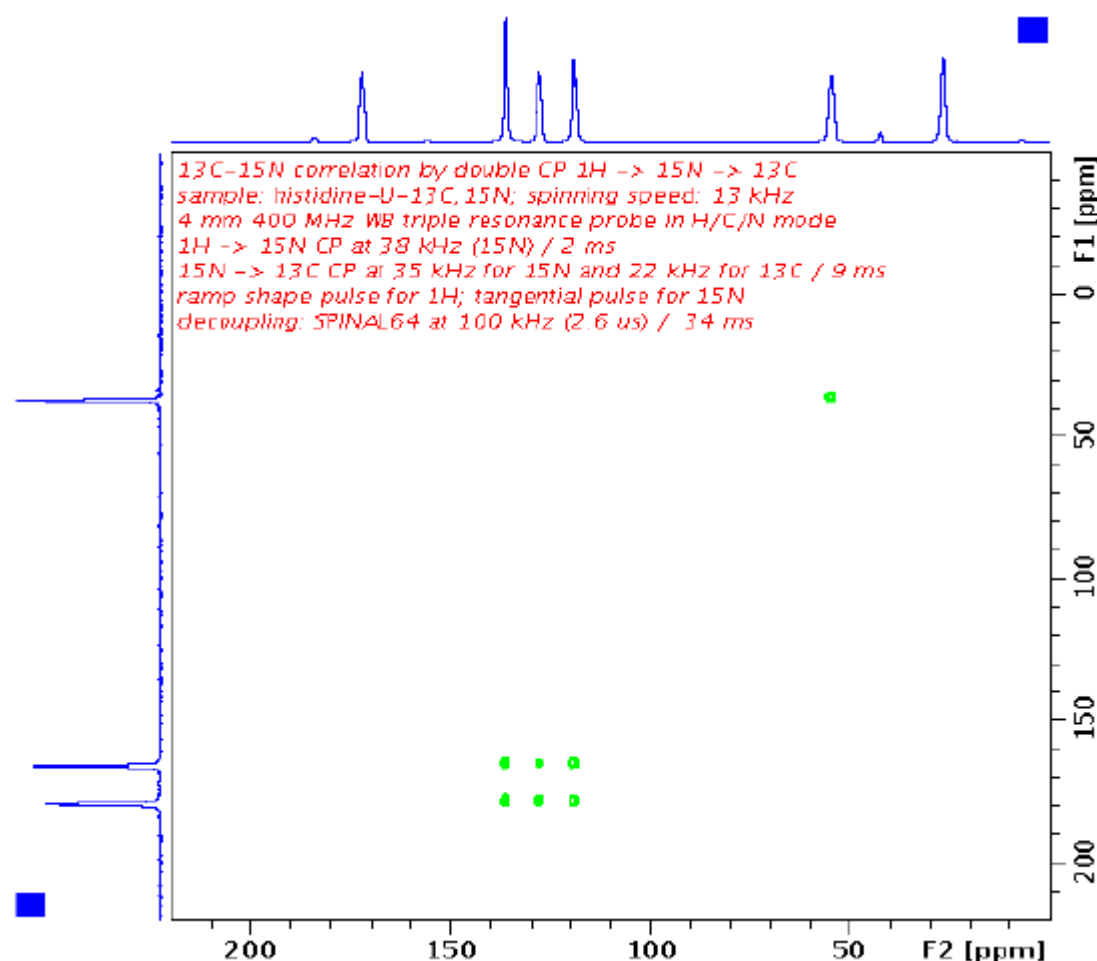


Figure 18.8. C-N correlation via Double CP in histidine (simple setup sample). 4mm Triple H/C/N Probe.

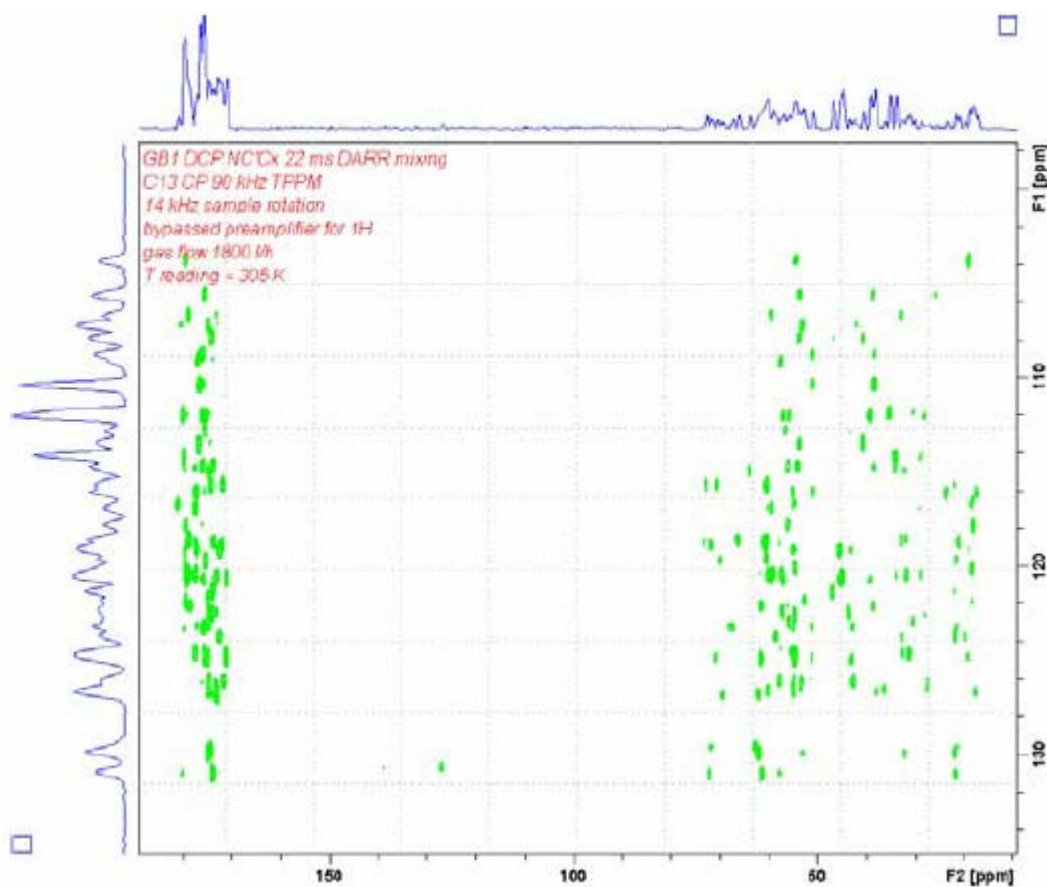


Figure 18.9.  $NC_\alpha C_x$  correlation experiment with 22 ms DARR mixing period for  $C_\alpha$ - $C_x$  spin diffusion on GB1 protein run using an  $E^{\text{FREE}}$ -Probe.

DARR transfer from  $C_\alpha$  to  $C_\beta$  or  $C_x$  generates positive cross peaks, HORROR or DREAM transfer generates negative cross peaks. See the chapter on spin diffusion experiments for more information about DARR or PDSD.

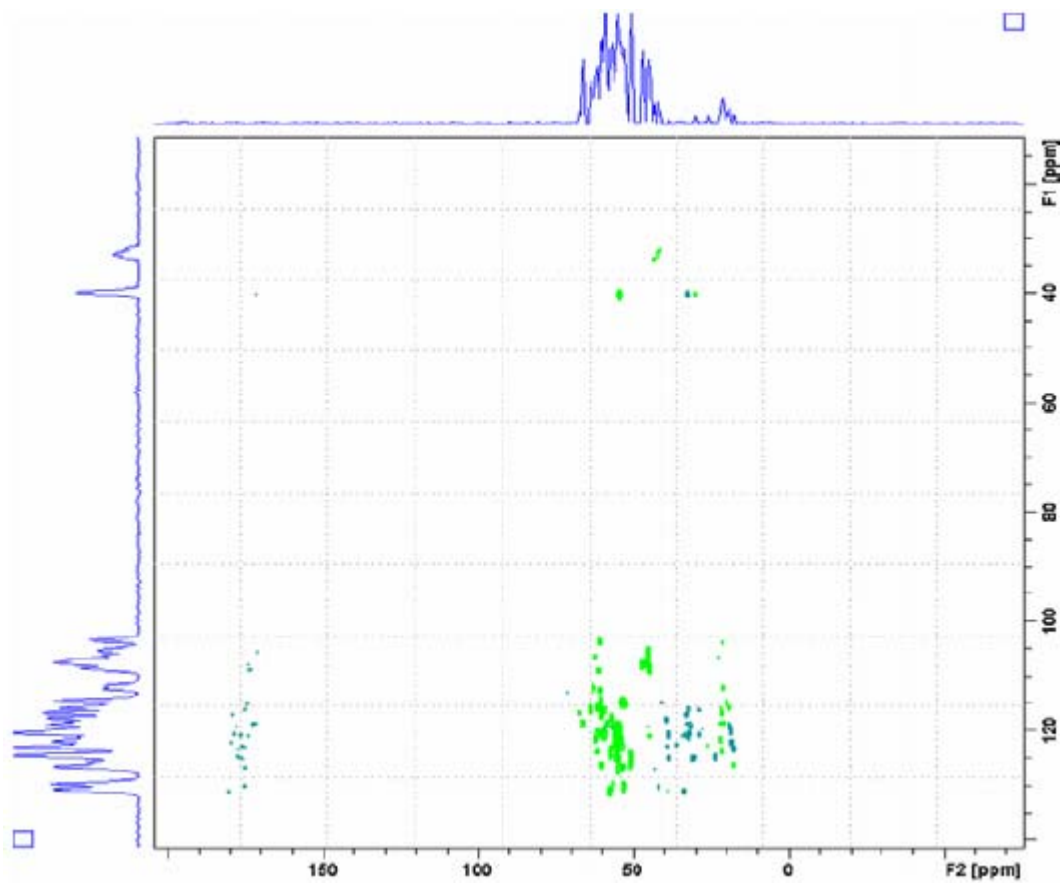


Figure 18.10. $^{13}\text{C}_a\text{C}_x$  correlation experiment with 4.2 ms SPC5-DQ mixing period for  $\text{C}_a\text{C}_x$  spin diffusion on GB1 protein run using an  $E^{\text{FREE}}$ -Probe at 14 kHz sample rotation and 100 kHz decoupling.

See the chapter on recoupling experiments for the SPC5 setup and for more information about DQ recoupling sequences. Note the inverse phase of the cross peaks generated by the DQ-mixing step.

# CRAMPS: General

19

CRAMPS is an acronym standing for “Combined Rotation And Multiple Pulse NMR Spectroscopy”. Multiple Pulse Spectroscopy had long been thought not to work under spinning around the magic angle, but in fact it does work, as long as the pulse cycle times are substantially shorter than the rotation period.

CRAMPS suppresses Homo-nuclear dipolar interactions between the abundant spins (mostly protons) and chemical shift anisotropy simultaneously through the combination of multiple pulse techniques and magic angle spinning. J-couplings and large hetero-nuclear dipolar couplings are not suppressed.

## Reference:

L.M. Ryan, R.E.Taylor, A. J. Patt, and B. C. Gerstein, *An experimental study of resolution of proton chemical shifts in solids: Combined multiple pulse NMR and magic-angle spinning*, J. Chem. Phys. 72 vol.1, (1980).

## Homo-nuclear Dipolar Interactions

19.1

Homo-nuclear dipolar interactions among spins with a strong magnetic moment and high natural abundance - mainly  $^1\text{H}$  or  $^{19}\text{F}$ , and to a much smaller extent  $^{31}\text{P}$  - are usually very large unless averaged by high mobility. Especially in the case of protons, spin exchange is usually rapid compared to routinely achievable rotation periods, meaning that MAS alone cannot suppress the Homo-nuclear dipolar broadening. Even spin rates in the order of 70 kHz, which is no longer a mechanical problem, cannot fully average this interaction in rigid solids. As chemical shift differences among the coupled nuclei become larger, the interaction becomes more heterogeneous and MAS can suppress it more efficiently. This is the reason why fast spinning alone works much better on  $^{19}\text{F}$  or  $^{31}\text{P}$  than on protons. hetero-nuclear dipolar coupling, such as between  $^{13}\text{C}$  and  $^1\text{H}$ , can in principle be spun out, but only if the Homo-nuclear coupling between protons is small, or averaged by motion or a suitable pulse sequence. CRAMPS sequences therefore play an important role also in experiments where X-nuclei are observed.

## Multiple Pulse Sequences

19.2

Dealing with a hetero-nuclear dipolar coupling is easy: continuous high power irradiation of one coupling partner will decouple it from the other nucleus, as in the case of  $^{13}\text{C}$  observation while decoupling protons. However observing a nucleus while decoupling it from like spins at the same time is obviously not trivial, since the signal cannot be observed under the much higher decoupling RF. Observation of the signal and decoupling pulses must therefore be alternately applied. Suppression of a Homo-nuclear dipolar interaction occurs when the magnetization vector of the coupled spins is rotated around the magic angle. This condition can be achieved either by  $4 \pi/2$  pulses of suitable phase and spacing (multiple-pulse methods), or by off-resonance irradiation of suitable offset and RF-field (Lee-Goldburg). To observe the signal, a gap within the pulse sequence must be supplied, which is long enough to observe one or several data points while the magnetization vector points along the magic angle. This condition obviously persists only for a time period short compared to the transverse relaxation of the signal.

To observe the time dependence of the signal, the sequence must be repeated and more data points accumulated until the signal has decayed under the influence of residual broadening. Obvious problems of this experiment are the requirement to observe a relatively weak signal shortly after a strong pulse (dead time problem) and the requirement to time the sequence in such a way that the magnetization vector is accurately aligned with the magic angle (requires precise pulse lengths and phases, and it requires RF fields strong compared to the interaction and shift distribution). Many sequences have been devised after the original WHH-4 (or WaHu-Ha) sequence which yield better results due to better error compensation (MREV-8, BR-24, C-24, TREV-8, MSHOT). Modern hardware has made the setup and application of these sequences a lot easier since pulse phase and amplitude errors are negligible, higher magnetic fields have led to better chemical shift dispersion and also to shorter dead times. The resolution achieved with long, highly compensated sequences like BR-24 is very good, but their applicability at limited spin rates (because of the need for the cycle time to be short with respect to the rotor period) often presents a problem.

### References:

- S. Hafner and H.W. Spiess, *Multiple-Pulse Line Narrowing under Fast Magic-Angle Spinning*, J. Magn. Reson. A 121, 160-166 (1996) and references therein.  
M. Hohwy, J. T. Rasmussen, P. V. Bower, H. J. Jakobsen, and N. C. Nielsen. *<sup>1</sup>H Chemical Shielding Anisotropies from Polycrystalline Powders Using MSHOT-3 Based CRAMPS*, J. Magn. Res. 133 (2), 374 (1998), and references cited therein.

## W-PMLG and DUMBO

## 19.3

W-PMLG and DUMBO are shorter sequences which avoid turning high power pulses rapidly on and off, which is what most multiple pulse sequences do. This avoids undesired phase glitches. Also, they use higher duty cycles during the decoupling period. As a result, the sequences are simpler and shorter, requiring fewer adjustments and allowing higher spin rates.

Both sequences use repetitive shaped pulses with detection in between. PMLG uses the principle of a *Frequency Switched Lee Goldburg* (FSLG) sequence (continuous irradiation with a net RF field along the magic angle), where the frequency shifts are replaced by a phase modulation. DUMBO basically works like a windowless MREV-type pulse sequence where the individual pulses are replaced by a single pulse with phase modulation.

### References:

- E. Vinogradow, P.K. Madhu, and S. Vega, High-resolution proton solid-state NMR spectroscopy by phase-modulated Lee-Goldburg experiment, Chem. Phys. Lett. 314, 443-450 (1999).  
D. Sakellariou, A. Lesage, P. Hodgkinson and L. Emsley, *Homo-nuclear dipolar decoupling in solid-state NMR using continuous phase modulation*, Chem. Phys. Lett. 319, 253 (2000).

## Quadrature Detection and Chemical Shift Scaling

## 19.4

Under Homo-nuclear decoupling, the magnetization precesses in the transverse plane of a tilted rotating frame whose new z-axis is along the direction of the effective field. The projection of this plane into the X-Y plane is therefore an ellipse, and the signal intensities sampled in the two quadrature channels along the x and y direction are different, since these are the major and the minor axes of the projected ellipse. As can be seen from fig. 1, the X and Y observe direction will see a signal of different amplitude. This means that quadrature images will always be present, if quad detection is used. In the case of single detection, the signal may be smaller or larger depending on the receiver phase. The standard procedure is to use quad detection and suppress the quad images by a suitable phase cycling scheme. This is however not as

straightforward as it is with standard excitation/observation. The quad phase cycling must occur in the precession plane, so a prepulse is required to tilt the initial magnetization into the direction of the precession axis. Usually, a combination of 2 pulses is used for initial excitation ( $90^\circ_{x,y,-x,-y} + (90^\circ - 55^\circ)$  adjust).

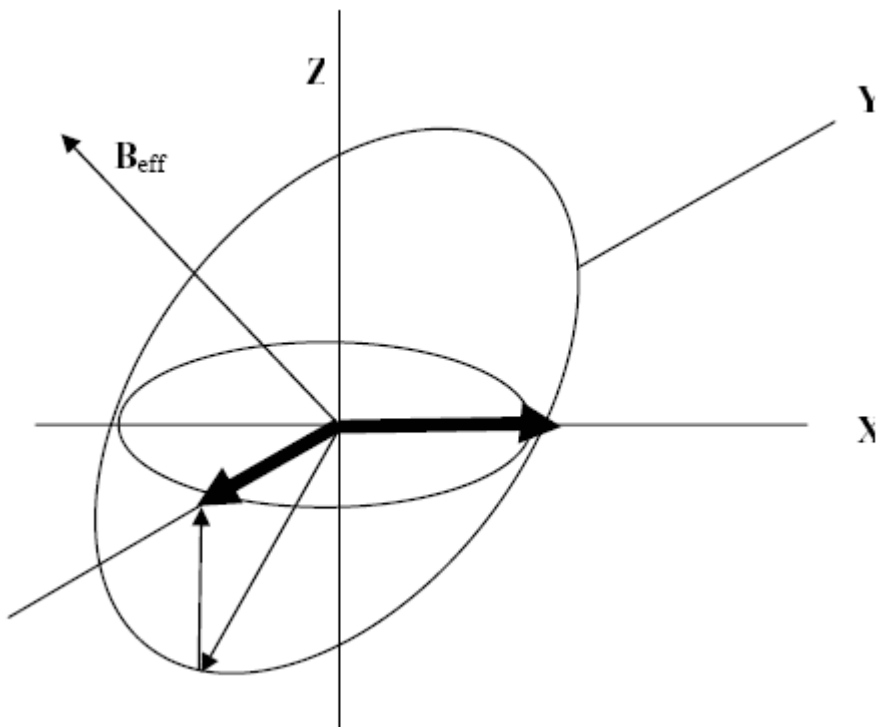


*Figure 19.1. Difference in Amplitude of the Quadrature Channels X and Y*

The difference in amplitude of the quadrature channels X and Y, caused by the tilted precession plane. Along X, the full amplitude is observed, along Y only the component in the XY-plane is detected.

As the spins precess around a tilted effective field and not only around the direction of the external field, the precession frequencies are changed, which means that the observed chemical shifts are changed. As the frequencies are always smaller than in the standard excitation/observation scheme, the chemical shift range appears scaled down. The scaling factor depends on the pulse sequence used. To achieve a spectrum comparable to spectra acquired conventionally, the shift range must be scaled up again by this scaling factor, i.e. the spectral window given by the repetition rate of the pulse sequence must be multiplied by this scaling factor in order to place the resonances correctly. This scaling factor can be calculated from the tilt angle, but is also slightly dependant on the offset and RF-field. Since the correct chemical shifts are usually unknown, one must be aware of the fact that the shifts may not be as precise as they are in high resolution liquids experiments. An example of shift calibration, taking the scaling factor into account, will be given in the practical chapter.



# CRAMPS 1D

# 20

As outlined above, many sequences are available to achieve Homo-nuclear dipolar decoupling. We want to concentrate on those that allow fast spin rates and are easy to set up. The performance of DUMBO and W-PMLG is very similar. The pulse sequence is also very similar on AV3 instruments, just different shapes and different timings are loaded.

## Pulse Sequence Diagram of W-PMLG or DUMBO

20.1

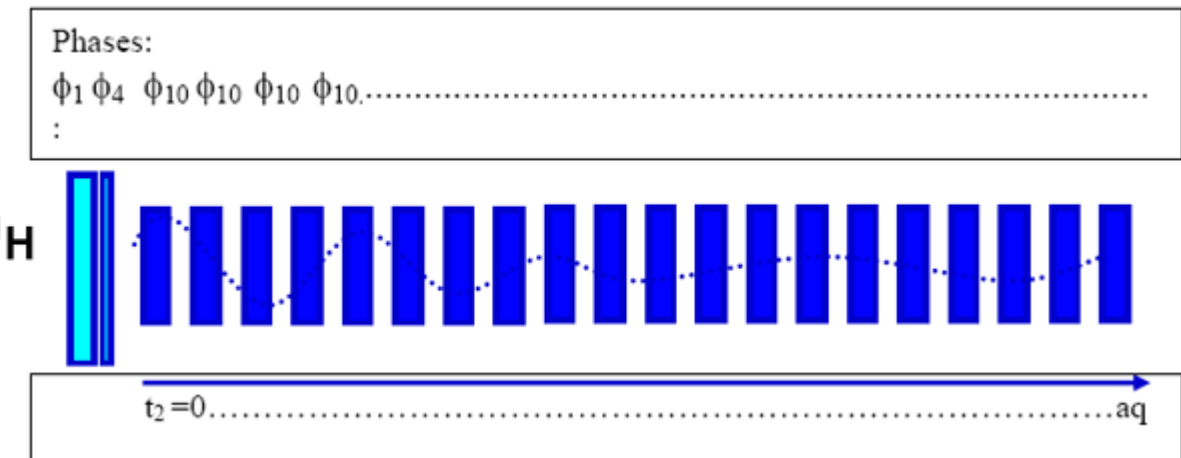


Figure 20.1. Pulse Sequence Diagram

Table 20.1. Phases, RF-Levels, Timings

Phases	RF Power Levels	Timing
$\phi_1$ = CYCLOPS, 1 2 3 0	p12=set for around 100 kHz	p1 around 2.5 $\mu$ sec.
$\phi_4$ = 0 +cnst25, adjust	ditto.	p4 about 45 degrees, adjust.
$\phi_{10}$ = 0	sp1: set for 100-130 kHz	WPMLG: p5, 1.2-1.5 $\mu$ sec or calculated from cnst20=RF field DUMBO: p10 set by xau dumbo.
$\phi_{31}$ = CYCLOPS, 0 1 2 3		

Both shapes are purely phase modulated pulses, their amplitudes are constant throughout. The PMLG shape is a standard shape delivered with the software (**wpmig1**, **m5m**, **m5p**). DUMBO shapes are generated using the standard AU-program dumbo. Calling dumbo with **xau dumbo** will ask for the slice length of the shape (usually 1  $\mu$ sec), the number of slices (usually 32), generate the shape and load the name of this shape into the current parameter set, it will also set the length of the shaped pulse, **p10**, to 32  $\mu$ sec. N.B.: at magnetic fields higher than 500 MHz, it is recommended to replace the standard 32  $\mu$ sec timing by 24  $\mu$ sec timing and increasing the power level accordingly, since this has been found to give better results.

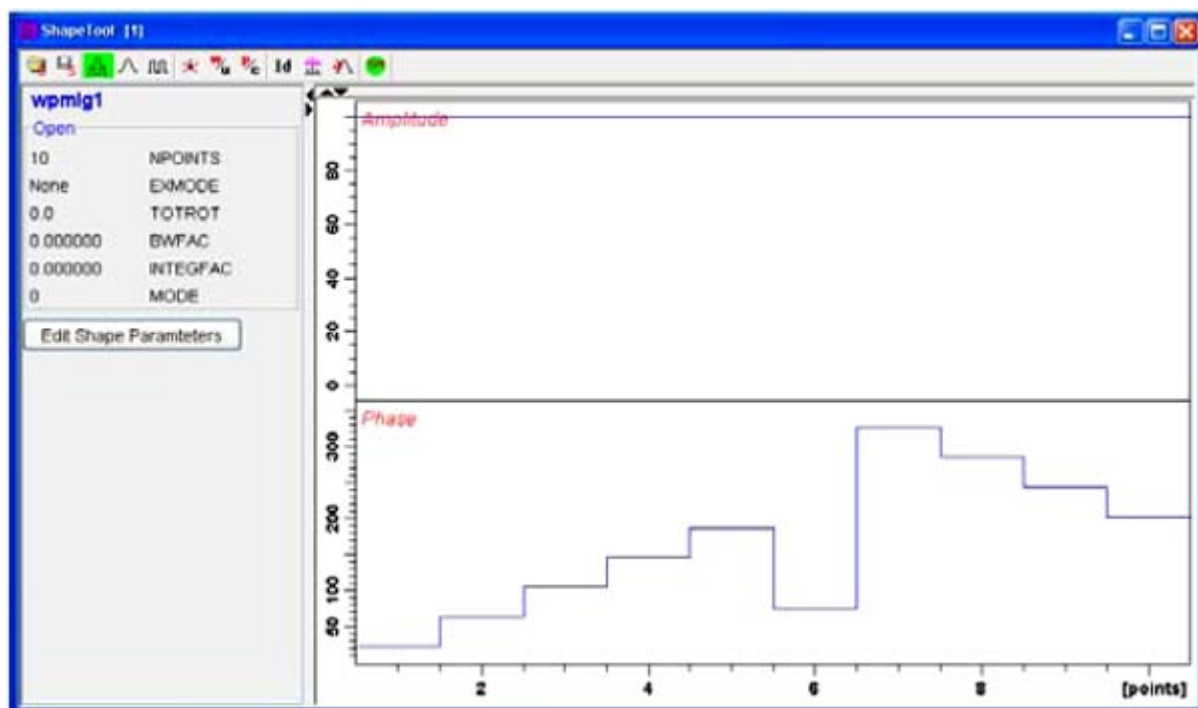


Figure 20.2. PMLG Shape for *wpmig*, *sp1*

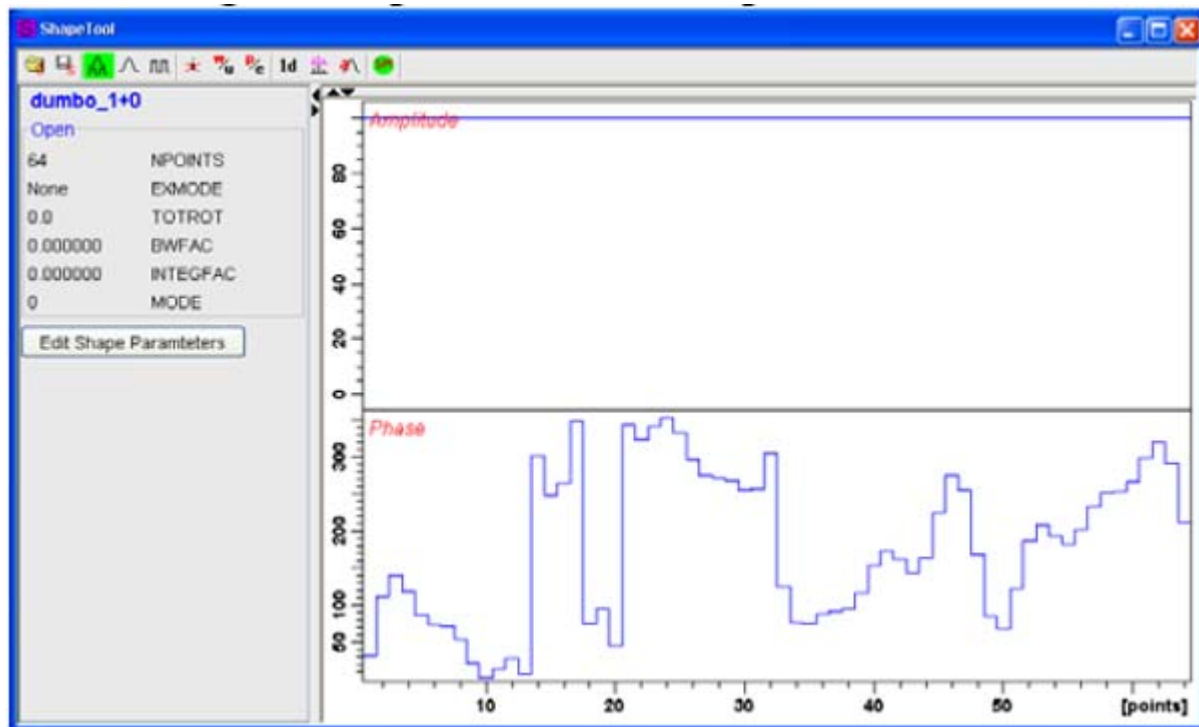


Figure 20.3. Shape for DUMBO, sp1

### Analog and Digital Sampling Modi

### 20.3

AV3 instruments allow different acquisition modi, one which resembles the previous mode of analogue filtering in so far as the down-conversion is done without simultaneous digital filtering, whereas the digital mode always down converts and filters simultaneously. Remember that at a standard sampling rate of 20 MHz (the fixed sampling rate of the DRU) down-conversion must be done to obtain data sets of reasonable sizes. The pulse programs dumboa and wpmlga are written for the pseudo analog mode without digital filtering, **dumbod** and **wpmldg** are written for the digitally filtered mode.

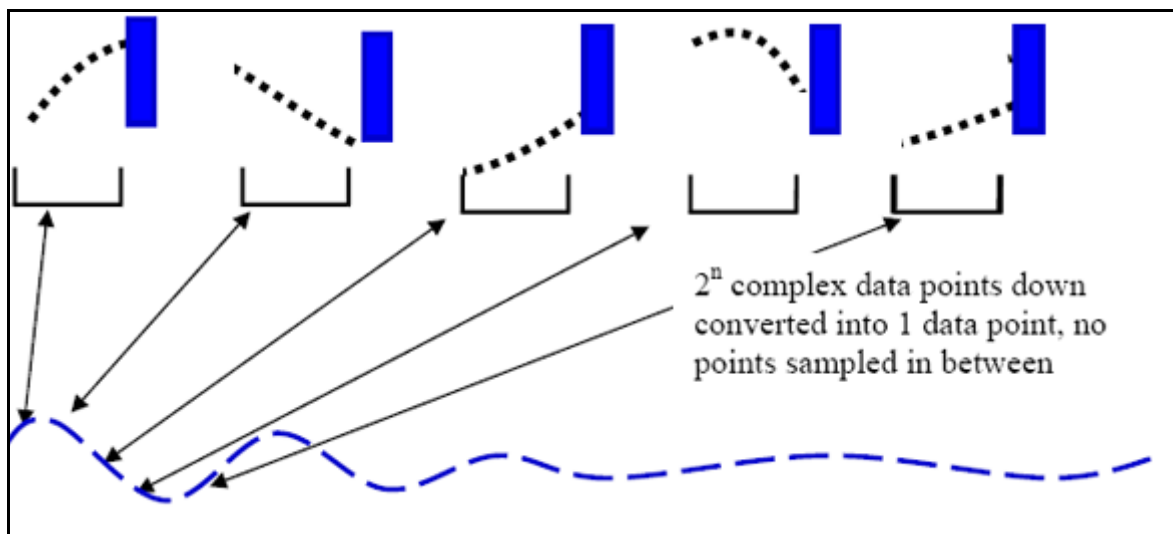


Figure 20.4. Analog Sampling Scheme

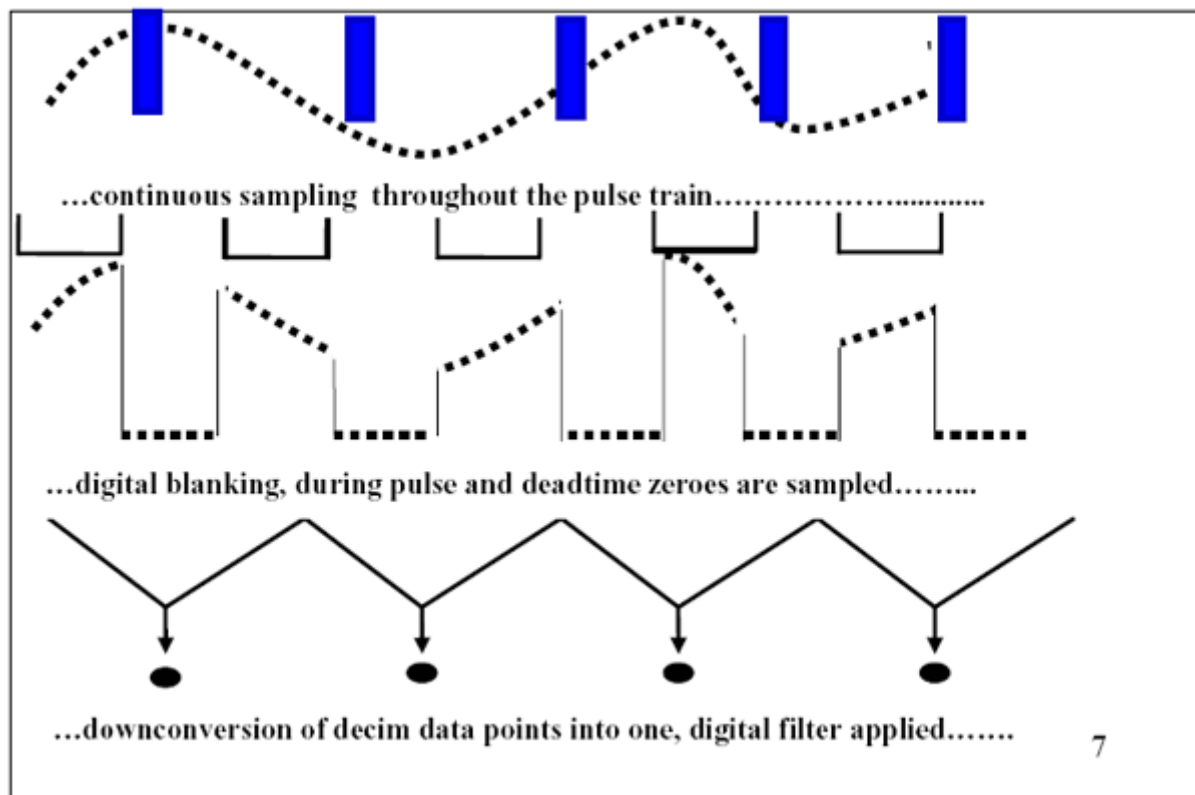


Figure 20.5. Digital Sampling Scheme

At frequencies of 400 MHz and higher, double or triple resonance CP-MAS probes may be used on the proton channel, at lower fields a CRAMPS probe is required due to the increased ring down time at lower field. Spinner diameters of 4mm or smaller are preferred, since we want to spin over 10 kHz. Since only one nucleus is observed, no filters are required and should be avoided. Good impedance matching between probe and transmitter is important in order to optimise the effect of the pulses on the spins. If the RF cable has been too strongly bent or the connectors been twisted, the cable may not have 50 Ohms and the result will always be bad. Likewise, if the preamp is burnt, it is not possible to get good results.

The fewer connectors are between probe and preamp, the better you can expect the 50 Ohm match to be. In **edasp**, set F1 for  $^1\text{H}$ -observation, select the high power proton amplifier and high power preamplifier. Tune and match as usual. It is assumed that the magic angle is precisely set, which can easily be achieved with KBr on a double resonance probe, or on  $\text{BaClO}_3 \cdot \text{H}_2\text{O}$ , looking at the proton signal, much like one does on the  $\text{Br}^{79}$  resonance.

Shimming will also be important, since protons are observed, and on some samples, good resolution is expected. Looking at the protons in adamantane, find the power level for a 2.5  $\mu\text{sec}$  90° pulse. Set the  $B_0$ -field or **o1** to be close to resonance (see chapter Basic Setup Procedures for more details). Calibrate the adamantane proton shift to 1.2 ppm. Then load a spinner with  $\alpha$ -glycine (precipitate from cold water with acetone and dry, if you are not sure about the composition of your sample). A spinner with 50  $\mu\text{l}$  or less sample volume is preferred since high  $\text{H}_1$ -homogeneity is desired, although it is by far less important than is commonly stated in the literature.

## Parameter Settings for PMLG and DUMBO

20.5

Table 20.2. PMLG Analog Mode

Parameter	Value	Comment
pulprog	wpm1ga	Runs on AV 3 instruments only.
pl12 sp1	for 100 kHz RF field dto, set cnst20=100 000	To be optimized during setup.
spnam1	wpm1g1, m5m or m5p	
p1	2.5 $\mu\text{sec}$	As for 100 kHz RF field.
p8	1.2 $\mu\text{sec}$	
p14	0.7 $\mu\text{sec}$	To be optimized.
cnst25	140	To be optimized.
p9	4 – 2.6 $\mu\text{sec}$	To be optimized.
p5	1.5 $\mu\text{sec}$ or calculated from cnst20	To be optimized.
d1	4s	For $\alpha$ -glycine.
l11=anavpt	4	2, 4, 8, 16 or 32.
o1p	10 or -1	To be optimized.

Table 20.2. PMLG Analog Mode

swh	$1e^6/2*(2*p9+10*p5)*0.6$	To be corrected for proper scaling.
rg	16-64	
td	512	Up to 1024.
si	4k	
digmod	analog	
MASR	12-15 kHz	Depending on cycle time.

Table 20.3. DUMBO, Analog Mode

Parameter	Value	Comment
pulprog	dumboa	Runs on AV 3 instruments only.
pl12 sp1	for 100 kHz RF field up to 130 kHz	To be optimized during setup.
spnam1	dumbo1_64	Set by xau dumbo.
p1	2.5 $\mu$ sec	For 100 kHz RF field.
p8	1.2 $\mu$ sec	
p14	0.7 $\mu$ sec	To be optimized.
cnst25	140	To be optimized.
p9	4 – 2.6 $\mu$ sec	To be optimized.
p10	32 $\mu$ sec or 24 $\mu$ sec	Set by xau dumbo.
d1	4s	For $\alpha$ -glycine.
I11=anavpt	4	2, 4, 8, 16 or 32.
o1p	5	To be optimized.
swh	$1e^6/2*(2*p9+p10)*0.5$	To be corrected for proper scaling.
rg	16-64	
td	512	Up to 1024.
si	4k	
digmod	analog	
MASR	10-12 kHz	Depending on cycle time.

**Fine Tuning for Best Resolution****20.6**

For fine tuning, the following parameters are important:

**P9** sets the width of the observe window. The shorter it is, the better the resolution. However, the natural limit is the size of the sampling period and the dead time of the probe. Preamp and receiver play no significant role in the total dead time. A CP/MAS probe usually has a fairly narrow bandwidth (long dead time), so **p9 <3μsec** is only possible at frequencies 400 and higher. With **I11 4-8**, **p9** can be chosen shorter for better resolution, but at the cost of S/N. Sampling more data points during **d9=I11\*0.1 μsec** with larger values of **I11**, will increase S/N slightly but requires more time within the window, may require a longer **p9** and therefore degrade resolution.

Since the decoupling bandwidths are not very large, **o1** should be close to resonance, especially for DUMBO. For PMLG, this is less critical. The power level for the shapes should be adjusted in steps of 0.2 dB. The splitting of the two high field lines (the protons in the –CH<sub>2</sub>- are in equivalent in the solid state) should be below the 50% level.

**Fine Tuning for Minimum Carrier Spike****20.7**

The tilt pulse **p14** and its phase (**cnst25**) determine the size of the carrier spike. Optimise both parameters alternately for minimum spike, and make sure the spike does not overlap with a resonance by choosing **o1** appropriately. N.B: changing **o1** will lead to different values for **cnst25**.

**Correcting for Actual Spectral Width****20.8**

Since the sampling rate is governed by the multi-pulse sequence repetition rate, the foreground parameter **swh** has no real meaning. Once all tuning procedures are done, calculate the real spectral width **swh** according to the formula given in the parameter tables and run a new experiment. After FT, the spectrum should have an approximately correct spectral width. Calibrate the middle position between the two –CH<sub>2</sub>- peaks to 3.5 ppm, the NH<sub>3</sub>-peak should then be at about 7.5 ppm. Since the actual peak positions depend on the probe tuning, you will have to recalibrate for your sample using one or more known chemical shifts. If the peak separation is incorrect, change the status parameter **swh** by typing **s wh** and scaling it appropriately. Some pulse programs are written such that upon **ased**, the (approximately) correct sweep width is shown and can be set as an acquisition parameter.

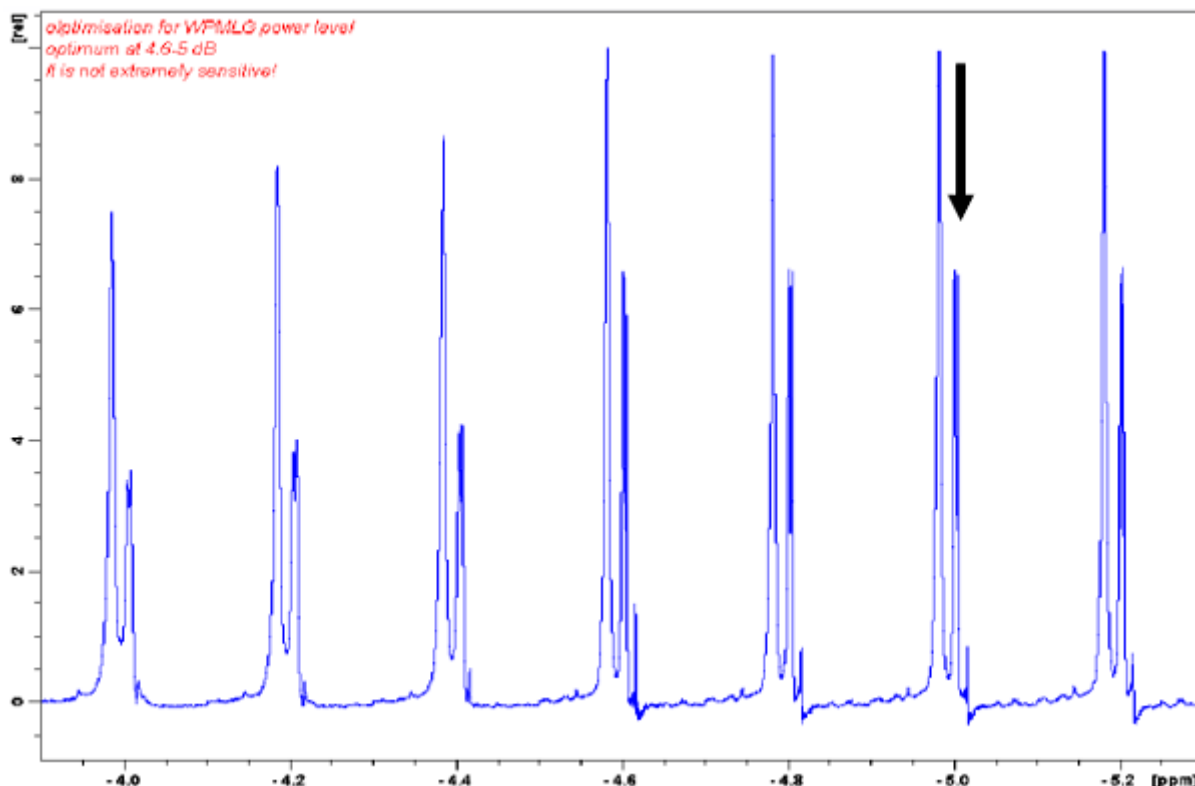
**Digital Mode Acquisition****20.9**

Most parameters stay the same as adjusted in analog mode.

**Table 20.4. Parameters for Digital Mode**

Parameter	Value	Comment
pulprog	dumbod or wpmlgd	AV 3 instruments only.
digmod dspfirm	digital sharp or medium	
aqmod	qsim or dqd	
swh	50000-10000	Depending on spectral range and o1.

The correction for the scaling factor must be done after acquisition, changing the status parameter **swh** by typing **s swh** and dividing the value by the scaling factor (about 0.578 for WPMLG, 0.47 for wpmlgd2 and 0.5 for DUMBO). Some pulse programs are written such as to show the correct sweep width in **ased**, which can then be set appropriately as **s swh** before transform.

**Examples****20.10****Figure 20.6. Optimizing sp1 for Best Resolution**

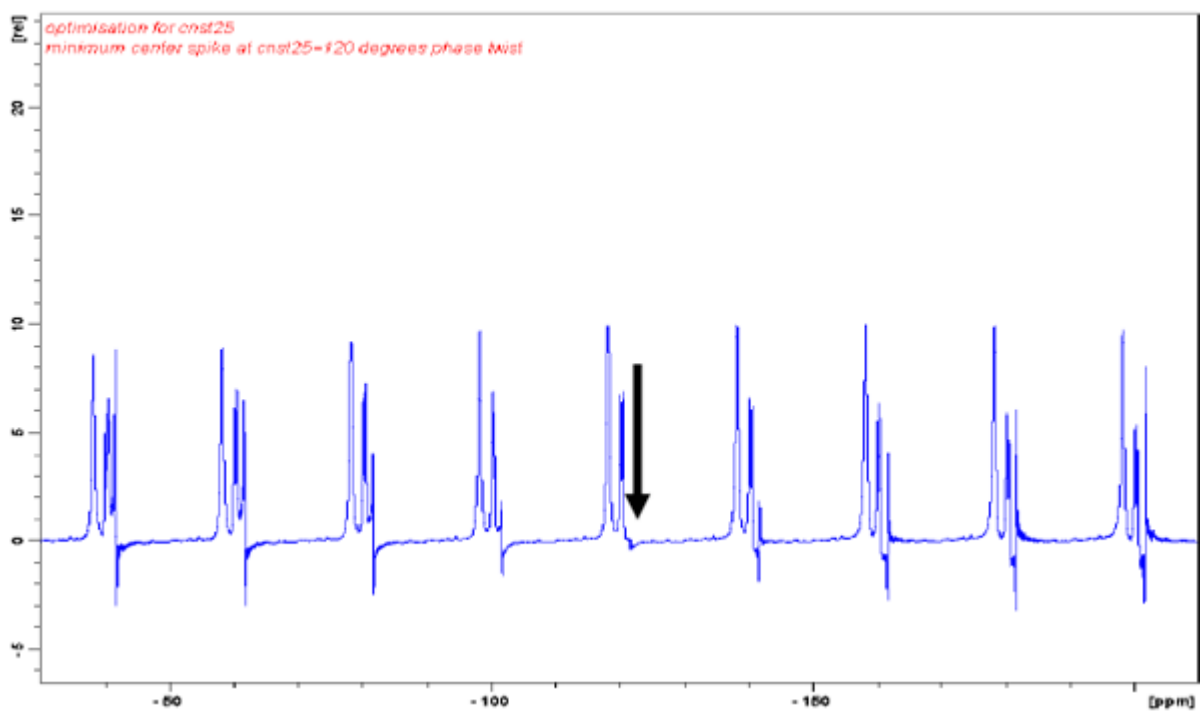


Figure 20.7. Optimizing cnst25 for Minimum Carrier Spike, Optimized at 120°C

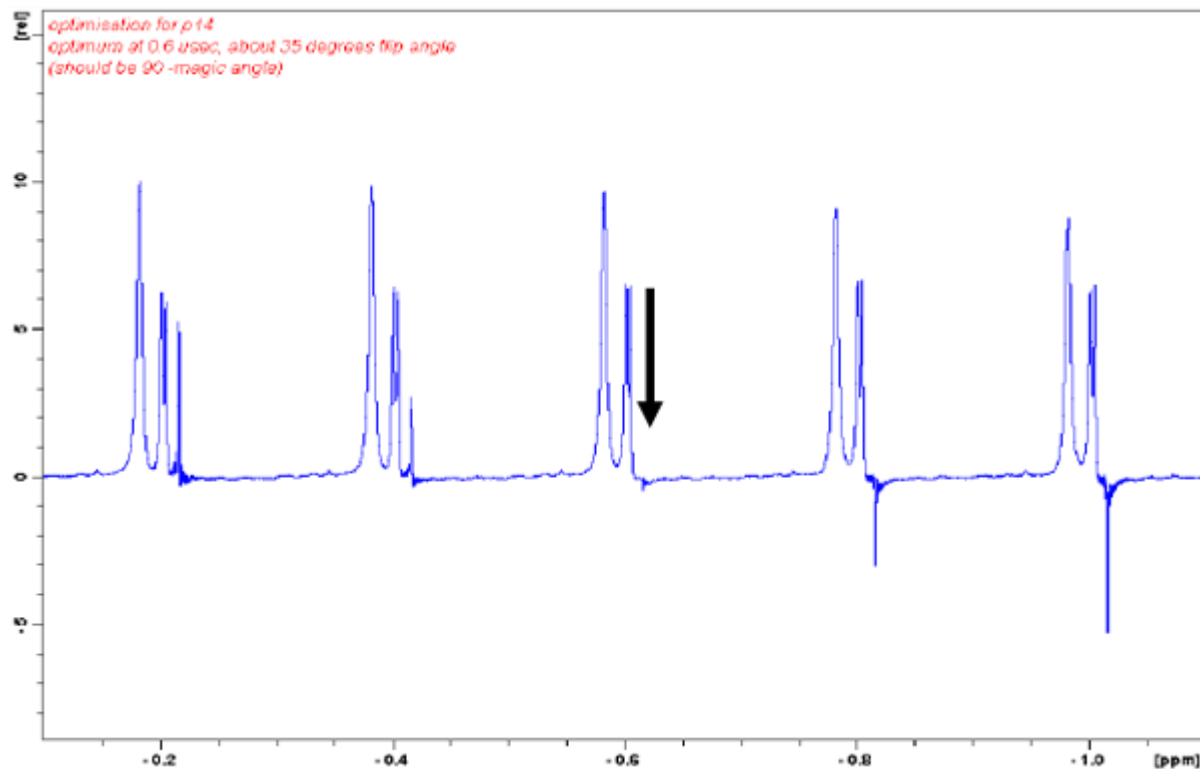
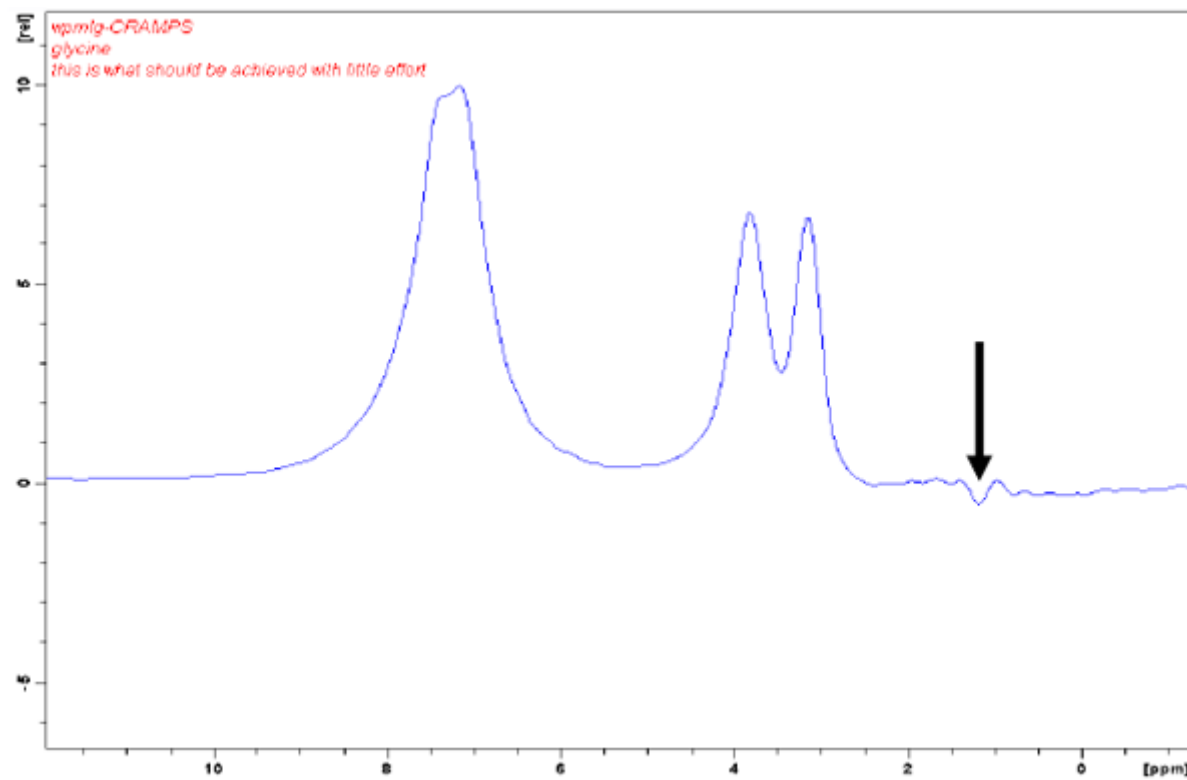


Figure 20.8. Optimizing p14 for Minimum Carrier Spike, Optimized at 0.6  $\mu$ sec



*Figure 20.9. WPMLG-CRAMPS After Optimization, Digital Acquisition*

# Modified W-PMLG

# 21

Recently, a modified version of WPMLG was published by Leskes et al., which suppresses the carrier spike completely and therefore allows placing the carrier frequency  $\omega_1$ ,  $\omega_{1p}$  arbitrarily. This is achieved by a 180 degree phase alternation between consecutive WPMLG-pulses. The magic angle tilt pulse is then not required anymore. This reduces setup time and enhances experimental possibilities significantly.

## Reference:

M. Leskes, P.K. Madhu and S. Vega, *A broad-banded z-rotation windowed phase-modulated Lee–Goldburg pulse sequence for  $^1H$  spectroscopy in solid-state NMR*, Chem. Phys. Lett. **447**, 370 (2007).

## Pulse Sequence Diagram for Modified W-PMLG

21.1

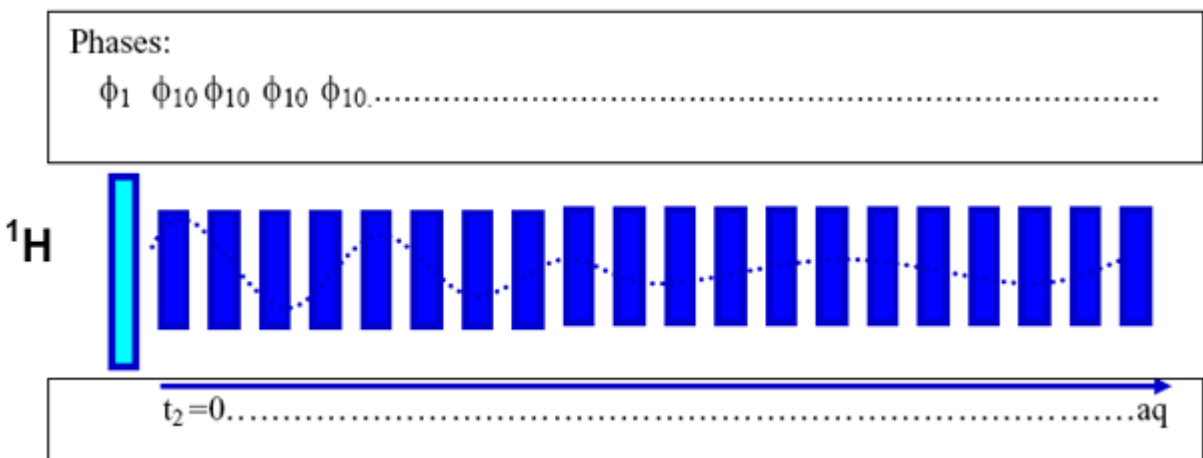


Figure 21.1. Pulse Sequence Diagram

Table 21.1. Phrases, RF-Levels, Timings

Phases	RF Power Levels	Timing
$\phi_1 = \text{CYCLOPS, 1 2 3 0}$	pl12=set for around 100 kHz	p1 around 2.5 $\mu\text{sec}$
$\phi_{10} = \mathbf{0 2}$	sp1: set for 100-130 kHz=cnst20	WPMLG: calculated from cnst20=RF field
$\phi_{31} = \text{CYCLOPS, 0 1 2 3}$		

**PMLG-shapes: m3p, m3m, m5m, m5p**

All these shapes perform similarly. M3p and m3m use 6 phases, m5p and m5m use 10 phases to generate the phase ramp. Obviously, 6 phases generate a phase ramp with less resolution, but shorter possible duration. With the timing resolution available on AV instruments, there is no need to prefer the coarse phase ramp. The letters m and p refer to the sense of phase rotation which is opposite between m and p. If probe tuning is not perfect, m or p may give different results depending on the carrier position. The overall added phases of 0 and 180 degrees on consecutive shape pulses are set by the phase program (phase list ph10).

<pre> ##TITLE= m5p ##JCAMP-DX= 5.00 Bruker JCAMP library ##DATA TYPE= Shape Data ##ORIGIN= Bruker BioSpin GmbH ##OWNER= &lt;hf&gt; ##DATE= 2005/11/29 ##TIME= 14:47:39 ###\$SHAPE_PARAMETERS= ##MINX= 1.000000E02 ##MAXX= 1.000000E02 ##MINY= 1.125000E01 ##MAXY= 3.487500E02 ###\$SHAPE_EXMODE= None ###\$SHAPE_TOTROT= 0.000000E00 ###\$SHAPE_TYPE= Excitation ###\$SHAPE_USER_DEF= ###\$SHAPE_REPHFAC= ###\$SHAPE_BWFAC= 0.000000E00 ###\$SHAPE_BWFAC50= ###\$SHAPE_INTEGFAC= 6.534954E-17 ###\$SHAPE_MODE= 0 ##NPOINTS= 10 ##XYPOINTS= (XY...XY) 1.000000E02, 20.78 1.000000E02, 62.35 1.000000E02, 103.92 1.000000E02, 145.49 1.000000E02, 187.06 1.000000E02, 7.06 1.000000E02, 325.49 1.000000E02, 283.92 1.000000E02, 242.35 1.000000E02, 200.78 ##END </pre>	<pre> ##TITLE= m3p ##JCAMP-DX= 5.00 Bruker JCAMP library ##DATA TYPE= Shape Data ##ORIGIN= Bruker BioSpin GmbH ##OWNER= &lt;hf&gt; ##DATE= 2005/11/29 ##TIME= 14:47:39 ###\$SHAPE_PARAMETERS= ##MINX= 1.000000E02 ##MAXX= 1.000000E02 ##MINY= 1.125000E01 ##MAXY= 3.487500E02 ###\$SHAPE_EXMODE= None ###\$SHAPE_TOTROT= 0.000000E00 ###\$SHAPE_TYPE= Excitation ###\$SHAPE_USER_DEF= ###\$SHAPE_REPHFAC= ###\$SHAPE_BWFAC= 0.000000E00 ###\$SHAPE_BWFAC50= ###\$SHAPE_INTEGFAC= 6.534954E-17 ###\$SHAPE_MODE= 0 ##NPOINTS= 6 ##XYPOINTS= (XY...XY) 1.000000E02, 214.64 1.000000E02, 283.92 1.000000E02, 353.21 1.000000E02, 173.2 1.000000E02, 103.92 1.000000E02, 34.64 ##END </pre>
---	--

Fine tuning is done in the same way as with the original sequence, except that the carrier is placed on a convenient position within the spectrum. There is no need to minimise the carrier spike, it should be all gone. Somewhat higher power is required for the wpmlg-shapes.

Table 21.2. PMLG, Analog Mode

Parameter	Value	Comment
pulprog	wpmiga2	Runs on AV 3 instruments only.
pl12 sp1	for 100 kHz RF field dto, set cnst20=100 000	To be optimized during setup.
spnam1	m5m or m5p	
p1	2.5 $\mu$ sec	As for 100 kHz RF field.
p8	1.2 $\mu$ sec	
p9	4 – 2.6 $\mu$ sec	To be optimized.
p5 not used	calculated from cnst20	To be optimized.
d1	4s	For $\alpha$ -glycine.
l11=anavpt	4	2, 4, 8, 16 or 32.
o1p	3 - 8	To be optimized.
swh	$1e^6/2*(2*p9+10*p5)*0.47$	To be corrected for proper scaling.
rg	16-64	
td	512	Up to 1024.
si	4k	
digmod	analog	
MASR	12-15 kHz	Depending on cycle time.

Table 21.3. DUMBO, Analog Mode

Parameter	Value	Comment
pulprog	dumboa2	Runs on AV 3 instruments only.
pl12 sp1	For 100 kHz RF field up to 130 kHz	To be optimized during setup.
spnam1	dumbo1_64	Set by xau dumbo.
p1	2.5 $\mu$ sec	For 100 kHz RF field.
p8	1.2 $\mu$ sec	
p9	4 – 2.6 $\mu$ sec	To be optimized.
p10	32 $\mu$ sec or 24 $\mu$ sec	Set by xau dumbo.
d1	4s	For $\alpha$ -glycine.

Table 21.3. DUMBO, Analog Mode

I11=anavpt	4	2, 4, 8, 16 or 32.
o1p	5	To be optimized.
swh	$1e^6/2*(2*p9+p10)*0.5$	To be corrected for proper scaling.
rg	16-64	
td	512	Up to 1024.
si	4k	
digmod	analog	
MASR	10-12 kHz	Depending on cycle time.

**Fine Tuning for Best Resolution****21.5**

Fine tuning is done by optimizing power levels, pulse widths and carrier offset as before, the carrier spike is gone, spikes at both sides may appear.

**Correcting for Actual Spectral Width****21.6**

The modified sequence has a slightly different scaling factor of 0.47.

**Digital Mode Acquisition****21.7**

Most parameters stay the same as adjusted in analogue mode.

Table 21.4. Parameters for Digital Mode

Parameter	Value	Comment
pulprog	dumbod2 or wpmlgd2	AV 3 instruments only.
digmod dspfirm	digital sharp or medium	
aqmod	qsim or dqd	
swh	50000-10000	Depending on spectral range and o1.

The correction for the scaling factor must be done after acquisition, changing the status parameter **swh** by typing **s swh** and dividing the value by the scaling factor (about 0.47 for WPMLG and 0.5 for DUMBO).

# CRAMPS 2D

# 22

CRAMPS methods allow measurement of chemical shifts in the presence of strong Homo-nuclear dipolar interactions. Therefore, CRAMPS-type sequences can be applied to measure chemical shifts of protons (where these sequences work most efficiently, and where fast spinning cannot easily be used). As an example, the proton-X hetero-nuclear chemical shift correlation experiment (see chapter 5) uses FSLG to suppress Homo-nuclear dipolar couplings between protons to resolve the proton chemical shifts. CRAMPS-type pulse sequences must be used in both dimensions if proton chemical shifts are to be correlated.

Two types of proton-proton correlation experiment will be described here:

1. Proton-proton shift correlation via spin diffusion (similar to the high resolution NOESY-experiment). In this case, the dipolar coupling between protons acts during the mixing period. The size of the off-diagonal cross peaks indicates the size of the dipolar coupling between the correlated sites.
2. Proton-proton DQ-SQ correlation (similar to the high resolution INADEQUATE) correlates proton chemical shifts with DQ-frequencies of dipolar coupled sites.

## References:

1. P. Caravetti, P. Neuenschwander, R.R. Ernst, *Macromolecules*, **18**, 119 (1985).
2. S.P. Brown, A. Lesage, B. Elena and L. Emsley, *Probing Proton-Proton Proximities in the Solid State: High-Resolution Two-Dimensional  $^1\text{H}$ - $^1\text{H}$  Double-Quantum CRAMPS NMR Spectroscopy*, *J. Am. Chem. Soc.* **126**, 13230 (2004).

The modifications according to the chapter "**Modified W-PMLG**" are implemented in order to remove the carrier spike. Without a carrier spike, 2D experiments are much easier and faster to set up. Being able to set the carrier close to the desired spectral range, one can make the total acquired window smaller as well along F2 (using digital mode) as along F1.

## Proton-Proton Shift Correlation (spin diffusion)

22.1

The standard CRAMPS setup must be executed first (see chapter [20](#), [21](#)). Any Homo-nuclear dipolar decoupling scheme may be used, but in the following the experiment is described using windowed pmlg (w-PMLG). The reasons are the following:

1. At fast spin rates over 10 kHz, only w-PMLG and DUMBO work well. The sequence can easily be modified to use DUMBO, replacing the w-PMLG shapes by DUMBO-shapes and modifying the shape timing accordingly.
2. W-PMLG is easy to set up, since it is rather insensitive to power level missets and frequency offsets. When the experiment setup for the 1D experiment has been executed, no further setup is required for the 2D experiment. Start from the 1D experiment on your sample (the recommended setup sample is glycine) and generate a 2D data set by clicking on the symbol 1, 2 in the headline of the acquisition parameters.

Phases:  
 $\phi_1 \quad \phi_{11} \quad \phi_{11} \quad \phi_5$        $\phi_1$        $\phi_{10}$        $\phi_{10} \dots$

Pulses and delays:  
 $p1 \quad LG$        $d3 \quad d3 \quad d3$        $d3 \quad p1^3$        $d8$        $p1 \quad LG$        $d3 \quad d3$        $d3 \quad d3$        $d3 \quad d3$        $d3 \quad d3$        $d3 \quad d3$

Pulse power:  
 $p112 \quad p113$        $p112$        $p112 \quad p113$

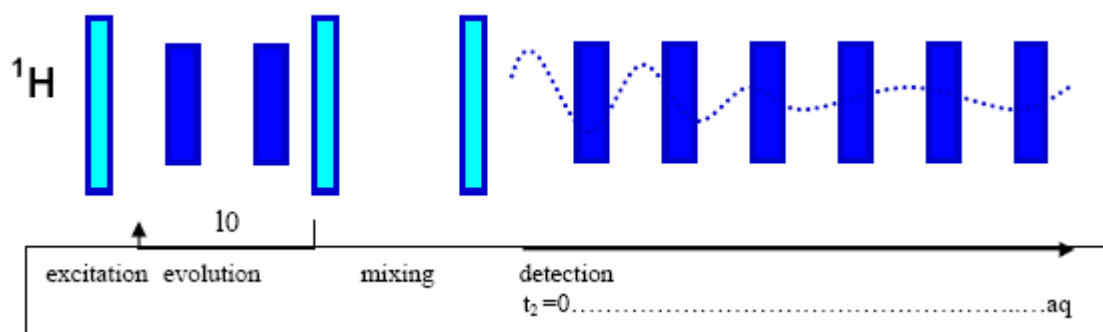


*Figure 22.1. Pulse Sequence Diagram*

This sequence is written in such a way that the windowed PMLG-unit is used both for detection and for the shift evolution along F1. This was done to minimize the setup requirements. In principle, a windowless sequence can be used as well and should give better resolution along F1. The power level for a windowless sequence is however usually slightly different from the windowed sequence, so this needs to be adjusted separately. Likewise, decoupling during t1 could be implemented using real frequency shifts as in the HETCOR sequence (see "[Decoupling Techniques](#) [on page 45](#)"). If a windowless sequence is incorporated, the windows d3 must of course be removed. A simple windowless FSLG-unit can be used, with a shape like lgs-2 or lgs-4 having duration of twice or 4 times the length of the w-pmlq pulse.

*Table 22.1. Acquisition Parameters*

Parameter	Value	Comment
pulprog	wpmlg2d.	AV 3 instruments only, topspin 2.1 or later.
FnMODE	STATES-TPPI.	Any other method may be used with appropriate changes in ppg.
NUC1, NUC2	1H.	
sw, swh along F1	Same as for F2.	Needs to be corrected before transform pulse program calculates approximate values to be set before transform ( <b>ased</b> ).
td	512-1k.	Depending on resolution.

*Table 22.1. Acquisition Parameters*

1 td	128-256.	Depending on resolution.
spnam1	wpmlg1, m5m or m5p as in 1d.	DUMBO may be used with modified timing.
spnam2	lgs-2 or lgs-4 if used.	Set l3=2 or 4, depending on desired sw1 DUMBER-22 with modified timing.

*Table 22.2. Phases, RF-levels, and Timings*

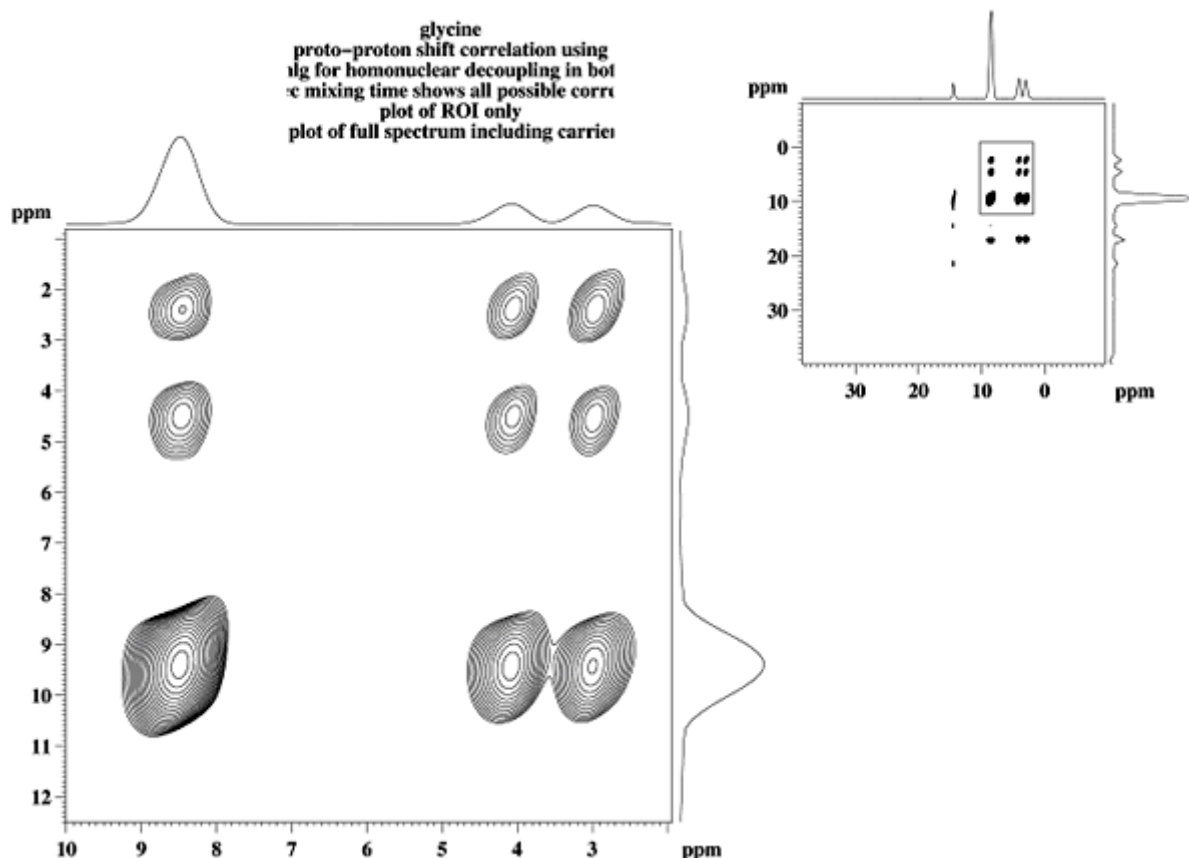
Phases	RF Power Levels	Timing
$\phi_0 = 0$ , STATES-TPPI	pl12 = set for around 100 kHz	p1 around 2.5 $\mu$ sec.
$\phi_1 = \text{CYCLOPS}, 1\ 2\ 3\ 0$	pl12	p1
$\phi_5 = 2$		
$\phi_{10} = 0\ 2$	sp1,sp2: set for 100-130 kHz RF-field or pl13 for both set in ppg	WPMLG: calculated via cnst20. DUMBO: p10 set by xau dumbo.
$\phi_{11} = 0\ 2$	dto.	dto.
$\phi_{31} = \text{CYCLOPS}, 0\ 1\ 2\ 3$		d8 = desired mixing time, 50-1000 $\mu$ s.

**Data Processing****22.3**

The spectral width in both dimensions assumes the absence of shift scaling. In order to account for the shift scaling effect of the sequence, one has to increase the spectral width by the scaling factor. Before doing the 2D-fourier transformation, type **s sw** to call the status parameters for both F2 and F1 and replace both values by <current value>/0.6. After **xfb**, the relative peak positions will be (approximately) correct, but the absolute peak positions must be corrected by calibrating a known peak position to the correct value. The pulse program is written such that the correctly scaled sweep widths are calculated and indicated upon **ased**. These values are set as status parameters before transform as indicated above.

*Table 22.3. Processing Parameters*

Parameter	Value	Comment
<b>mc2</b>	STATES-TPPI	
<b>wdw</b>	QSINE	Slight-moderate resolution enhancement is usually required.
<b>ssb</b>	3 or 5	
<b>si</b>	2k -4k	
<b>1 si</b>	512 – 1k	

**Examples**

*Figure 22.2. Setup and Test Spectrum of Alpha-glycine*

The figure above shows the setup and test spectrum of alpha-glycine (N.B. glycine samples containing gamma glycine will show additional peaks!). The protons attached to the alpha-carbon are in equivalent and strongly coupled. The cross peaks at 3 and 4 ppm will show at a mixing time as short as 50  $\mu$ sec, the cross peaks to the  $\text{NH}_3$ -protons at 9 ppm require 200 -300  $\mu$ sec to show. The mixing time here was 500  $\mu$ sec. A sequence without carrier spike suppression was used here.

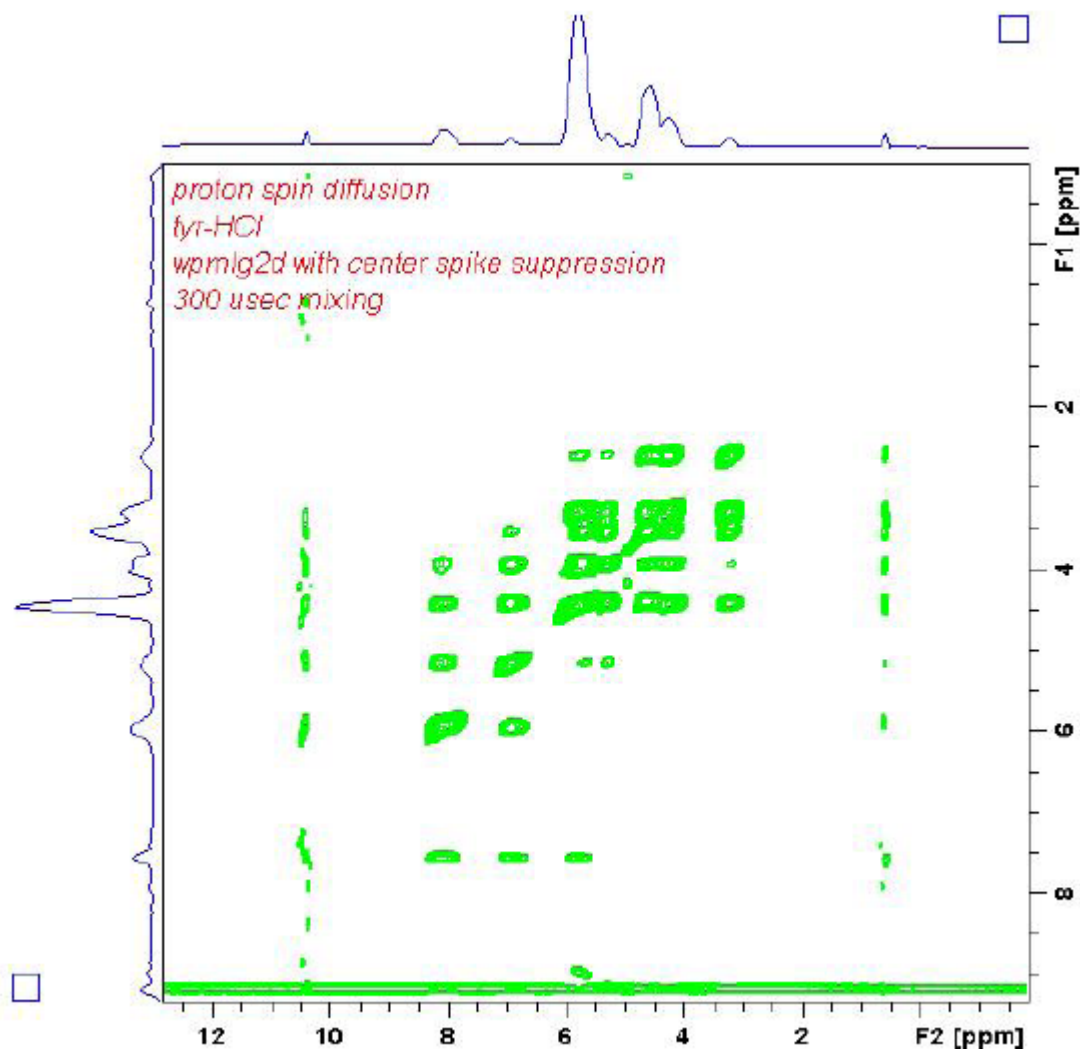


Figure 22.3. Spectrum of Tyrosine-hydrochloride

The mixing time was 300  $\mu$ sec to show all connectivity. Full plot to show that smaller sweep widths can be chosen when the carrier can be conveniently placed within the spectrum.

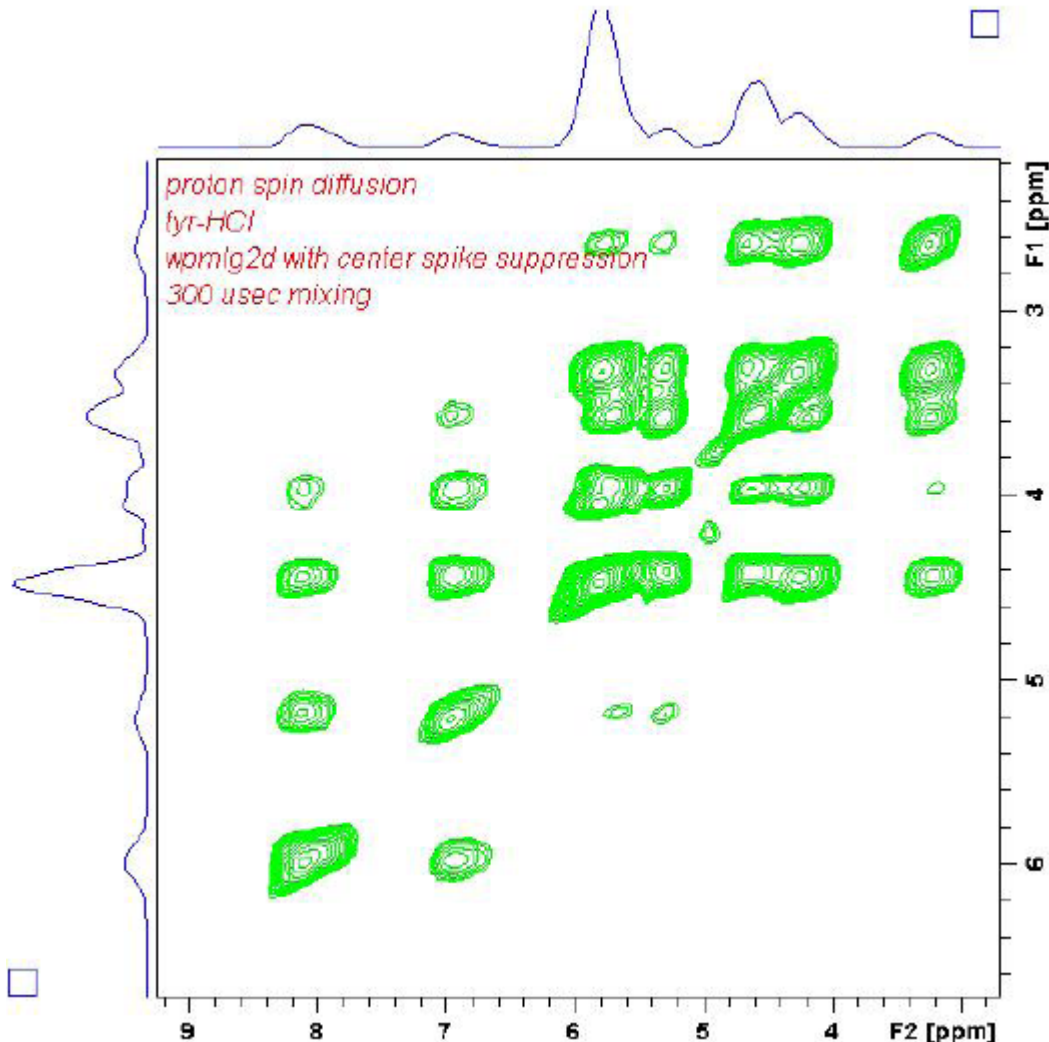


Figure 22.4. Expansion of the Essential Part of the Spectrum

### Proton-Proton DQ-SQ Correlation

### 22.5

This experiment correlates proton shifts (F2) with double quantum frequencies (sum of shifts of the correlated sites). Double quantum transitions are excited and reconverted by a post-C7 or similar sequence.

## Pulse Sequence Diagram

22.6

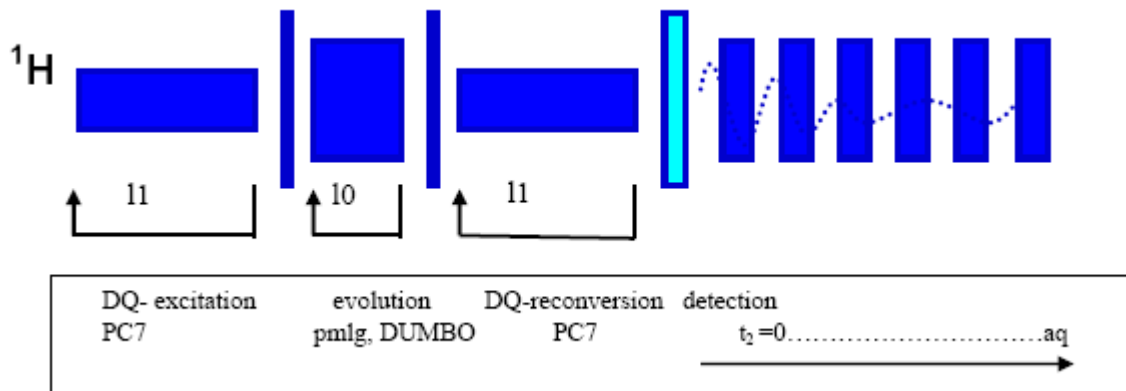
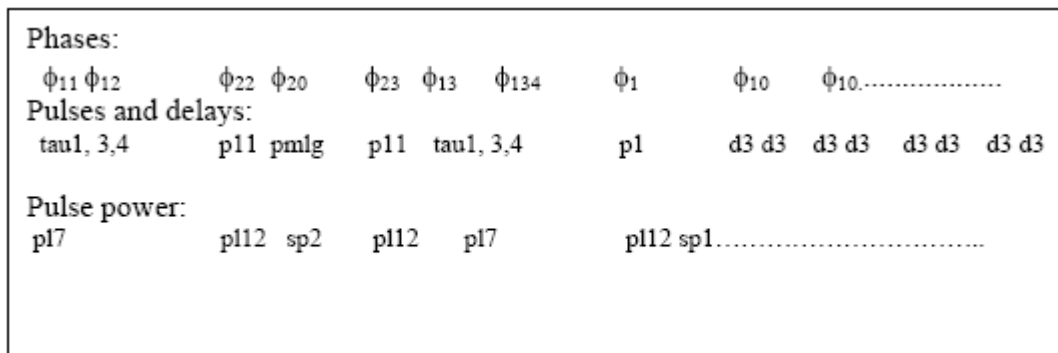


Figure 22.5. Pulse Sequence Diagram

When applied to X-nuclei like  $^{13}\text{C}$ , the RF field during this sequence must be carefully matched to the 7-fold spin rate, since the dipolar couplings are small, and care must be taken that the excitation bandwidth of the sequence chosen covers the whole shift range of the X-nucleus. In the case of protons, this is rather forgiving, since the shift range to be covered is small, and the required power levels are easily achieved for protons. Usually it is enough to calculate the required power level from the spin rate and the known proton 90 degree pulse using the au program **calcpowlev**. Assume the spin rate is 14000 Hz and post-C7 is used. The required RF field is then  $7 * 14000 = 98000$  Hz. The known proton 90 degree pulse is  $2.5 \mu\text{sec} = 1/4 * 2.5 \text{e-6} = 100000$  Hz. Type **calcpowlev** and enter 100000, return, then enter 98000, return. The output will be "change power level by 0.18 dB". The power level for the p-C7 sequence is therefore 0.18 dB to higher attenuation than what is required for a 2.5  $\mu\text{sec}$  pulse.

Table 22.4. Acquisition Parameters

Parameter	Value	Comment
pulprog	wpmlgdqsq	AV 3 instruments only, topspin 2.1 or later.
FnMODE	STATES-TPPI	Any other method may be used with appropriate changes in ppg.
NUC1, NUC2	1H	
sw, swh along F1	same as for F2	Needs to be corrected before transform pulse program calculates approximate values upon <b>ased</b> .
td	512-1k	Depending on resolution.
1 td	128-256	Depending on resolution.
cnst31	spin rate, 10-15 000	Depending on available RF field.
I1	number of pc7-cycles	2-7 depending on dipolar coupling.
spnam1	m5m or m5p as in 1d setup	DUMBO may be used with modified timing.
spnam2	lgs-2 or lgs-4 if used.	Set I3=2 or 4, depending on desired sw1 DUMBER-22 with modified timing.

Table 22.5. Phases, RF-Levels and Timing

Phases	Rf Power Levels	Timing
$\phi_{11,12} = \text{POST-C7} = \phi_{13,14}$ $\phi_{11,12}$ incremented for DQ-evol. $\phi_{11,12}$ incremented for DQ-select	pl7 set for RF=7*spin rate	tau1,3,4 calculated from cnst31.
$\phi_1 = \text{CYCLOPS}$	pl12	p1
$\phi_{22} = 3$	pl12	p11, ~45°
$\phi_{23} = 1$	pl12	p11
$\phi_{10} = 0$	sp1: set for 100-130 kHz RF-field	WPMLG: calculated via cnst20 DUMBO: p10 set by xau dumbo.
$\phi_{31} = \text{DQ selection}$		

**Data Processing****22.7**

The spectral width in both dimensions assumes the absence of shift scaling. In order to account for the shift scaling effect of the sequence, one has to increase the spectral width by the scaling factor. Before doing the 2D-fourier transformation, type **s sw** to call the status parameters for both F2 and F1 and replace both values by <current value>/0.6. After **xfb**, the relative peak positions will be (approximately) correct, but the absolute peak positions must be corrected by calibrating a known peak position to the correct value.

*Table 22.6. Processing Parameters*

Parameter	Value	Comment
<b>mc2</b>	STATES-TPPI	Or whatever used.
<b>wdw</b>	QSINE	Slight-moderate resolution enhancement is usually required.
<b>ssb</b>	3 or 5	
<b>si</b>	2k -4k	
1 si	512 – 1k	

**Examples****22.8**

These spectra were both taken without the modification according to "["CRAMPS 2D" on page 225](#)", so the offset is placed to the down field side and the spectrum width was chosen larger than necessary. The small plots show the full spectrum.

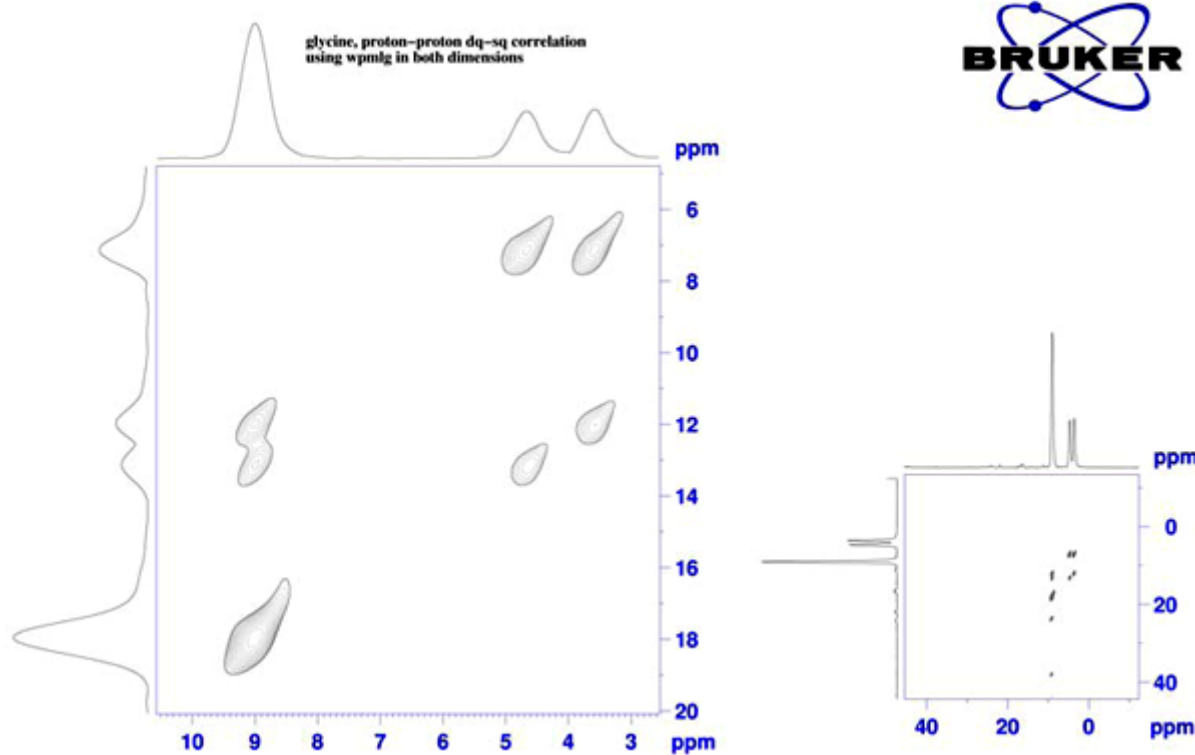


Figure 22.6. Glycine, Proton-Proton DQ-SQ Correlation Using WPMLG in Both Directions

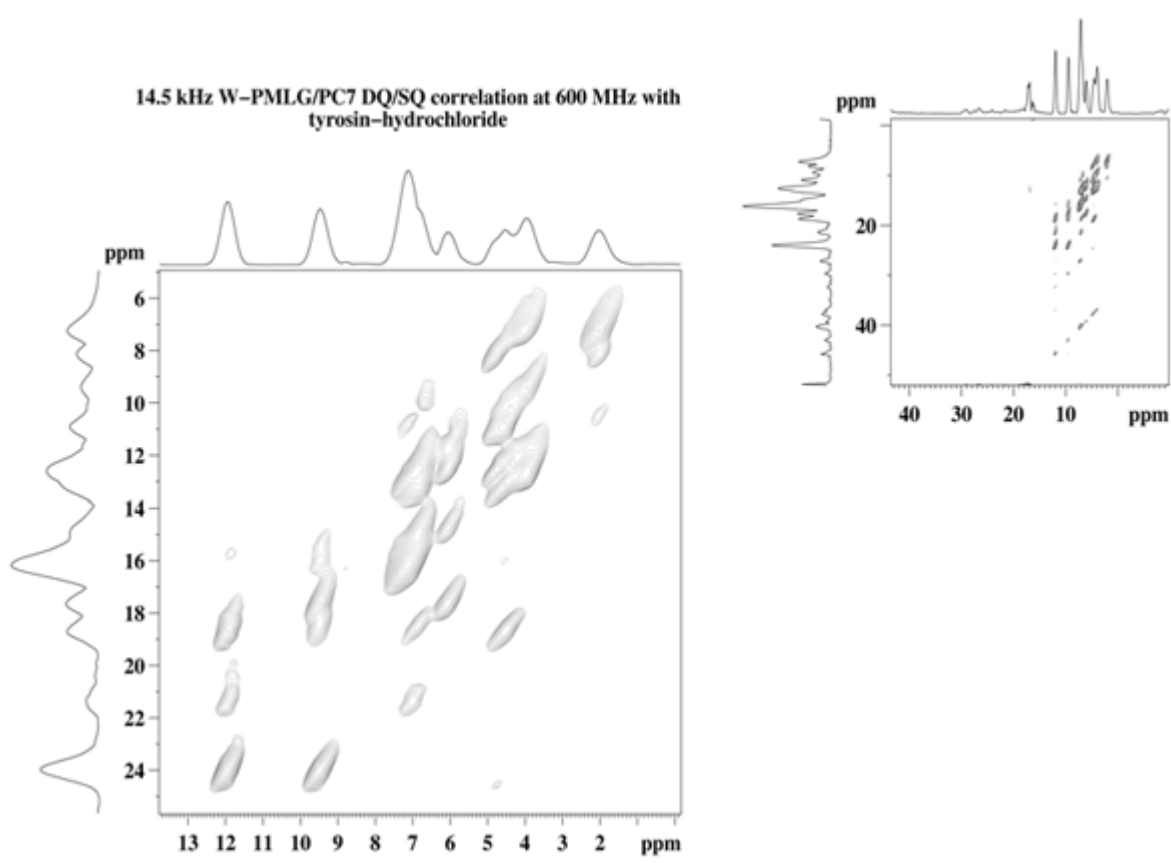


Figure 22.7. 14.5 kHz W-PMLG/PC7 DQ/SQ Correlation at 600 MHz with Tyrosine-Hydrochloride



# Appendix A

## Form for Laboratory Logbooks

A.1

The form on the following page may be printed and filled out by every user using the instrument to trace eventual problems and provide information for the next user.

Another copy may be printed for every user's own laboratory notebook. One form per probe used should be filled out. The following form serves as an example:

<b>Operator</b>	<b>used from:</b>		<b>to:</b>						
HF	10.12.07 10.00h		13.12.07 18.00h						
<b>Probe:</b>	<b>shim file:</b>		<b>B<sub>0</sub>-field:</b>						
4mm triple C/N/H	triple4.hf		390 SR -360.14						
<b>Sample:</b>	<b>Experiment:</b>		<b>pulses</b>	<b>(us)</b>	<b>pl(n)</b>	<b>(dB/watt)</b>		<b>ok?</b>	<b>S/N:</b>
Glycine	CP S/N test	F1 <sup>13</sup> C	p90: contact: mix: else:	3.5 2m - -	pl11 pll 3.5 120	3 3.5 150 120		y	100
		F2 <sup>1</sup> H	p90: contact: decouple: mix: else:	2.5 2m 4.6 -	pl12 sp0 pl12 -	4 5 120 100			
		F3	p90: contact: decouple: mix: else:	- - - -					
<b>stored under filename:</b> glycine-4 /opt/topspin/reference 1 1									
<b>comments:</b> spinning at 10 kHz ok, mains pressure at 6 bars, linewidth $\alpha$ -C 50 Hz, O2= 1500, spinal decoupling									



<b>Operator</b>	<b>used from:</b>	<b>to:</b>							
<b>Probe:</b>	<b>shim file:</b>	<b>B<sub>0</sub>-field:</b>							
		SR:							
<b>Sample:</b>	<b>Experiment:</b>		<b>pulses</b>	<b>us</b>	<b>pl(n)</b>	<b>dB</b>	<b>watt</b>	<b>ok?</b>	<b>S/N:</b>
		F1	p90: contact: mix: else: p90: contact: decouple: mix: else: p90: contact: decouple: mix: else						
<b>Sample:</b>	<b>Experiment:</b>								
<b>stored under filename:</b>									
<b>comments:</b>									

## 2. Pulse program cpopt:

```
;cpopt (TopSpin 2.1)

;single pulse excitation, acquisition without decoupling

;Avance III version
;parameters:
;d1 : recycle delay
;p3 : proton excitation pulse length as in cp
;p112 : decoupling/excitation power level for cp
;spnam0 : usual shape for cp
;sp0 : usual shape power for cp contact

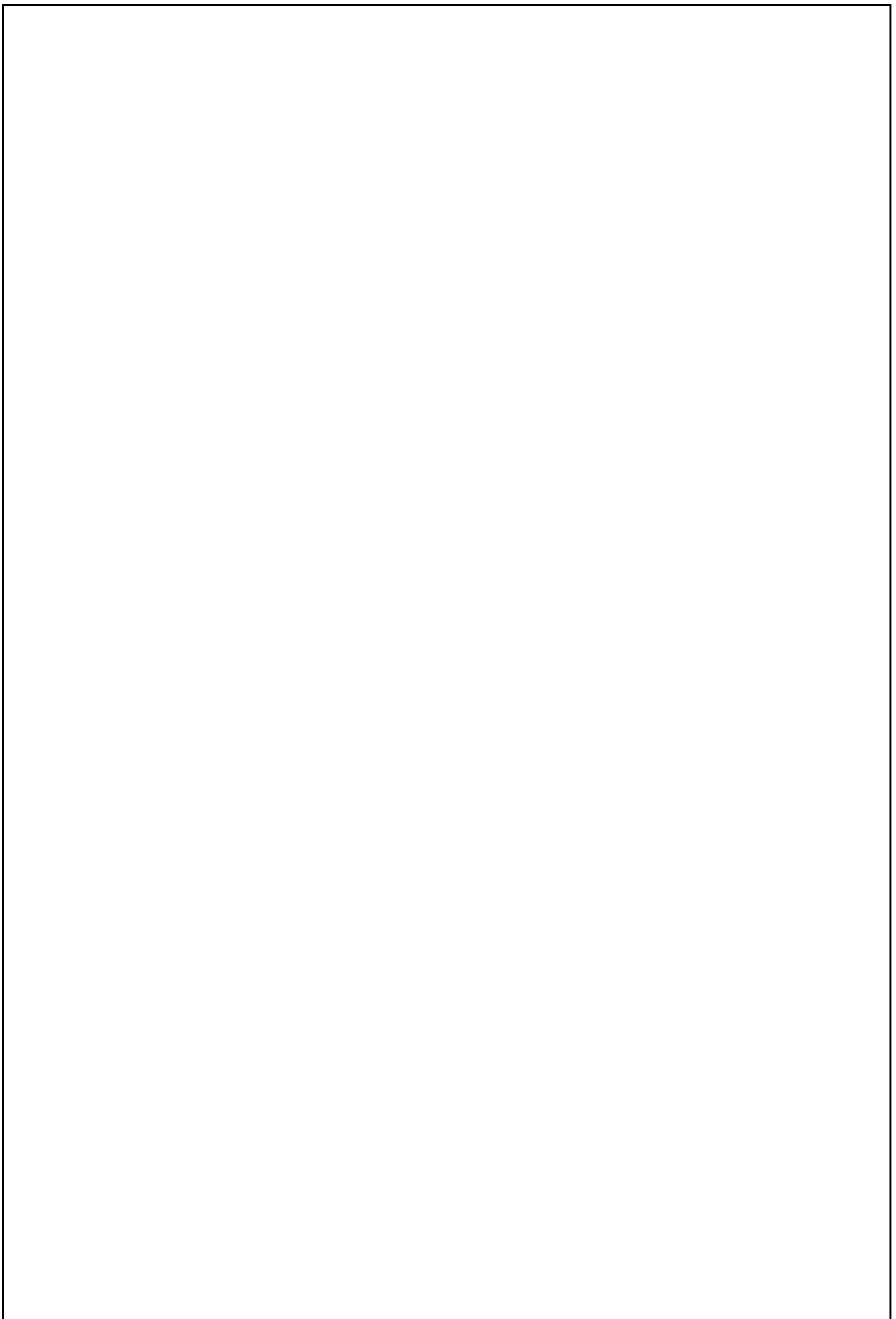
;$COMMENT=single pulse excitation, acquisition without decoupling
;$CLASS=Solids
;$DIM=pseudo-2D
;$TYPE=direct excitation
;$SUBTYPE=relaxation measurement
;$OWNER=Bruker
;cnst11 : to adjust t=0 for acquisition, if digmod = baseopt
"acqt0=lu*cnst11"

1 ze
2 d1
  (p3 p112 ph1):f1
  (p15:sp0 ph10):f1
  go=2 ph31
  wr #0
exit

ph1= 0 2
ph10= 1
ph31= 0 2
```

### 3. Power conversion table:

power conversion table				
probe: 4mm triple				
nucleus/frequency	p90 (us)	RF-field (kHz)	power (W)	remarks
<sup>1</sup> H/				
<sup>19</sup> F/				
<sup>15</sup> N/				
<sup>15</sup> N/				
<sup>29</sup> Si/				
<sup>13</sup> C/				
<sup>13</sup> C/				
<sup>119</sup> Sn/				
<sup>31</sup> P/				



# Figures

<b>1 Introduction</b>	<b>9</b>
<b>2 Test Samples</b>	<b>11</b>
<b>3 Basic Setup Procedures</b>	<b>13</b>
Figure 3.1. Routing for a Simple One Channel Experiment .....	15
Figure 3.2. Probe Connections to the Preamplifier .....	17
Figure 3.3. Pop-up Window for a New Experiment .....	18
Figure 3.4. used Table with Acquisition Parameters for the KBr Experiment .....	19
Figure 3.5. Graphical Pulse Program Display .....	20
Figure 3.6. Display Example of a Well-tuned Probe .....	21
Figure 3.7. Display Example of an Off-Matched and Off-Tuned Probe .....	22
Figure 3.8. Display Example Where Probe is Tuned to a Different Frequency .....	22
Figure 3.9. FID and Spectrum of the 79Br Signal of KBr used to Adjust the Magic Angle .....	23
Figure 3.10. Routing for a Double Resonance Experiment using High Power Stage for H and X-nucleus .....	24
Figure 3.11. Routing for a Double Resonance Experiment, Changed for Proton Observation .....	25
Figure 3.12. Proton Spectrum of Adamantane at Moderate Spin Speed .....	26
Figure 3.13. Setting the Carrier on Resonance .....	27
Figure 3.14. Expanding the Region of Interest .....	28
Figure 3.15. Save Display Region to Menu .....	28
Figure 3.16. The popt Window .....	29
Figure 3.17. The popt Display after Proton p1 Optimization .....	30
Figure 3.18. Adamantane 13C FID with 50 msec aq. setsh Display .....	31
Figure 3.19. Adamantane 13C FID with 50 msec aq. setsh with Optimized Z-Shim Value .....	32
Figure 3.20. A cp Pulse Sequence .....	33
Figure 3.21. Hartmann-Hahn Optimization Profile .....	34
Figure 3.22. Hartmann-Hahn Optimization Profile Using a Square Proton Contact Pulse .....	35
Figure 3.23. Display Showing $\alpha$ -Glycine Taken Under Adamantane Conditions, 4 scans .....	36
Figure 3.24. Optimization of the Decoupler Offset o2 at Moderate Power, Using cw Decoupling .....	37
Figure 3.25. Glycine with cw Decoupling at 90 kHz RF Field .....	38
Figure 3.26. Glycine Spectrum with Spinal64 Decoupling at 93 kHz RF field .....	40
<b>4 Decoupling Techniques</b>	<b>45</b>
Figure 4.1. Optimization of TPPM Decoupling, on Glycine at Natural Abundance ....	46
Figure 4.2. Geometry for the FSLG Condition .....	49
Figure 4.3. FSLG Decoupling Pulse Sequence Diagram .....	50

Figure 4.4. Adamantane, FSLG Decoupled. The C-H J-Couplings Shown. ....	50
Figure 4.5. Shape with Phase Gradients .....	52
Figure 4.6. Pulse Program for Hahn Echo Sequence .....	54

## **5 Practical CP/MAS Spectroscopy on Spin 1/2 Nuclei** 55

### **6 Basic CP-MAS Experiments** 61

Figure 6.1. Pulse Program for CP with Flip-back Pulse .....	61
Figure 6.2. Pulse Program for CPTOSS. ....	63
Figure 6.3. Comparison of a CPTOSS and CPMAS Experiment .....	64
Figure 6.4. CPTOSS243 Experiment on Tyrosine HCl at 6.5 kHz .....	65
Figure 6.5. CPTOSS Experiment on Tyrosine HCl at 6.5 kHz .....	66
Figure 6.6. Pulse Program for SELTICS. ....	67
Figure 6.7. SELTICS at 6.5 kHz Sample Rotation on Tyrosine HCl. ....	67
Figure 6.8. Cholesterylacetate Spectrum Using Sideband Suppression .....	68
Figure 6.9. Block Diagram of the Non-quaternary Suppression Experiment .....	69
Figure 6.10. Glycine <sup>13</sup> C CPMAS NQS Experiment with a Dephasing Delay .....	70
Figure 6.11. Tyrosine <sup>13</sup> C CPMAS NQS Experiment with TOSS .....	71
Figure 6.12. Block Diagram of the CPPI Experiment. ....	72
Figure 6.13. CPMAS Spectrum of Tyrosine.HCl at 6.5 kHz .....	73

### **7 FSLG-HETCOR** 75

Figure 7.1. The FSLG Hetcor Experiment .....	76
Figure 7.2. The "12.." icon, and the ased icon in eda. ....	77
Figure 7.3. The ased Display .....	78
Figure 7.4. FSLG Hetcor Spectrum Tyrosine HCl .....	81
Figure 7.5. FSLG Hetcor Spectrum Tyrosine HCl .....	82

### **8 Modifications of FSLG HETCOR** 83

Figure 8.1. Comparison of HETCOR with and without <sup>13</sup> C-decoupling .....	84
Figure 8.2. HETCOR Using Windowless Phase Ramps .....	86
Figure 8.3. HETCOR on tyrosine *HCl without (left) and with LG contact (1msec contact) .....	92

### **9 RFDR** 93

Figure 9.1. RFDR Pulse Sequence for 2D CPMAS Exchange Experiment. ....	94
Figure 9.2. The "123" Icon in the Menu Bar of the Data Windows Acquisition Parameter Page .....	95
Figure 9.3. <sup>13</sup> C Histidine Signal Decay as a Function of the RFDR Mixing Time ....	97
Figure 9.4. 2D RFDR Spectrum of <sup>13</sup> C fully Labelled Histidine (RFDR mixing time 1.85 ms). ....	97

### **10 Proton Driven Spin Diffusion (PDSD)** 99

Figure 10.1. CPSPINDIFF Pulse Sequence .....	101
Figure 10.2. The Acquisition Parameter Window (eda) .....	102
Figure 10.3. POPT Result for the cw Decoupling Power Variation .....	105
Figure 10.4. <sup>13</sup> C CPSPINDIFF of fully labeled tyrosine*HCl, spinning at 22 kHz, 4.6 msec mix. Upper: PDSD, lower: DARR .....	106
Figure 10.5. Comparison of DARR/PDSD .....	107

Figure 10.6.13C DARR of Fully Labelled Ubiquitine Spinning at 13 kHz .....	108
<b>11 SUPER</b>	<b>109</b>
Figure 11.1.Pulse Sequence for 2D CPMAS exchange experiment .....	110
Figure 11.2.The “123” Icon in the Menu Bar of the Data Windows Acquisition Parameter Page. ....	111
Figure 11.3.The Acquisition Parameter Window (eda) .....	112
Figure 11.4.The SUPER Spectrum of Tyrosine HCl After Processing Using “xfb” ...	115
Figure 11.5.SUPER spectrum after tilting the spectrum setting “1 alpha” = -1 .....	116
Figure 11.6.Various Cross Sections from the Upper 2D Experiment .....	117
<b>12 Symmetry Based Recoupling</b>	<b>119</b>
Figure 12.1.C7 SQ-DQ Correlation Experiment .....	121
Figure 12.2.Optimization of the RF power level for DQ generation/reconversion on glycine. ....	123
Figure 12.3.Variation of DQ-generation/reconversion time on a uniformly 13C labeled peptide (fMLF). ....	124
Figure 12.4.PC7 Recoupling Efficiency at a Spinning Speed of 13 kHz .....	125
Figure 12.5.SC14 2d SQ-DQ correlation on tyrosine-HCl .....	128
Figure 12.6.PC7 2d SQ-SQ correlation on tyrosine-HCl .....	130
<b>13 PISEMA</b>	<b>131</b>
Figure 13.1.Pisema Pulse Sequence .....	132
Figure 13.2.The “123” Icon in the Menu Bar of the Data Windows Acquisition Parameter Page. ....	134
Figure 13.3.ASED Display for the PISEMA Setup. ....	135
Figure 13.4.A) PISEMA Spectrum of 15N Labeled Acetylated Valine, B) FID in t1 over 3.008 ms 64 Data Points .....	138
Figure 13.5.PISEMA Spectrum of 15N Labeled Kdpf Transmembrane Protein. ....	139
<b>14 Relaxation Measurements</b>	<b>141</b>
Figure 14.1.The CPX T1 Pulse Sequence .....	143
Figure 14.2.Relaxation of Alpha-carbon Signal in Glycine .....	146
<b>15 Basic MQ-MAS</b>	<b>151</b>
Figure 15.1.A 3-Pulse Basic Sequence with Z-Filter. ....	152
Figure 15.2.A 4-Pulse Basic Sequence with Z-Filter. ....	152
Figure 15.3.Comparison of 87Rb MAS spectra of RbNO <sub>3</sub> excited with selective and non-selective pulses. ....	155
Figure 15.4.Nutation profiles of selective and non-selective pulses. ....	156
Figure 15.5.Example for popt Set-up for Optimization of p1 and p2. ....	157
Figure 15.6.Signal Intensities of 87Rb Resonances in RbNO <sub>3</sub> as Function of p1 and p2. ....	158
Figure 15.7.2D 87Rb 3QMAS Spectrum of RbNO <sub>3</sub> . ....	161
Figure 15.8.Comparison of Differently Processed 2D 23Na 3Q MAS Spectra of Na <sub>4</sub> P2O <sub>7</sub> . ....	162
Figure 15.9.Calculated Shift Positions dMQ .....	163
Figure 15.10.17O MQMAS of NaPO <sub>3</sub> at 11.7 T (67.8 MHz) on the left and 18.8 T (108.4 MHz) on the right. ....	166

## Figures

Figure 15.11.Slices and Simulations of the 18.8 T 17O MQMAS of NaPO3. ....	167
Figure 15.12.Graphical Interpretation of the Spectrum from <u>Figure 15.10.</u> .....	168

## 16MQ-MAS: Sensitivity Enhancement 169

Figure 16.1.Hahn Echo Pulse Sequence and Coherence Transfer Pathway. ....	170
Figure 16.2.Processing of Hahn Echo. Left is the Shifted Echo. ....	171
Figure 16.3.Four Pulse Sequence and Coherence Transfer Pathway for the 3Q MAS Experiment .....	172
Figure 16.4.Three Pulse Sequence and Coherence Transfer Pathway .....	172
Figure 16.5.Example for popt to Set-up for Optimization of DFS. ....	175
Figure 16.6.Signal Intensities of 87Rb in RbNO3 .....	176
Figure 16.7.Pulse Sequence and Coherence Transfer Pathways for SPAM 3QMAS. ...	181

## 17STMAS 183

Figure 17.1.Principle of 2D Data Sampling in STMAS Experiments. ....	183
Figure 17.2.Four-pulse sequence and coherence transfer pathway for the double quantum filtered STMAS experiment with z-filter (stmasdqfz.av). ....	185
Figure 17.3.Four pulse sequence and coherence transfer pathway .....	186
Figure 17.4.87Rb STMAS Spectra of RbNO3. ....	190

## 18Double-CP 193

Figure 18.1.Pulse sequence diagram for 1D (t1=0) and 2D double CP experiments. ...	194
Figure 18.2.The edasp routing tables for H-C-N double CP. ....	195
Figure 18.3.Routing table for triple resonance setup change for 15N pulse parameter measurement and CPMAS optimization. ....	196
Figure 18.4.Shape Tool display with ramp shape from 45 to 55%. ....	198
Figure 18.5.Shape Tool display with a tangential shape for adiabatic cross polarization. ....	199
Figure 18.6.Double CP optimization of PL5 in increments of 0.1 dB. ....	200
Figure 18.7.Double CP yield, measured by comparing CPMAS and DCP amplitudes of the high field resonance. ....	201
Figure 18.8.C-N correlation via Double CP in histidine (simple setup sample). 4mm Triple H/C/N Probe. ....	204
Figure 18.9.NCaCx correlation experiment with 22 ms DARR mixing period for Ca-Cx spin diffusion on GB1 protein run using an EFREE-Probe. ....	205
Figure 18.10.NCaCx correlation experiment with 4.2 ms SPC5-DQ mixing period for CaCx spin diffusion on GB1 protein run using an EFREE-Probe at 14 kHz sample rotation and 100 kHz decoupling. ....	206

## 19CRAMPS: General 207

Figure 19.1.Difference in Amplitude of the Quadrature Channels X and Y .....	209
--	-----

## 20CRAMPS 1D 211

Figure 20.1.Pulse Sequence Diagram .....	211
Figure 20.2.PMLG Shape for wpmlg, sp1 .....	212
Figure 20.3.Shape for DUMBO, sp1 .....	213
Figure 20.4.Analog Sampling Scheme .....	214

Figure 20.5.Digital Sampling Scheme .....	214
Figure 20.6.Optimizing sp1 for Best Resolution .....	218
Figure 20.7.Optimizing cnst25 for Minimum Carrier Spike, Optimized at 120°C .....	219
Figure 20.8.Optimizing p14 for Minimum Carrier Spike, Optimized at 0.6 $\mu$ sec .....	219
Figure 20.9.WPMLG-CRAMPS After Optimization, Digital Acquisition .....	220
<b>21Modified W-PMLG</b>	<b>221</b>
Figure 21.1.Pulse Sequence Diagram .....	221
<b>22CRAMPS 2D</b>	<b>225</b>
Figure 22.1.Pulse Sequence Diagram .....	226
Figure 22.2.Setup and Test Spectrum of Alpha-glycine .....	228
Figure 22.3.Spectrum of Tyrosine-hydrochloride .....	229
Figure 22.4.Expansion of the Essential Part of the Spectrum .....	230
Figure 22.5.Pulse Sequence Diagram .....	231
Figure 22.6.Glycine, Proton-Proton DQ-SQ Correlation Using WPMLG in Both Directions .....	234
Figure 22.7.14.5 kHz W-PMLG/PC7 DQ/SQ Correlation at 600 MHz with Tyrosine-Hydrochloride .....	235
<b>A Appendix</b>	<b>237</b>

## Figures

# Tables

<b>1 Introduction</b>	<b>9</b>
<b>2 Test Samples</b>	<b>11</b>
Table 2.1. Setup Samples for Different NMR Sensitive Nuclei .....	11
<b>3 Basic Setup Procedures</b>	<b>13</b>
Table 3.1. Summary of Acquisition Parameters for Glycine S/N Test .....	39
Table 3.2. Processing Parameters for the Glycine S/N-Test .....	40
Table 3.3. Reasonable RF-fields for Max. 2% Duty Cycle .....	41
<b>4 Decoupling Techniques</b>	<b>45</b>
Table 4.1. Acquisition Parameters .....	51
Table 4.2. Processing Parameters .....	52
<b>5 Practical CP/MAS Spectroscopy on Spin 1/2 Nuclei</b>	<b>55</b>
Table 5.1. Power Conversion Table .....	57
<b>6 Basic CP-MAS Experiments</b>	<b>61</b>
Table 6.1. Acquisition Parameters .....	62
Table 6.2. Acquisition Parameters .....	63
Table 6.3. Acquisition Parameters .....	69
<b>7 FSLG-HETCOR</b>	<b>75</b>
Table 7.1. Acquisition Parameters for FSLG-HETCOR (on tyrosine-HCl) .....	79
Table 7.2. Processing Parameters for FSLG-HETCOR (on tyrosine-HCl) .....	80
<b>8 Modifications of FSLG HETCOR</b>	<b>83</b>
Table 8.1. Acquisition Parameters for pmlg-HETCOR (on tyrosine-HCl) .....	86
Table 8.2. Processing Parameters for pmlg-HETCOR (as for FSLG on tyrosine-HCl) .....	87
Table 8.3. Acquisition Parameters for wpmlg-HETCOR (on tyrosine-HCl) .....	88
Table 8.4. Acquisition Parameters for e-DUMBO-HETCOR (on tyrosine-HCl) .....	89
Table 8.5. Acquisition Parameters for DUMBO-HETCOR (on tyrosine-HCl) .....	90
<b>9 RFDR</b>	<b>93</b>
Table 9.1. Acquisition Parameters .....	95
Table 9.2. Processing Parameters .....	96
<b>10 Proton Driven Spin Diffusion (PDS)</b>	<b>99</b>
Table 10.1. Acquisition Parameters .....	103

## Tables

Table 10.2. Processing Parameters .....	104
<b>11 SUPER</b>	<b>109</b>
Table 11.1. Acquisition Parameters .....	113
Table 11.2. Processing Parameters .....	114
<b>12 Symmetry Based Recoupling</b>	<b>119</b>
Table 12.1. Recommended Probe/Spin Rates for Different Experiments and Magnetic Field Strengths .....	122
Table 12.2. Acquisition parameters for DQ-SQ correlation experiments using symmetry based recoupling sequences .....	126
Table 12.3. Processing parameters for DQ-SQ correlation experiments using symmetry based recoupling sequences .....	127
<b>13 PISEMA</b>	<b>131</b>
Table 13.1. Acquisition Parameters .....	136
Table 13.2. Processing Parameters .....	137
<b>14 Relaxation Measurements</b>	<b>141</b>
Table 14.1. Parameters for the 1D CP Inversion Recovery Experiment .....	143
Table 14.2. Parameters for 2D Inversion Recovery Experiment .....	144
Table 14.3. Processing Parameters for CP T1 Relaxation Experiment .....	145
Table 14.4. Parameters for the Saturation Recovery Experiment .....	148
<b>15 Basic MQ-MAS</b>	<b>151</b>
Table 15.1. Some Useful Samples for Half-integer Spin Nuclei .....	154
Table 15.2. Initial Parameters for Setup .....	157
Table 15.3. F1 Parameters for 2D Acquisition .....	158
Table 15.4. Processing Parameters for 2D FT .....	160
Table 15.5. Values of  R-p  for Various Spins I and Orders p .....	164
Table 15.6. Chemical Shift Ranges for all MQ Experiments for All Spins I .....	165
<b>16 MQ-MAS: Sensitivity Enhancement</b>	<b>169</b>
Table 16.1. Initial Parameters for the DFS Experiment .....	174
Table 16.2. Parameters for 2D Data Acquisition of 3-pulse Shifted Echo Experiment mp3qdfs.av. ....	177
Table 16.3. Parameters for 2D Data Acquisition of 4-pulse Z-filtered Experiment mp3qdfsz.av. ....	178
Table 16.4. Processing Parameters .....	179
Table 16.5. Parameters for FAM .....	180
Table 16.6. Further Parameters for 2D Data Acquisition of SPAM MQMAS Experiment mp3qspam.av .....	181
<b>17 STMAS</b>	<b>183</b>
Table 17.1. Time deviation of the rotor period for spinning frequency variations of $\pm 1$ and $\pm 10$ Hz for various spinning frequencies. ....	184
Table 17.2. Some Useful Samples for Some Nuclei with Half Integer Spin .....	187
Table 17.3. Initial Parameters for the Set-up of stmasdfqz.av. ....	188

Table 17.4. Initial Parameters for the Set-up of stmasdfqe.av .....	189
Table 17.5. F1 Parameters for the 2D Data Acquisition. ....	190
Table 17.6. Processing Parameters for the 2DFT .....	191
Table 17.7. Values of R and $\zeta R - \rho \zeta$ for the Various Spin Quantum Numbers Obtained in the STMAS Experiment .....	192
<b>18Double-CP</b>	<b>193</b>
Table 18.1. Recommended Parameters for the DCP Setup .....	197
Table 18.2. Recommended Parameters for the DCP 2D Setup .....	202
Table 18.3. Recommended Processing Parameters for the DCP 2D .....	203
<b>19CRAMPS: General</b>	<b>207</b>
<b>20CRAMPS 1D</b>	<b>211</b>
Table 20.1. Phases, RF-Levels, Timings .....	211
Table 20.2. PMLG Analog Mode .....	215
Table 20.3. DUMBO, Analog Mode .....	216
Table 20.4. Parameters for Digital Mode .....	218
<b>21Modified W-PMLG</b>	<b>221</b>
Table 21.1. Phrases, RF-Levels, Timings .....	221
Table 21.2. PMLG, Analog Mode .....	223
Table 21.3. DUMBO, Analog Mode .....	223
Table 21.4. Parameters for Digital Mode .....	224
<b>22CRAMPS 2D</b>	<b>225</b>
Table 22.1. Acquisition Parameters .....	226
Table 22.2. Phases, RF-levels, and Timings .....	227
Table 22.3. Processing Parameters .....	227
Table 22.4. Acquisition Parameters .....	232
Table 22.5. Phases, RF-Levels and Timing .....	232
Table 22.6. Processing Parameters .....	233
<b>A Appendix</b>	<b>237</b>

## Tables

# Index

## Symbols

(NH4)2SeO4 .....	12
(NH4)H2PO4.....	11

## Numerics

13C Matching Box.....	17
1H HP Preamplifier .....	17
79Br Signal.....	23
90° pulse .....	13

## A

Adamantane.....	11 – 12
ADP.....	59
AgNO3 .....	12
AlPO-14.....	12
analog mode .....	213
Anatas.....	12
as hydroquinon.....	11
ased .....	18
AU-program DUMBO .....	53

## B

B0-field .....	39
background signal .....	56
background suppression.....	56
BaClO <sub>3</sub> *H <sub>2</sub> O.....	215
Basic Setup Procedures.....	13
Beff.....	49
BF1.....	16
BLEW-12.....	48
BN .....	11
Boric Acid .....	11
BR-24 .....	48, 208
breakthrough .....	14
bsmsdisp .....	33
bypassing the preamp.....	31

## C

C-24 .....	208
calcpowlev.....	30
Calibrating .....	32

Carrier .....	27
Cd(NO <sub>3</sub> ) <sub>2</sub> *4H <sub>2</sub> O .....	12
Chemical Shifts .....	32
Clathrate.....	11
cnst20.....	77
Co(CN) <sub>6</sub> .....	12
Compressors.....	14
conductivity .....	55
contact time .....	33
CORTAB .....	16
cpdprg2 .....	38
CPPI.....	61, 72 – 73
CPPIRCP .....	72 – 73
CPPISPI .....	72 – 73
CRAMPS .....	207
Cross polarisation .....	33
cross polarisation .....	13
cross polarization under a LG frequency offset.....	75
Cu-metal powder.....	11
CW decoupling .....	45

**D**

D2O .....	12
d-DMSO <sub>2</sub> .....	12
Default.....	16
dielectric loss.....	55
digital mode .....	213
d-PE .....	12
dpl .....	28
d-PMMA .....	12
dry gas .....	14
dryers .....	14
DSS .....	12, 59
–Dtossb .....	62
DUMBO .....	53, 90, 208

**E**

eda .....	15, 77
EDASP .....	16
edasp .....	15
edc .....	17
e-DUMBO.....	89
experiment button .....	19

**F**

frequency .....	15
Frequency Switched Lee Goldburg.....	48, 208
Frequency Switched Lee Goldburg Heteronuclear Correlation.....	75
FSLG .....	208
FSLG Decoupling .....	48
FSLG pulse .....	75

**G**

Ga <sub>2</sub> O <sub>3</sub> .....	11
gas .....	14
gas in air.....	11
Glycine .....	11
Good Laboratory Practice .....	41
graphical display .....	19
group .....	29

**H**

H <sub>3</sub> SeO <sub>3</sub> .....	12
Hartmann-Hahn.....	34
Hartmann-Hahn-condition.....	33
Heteronuclear Decoupling.....	45
Hg.....	12
Hg(acetate)2 .....	12
HH conditions.....	35
HH profile .....	35
high .....	24
High power decoupling.....	14
Homonuclear decoupling .....	47
Homonuclear dipolar interactions.....	207
HP-HPPR modules .....	31
HPLNA 1H modules .....	31

**I**

IN_F1 .....	77
inversion-recovery.....	142
irradiation frequency.....	15

**K**

K <sub>2</sub> Pt(OH) <sub>6</sub> .....	12
K <sub>2</sub> S .....	12
KBr .....	12 – 13, 23
KCl .....	12
KMnO <sub>4</sub> .....	12

**L**

Lee Goldburg condition .....	48
LG Offset.....	91
Li (org.).....	12
LiCl .....	11 – 12
local motions .....	142
logical channel .....	15
longitudinal relaxation .....	141

**M**

magic angle .....	13, 47
Malonic Acid .....	11
matching box .....	16
monoexponential .....	147
MREV-8 .....	48, 208
MSHOT .....	208
Multiple Pulse Decoupling .....	48
Multiple pulse NMR .....	47

**N**

Na2HPO4 .....	11
Na3P3O9 .....	11
new .....	23
nexp .....	29
NH4Cl .....	12
NH4VO4 .....	11
nonexponential decay .....	148
NQS .....	69
nrf .....	13

**O**

observe nucleus .....	16
offset O1 .....	15
oil-free gas .....	14
optimize .....	29
optimum posmax .....	29

**P**

Pb(p-tolyl)4 .....	12
PbNO3 .....	12
PCPD2 .....	39
pcpd2 .....	40, 46
peakw .....	42
phase modulated pulses .....	75
phase-modulation .....	49
Pi-pulse decoupling .....	47
PMLG .....	49
pmlg .....	86
pmlghet .....	85
popf .....	29, 46
poptau.exe .....	29
power conversion factor .....	57
Power Conversion Table .....	57
powmod .....	16, 24
powmod high .....	24
preamp .....	16
preamplifier .....	16
Profile .....	34 – 35
Proton Bandpass Filter .....	17

proton T1 .....	55
proton T1p .....	35, 55
Proton-Proton DQ-SQ Correlation .....	230
pseudo-2D .....	145
PTFE .....	11
Pulprog .....	19
PVDF .....	11

**Q**

Q8M8 .....	12
------------	----

**R**

RbClO4 .....	11
RbNO3 .....	11
relaxation .....	141
Resonance .....	27
RF voltages .....	14
RFDR .....	93
RF-efficiency .....	13
RF-field .....	13
RF-performance .....	13
RF-power .....	13
RF-routing .....	13

**S**

Sampling .....	213
saturation recovery .....	147
saturation-recovery experiment .....	143
save button .....	29
Save Display Region to .....	28
SB probes .....	43
scaling factor .....	209, 218
SELTICS .....	63, 66 – 67
semi-windowless .....	48
sensitivity .....	13
setsh .....	31
SFO1 .....	16
SGU1 .....	16
shimming .....	13
Silicone paste .....	11
Silicone rubber .....	11
sinocal .....	40
skip .....	29
Skip optimization .....	29
Sm <sub>2</sub> Sn <sub>2</sub> O <sub>7</sub> .....	11
Sn(cyclohexyl)4 .....	11
SnO <sub>2</sub> .....	11
spin nutation frequencies .....	13
spin rate monitor .....	13
SPINAL .....	47
SPINAL decoupling .....	47

spin-lattice relaxation .....	141
spin-locking pulse.....	142
spinning gas .....	13
spin-spin relaxation .....	141
spnam0 .....	41
sr .....	33
SSNMR .....	13
start optimize.....	29
stop optimization .....	29
susceptibility compensated .....	32
SwitchF1/F2 .....	24

**T**

T1 .....	55, 141
T1/T2 relaxation .....	145
T1r .....	142
T1ρ .....	55
T2 .....	141
TI-S .....	55
TMSS .....	12
Torchia method .....	142
TOSS .....	63
tp90 .....	13
TPPM decoupling.....	46
transmitter .....	16
transverse magnetization .....	141
TREV-8 .....	208

**V**

variable delay .....	143
variable pulse list.....	149
varmod .....	29

**W**

WaHuHa.....	208
WHH-4 .....	208
windowless sequences .....	48
wobb.....	20
wobb high.....	25
W-PMLG .....	208

**X**

X Low Pass Filter .....	17
xau angle.....	23
X-BB Preamplifier.....	17
XiX decoupling .....	47

**Y**

Y(NO<sub>3</sub>)<sub>3</sub>\*6H<sub>2</sub>O ..... 12

**Z**

ZGoption -Dlacq ..... 32  
ZGOPTNS ..... 62  
 $\alpha$ -carbon at 43 ppm ..... 36  
 $\alpha$ -glycine ..... 12, 36  
 $\gamma$ -glycine ..... 36

## **Index**

**End of Document**

# Bruker BioSpin, your solution partner

Bruker BioSpin provides a world class, market-leading range of analysis solutions for your life and materials science needs.

Our solution-oriented approach enables us to work closely with you to further establish your specific needs and determine the relevant solution package from our comprehensive range, or even collaborate with you on new developments.

Our ongoing efforts and considerable investment in research and development illustrates our long-term commitment to technological innovation on behalf of our customers. With more than 40 years of experience meeting the professional scientific sector's needs across a range of disciplines, Bruker BioSpin has built an enviable rapport with the scientific community and various specialist fields through understanding specific demand, and providing attentive and responsive service.



[info@bruker-biospin.com](mailto:info@bruker-biospin.com)  
[www.bruker-biospin.com](http://www.bruker-biospin.com)